

AIRBORNE AND GROUND LEVEL FLASK SAMPLING FOR REGIONAL CARBON BUDGETS – THE POTENTIAL OF MULTIPLE TRACER AND ISOTOPE ANALYSES

Development of a new 'Investigation Strategy' and of an improved
'Sampling System'

Dissertation
zur Erlangung des Doktorgrades
der Naturwissenschaften im Fachbereich
Geowissenschaften
der Universität Hamburg

Vorgelegt von
Marcus Schumacher
aus
Gifhorn

Hamburg
2005

Als Dissertation angenommen vom Fachbereich Geowissenschaften der
Universität Hamburg

Auf Grund der Gutachten von Professor Dr. Hartmut Graßl
und Professor Dr. Martin Heimann

Hamburg, den 11. Juli 2005

Professor Dr. H. Schleicher
Dekan des Fachbereichs Geowissenschaften

PREAMBLE

Some of the most important problems and questions focussed on in this thesis were identified by field experiments performed within a major project initiated and carried out by several groups.

The investigations, as well as the resulting enhancements presented here are mainly reactions attributed to campaign observations. Therefore the newly designed sampling system, the ground reference unit and the sophisticated investigation strategy have arisen as means to an end – and were not the intended purposes of this study. To accomplish the findings a particular venture was the critical scrutiny and the adaptation of established assumptions.

Since the data acquisition was carried out within the restricting frame of the main project specific experiments were only possible in a limited fashion. More flights would have been desirable, also because the amount of data obtained from the field campaigns is low.

As a corollary, the result of this study is not a register with regional carbon ‘numbers’, but a list with aspects and impairments which have to be taken into account, providing the basis for further investigations focussing on airborne and ground based assessment of the carbon budget.

In spite of, or thanks to the adverse conditions, new findings and ideas could be deduced which shall be applied in succeeding projects.

‘And therefore as a stranger give it welcome ...’

PREAMBLE

1. INTRODUCTION

2. BASIC PRINCIPLES: THEORY AND EXPERIMENTAL SETUP

2.1. Theory

2.1.1.1. Long lived Trace Gases in the Atmosphere	4
<i>Carbon Dioxide in the Atmosphere</i>	5
<i>Additional Trace Gases</i>	7
2.1.1.2. Isotopic Signatures in Carbon Dioxide	13
2.1.2. RECAB Strategy	19
2.1.3. Convective Boundary Layer	25
2.1.4. Ground Characterization and References	28
2.1.5. Combined Investigations	
2.1.5.1. Modelling Approaches – Inverse Studies	29
2.1.5.2. Land Use Classification	31

2.2. System Configurations and Data Analysis

2.2.1. Campaign Equipment

2.2.1.1. Flight Sampling Unit	34
2.2.1.2. Continuous Flight Measurements	35
2.2.1.3. Ground Reference System	36

2.2.2. Equipment Gas Analyses

2.2.2.1. Trace Gas Mixing Ratios from Flask Sampling	38
2.2.2.2. Isotope Ratios	39

3. TEST FLIGHTS AND LABORATORY EXPERIMENTS

3.1. Test Flight Measurements	October 2000-May 2001	
 3.1.1. Description of the German Study Region		
3.1.1.1. Geography and Climate		40
3.1.1.2. Field Sites		41
 3.1.2. Hainich Flights	October 2000	43
 3.1.3. Winter Flights	January and February 2001	45
 3.1.4. Gebesee Flights	May 2001	47
3.2. Development of a modified Flask Sampling System		
 3.2.1. Conventional System:		
Test of the inlet tubing and of the gas exchange rate		48
October – December 2000		
3.3. Modified Flask Sampling System		
 3.3.1. Modified System:		
Adjustment of the flow rate and tests regarding effects of the drying reagent on the CO ₂ mixing ratio		51
September – December 2001		
3.3.1.1. Exchange characteristic		51
3.3.1.2. Influence of the drying medium on the CO ₂ mixing ratio		52
 3.3.2. Comparison of the different sampling systems	January 2002	54
3.4. Summary of the modifications and assessment of the improvements		57

4. RECAB FIELD EXPERIMENTS JUNE 2001 – AUGUST 2002

4.1. Data Acquisition and Observations

4.1.1. Valencia Summer Experiment	17 June – 7 July 2001	60
First experiment with the modified sampling system		
4.1.2. Thuringia Summer Experiment	15 July – 2 August 2001	62
4.1.3. Uppland Summer Experiment	11 August - 9 September 2001	63
Implementation of additional trace gases analyses		
4.1.4. Valencia Winter Experiment	16 November – 15 December 2001	66
Final configuration of the modified sampling system		
4.1.5. The Netherlands Winter Experiment	14 January – 10 February 2002	69
Test of improved sampling strategy		
4.1.5. Lazio Summer Experiment	27 May – 27 June 2002	73
4.1.7. The Netherlands Summer Experiment	10 – 28 July 2002	75
Enhancement of improved sampling strategy		
4.1.8. ‘SPA¹³CE’ Thuringia Summer Experiment	6 – 15 August 2002	77
Combined ground level and flight investigations		

4.2. Interpretation of the Results

Southern Europe

4.2.1. Valencia Summer Experiment	80
4.2.2. Valencia Winter Experiment	81
4.2.3.1. Lazio Summer Experiment	84
4.2.3.2. Inverse Study - Mesoscale Dispersion Model	86
4.2.3.3. Inverse Study - Back Trajectory Calculations	88

Northern Europe

4.2.4. Uppland Summer Experiment	90
---	-----------

Central Europe

4.2.5. Thuringia Summer Experiment	94
4.2.6. The Netherlands Winter Experiment	95
4.2.7. The Netherlands Summer Experiment	97
4.2.8.1. ‘SPA¹³CE’ Thuringia Summer Experiment	102
<i>4.2.8.2. Inverse Study - Adjoint of a Transport Model</i>	108

5. DISCUSSION

5.1. Comparison of the Study Regions using Multiple Tracer Data

5.1.1. CO₂ / delta¹³C and CO₂ / CO relationships	
<i>Carbon Dioxide and Isotopic Signature</i>	111
<i>Combustion Processes</i>	113
5.1.2. Comparison of the study regions	
5.1.2.1. <i>Seasonal Variations</i>	115
5.1.2.2. <i>Longitudinal Differences</i>	119
5.1.2.3. <i>Latitudinal Differences</i>	122

5.2. Theoretical and Conceptual Aspects

5.2.1. Time Dependence	127
<i>Variability - Air Mass Change</i>	129
<i>Day-to-day Variability</i>	130
<i>Local Characteristics – Land-Sea-Wind Circulation</i>	132
‘Signal Shift’ – Effects of time delayed Detection	133
<i>CH₄ and VOC Conversion</i>	135
5.2.2. Applicability of the ‘CBL-budget Approach’	141

5.3. Summary of Methodological Experiences	143
<i>Identified Impairments</i>	145
5.4. Enhanced Investigation Strategy	
5.4.1. Implementation of Ground Reference Measurements and Sampling	148
5.4.2. Adapted Flight Investigation Strategy – ‘Transect Approach’	151
6. CONCLUSIONS	
6.1. Relevance of the Results	155
6.2. Perspectives	156
7. SUMMARY	158
8. ANNEXES	
A1 ABBREVIATIONS and CONVERSION OF UNITS	161
A2 EQUIPMENT Configuration of Sampling Units	162
A3 EQUIPMENT Configuration of Analytical Instrumentation	163
A4 EQUIPMENT Instrument Manufacturers	164
A5 Laboratory Experiment January 2002	166
A6 Scale Basis for Triplet Calculations	168
A7 Trace gas mixing ratios and isotopic composition of CO₂ from the RECAB field campaigns for the lowest flight level and for the free troposphere	169
9. REFERENCES	170
10. ACKNOWLEDGEMENTS	198

1. INTRODUCTION

As soon as mankind appeared on the scene some hundred thousand years ago it formed its environment. But during the last few hundred years the human impact became more and more distinct, because of the broadening and intensification which came along with the growth of population and the increase of the living standards and economic demands.

These anthropogenic interferences are influencing not only the terrestrial surface but also the atmosphere. Effects, which became apparent during the last two decades, are for example the ozone hole, the acid rain and the summer smog phenomena, and more recently the ‘additional greenhouse effect’, which appears to provoke the rising of the global mean air temperature. A close relationship between observed temperature rise and the surge of the CO₂ release since the era of the ‘industrial revolution’ is being discussed. The rise of CO₂ concentration is resulting in particular from the increasing consumption of fossil fuels and from land use changes. An interdisciplinary assessment body was established with the *Intergovernmental Panel on Climate Change (IPCC)* in 1988, to provide basic information for policymakers on the status quo and for future scenarios of impacts and economics of climate change. The Kyoto Protocol manifested in 1997 the political efforts to react on the interferences with the climate system. More scientific investigations were initiated, among others the *CarboEurope* cluster.

As one part of the cluster the project *RECAB (Regional Assessment and Monitoring of the Carbon Balance within Europe)* focused on the link between local investigations and global modelling strategies [HUTJES ed. 2003]. Eleven groups from seven European countries cooperate since the summer of 2000 to improve theories and strategies and to develop new methods, with the aim to determine the carbon budget on regional scales by a close link between experimental and theoretical approaches.

One fundamental part of the project was the provision of data. During several field campaigns, of two to four weeks duration, flight and ground based data collections were conducted at different locations within Europe over the year. The *Max-Planck-Institut für Biogeochemie (MPI-BGC)* contributed with airborne studies within the lower troposphere to the project, supplementing ground level

measurements. The experimental concept based on the theory of the *CBL*- (convective boundary layer) *Budget-Approach* [LAUBACH AND FRITSCH 2002] should provide by comparison of repeated measurements information about the flux of carbon within the study region. To supply a data base for such task, air samples were taken in different heights and analysed for trace gas mixing ratios and for the composition of the stable isotopes in CO₂. Aim of this flask sampling was to

- distinguish between the contributions from anthropogenic sources and natural sources and sinks and to
- estimate carbon budgets for small regions ($\leq 10^4 \text{ km}^2$).

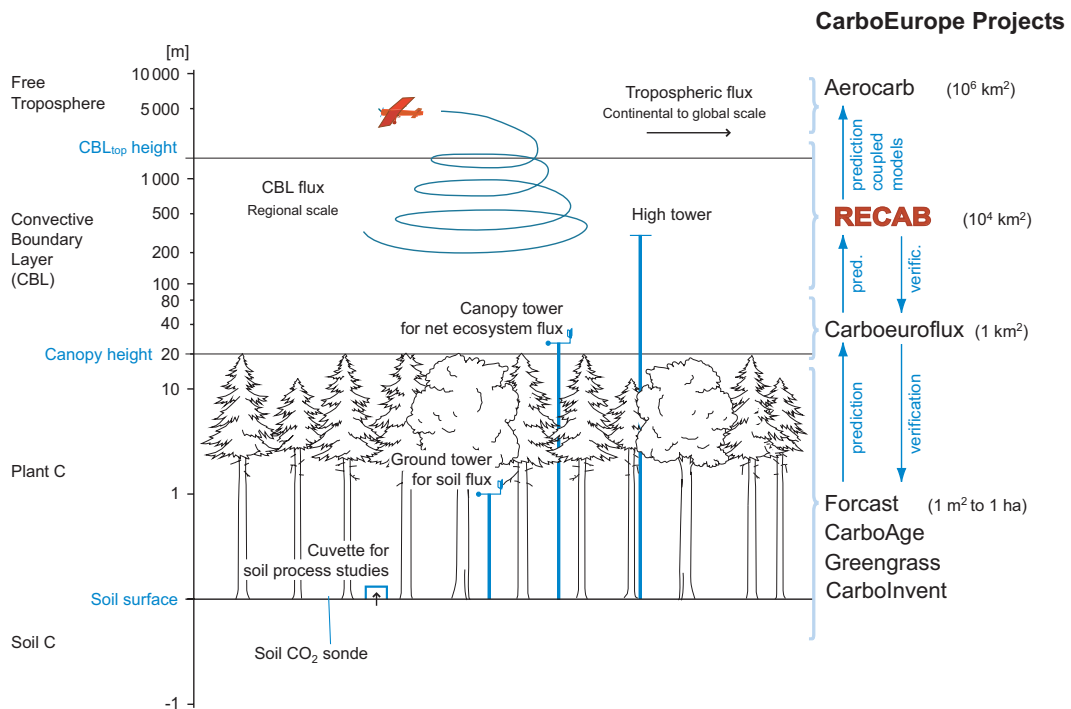


Figure 1. The RE CAB project within the frame of the CarboEurope cluster.
(from FREIBAUER 2002, modified)

However, after the analysis of the first measurements it became obvious, that fundamental theoretical and conceptual aspects might be affected in a crucial way by processes which had not been taken into account so far.

Hence the emphasis of this thesis became

- the identification and characterisation of these impairments and

- the evaluation of the potential of multiple trace gas and isotope analyses for
 - the construction of an improved sampling system,
 - the development of a new investigation strategy
 - the characterisation of the REcab study regions and their comparison.

Regarding this study the REcab project occupies an ambivalent position. On one hand the field campaigns were the base for the data acquisition. On the other hand, due to the constraints fixed in the primary concept, specific experiments could only be accomplished in a restricted frame.

The structure of this thesis: An introduction into the theoretical base and the methods used is given in the first section. Subsequently, the laboratory- and test flight experiments are discussed that were performed before and during the REcab field campaigns. To concentrate the technical aspects in one block also the new flight sampling system is examined, quasi in an anticipation of the findings from the field experiments.

The field observations are presented with respect to the development of instrumentation and measurement strategy in chronological order. Regarding the aim of the REcab project – the characterisation and comparison of the study regions - the interpretation of the results is according to regions.

The potential of multiple tracer studies is reflected with respect to the characterisation and the comparison of the REcab regions, followed by a discussion of more general theoretical and conceptual aspects. Finally an enhanced investigation strategy is presented.

In the conclusion section the significance of the findings and the perspectives of airborne studies regarding flask sampling and multiple tracer analyses are discussed.

Flight campaigns and ground sampling data are recorded on the attached CD-ROM. In addition, a photo documentation of the sampling equipment and of the study sites gives an impression of the campaign performance.

2. BASIC PRINCIPLES: THEORY AND EXPERIMENTAL SETUP

2.1. Theory

2.1.1. Long lived trace gases in the atmosphere

Carbon is a common component found in several compounds of the atmosphere, such as carbon dioxide (CO_2), carbon monoxide (CO), methane (CH_4) and the group of the volatile organic compounds (VOCs), but also in form of solid particles. For the estimation of the budget direct concentration measurements but also the examination of the variations of all carbonaceous constituents would be necessary. Since a full C-budget was not anticipated within the RECAB project the project focussed on the investigation of the most common atmospheric species with global warming potentials (CO_2 , CH_4 , later extended by CO).

In the atmosphere the gases are characterised by different mixing ratios as also by different contribution potentials to the greenhouse effect. The *absolute* amount of the individual gas species is thereby highly variable in time and space. Major causes are the distribution of sources and sinks on the land surface, as well as parameters which dominate biological and chemical activity, like temperature, radiation, the availability of potential reaction partners, and the synoptic weather pattern.

Furthermore information can be obtained from the *relative* ratios of the gases. On one hand the covariance provides information on chemical reaction chains, e.g. H_2 and CO, because they are involved in the oxidation of CH_4 . On the other hand, in particular from non reactive constituents, evidence for air mass change can be derived. As such a tracer SF_6 was included in the analysis scheme.

The occurrence of trace gases in the atmosphere is mainly dependent on three factors: a) the nature of the sinks and sources, b) their magnitude and persistence as well as c) their distribution [MAHRT 1997]. Often the generating and destructing mechanisms, defining the lifetime of a species, are coupled to biological and chemical activities, expressed in diurnal and annual cycles, but also the availability depends on nutrients or reaction partners. It might thus happen that a sink becomes a source and vice versa. Urban and rural environments, as point and

area sources are affecting the mixing ratio field of trace gases, which are additionally modified by topography and circulation.

Causes for the omnipresence of a gas species might be a uniform distribution of the sources and/or a long residence time. Characteristic for such species are concentrations barely differing from site to site.

A long life time is necessary to use an individual species as a tracer, for example due to air mass exchange. As a nearly purely anthropogenic gas species, which is also chemically rather inert without sinks at the surface or in the troposphere, SF₆ was chosen during the study.

CARBON DIOXIDE CO₂

Of all analyzed gas species CO₂ is the one which occurs with the highest mixing ratio and shows the most distinct periodicity. For the year 2000 the global average of the volume mixing ratio was calculated to be 368 ppmv [HOUGHTON et al. 2001], with higher absolute values and a larger seasonal variation in the northern hemisphere. This is related to the fact that the strongest sources and sinks are located on the northern hemisphere continents [CIAIS et al. 1995, PRENTICE et al. 2000]. While the uptake of CO₂ by vegetation or oceans occurs over large areas, the major part of the anthropogenic CO₂ is released from point sources, like cities and industrial complexes. The long life time of 50 to 200 years [U.S. GREENHOUSE GAS INVENTORY PROGRAM 2002] is the main cause for the observed average concentration increase indicated in figure 2.2.

Most significant terrestrial sources are the respiration of autotrophic and heterotrophic organisms, and the combustion of organic material, especially the use of fossil fuels, by traffic, industry and households [WITTENBERG et al. 1998, ANDRES et al. 1999, LANGENFELDS et al. 2002]. Since the beginning of the industrial revolution the average atmospheric volume mixing ratio of CO₂ increased by about 30% from 280 ppm to the actual value [HOUGHTON et al. 2001]. Assimilation of CO₂ by plants is the major terrestrial sink. Depending on the organism, whether annual or persistent, the storage time may vary from a growing season to centuries. However, a part of the carbon is recycled immediately by respiration. Driven by plant activity a diurnal and an annual cycle can be

distinguished, where the contribution of the uptake exceeds the release of CO₂ during the growing season – which can be divided in an assimilation uptake during day time and a respiration release during night time. In dormant seasons, such as winter time respiration is in general dominant [RANDERSON et al. 1997, WINSTON et al. 1997, RAYNER & LAW 1999]. Because of the covariance of radiation and temperature with the development of the boundary layer depths, the stable nocturnal layer is characterised by high CO₂ mixing ratios. Whereas in the CBL the mixing ratio is depleted because of the extension of the layer depths - and during the growing season plant uptake.

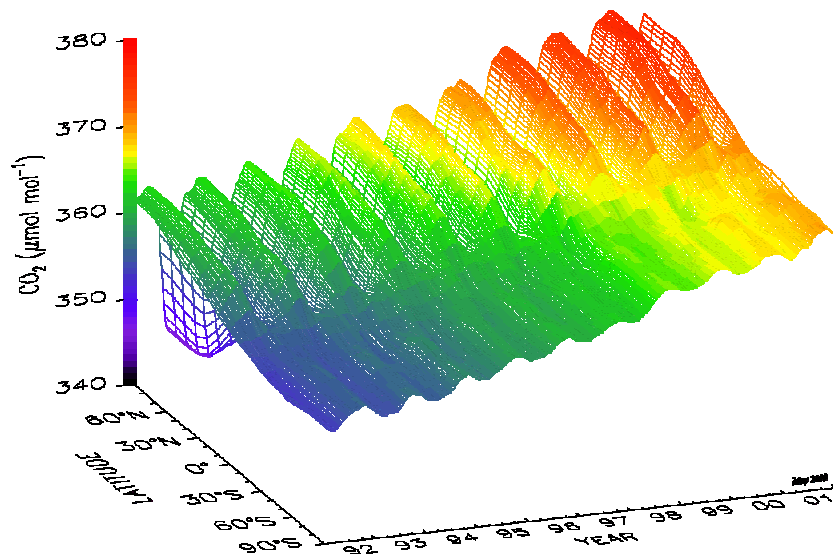


Figure 2.1. Latitudinal distribution of atmospheric carbon dioxide mixing ratio in the marine boundary layer air. The surface represents data smoothed in time and latitude, from the NOAA / CMDL cooperative air sampling network (PI: P. Tans and T. Conway, NOAA / CMDL)

The terrestrial stocks of natural carbon are estimated to be 1500 Pg in soils and 500 Pg in plants [IPCC 2001]. The atmospheric reservoir contains about 730 Pg, whereby the flux between atmosphere and land is estimated to be around 122 PgC/a and from the land to the atmosphere to be about 120 PgC/a [HOUGHTON et al. 2001]. In total the carbon-pool of the oceans (39000 Pg) exceeds the terrestrial sinks by more than a factor 50, the assumed natural influx into the ocean is calculated to be 90 Pg per year. Human perturbation adds an annual flux of 5.4 PgC/a from geological reservoirs (5.3 PgC/a from fossil fuel burning,

0.1 PgC/a from cement production) to the atmosphere. A net uptake by land of 1.9 PgC/a is nearly balanced by a release of 1.7 PgC/a from land use changes. The ocean net uptake is estimated to be 1.9 PgC/a.

Besides for CO₂ the air samples were also analyzed for the mixing ratios of five additional trace gases. Two carbonaceous compounds, CO and CH₄, and N₂O, SF₆ as well as H₂ also are having a direct or indirect greenhouse warming potential. Additional information can be obtained from the ratios of the individual species when back tracking the air masses with the aim to identify the sources origin.

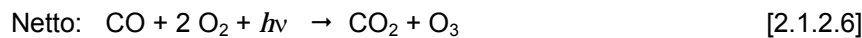
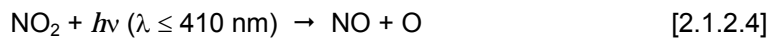
CARBON MONOXIDE CO

Formation processes and the occurrence of CO in the atmosphere are described by many studies [NOVELLI et al. 1992, NOVELLI et al. 1994, BAKWIN et al. 1994, NOVELLI et al. 1998, BERGAMASCHI et al. 2000, WOTAWA et al. 2001]. A main source of CO are combustion processes [LAURSEN et al. 1992, KATO et al. 1999, WARNECK 2000, ANDREAE & MERLET 2001]. Different materials and burning temperatures lead to characteristic CO to CO₂ ratios in emissions, for example the volume percentage ratio of CO / CO₂ from biomass burning of forest wild fires is 11 – 25 %, for burning of agricultural wastes 3 – 16 % or for burning of wood 6 – 18 %. In the smoldering stage CO emission can, depending on the temperature, rise up to 80 % [WARNECK 2000]. Characteristic ratios emitted by car engines are estimated to be between 0.02 – 1.34 %. Typical values for power plants are 0.03 % and for industrial production processes 2.15 %. Distinctly higher rates are obtained for emissions from metal production 71.2 % (ranges calculated from data published by the KRAFTFAHRT-BUNDESAMT 2003 and by the UMWELTBUNDESAMT 2003). CO can therefore be used as a tracer for CO₂ from combustion processes.

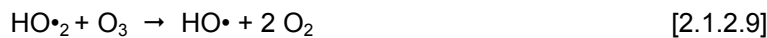
On the other hand CO is a direct precursor of CO₂. The reaction of CO with the OH radical, the major sink process for carbon monoxide, leads to CO₂ [ATKINSON 1989, BLAKE et al. 1993, TYLER et al. 1997, RÖCKMANN et al. 1998]. Thus, the ratio

of CO / CO₂ changes with the distance from the source and the concentration of OH radicals.

There are two reaction cycles (net equations [2.1.2.6. and 2.1.2.10.]), depending on whether NO_x is available or not. Beside the role of NO_x as a catalyst for the formation of O₃ its presence is also important for the regeneration of OH radicals.



Or if the NO_x concentration is low:



Another sink, however less important than the reaction with the hydroxyl radicals, is the microbiological uptake in soils. The sources of CO are, with nearly equal amounts, fossil fuel combustion and related activities, biomass burning, the oxidation of CH₄ (see below [2.1.2.11. – 2.1.2.16.]) and the oxidation of natural hydrocarbons [CONWAY et al. 1994, WARNECK 2000].

Since the late 1980s a decrease of the CO mixing ratio can be observed because the actual sink strength exceeds source strength [HOUGHTON et al. 2001].

Table 2.1: The Global and North Hemispheric Budget of Carbon Monoxide in the Troposphere (Tg CO per year)¹⁾

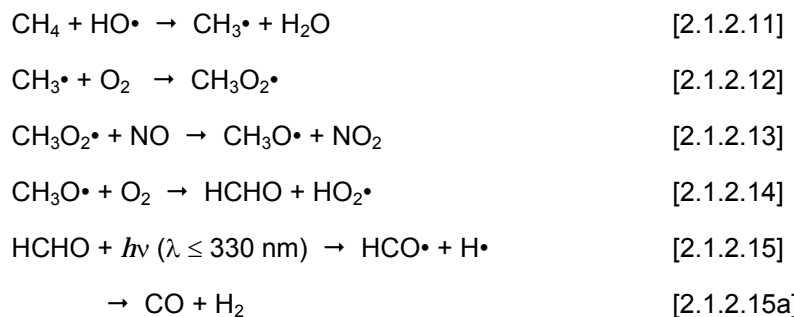
	Logan et al. (1981) Global	NH	Pacyna & Graedel (1995) Global
Sources			
Fossil fuel combustion and related activities	450	425	440 ± 150
Biomass burning	655	415	700 ± 200
Oxidation of human-made hydrocarbons	90	85	—
Oxidation of natural hydrocarbons	560	380	800 ± 400
Ocean emissions	40	13	50 ± 40
Emissions from vegetation	130	90	75 ± 25
Oxidation of methane	810	405	600 ± 20
Total source strength	2735	1813	2700 ± 1000
Sinks			
Reaction with OH radical	3170	1890	2000 ± 600
Consumption by soils	250	210	250 ± 100
Flux into the stratosphere	—	—	110 ± 30
Total sink strength	3420	2100	2400 ± 750

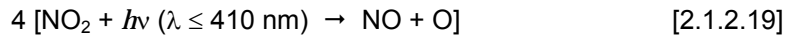
1) from Warneck (2000)

METHANE CH₄

In air samples the highest volume mixing ratios following CO₂ are found for CH₄. Sources of CH₄ are wetlands, rice paddies, landfills and ruminants [THOM et al. 1993, ETHERIDGE et al. 1998, KUHLMANN et al. 1998, SASS et al. 1999, WALTER et al. 2000, WALTER et al. 2001b]. Because of the formation by mostly biological activity a clear annual cycle for CH₄ can be observed.

Major sink for CH₄ is the oxidation by OH radicals via formaldehyde (HCHO) to CO and H₂ [ATKINSON 1994, TYLER et al. 1997].





The net reaction equation describes the formation of one molecule CO, four molecules ozone and two molecules hydroxyl radicals (and of water) per methane molecule, in an environment characterised by NO_x concentrations above a threshold of about 5 – 10 ppt [GRAEDEL & CRUTZEN 1993].

HYDROGEN H₂

For the formation of hydrogen in general similar processes as for CO are important: mainly the oxidation of CH₄ [2.1.2.15a] and of non methane hydrocarbons (NMHCs), as well as combustion [NOVELLI et al. 1999, BARNES et al. 2003].

The major sink for H₂ is the uptake by soils, with a minimum in winter and a maximum in early autumn. Another sink, but less important, is the reaction of H₂ with OH radicals, forming H₂O and H.

In the literature no information about the pre industrial concentration of H₂ could be found, but since the formation processes are comparable to the production paths of CO also an increase since the beginning of the industrial revolution might be expected.

NITROUS OXIDE N_2O

Major sources for N_2O are losses from soils during denitrification and nitrification processes [SCHMIDT et al. 1988, MEIXNER et al. 2000]. Since the nitrogen conversion is due to microbiological activity under both aerobic (nitrification) and anaerobic (denitrification) conditions, seasonal variations are occurring because of a strong temperature and humidity dependence. On account of the introduction of artificial fertilizers and their increased use the global mean mixing ratio of N_2O is rising as well [DOBBIE et al. 1999, RÖCKMANN et al. 2003]. There are no known sinks of N_2O in the troposphere, removal occurs only by transport to and photochemical destruction in the stratosphere.

Table 2.2: Tropospheric Budget of Nitrous Oxide (Tg per year)¹⁾

Bouwman et al, (1995)

Natural Sources	
Tropical forests	5.2
Temperate forests	0.8
Grasslands	2.3
Arable land	1.5
Total land surface	10.7 ± 0.3
Oceans	5.7 (4.4 - 8.9)
Total	16.4 (14.8 – 19.9)
Anthropogenic Sources	
Fossil fuel combustion	0.47 (0.16 – 0.94)
Adipic acid production	0.47 (0.30 – 0.61)
Nitric acid production	0.3 (0.12 – 0.47)
Nitrogen fertilizers	1.6 (0.64 – 2.6)
Domestic animal excreta	1.6
Biomass burning	0.36
Land use change	0.6
NH_3 conversion	0.63 (0.47 – 1.9)
Total	9.4 (4.3 - 8.9)
Total identified sources	25.8 (19.1 – 28.8)

Houghton et al. (1995)

Stratospheric sink	19.3 (14.1 – 25.1)
Atmospheric increase	6.1 (4.9 – 7.4)

1) from Warneck (2000)

SULPHUR HEXAFLUORIDE SF₆

Anthropogenic emissions are accounting nearly completely for the origin of SF₆. Major sources are releases through leakages of insulation glass and tire fillings, exhalations from aluminium production and high voltage plants. Less than 1% is of radiochemical origin, released from the geosphere [HAASE 1999]. SF₆ is chemically inert and no sinks are known for the troposphere, therefore it can be used within this study as the most probable tracer with regard to anthropogenic emissions and air mass changes [MAISS et al. 1994, MAISS et al. 1996].

Table 2.3: Characterisation of the Atmospheric Trace Gases¹

	Terrestrial Sources	Terrestrial Sinks	Mixing ratio ²		Average change rate ³ (yr ⁻¹)	Lifetime (yr ⁻¹)
			Actual	'1750'		
CO ₂	<ul style="list-style-type: none"> ▪ combustion ▪ respiration ▪ CO oxidation 	<ul style="list-style-type: none"> ▪ assimilation / organic material ▪ carbonates 	368 ppm	280 ppm	1,6 ppm	50-200
CO	<ul style="list-style-type: none"> ▪ combustion ▪ oxidation of CH₄ and VOCs ▪ soils 	<ul style="list-style-type: none"> ▪ oxidation → CO₂ ▪ uptake by soils 	95 ppb		-0,4 ppb	0,2
CH ₄	<ul style="list-style-type: none"> ▪ methanogenic bacteria (swamps and bogs, landfills, ricefields) ▪ ruminants ▪ biomass burning 	<ul style="list-style-type: none"> ▪ oxidation → CO and H₂ 	1784 ppb	700 ppb	8 ppb	7,9
N ₂ O	<ul style="list-style-type: none"> ▪ nitrification and denitrification in soils 	- only stratosphere -	314 ppb	270 ppb	1 ppb	122
H ₂	<ul style="list-style-type: none"> ▪ CH₄ oxidation ▪ combustion of fossil fuels 	<ul style="list-style-type: none"> ▪ uptake by soils 	531 ppb			1,9
SF ₆	<ul style="list-style-type: none"> ▪ nearly completely anthropogenic (insulation for glass filling, high voltage plants, aluminium production), ▪ natural radiochemical release from the geosphere ~ 1% 	<ul style="list-style-type: none"> ▪ chemically inert 	4,2 ppt	0 ppt	0,25 ppt	3200

¹ Data from WARNECK [2002], IPCC [HOUGHTON et al. 2001], HAASE [1999], WDCGG [2003],

USGreenhouseGasInventoryProgram [2002]

² Global average

³ for the observation period 1980 - 2000

2.1.1.2. Isotopic Signatures in Carbon Dioxide

Because of the active discrimination by vegetation characteristic signatures can be found in the surrounding atmosphere and the plant material itself [LLOYD et al. 1996, EHLERINGER et al. 1997, FLANAGAN & EHLERINGER 1998]. Thus, stable isotopes can be used to distinguish and estimate the contribution of different sources of spatially and temporally varying quantities like CO₂ [TRUMBORE 1999]. By the implementation of isotope analyses a differentiation between contributions by the vegetation and by the insertion of anthropogenic material might be achieved [CIAIS et al. 1995, ZONDERVAN & MEIJER 1996, BAKWIN et al. 1998, YAKIR et al. 2000].

Isotopes are nuclides of a chemical element, which have equal atomic numbers but differ by the number of neutrons, the nucleon number. In CO₂ several stable isotopomeres can be found, e.g. C¹²O¹⁶O¹⁶, C¹³O¹⁶O¹⁶, C¹³O¹⁸O¹⁶, C¹³O¹⁸O¹⁸, C¹²O¹⁶O¹⁸, C¹²O¹⁸O¹⁸. Here the CO₂ of the sampled air was analyzed for delta¹³C and delta¹⁸O [WERNER et al. 2001], whereby the focus is on the carbon isotopes. The data are expressed in the common delta nomenclature, expressing the relative deviation of the sample ¹³C/¹²C ratio from a reference isotopic ratio in per mill [%]:

$$\delta^{13}\text{C} [\%]_{\text{V-PDB}} = (R_{\text{sample}} / R_{\text{V-PDB}} - 1) \cdot 1000 \quad [2.1.1.2.1.]$$

Primary international standards are the V-PDB (Vienna PeeDeeBelemnite) for delta¹³C and the V-SMOW (Vienna Standard Mean Ocean Water) for delta¹⁸O.

CARBON ISOTOPES

When building up organic material plants consume CO₂ and release O₂. The gas exchange takes place through the stomata and can (mostly) actively be regulated by a more or less wide opening of these pores. Since the period of the highest photosynthetic activity around noon comes along with the decrease of relative humidity and thus an increase in drought stress different strategies of adaptation have been developed during evolution. Due to specific assimilation strategies three classes of plants can be distinguished: C₃, C₄ and CAM (with a crassulacean

acid metabolism). Most of the plant species, like bushes and trees, are belonging to the C₃ type, whereas in the group of the C₄ class grasses are most prominent. CAM plants are specifically adapted to semiarid / arid conditions.

Under normal conditions plants tend to assimilate the lighter CO₂ molecules easier than the ones containing the heavier ¹³C isotope. By this discrimination the ratio of the carbon isotopes, compared to the original air, changes. Plants contain more of the ¹²C isotope, whereas the concentration of the heavier ¹³C isotope increases in the ambient air [FARQUHAR 1989, LLOYD & FARQUHAR 1994, FLANAGAN ET AL. 1996, FLANAGAN & EHLERINGER 1998]. Because the discrimination against ¹³C is much higher for C₃ than for C₄ plants, delta¹³C values in biomass are -20 to -35 ‰ and -9 to -14 ‰ for C₃ and C₄, respectively [EHLERINGER & RUNDEL 1989]. But also ambient air will show a plant related isotope ratio. A less negative delta¹³C value indicates the assimilation rate of the plants [TROLIER et al. 1996, TRUDINGER et al. 1999]. On the other hand respiration from plants is depleted in ¹³C relative to the atmospheric CO₂, which leads to a dilution resulting in a more negative delta¹³C value [LEVIN et al. 1995, FUNG et al. 1997, KAPLAN et al. 2002].

Baseline air has a delta¹³C value about -8 ‰ and possesses a seasonal cycle with a peak to peak amplitude of 0.05 ‰ at the South Pole and 0.8 ‰ at high northern latitudes.

Fossil organic material reflects the isotopic signature of the original plant substance, mostly C₃ vegetation. Depending on the kind of fuel and the formation process further differentiations can be made [TANS 1989]. Natural gas contains a high amount of CH₄ which can be highly depleted in ¹³C [HOEFS 1996]. CO₂ from oxidation processes reflects the isotopic ratios from the source substances [BOSINGER et al. 1988, BERGAMASCHI et al. 1998]. Under diagenic conditions, characterised by high pressure and temperature, additional alterations may occur, for example during the formation of coal and lignite.

Isotopic ratios of atmospheric air vary on different time scales. Beside the diurnal cycle there is also a seasonal variation, due to changes of the assimilation activity [BUCHMANN et al. 1996, FLANAGAN et al. 1999]. The activity of the soil organisms, which are recycling plant material, is affected by temperature and humidity [CIAIS et al. 1999]. Likewise the contribution of anthropogenic emissions, especially from fossil fuel consumption, reflects seasonality.

The actual annual decline rate is around 0.025 ‰ (see figure 2.2. and [<http://www.cmdl.noaa.gov/ccgg/figures/co2c13rug.jpg>]).

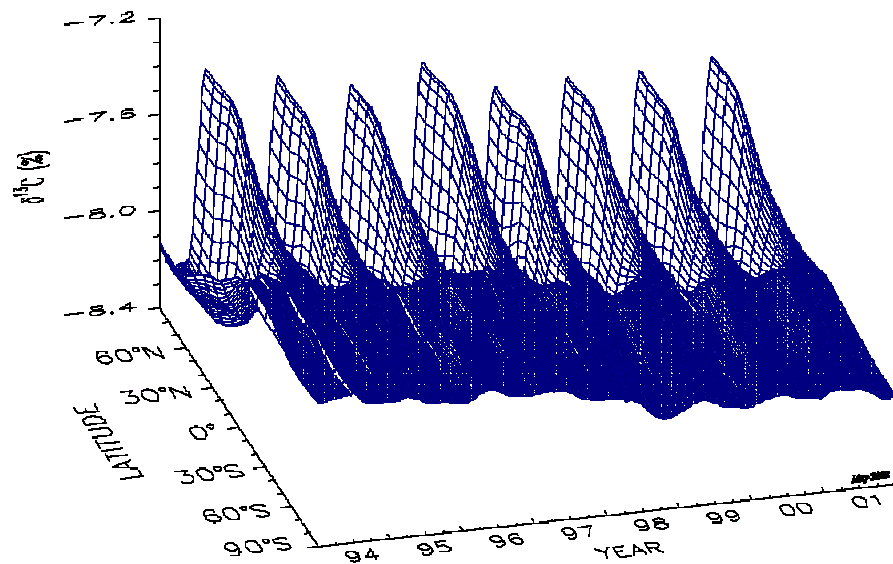


Figure 2.2. Latitudinal distribution of the carbon isotopic composition of atmospheric carbon dioxide concentration in the marine boundary layer air. The surface represents data smoothed in time and latitude from the NOAA / CMDL cooperative air sampling network analyzed at the University of Colorado INSTAAR (PI: J. White, NOAA / CMDL)

For ^{13}C a direct relationship is given with the CO_2 gas mixing ratio: A reduction of the CO_2 mixing ratio with a simultaneous enrichment in ^{13}C indicates an uptake by vegetation, whereas an increase of the CO_2 mixing ratio and a depletion of ^{13}C can be attributed to the consumption of organic material.

The ‘Keeling plot approach’ is commonly used for the determination of the carbon isotope composition of the source. It is assumed that a measured air sample mixing ratio C_m is the sum of an atmospheric background C_b and a contribution from an individual source or sink C_s .

$$C_m = C_b + C_s \quad [2.1.1.2.2.]$$

and for the isotopic ratio respectively

$$\delta_m C_m = \delta_b C_b + \delta_s C_s \quad [2.1.1.2.3.]$$

The background should be represented by the tropospheric delta¹³C ratio (at least by the global average; -8‰), the ground source/sink is characterised by its specific carbon isotope discrimination behaviour. This discrimination can be calculated from the intercept of the linear regression between the carbon isotope ratios and the inverse of the CO₂ mixing ratio [KEELING 1958, PATAKI et al. 2003], described by the equation

$$\delta_m = \delta_s + \frac{1}{C_m} \cdot M \quad \text{with} \quad [M = C_b(\delta_b - \delta_s)] \quad [2.1.1.2.4.]$$

where δ_m is the isotopic value and C_m the measured CO₂ mixing ratio. The subscript b denotes the background value, s respectively the source signal.

OXYGEN ISOTOPES

Also the delta¹⁸O in CO₂ was determined. Even if the focus of this study was not on the oxygen isotopic ratios a brief introduction shall be given for the sake of completeness.

Changes of delta¹⁸O in atmospheric CO₂ are induced by plants, similar to the carbon isotopes. Thereby three different sources have to be distinguished: oxygen from soil water taken up by the plants, oxygen that exchanges with the CO₂ of the ambient air, and CO₂ from the photorespiration.

In the water cycle a discrimination of the heavier water molecules exists during evaporation, which leads in a first step to an ¹⁸O-depletion in the water vapour. During the formation of precipitation more ¹⁸O condenses, hence the remaining water vapour becomes lighter, whereas the delta¹⁸O of the cloud water increases during ageing [CIAIS et al. 1997]. When the plants are taking up the soil water no discrimination occurs, but through reduced evaporation of the H₂¹⁸O compared to H₂¹⁶O a relative accumulation of ¹⁸O takes place in the leaf water.

Atmospheric CO₂ enters the plants through the stomata. Hereby the uptake is restricted on one hand by a diffusive kinetic isotope effect, on the other hand only a few of the oxygen atoms are fixed via photosynthesis [FLANAGAN et al. 1997]. The majority are leaving the plants again, but some of them have exchanged in an

equilibrium reaction with atoms of the relative enriched leaf water. Both effects are leading to a relative increase of delta¹⁸O in the ambient atmospheric CO₂. Contrary to this, CO₂ from respiration is more characterised by the signal of the soil or precipitation water, which results in lower delta¹⁸O values [FARQUHAR et al. 1993]. Isotope discrimination in plant metabolism occurs during biosynthesis of carbohydrates and other primary or secondary products; e.g. STERNBERG [1989] describes for cellulose oxygen isotope ratios to be 27‰ (±3‰) higher relative to leaf water. Caused by further kinetic and equilibrium isotopic effects the delta¹⁸O ratio decreases for secondary products; total plant dry matter has a delta¹⁸O value of about 18‰ [YAKIR 1998]. C₃ and C₄ plants differ in delta¹⁸O in the organic material. Since C₃ plants are, compared to C₄ species, more sensitive to water stress assimilation via photosynthesis is only active when no vapour pressure deficit occurs, leading to a relative low ¹⁸O fraction in the leaf water [STERNBERG 1989].

Because of the isotope fractionation processes during evaporation and condensation delta¹⁸O varies also on spatial scales [PEYLIN et al. 1999]. Due to the increasing depletion in ¹⁸O inland areas reflecting continentality. Also specific environmental conditions, like the low evaporation rate in higher latitudes, are provoking characteristic isotopic signals. By the enhanced oxygen isotope ratios in organic material relative to water at the site of synthesis (as described by STERNBERG to be about 27‰) environmental conditions during the assimilation period can be obtained also from the plant material, as practised for example by palaeo-climatic studies via the analysis of tree rings [BURK & STUIVER 1981].

An example for zonal differentiations can be obtained when focus on higher latitudes.

In addition to the plant activity, also soil respired ¹⁸O is contributing to the delta¹⁸O ratio of the atmospheric CO₂. Therefore estimates of this rate have to be taken into account when calculating the fraction of plant activity [MILLER et al. 1999].

Reasons for neglecting delta¹⁸O for the estimates within this study were: Oxygen isotopes are very sensitive with respect to alterations, in particular for interactions with water and surface processes during the sampling and the transport / storage of the flasks [GEMERY et al. 1996]. One crucial uncertainty, but still not verified,

might be provoked by the drying unit. However, the main reason for dropping a detailed investigation of delta¹⁸O was caused by the fact that the real vegetation signal was unduly affected and masked by interferences (as described in the more detailed presentation of the findings).

2.1.2. RECAB Strategy

The main objective of RECAB (Regional Assessment and Monitoring of the Carbon Balance within Europe) was the development of methodologies and techniques to qualify and quantify the carbon budget on regional scales [HUTJES ed. 2003]. This goal should be achieved by the linkage of experimental investigations and modelling studies, combining bottom-up with top-down approaches. The bottom-up attempt should be pursued by local tower measurements and profile flights. Information for the top-down part should come from model calculations and also from profile flights, which therefore connect both concepts.

Part of the MPI-BGC was to collect data by vertical profile flights within the lower part of the atmosphere for estimations of the carbon fluxes, the determination of source and sink processes and the provision of data for the modelling groups.

A primary aim of RECAB was to acquire data from characteristic regions within Europe, whereby a region was defined as an area of typical appearance and a spatial extension of roughly 10^4 km^2 ($100 \times 100 \text{ km}$). An intention was also to carry out the campaigns in zones with different climatic and vegetation conditions, at least once during summer and winter time. Additionally the investigations should be performed at places where information would be available also from local measurements.

Both, the study regions and the time frame, where and when the data acquisitions should take place, had been specified by the principal investigators of RECAB at the beginning of the project. Because of tower measurements operational within the regions, five field sites were defined: *Uppland* in Sweden, the central part of The Netherlands – both regions including one tall tower site (Norunda in Sweden, Cabauw in the Netherlands). At the study areas *Thuringia* in Germany, *Valencia* in Spain and *Lazio* in Italy several small towers are operational.

Beside the rough classification into three zonal districts (Northern, Central and Southern Europe) a further longitudinal differentiation was an intention of the project, regarding the sites in Central Europe between the region in The

Netherlands and the more continental site in Germany. In Thuringia additional flights were performed between fall 2000 and spring 2001.



Figure 2.3. RECAB study regions

The square sizes are scaled to the defined extension of the 'region' ($\leq 10^4 \text{ km}^2$).

(Picture from DFD: <http://www.caf.dlr.de/caf/satellitendaten/bildergalerie/>)

The importance of RECAB for this study is given by two aspects: Data were acquired during the field campaigns, which also provided (in a constricted frame) the opportunity for specific experiments. On the other hand, the field studies had to serve primarily the aims and the time schedule of RECAB, which meant rather a constraint.

Focus of this study are the analyses of flask samples with respect to information on composition and trace gas mixing ratios (CO_2 , CH_4 , N_2O , additionally CO , H_2 and SF_6 since August 2001) as well as on stable isotopes in CO_2 . Through the multiple tracer studies specific carbon sources and sinks should be identifiable. This primary contribution to the project was enhanced by additional investigations, helping the RECAB strategy to link bottom-up and top-down approaches: Development of a ground reference and sampling unit, adaptation of the flight strategy and modelling studies for specific flights.

Field Campaigns

During two to four weeks several intensive combined flight- and ground based investigations were performed on selected days. The local partners led the coordination of the different combined investigations.

Measurements were performed continuously at meteorological and flux towers, whereas the low level horizontal flux transects, using the *mobile flux plane* 'Sky Arrow' (abbreviated 'MFP'), and the vertical CBL-profile flights were carried out as frequently as possible, weather permitting.

The activities included:

- CBL vertical profile flights with flask sampling and continuous measurements (part of the MPI-BGC; for observed parameter and system configuration see chapter 2.2.1); additional ground reference sampling and measurements (using the new implemented mobile mast; see chapters 2.2.1.3. & 5.2.1.)
- Horizontal transect flights with high frequency measurements (CO_2 mixing ratio and water vapour by an open-path infrared gas analyzer, as well as air temperature, pressure, radiation, 3D-wind field) by the MFP [for detailed description of instrumentation see GIOLI et al. 2004]
- Continuous eddy-covariance measurements and recording of meteorological parameter from local towers
- Tethered balloon (Valencia) and SODAR profiles (The Netherlands) for wind profile observation and the determination of the CBL top height
- Data processing and submission to the 'Carbis' data base
- Forward and inverse modelling of the individual campaigns

Flight activity was limited by the fixed budget for the operational costs, maintenance intervals of the MFP and the number of the sampling flasks.

Because the MPI-BGC does not possess its own aircraft a plane had to be hired at each site. Therefore the equipment had to be adapted to the individual configurations at each air field (see also the documentation of the 'Flask Sampling Unit' on the CD-ROM).

Table 2.4. Nomenclature of the study regions and basic data describing the measurement campaigns

Region	Coordinates ¹	Land Type	Period ²
Valencia (Spain)	39°15'N 00°30'W	southern coastal zone; very intensive agriculture, Valencia urban area	17.06.-07.07.2001 16.11.-15.12.2001
Uppland (Sweden)	60°10'N 17°50'E	Nordic coniferous forest and wetlands; extensive agriculture, rural structure	11.08.-09.09.2001
The Netherlands	52°10'N 05°40'E	very intensive agriculture, high level of urban sprawl	14.01.-10.02.2002 10.07.-28.07.2002
Lazio (Italy)	42°25'N 11°55'E	southern plains; forests and agriculture, urban character	27.05.-27.06.2002
Thuringia (Germany)	51°05'N 10°30'E	very intensive agriculture within the basin, ridges covered by forests, scattered villages and cities	20.10.-23.10.2000 13.01.-17.01.2001 10.02.-16.02.2001 09.05.-11.05.2001 15.07.-02.08.2001 06.08.-16.08.2002

Also the sampling sites and the flight patterns had to be specified. In addition characteristic field sites had to be selected and the ground reference unit had to be installed. Ground level flask sampling was mostly carried out, due to the lack of man power, before or after the flights, whereas the meteorological measurements are available for mostly the whole period.

FLIGHT OPERATION

Measurement flights were executed at least twice per day. The first or morning flight was scheduled to take place around one hour after sunrise, in order to sample an average of the regional respiration signal. To record a clear signal of the plant activity the second flight was scheduled around the maximum assimilation rate. Flask sampling was carried out at four to five pre-defined levels within the boundary layer and at one height clearly above the inversion. Thereby

¹ Central / main point of the study region

² Summer campaigns (bold)

the vertical profile had to reach a maximum height of about 3000 m above ground, depending on the thermal conditions. Oriented at ground reference points the flight pattern enclosed a quadratic air column with a typical leg length of 2 km, realized by GPS guidance.

For system comparisons, and to obtain further information, also intermittent flights with the 'Sky Arrow' were performed.

Because airborne measurements are highly depending on weather conditions the decision whether to fly or not had to be made spontaneously in the early morning of the scheduled flight days. In addition, the flights were affected by fixed operational hours of the airfields, restrictions caused by local flight regulations, the availability of pilots and aircraft capability.

GROUND REFERENCES

Reference samples were taken over characteristic land units within the study region. On one hand the prevalent conditions should be recorded and samples be taken simultaneously with the airborne measurements. On the other hand we aimed to collect data from the individual sites for different microclimatic situations. Therefore the sensor mast was erected at the characteristic field sites for defined periods and shifted between them. Flask sampling was performed at five heights (0.1, 0.5, and 1.0, 2.0 and 5.0 m above ground) at least once for each site, twice a day. 'Night time measurements' had to be accomplished around sunrise, to gain a clear respiratory signal. The day time sampling, reflecting assimilation, was executed in the early afternoon.

Additional mapping of the environment was performed with specific focus on the vegetation (kind, composition, distribution and status of development), the geomorphic appearance (soils, topography, exposition) and with respect to anthropogenic influences like buildings, obstacles, and intensive utilisation – in particular fertilization, animal stocks, harvest and tillage.

Table 2.5. Nomenclature and land use character of the study sites

Region	Ground Reference Sites	Land Use Character	Flight Profile Location
Thuringia (Germany)	Hainich	beech forest	Hainich
		agricultural utilisation	Gebesee
Valencia (Spain)	Rice	rice fields	Rice
	Orchard	citrus and apricot plantations	Orchard
	Macchia	quasi natural shrubland	Macchia
		Mediterranean Sea	Mare
	Highway	main road	
Uppland (Sweden)		coniferous forest	Norunda
	Florarna Swamp	open wetland	Florarna
	Forest	mixed forest	
The Netherlands	Loobos	coniferous forest	
	Maize	agricultural utilisation	Maize
	Marshland	grassland	Cabauw
		mixed forest	Forest
Lazio (Italy)	Roccarespampani	deciduous forest	
		deciduous forest surrounded by agricultural land	Tuscania
	Orvinio Meadow Valley	grassland forested mountain slope	Orvinio

Coloured are the sites where only ground or flight investigations were performed. For a more detailed description of each study location see the individual campaign folders on the CD-ROM.

All campaigns were documented in a uniform scheme. Data gained from the continuous systems were logged and frequently saved on hard disks. The flight- and ground operations were recorded in specific forms. Sketches and photographs, in particular aerial views, were prepared to record the environmental conditions during the investigations. Plant material was sampled and dried. A detailed depiction of all activities was kept in a campaign diary.

2.1.3. Convective Boundary Layer

During the last years several theoretical studies have proposed the idea to use the atmospheric boundary layer for the description of larger areas [KLAASSEN 1992, RAUPACH et al. 1993, RAUPACH 1995, RAUPACH & FINNIGAN 1996, RAUPACH 1998, DENMEAD et al. 1996, CLEUGH 1998].

Based on this approach several scientific groups started to investigate parameters, such as energy fluxes or fluxes of climatic relevant trace gases, by aircraft measurements on larger scales [CRAWFORD et al. 1996, LANGENFELDS et al. 1996, DESJARDINS et al. 1997, NAKAZAWA et al. 1997, LLOYD et al. 2001, LEVIN et al. 2002, LLOYD et al. 2002, RAMONET et al. 2002]. These investigations were performed over wide-stretched areas of homogeneous character, such as in Siberia or the Amazonian Basin. Part of this study will be therefore to focus also on answering the question if and to what extent a transfer of the approach will be possible to areas with differing conditions, in particular with a mosaic of different surface characteristics.

The boundary layer can be defined '*as that part of the troposphere that is directly influenced by the presence of the earth's surface, and responds to surface forcings with a timescale of about an hour or less*' [STULL 1988, p.2].

Characteristic for the convective boundary layer is its strong diurnal development, with different behaviours depending on the surface conditions [SHUTTLEWORTH 1988, DE WEKKER 1995]. The typical height of the boundary layer top varies between 100 and 3000 m, forced in particular by solar irradiance. Thereby the shallow night time 'stable boundary layer' (NBL), growing during day time because of thermal convection, converts into the 'convective boundary layer' (CBL). During this expansion the air that had been trapped during the night, characterised by high mixing ratios of CO₂ from plant respiration for example, is modified by entrainment of air from the 'residual layer' located above the NBL. Further contribution occurs by vertical motion on synoptic scales, like subsidence in high pressure systems, and by horizontal advection [LEHNING 1996, SAMUELSSON & TJERNSTROM 1999].

Based on this concept a budget approach was developed using the CBL as an ‘integration chamber’ for monitoring larger areas. It can be characterised in a simplified manner: if mass conservation can be assumed and the fluxes through the walls and the top of the air column are known, it should be possible to calculate surface-atmosphere exchange rates from the variation of the amount of scalars inside the air column.

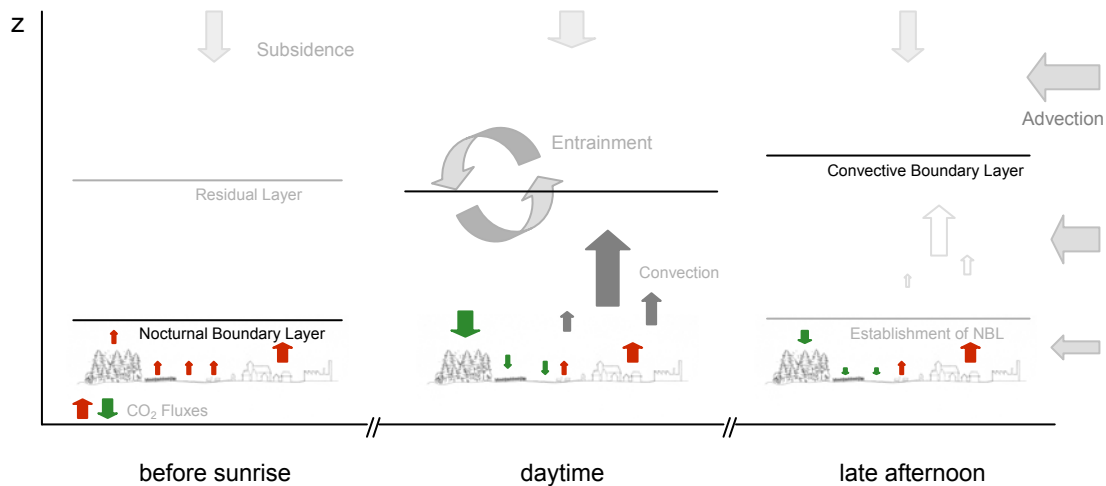


Figure 2.4. Scheme of the CO₂ fluxes and of the CBL behaviour on a summer day, showing CBL development from a nocturnal / stable boundary layer until the establishment of the next night time boundary layer.

‘CBL-BUDGET APPROACH’

The CBL-budget concept was already practised from small aircrafts for studies carried out by the MPI-BGC over Siberia and the Amazon Basin [LLOYD et al. 2001]. It was the objective within RECAB to utilise the budget approach for the determination of CO₂ fluxes in a similar way.

However, here the role of the ‘CBL-budget approach’ is not well defined by its application. Since serious questions about fundamental assumptions arose from the flask sampling observations, general conceptual aspects became the most import topic.

A detailed specification of the ‘CBL budget approach’ theory is given by LAUBACH & FRITSCH [2002]. The aim of the concept is the explanation of the surface fluxes

(F_s^G) by the measured change in the CBL content from two profiles ($dN/dt = F_s^C$) and estimates of the fluxes from the top and the sides of the CBL: Entrainment (F_s^E), Subsidence (F_s^S) and horizontal advection (F_s^H).

$$F_s^G = F_s^C - F_s^E - F_s^S - F_s^H \quad [2.1.3.1.]$$

The time integral can be expressed respectively

$$I_s^G = I_s^C - I_s^E - I_s^S - I_s^H \quad [2.1.3.2.]$$

Basic for the calculation is the scalar conservation equation, which is integrated from the ground to the top of the CBL column, leading finally to [2.1.3.3.]

$$I_s^G = \alpha_s \left\{ \left[\langle \rho \rangle_i z_i \langle s \rangle_i \right]_{t_1}^{t_2} - \int_{t_1}^{t_2} \langle s \rangle_i \frac{\partial}{\partial t} (\langle \rho \rangle_i z_i) dt - \int_{t_1}^{t_2} \rho_+ (s_+ - \langle s \rangle_i) \frac{\partial z_i}{\partial t} dt + \int_{t_1}^{t_2} \rho_+ (s_+ - \langle s \rangle_i) w_+ dt \right\}$$

----- I_s^C ----- ----- I_s^E ----- ----- I_s^S -----

Horizontal advection is neglected

For the application several assumptions have to be made, inter alia 1) constant vertical gradients of the scalars and the vertical wind component in z and t, 2) linearity of the CBL growth and 3) linearity regarding the trend of the scalar changes in t.

Table 2.6. Nomenclature used in the equations

Roman letters	Greek symbols	Operators	Subscripts
M mass per surface area of the air column	Δs drawdown difference of s at $z = z_{top}$	$\langle \dots \rangle_h$ vertical average from $z = 0$ to $z = z_{top}$	$+$ just above $z = z_i$
s mixing ratio	α_s conversion factor		top at $z = z_{top}$
t time	ρ air density		$1, 2$ time, respect. flight count
w vertical wind component			
z_i CBL height			

LAUBACH & FRITSCH presented additionally a second, so called ‘fixed-mass column’ approach. Since mass conservation is required changes of the scalars within the entire column are including already the entrainment flux ($I_s^C - I_s^E$).

Regarding the subsidence term a linear time dependency has to be assumed for the drawdown gradient.

Similar to the CBL column approach horizontal advection is neglected. From these the cumulative surface flux is expressed as:

$$I_s^G = \alpha_s \left\{ M_{top} \left(\langle s \rangle_{top_2} - \langle s \rangle_{top_1} \right) + \frac{1}{2} w_{top} \rho_{top} (\Delta s_2 + \Delta s_1) (t_2 - t_1) \right\} \quad [2.1.3.4]$$

----- $I_s^C - I_s^E$ ----- ----- I_s^S -----

In principle the strategy can be divided into three parts: a) the estimation of the boundary layer top height for each profile, by analysis of the potential temperature Θ and the humidity f gradients, b) the calculation of the amounts contributed by the fluxes through the walls and the top of the column within the time step and c) the determination of the scalar fluxes from the residual of the mixing ratio change.

The utilisation of the ‘CBL-budget approach’ for the determination of CO₂ fluxes could not be achieved in this study, since general questions regarding the concept arose from the flask sampling observations.

Another attempt to estimate surface fluxes focuses on a ‘Lagrangian’ concept. By a field experiment carried out in June 2001 above a forest in south-western France, loosely associated to the RECAB project, the potential was evaluated [SCHMITGEN et al. 2004]. A brief discussion of this experimental approach will be given when introducing finally the enhanced investigation strategy, derived from the multiple tracer and isotope analyses, in chapter 5.4.

2.1.4. Ground Characterisation and References

Most of the processes affect the CO₂ concentration in air samples, as the majority of the sources and sinks are related to or located at the ground. Also atmospheric dynamics are coupled to the surface, like turbulence driven by thermal inhomogeneity, the formation of eddies and the horizontal air flow influenced by the topography [LEHNING 1996, SCHMID & LLOYD 1999]. Therefore the incorporation of ground reference information is a fundamental requirement.

To get the basic information about the composition of the trace gases and of their individual mixing ratios and isotope signature, investigations were performed directly at ground level. Since the variations are affected by the individual source and sink characteristics, whose variability is mostly driven by climatic parameters, records of the climatic conditions have to be performed for the most prominent landscapes of the study regions. Around this ‘ground reference sites’ also detailed investigations were carried out with regard to the kind of vegetation, its extension and distribution.

High productivity of plants is linked in particular to temperature, humidity and radiation and the complex interplay of these factors. Because of the missing solar irradiance during night time the photosynthetic activity stops and the vegetation respires CO₂. A reduction of the uptake (or even a change from a CO₂ sink into a source) can also occur during day time under favorable radiation conditions, provoked for example by drought stress. The incidence of air pollutants, like ozone, or the infestation by herbivores can likewise provoke rapid perturbations.

Heterotrophic organisms, which are respiring organic material in the soils, also require specific optimal conditions. In frozen, as well as in dry soil the activity is reduced to a minimum. Variability occurs also in subjection due to the supply of organic material or decomposition products. Furthermore some of the organisms need aerobic, others, like the methanogenic bacteria, anaerobic conditions. The pathways of the disintegration can change with the time, for example depending on the oscillation of the water table, which has to be taken into account especially for wetland regions.

In particular temperature and irradiance are of interest with respect to the situation and the development of the boundary layer. Also information about wind velocity and direction are mandatory for an estimation of transport and mixing processes.

2.1.5. Combined Investigations

2.1.5.1. Modelling Approaches – Inverse Studies

Intention for the implementation of a transport model within this study was to obtain further information for quality estimations, in particular with regard to contaminations, and to determine the origin of the sampled air. In cooperation with

CHRISTIAN RÖDENBECK from the modelling group of the MPI-BGC, analyses were performed for several flights of the SPA¹³CE experiment (see chapter 4.2.8.). The sensitivities were calculated using the global 3D atmospheric tracer transport model TM3 with the vfg grid (192 x 96 L28) configuration [HEIMANN & KÖRNER 2003, RÖDENBECK 2003], driven by observed meteorology [NCEP reanalysis, www.ncep.noaa.gov]. By the implementation of diverse specific inventories (EDGAR data base for fossil fuel) and model results (BiomBGC for biosphere influence) individual spatial contribution probabilities were calculated. Estimates of the ‘regional footprint’ were performed by the comparison with the interpretation results of the gas and isotope analysis. In addition the model could be tested using real data with respect to some specific sensitivities.

Further calculations were carried out in cooperation with GORKA PÉREZ-LANDA, from the RECAB partner CEAM in Valencia, for individual study sites in Spain and Italy. Our intention was to identify the spatial origin and to derive by comparisons and interpretation of the sampled data the probable formation process.

The simulation was performed with the non-hydrostatic PSU/NCAR Mesoscale Model MM5, combined with the Lagrangian Particle Dispersion (LPD) model FLEXPART. Data assimilation was applied with NCEP reanalyses. To enhance the resolution within the surroundings of the study areas nested-grid configurations were used with 130 x 130 and 202 x 301 grid cells at 27 and 9 km grid size, respectively, centred over the Western Mediterranean Basin [PÉREZ-LANDA et al. 2002].

To obtain quick information with respect to tendencies of the origin and the pathway of the sampled air masses additional back trajectory calculations were performed. One motivation therefore was to improve the interpretation of the free troposphere samples from the Italian mountain site with their specific gas composition (see chapter 4.2.3).

The calculations were performed using the back trajectory particle model ‘HYSPLIT’ (HYbrid Single-Particle Lagrangian Integrated Trajectory, Version 4) developed by NOAA and Australia’s Bureau of Meteorology [DRAXLER & HESS 2002]. A fixed number of particles are tracked backwards from the receiving point, which are assumed to be advected by the mean wind field, but

taking also a turbulent component into account. The calculations were driven by the observed meteorology from the NCEP reanalyses, running in one hourly time-steps for a period of 14 days. Horizontal resolution of the model is adapted to the grid system of the meteorological data. The internal model heights above ground level can be determined at any interval; the top height was defined to be 9000 m.

An introduction to back trajectory calculations was given by MANUEL GLOOR (MPI-BGC), who also made the model available for these studies.

2.1.5.2. Land Use Classification

Europe is characterised by a nearly complete anthropogenic landscape. Thus a patchy surface is formed by the heterogeneous distribution of urban agglomerations, agriculturally used areas, managed forests, water spaces and a few unmanaged smaller parts. Even at the scale of the individual study region a homogenous distribution of the sources and sinks can not be expected. In consequence, an inventory of the different land use classes, within the region and extended to the areas affecting the study space, is required to provide the basic information with respect to the interpretation of the air samples.

A land use classification, using remote sensing data from the Landsat ETM+ sensor (path 194 / row 24), was performed within the frame of a diploma thesis study [REITHMEIER 2003]. The area covered by a scene encloses a square with a leg length of roughly 185 km, at a spatial resolution of 30 x 30 m. Since the classification was not finished in time only a first draft could be used for this study. Nevertheless, by the implementation of the remote sensing based land use classifications additional information about the spatial distribution of the individual sources and sinks became available. Primary intention was to obtain a tool for the verification of the findings from the 'regional' measurements. Therefore data should be derived from the spatial percentages of the classified areas (as presented in table 2.8.), related to their characteristic gas composition and isotopic signatures. The focus should be on the differentiation of forested lands, agricultural areas and urban settlements, deduced from satellite images for the campaign periods at the Hainich site in 2001 and 2002.

For the analyses the images, already radiometrically and systematically precorrected (*Level 1G* data from NASA's Earth Observing System [<http://edcimswww.cr.usgs.gov>]), have been further processed with respect to geometric and atmospheric corrections. Additionally cloud-covered pixels were identified and excluded for the subsequent land use classification. For the identification of training areas additional spectral transformations were performed prior to the classifications with the standard maximum likelihood classifier of the image processing software *ENVI® Version 3.5* (see figure 2.5.).

The high spatial resolution of ETM+ images enables to distinguish most of the surface characteristics, e.g. agricultural or urban use. By the comparison of the back scattering spectra for several pictures vegetation type can be derived. An advantage over topographic maps or land use databases like 'Corine' is the actuality.

A differentiation between the most common crops could be obtained by comparing two scenes from April and July (for the characteristics see table 2.7.).

Table 2.7. Individual crops and their differential characteristics

	Vegetation Type	Characteristic behaviour	
		Spring	Summer
Summer crops	summer wheat, barley	bare soil	development peak
Summer crops 2	sugar beets	shallow growing height bare soil visible throughout the growing period	development peak
Winter crops	winter wheat, rye	development peak	harvested
Winter crops 2	potatoes	shallow growing height bare soil visible throughout the growing period	harvested

When it became obvious that the 'regional character' of trace gas composition is affected seriously by horizontal transport processes an utilisation of satellite remote sensing data became even more interesting. Since the 'regional footprint' is more extended than assumed so far, land use classifications could provide the information for better interpretation and also for model applications. It was hoped to incorporate the land use information for analyses of the grid boxes along the footprint and, if practicable, also for the description of a nested model area in the surroundings of the location of an air sample.

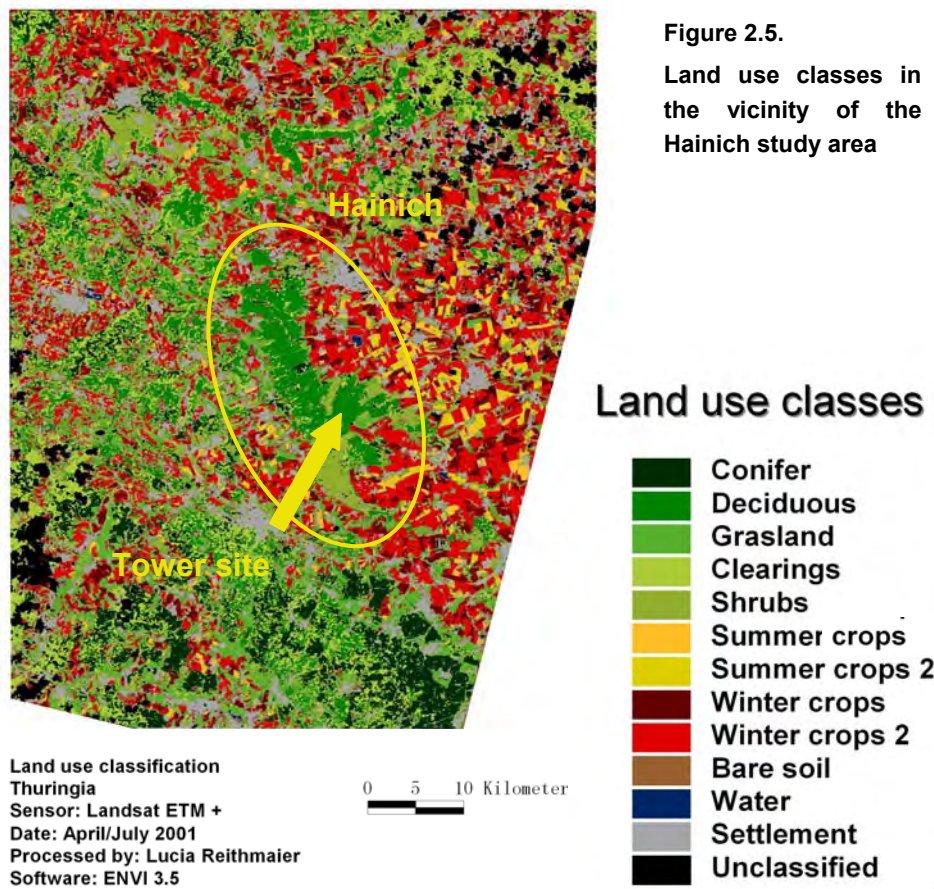


Figure 2.5.

Land use classes in the vicinity of the Hainich study area

Therefore the land use classes should be combined with their gas and isotopic signatures in a geographical information system (GIS).

Table 2.8. Summary of the land use percentages within the study area in Thuringia

Landuse class	Pixels	Percent
Coniferous forest	332837	6.60 %
Deciduous forest	361068	7.16 %
Clearings	519838	10.30 %
Shrubs	555264	11.01 %
Grasland	440448	8.73 %
Summer crops	91493	1.81 %
Summer crops 2	60718	1.20 %
Winter crops	274158	5.43 %
Winter crops 2	879199	17.43 %
Bare soil	212993	4.22 %
Urban areas	665995	13.20 %
Lakes	7605	0.15 %
unclassified	642934	12.75 %
	5044550	99.99 %

2.2. System Configurations and Data Analysis

2.2.1. Campaign Equipment

2.2.1.1. Flight Sampling Unit

From the analysis of flight data and laboratory experiments it had become obvious that the flask sampling system, used so far by the MPI-BGC, did not comply with the requirements of the intended project goals. The necessary modifications had to be tested further in the laboratory and during field investigations. The most important technological changes permit: a) to flush and sample the flasks under constant pressure, b) to allow a permanent air flow through the tubing and the system up to the flasks in order to avoid contamination by residual air, and c) to regulate the flow rate individually for the flushing and sampling procedure, according to the environmental conditions, like aircraft velocity and surface structure (see table 3.6). A detailed comparison of the old and the new unit can be found in Appendix A2 and on the CD-ROM.

The installations were also determined by the configuration of the individual aircraft. To avoid contamination caused by the aircraft itself (e.g. exhausts, fuel and oil steams) the sampling inlet had to be fixed strictly at the outermost tip of the wing, in spite of the negative effects for aircraft behaviour.

CONFIGURATION OF THE SAMPLING SYSTEM AND SAMPLING EXECUTION

The sampling unit can be divided into three major components: a) the inlet, with its tubes and the pump, b) the drying device, particle filter, mass flow controller and switch to c) the flask compartment. Bor silicate glass flasks with 1000 ml volume were used, flushed and prefilled with air of known gas composition and mixing ratios at 2 bar pressure (absolute).

From the inlet at the wing tip the air was sucked in by a double-head membrane pump. Passing a coalescence filter, to trap a large part of water vapour, the gas flowed at different throughput during flushing and sampling to the vertically orientated drying column, filled with magnesium perchlorate $[Mg(ClO_4)_2]$. After the particle filter the air enters the flask section, or leaves the system into the cabin, when no sampling is carried out. For sampling the air flushes the flasks, which are arranged in a line, first for 2 minutes with a flow rate of $\sim 10 \text{ l min}^{-1}$ and further

2 minutes with $\sim 3 \text{ l min}^{-1}$, before the sample is taken after another 2 minutes at the reduced flow rate of $\sim 3 \text{ l min}^{-1}$. To secure a constant pressure of 2 bar inside the drying section and the flasks an electronic mass flow controller was installed in front of the drying column and a pressure conditioner was located at the outlet.

2.2.1.2. Continuous Flight Measurements

It was our intention to obtain information about the CBL structure in general and in particular the local environmental conditions when taking the air samples.

Therefore meteorological parameters, dynamic pressure, geographical latitude and longitude of the aircraft and the CO₂ mixing ratio were continuously recorded with a frequency of 1Hz [LAUBACH & FRITSCH 2002].

Meteorological parameters measured were air temperature, humidity [Vaisala HMP 233] and air pressure [Vaisala PTB 101B]. The temperature and humidity sensors, capsulated into a radiation shield, were mounted on the front section of the wing, outside the area affected by the slip stream. Close to it the wind / pressure inlet was installed, roughly 50 cm in front of the wing nose. The GPS receiver [d-black Box, DGPS] was fixed on the cabin ceiling and the gas inlet for the continuous CO₂ measurements was placed close to the sampling unit.

For the continuous measurement of the CO₂ mixing a Licor 6251 gas analyser was used. Since the system is very sensitivity to pressure and temperature variations, regular in flight calibrations were carried out at each flight level where flask samples were taken (see for example figure 2.6). Therefore two standard gases of known mixing ratio, one with a ratio at the lower and upper end of the expected atmospheric value, were measured at existing pressure instead of the ambient air for one minute each. From the comparison of the measured ambient air and the 'calibration gas' with known mixing ratios the pressure dependency of the Licor instrument can be estimated and corrected.

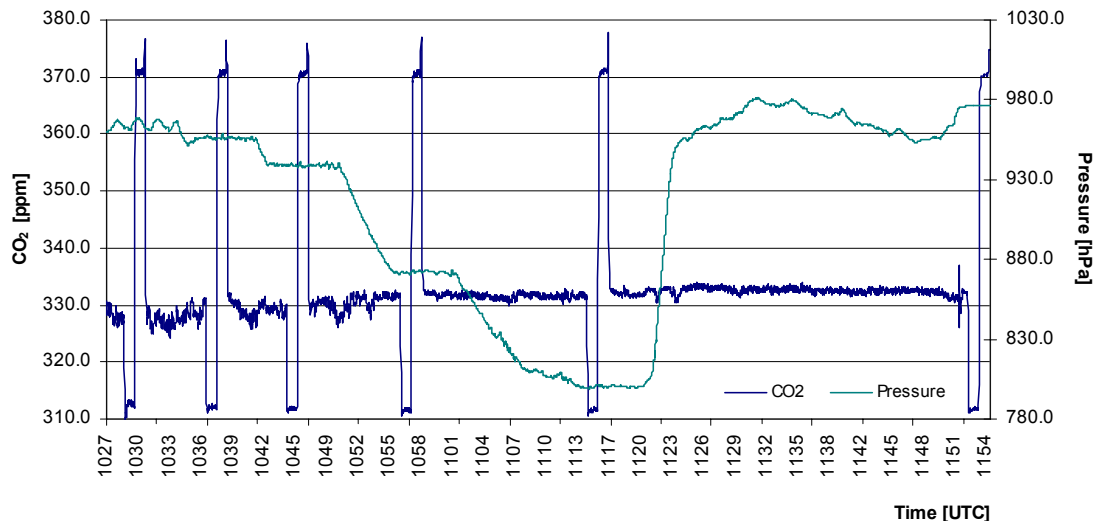


Figure 2.6. Records of CO₂ mixing ratio (raw data, not corrected for temperature and pressure effects) and ambient air pressure from the SPA¹³CE midday flight on 14 August 2002. The spikes in the mixing ratio curve are indicating the calibration events, the steps in the air pressure graph are related to the individual sampling levels. At the lowest sampling height (10:27 – 10:34 UTC) the flight track is following the canopy top, clearly reflected by the oscillating curve. For processed data see for example figure 4.28.

2.2.1.3. Ground Reference System

To gain additional information concerning the surface conditions a mobile ground reference system was developed. A small sized and light weight mast was constructed, for operations in particular at remote sites. Therefore an autonomous power supply by rechargeable batteries and solar panels was necessary. The installation and operation of the system should be possible by a single person.

The mast was equipped with instrumentation for near surface profile measurements of meteorological parameters and for air sampling at different levels. Additional data were taken in the upper soil layers. Air temperature and humidity were measured continuously at 0.5, 2.0 and 5.0 m above ground (active ventilated KPK 1/5-Me, Galltec Mela), wind direction (potentiometric wind vane W200P, Vector Instruments) and velocity (potentiometric cup anemometer A100R, Vector Instruments) at 6m, photosynthetic active radiation (PAR), net radiation (LXG055, Dr. Bruno Lange), soil temperature in 5, 10 and 20 cm depth as well as the temperature within the litter layer and 10 cm above ground (107-Temperature Probe, Campbell Scientific), and finally heat flux into and from the soil (heat flux

plates Rinco HFP-CN3, McVan Instruments). During the campaign in Sweden the CO₂ mixing ratio was continuously measured in 2.0 m height by a Licor 6262, for the other field studies a simpler CO₂ sensor was used (GMT222, 0–3000 ppm, Vaisala), because the Licor was no longer available. Sporadically CO₂ soil respiration measurements were carried out (GMT222, 0–2000 ppm, Vaisala). Depending on the intervals for the routine operations the measurement frequency could be fixed between 1Hz up to averages of about 30 sec. The data were recorded by a Campbell CR23X data logger.

For the ground reference flask sampling the system was adapted to the configuration of the flight sampling unit. Sucked in by two pumps, arranged in line, the air was pressed via a drying tube, filled with magnesium perchlorate [Mg(ClO₄)₂], through the flask compartment. As for the flight sampling similar preconditioned bor silicate 1000 ml flasks were used. The flow rate was held constant during the 10 minutes for flushing and sampling at 5 l min⁻¹. The pressure was regulated by a restriction valve at 1bar relative. Five inlets were placed at 0.1, 0.5, 1.0, 2.0 and 5.0 m above the ground.

A detailed list of the sampling system components is given in the appendix A2 and on the CD-ROM.

2.2.2. Equipment for Gas Analyses

The analysis of trace gas mixing ratios and the isotope ratios were carried out by the ‘isolab’ gas department of the MPI-BGC [BRAND 1996, JORDAN & BRAND 2001, WERNER et al. 2001, WERNER & BRAND 2001].

Besides air samples from the field campaigns also samples from the system configuration experiments, and finally the calibration gases were analysed.

2.2.2.1. Trace Gas Mixing Ratios from Flask Sampling

Gas mixing ratios were derived using a modified *Hewlett Packard 6890* gas chromatograph. For individual trace gases different system configurations and detectors are used: Flame Ionization Detector (FID) for CO₂ and CH₄, Electron Capture Detector (ECD) for N₂O. In a second loop the samples are analysed for

the mixing ratios of CO and H₂ using a Reduction Gas Analyzer (RGA), SF₆ is analyzed by another ECD.

All sample and reference gas analyses are performed alternating with a working standard gas. A daily quality control analysis is routinely executed against three standard gases. Calibration routines are carried out at different time intervals. For a scale setup monthly to bi-monthly analyses of calibration standard gases are scheduled, measurements are compared with CSIRO (Commonwealth Scientific and Industrial Research Organisation / Australia), Institut für Umweltphysik, Heidelberg (bi-weekly 4 flasks) and bi-monthly 6 flasks with TACOS (Terrestrial and Atmospheric Carbon Observing System; Laboratory Network of the Carbo Europe cluster).

Special corrections of the analysed results are accomplished with respect to the system offset (reference and working standard, intercomparison) as due to storage time shift, mainly caused by surface processes. The reached analysis precision for the trace gas mixing ratios is listed in table 2.9.

Table 2.9. Precision of the gas mixing ratio analyses

Gas species	Unit	Precision
CO ₂	ppm	0.08
CO	ppb	1.0
CH ₄	ppb	1.3
N ₂ O	ppb	0.15
H ₂	ppb	5.0
SF ₆	ppt	0.08

A detailed list with the instrument configuration, the analytical procedure as also the calibration specifications can be found in Appendix A3.

2.2.2.2. Isotope Ratios

For the determination of the isotopic ratios $^{13/12}\text{C}$ and $^{18/16}\text{O}$ in CO_2 an advanced Isotope Ratio Mass Spectrometer (IRMS) *Finnigan MAT 252 IRMS* was used. With an additional CO_2 pre separation (*BGC-Air-Trap*), a precision of 0.012 ‰ for ^{13}C and 0.02 ‰ for ^{18}O , respectively, is reached.

To keep high accuracy, calibration routines are executed with a working standard gas twice at the beginning and twice at the end of the analyses; an additional reference standard is included within the flask sample loop. Further on measurements are performed from the ‘comparison CSIRO standard air tanks’.

The data are corrected with respect to the system offset and the shift because of storage time. Additional corrections due to cross contaminations in the dual inlet system, effects depending on mass overlap [N_2O isobaric to CO_2 (molecular mass = 44, mixing ratio taken from the GC measurements) and the ^{17}O contribution to mass = 45 ($^{12}\text{C}^{17}\text{O}^{16}\text{O} / ^{13}\text{C}^{16}\text{O}^{16}\text{O}$)] were accomplished.

A systematic scheme of the instrumentation and operation is presented in Appendix A3, together with the calibration parameters.

3. TEST FLIGHTS AND LABORATORY EXPERIMENTS

DEVELOPMENT OF AN IMPROVED SAMPLING SYSTEM

The studies are divided with respect to their intentions into two sections: 1) the test flights carried out before the RECAB campaigns, and 2) the laboratory experiments aiming at the identification of technical problems regarding the modification of the flight sampling system.

Since the test flights provided basic information for the further investigations a brief discussion of the observations and their relevance is given already in this part. A summary of the realized modifications and an assessment of the improvements are given at the end of this chapter.

3.1. Test Flight Measurements

October 2000–May 2001

Before the first complete RECAB field campaign took place (Spain, June 2001) several test flights have been carried out with respect to training of personnel and system testing during fall, winter and spring 2000/2001. Flights were performed above two different sites in Central Germany (Hainich and Gebesee), where the MPI-BGC is operating towers for eddy covariance and meteorological measurements.

3.1.1. Description of the German Study Region

3.1.1.1. Geography and Climate

GEOGRAPHY

The study area, located nearly in the center of Germany, is part of the geographical landscape unit of the ‘Thüringer Becken’ (Thuringian Basin), that is part of the geomorphological major zone of the ‘Deutsche Mittelgebirgsschwelle’. The southern border is marked by the mountain ridge of the Thüringer Wald (Großer Finsterberg, 944 m a. MSL), the western rim is formed by the ranges of the Hainich (Alter Berg, 494 m a. MSL) and the Dün, and by the Werra valley. To the north the Harz (Brocken, 1142 m a. MSL) and to the east the Saale River are

defining this entity. The small river 'Unstrut' drains the region along a west-east direction, tributing to the Elbe.

Agricultural landuse dominates the inside part of the basin, characterised by a slight rolling morphology, only the west-east striking ridges of the 'Fahnersche Höhe' and the 'Ettersberg' are covered by forests. Common field sizes are up to more than 1 km², dominant crops are wheat, barley, rape, beets and maize. West of the Werra River a more scattered region follows, where also the rate of forested areas, especially on hill tops, become larger.

Along an old trade road the major cities Eisenach (44.000 inhabitants), Gotha (49.000) and Erfurt (197.000) are located south of the flight paths within a west-east distance of 50 km. The towns of Mühlhausen (38.000) and Bad Langensalza (22.000) were enclosed by the flight pattern of the flux aircraft, many small villages are unequally distributed within the whole study area (see figure 3.1 on next page).

CLIMATE

With respect to the topography the study region can be divided into subatlantic and submountain climate zones. South-westerly winds prevail. Yearly mean temperature for Mühlhausen (300 m a. MSL) and Erfurt (316 m a. MSL) is 8.7°C, the yearly mean sum of precipitation is 736 mm, respectively 581 mm (averaging period 1961 – 1990).

3.1.1.2. Field Sites

HAINICH TOWER

Within the Hainich National Park, a small mountain range north of Eisenach, the Max-Planck-Institute for Biogeochemistry operates a field site at a 43.5 m micrometeorological / flux tower, operational since 1999. The Hainich, a limestone ridge, stretches over a distance of 20 km in north-west / south-east direction, the extension from west to east is about 7 km. At the western side a steep slope leading to the Werra valley, whereas the decline to the eastern basin is not as steep and more gently. The typical form of silviculture is selective cutting ('Plenterwaldwirtschaft'), where only single trees are harvested and replaced by natural young growth. As large parts of the area were intensively used from the mid of the 1930s for military training the forest looks rather primeval. Beech, ash

and oak are the predominant tree species, with all age classes up to 250 years. The mean tree height around the tower site is ~ 33 m, the height of the herbal understory ~ 0,3 m.

Hainich Tower; 51°04,7'N / 10°27,1'E, 439 m above MSL

GEBESEE MAST

Since January 2001 a 6 m micrometeorological mast is operational within a intensively used agricultural area 2 km southwest of Gebesee. Predominant in the direct surroundings of the site are wheat, barley, rape and maize. To the south also some small patches were planted with peppermint and sunflowers. During the RE CAB summer campaign in July 2001 the harvest of the cultivated crops started. Wheat, barley and rape were harvested successively during the flight days, which become also obvious from the aerial photograph presented in the documentation folder.

Gebesee Mast; 51°06,1'N / 10°55,0'E, 162 m a. MSL

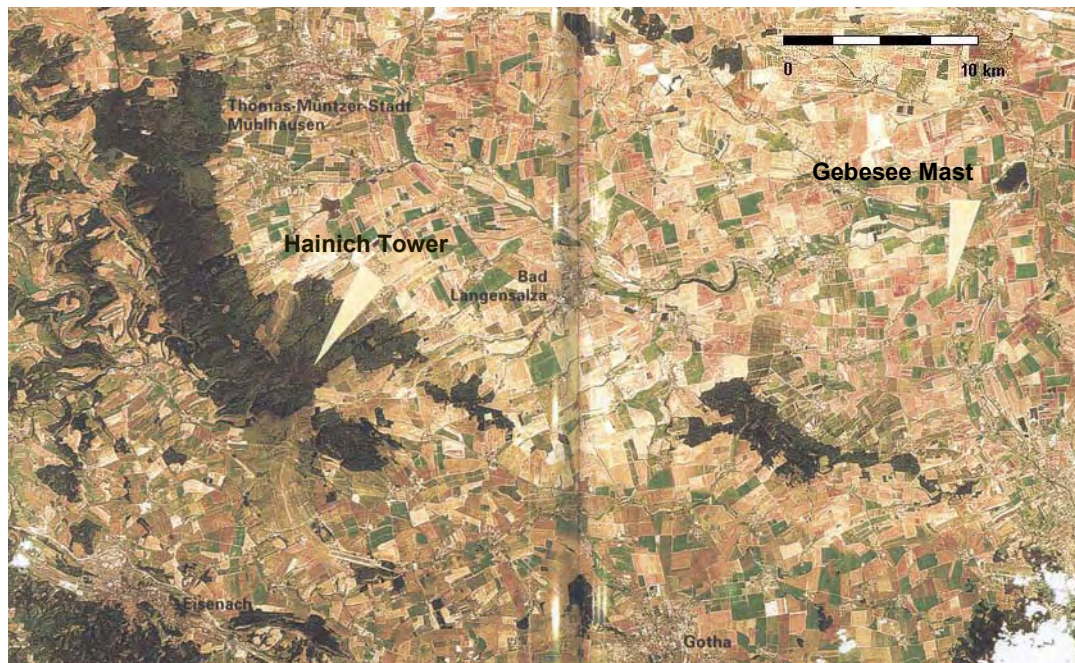


Figure 3.1. Satellite image of the German study area (picture from WINTER et al. 1998, modified)

3.1.2. Hainich Flights October 2000

First flight samplings were performed following the sampling strategy and using a similar flask sampling system as described by LAUBACH & FITSCH [2002] and by LLOYD et al. [2002] above the Hainich between 20 to 23 October 2000. Surprisingly the results were completely contrary to what was expected: in between paired flasks CO₂ mixing ratio differences of up to 4 ppm occurred (displayed in figure 3.2). And as shown in figure 3.3, on 23 October the data from the morning and the afternoon sampling did not decrease over time but increase.

Since the 'isolab' aimed to use the paired flasks also as an internal quality control, the first tests were focussing on the differences between twin flask samples. In almost all cases the CO₂ mixing ratio of the second flask was higher than the first. Two reasons seemed to be responsible: 1) the problem is generated by the system configuration. Perhaps caused by an insufficient flow rate, so that remnants of the calibration gas were left in the flasks. Or cabin air entered through a leakage or a dead end. 2) The ambient air might be less well mixed than expected. Therefore a highly variable mixing ratios occur on small spatial scales. A corollary would be that the flask pairs can not be used as a quality criterion for the laboratory.

In a first step the sampling unit was checked for leakages with a negative result, but, regarding a contribution from 'dead end residual air', the outlet was identified as a potential error source. However, in laboratory experiments it was not possible to attribute the high mixing ratios in the second flask solely to the system configuration.

The second attempt focused on the distribution of the CO₂ mixing ratios at each individual sampling level. If small scale variability exists, this should be noticeable as well in the continuous records. Therefore the calibrated Licor measurements were analysed with regard to mixing ratio variability for the time frames, when the flask sampling procedures were performed (see figure 3.2). Thereby variability up to 13 ppm was identified at the lowest levels; the absolute variation levelled off with increasing sampling height. Hence high variability of the gas mixing ratios on small spatial scales has to be assumed, even above relative uniform vegetation.

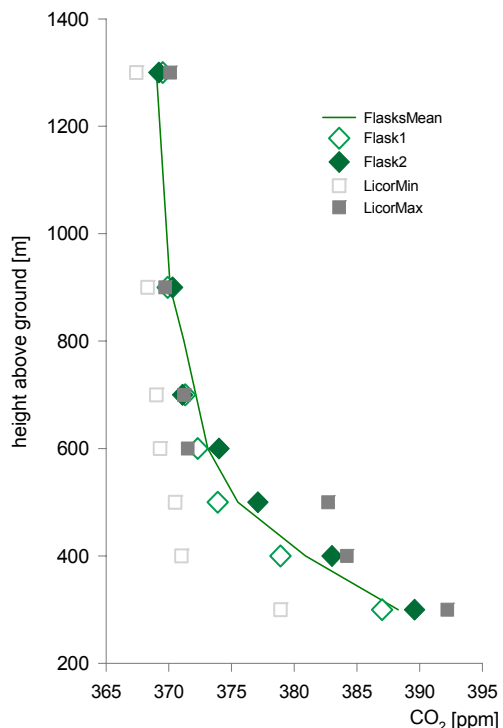


Figure 3.2.

CO_2 mixing ratio variability obtained from a vertical profile flask sampling flight on 23 October 2000 (*Hainich / Germany*)

Flask sampling vs. the Licor online minima and maxima values, recorded during the period the flask sampling procedures were performed

Also the sudden increase of the CO_2 mixing ratio during day time, as observed on 23 October, was unexpected. Even if the photosynthetic CO_2 uptake was reduced because of the beginning senescence, the results from the days before reflected an activity high enough to decrease the atmospheric CO_2 by a recognizable amount.

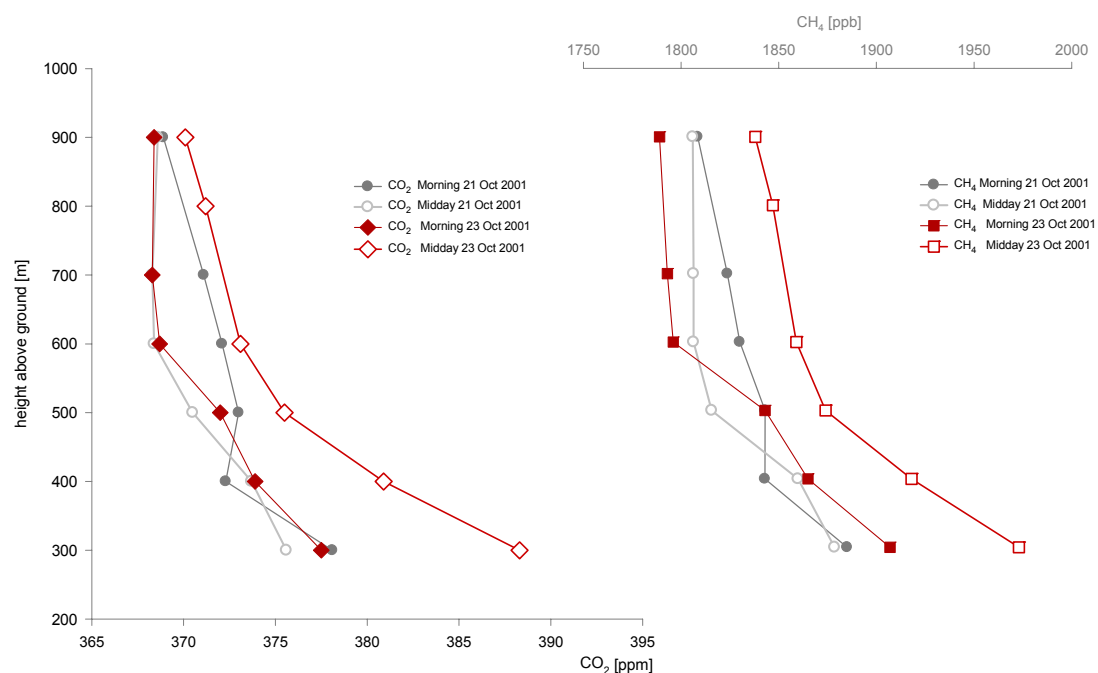


Figure 3.3. CO_2 and CH_4 mixing ratios from flasks sampled during morning and midday flights on 21 and 23 October 2000 (*Hainich / Germany*)

Since the highest values were observed near the ground comparisons were performed with the meteorological records and the CO₂ profile data of the Hainich tower (see figure 3.4.).

As expected, the CO₂ mixing ratio increased with the night time respiration until the photosynthesis became more active around 8:00 AM. In the following the mixing ratio decreased, despite several CO₂ peaks a minimum of 373 ppm was observed at noon, when a rapid increase occurred, leading to values much higher than during night time. These observations can be explained by the analysis of the wind data. During day time a change from westerly to more southerly directions was recorded. Thereby the study site was affected in the afternoon by air of urban origin from the surroundings of Eisenach. During the previous night and the early morning hours of the day air of more rural character passed the Hainich.

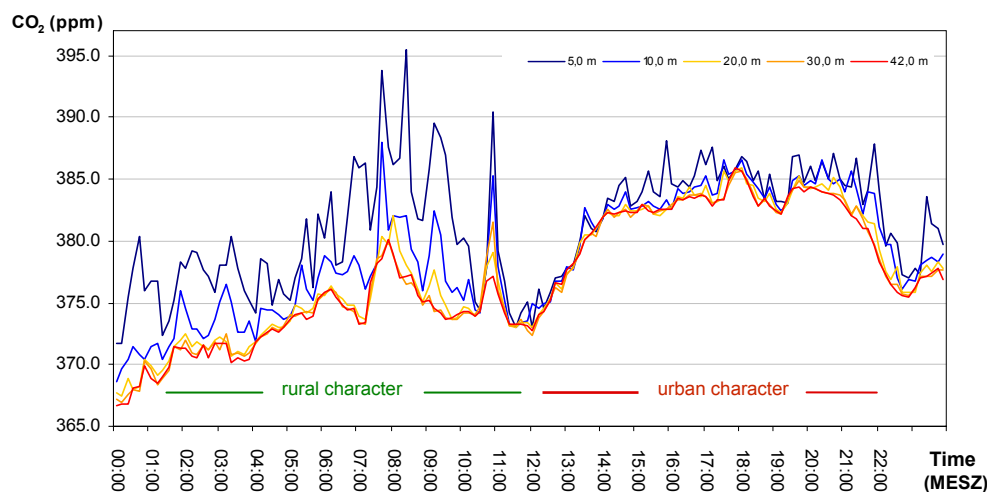


Figure 3.4. CO₂ profile data recorded at the *Hainich* Tower on 23 October 2000

Thus it has to be noticed, that changes of the main wind direction and air mass changes may prevent the CBL budgeting.

3.1.3. Winter Flights January and February 2001

To monitor the seasonal characteristics, the next series of flights were performed during January above the 'Hainich', and in February above the agricultural site 'Gebesee'.

Compared with the data from October the winter time samples contained higher CO₂ mixing ratios with an elevated amount of ¹²C, but lower mixing ratios of N₂O and CH₄, which are both related to soil processes. The averaged data from the flights in autumn and winter, respectively, are listed in table 3.1.

Table 3.1. Average CO₂ and N₂O mixing ratios and delta¹³C values for October and January sampling flights above the 'Hainich'

	October	January
CO ₂ [ppm]	377.5	384.3
N ₂ O [ppb]	319.0	318.5
δ ¹³ C [%]	-8.147	-8.826

Similar to the autumn experiment small scale variability and a decrease of the CO₂ mixing ratio with height for the entire flight profile were observed. Also strong day-to-day variation was monitored. However the tower measurements showed a deviation of approximately -10 ppm. 3 to 4 ppm of the discrepancy might be attributed to uncontrolled calibration gases used for the tower instrumentation.

On 15 January 2001 the CO₂ mixing ratio decreased during the day at the tower, whereas the flight flask samples showed an increase. Thus the tower data could not be consulted as direct ground references.

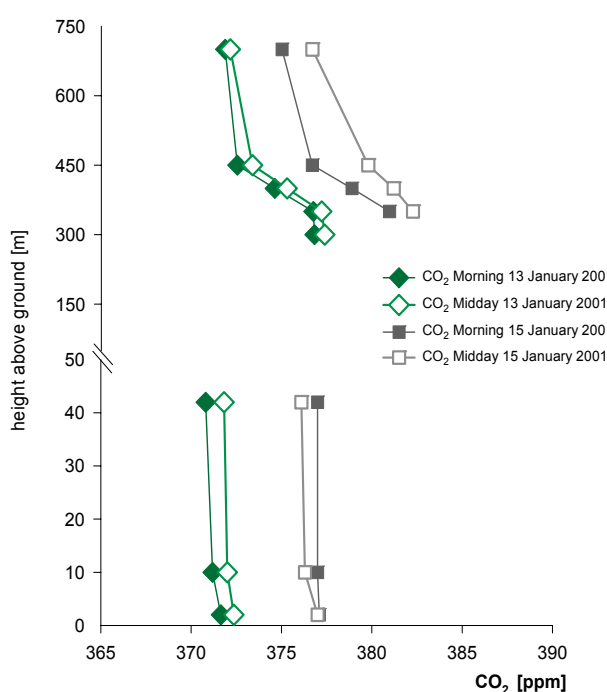


Figure 3.5.

CO₂ mixing ratios measured at the *Hainich* Tower and obtained from flight samples above the *Hainich* on the 13 and 15 January 2001.

3.1.4. Gebesee Flights May 2001

Flights were performed above the agricultural site at Gebesee three times per day from 9 to 11 May 2001 (see figure 3.6). One additional flight for specific tests of the pump system was performed on 26 May. Caused by flight restrictions the lowest level was 150 m above ground.

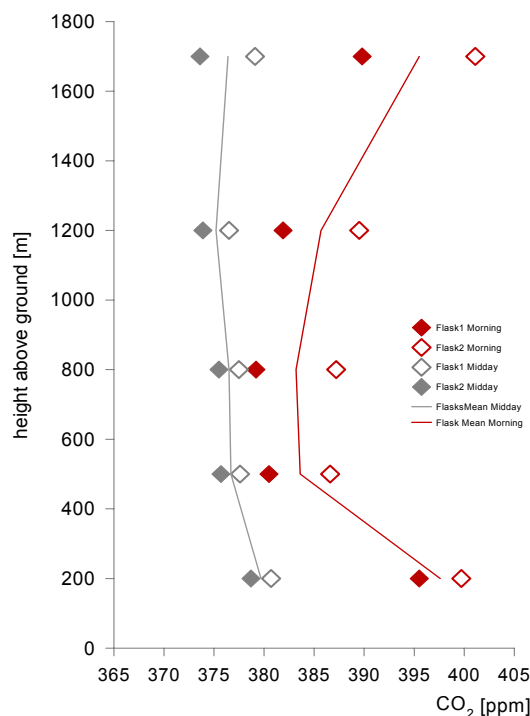


Figure 3.6.
CO₂ mixing ratios from flasks sampled on 10 May 2001 above the agricultural measurement site Gebesee (shown are the results from the morning and from the midday flight). Notice the increasing flask pair differences with height.

Remarkable are the strong decrease of the CO₂ mixing ratio within the course of the day, the flask pair difference increasing with height and that the much higher mixing ratios of the second flask from the morning flight could not be recognized anymore in the midday data.

Even if the results can be explained as being due to assimilation by vegetation the functionality of the modified sampling unit was unsatisfactory. At the lower levels the pump configuration met the requirements. But the flow rate became insufficient with increasing height, caused by the loss of efficiency at reduced ambient air pressure. The decreasing flow rate caused an insufficient flushing of the flasks. Further tests and calculations were carried out (see chapter 3.2.1) to define the requirements for the improvements of the inlet and of the pump section.

Because of the difficulties caused by the insufficient flushing an interpretation of the observed flask pair differences is not appropriate here.

3.2. Development of a modified Flask Sampling System

Since it had become obvious from the test flights that there are big discrepancies between mixing ratios of paired flasks laboratory experiments were carried out to identify disturbances provoked by the original sampling system, and to verify the modifications of the new flight sampling unit.

3.2.1. Conventional Flight Sampling System: Test of the inlet tubing and of the gas exchange rate

October 2000 – May 2001

The original system was configured with different materials, in particular plastics, which might be unsuited due to adsorption at surfaces or permeability. Especially the inlet tubes seemed to be highly sensitive, because of its length of more than 7 meter.

For the laboratory experiment the common sampling flasks and conditioner gas were used. The air samples were analyzed for the mixing ratios of CO₂, CH₄ and N₂O as well as for delta¹³C and delta¹⁸O. Two samples were taken, one direct from the gas tank (for reference) and one after passing the tube.

Table 3.2. Isotopic ratios of the calibration gas filled into sample flasks either directly from the air tank or via the plastic tube used for the flight sampling

Flask	conditioner gas direct		conditioner gas via plastic pipe	
	del ¹³ C [%‰]	del ¹⁸ O [%‰]	Flask	del ¹³ C [%‰]
1A-MS	-8.516	-2.180	IA-MS	-8.515
1B-MS	-8.550	-2.203	IB-MS	-8.498
2A-MS	-8.514	-2.153	IIA-MS	-8.472
2B-MS	-8.518	-2.218	IIB-MS	-8.492
3A-MS	-8.522	-2.202	IIIA-MS	-8.516
3B-MS	-8.543	-2.231	IIIB-MS	-8.489
4A-MS	-8.511	-2.151	IVA-MS	-8.506
4B-MS	-8.535	-2.224	IVB-MS	-8.509
5A-MS	-8.503	-2.198	VA-MS	-8.470
5B-MS	-8.504	-2.173	VB-MS	-8.489
Mean	-8.522	-2.193	Mean	-8.496
Std.Dev.	± 0.016	± 0.028	Std.Dev.	± 0.016
				± 0.013

Mean direct and via plastic pipe: del¹³C [%‰] = -8.509 del¹⁸O [%‰] = -2.170

From the results of the trace gas analysis and the isotope ratios (see Table 3.2.) a differentiation caused by material related interferences could not significantly be excluded. In consequence the complete PVC pipes were replaced by decabon® tubes.

Because residual humidity was detected in the samples from the former flights the horizontal drying tube was removed and a vertically orientated column installed.

To enable a constant operation under final pressure conditions an experimental system with two pumps of higher capacity was constructed and tested in the laboratory. During the flight series in May 2001 the modified set up was verified under real operational conditions (see 3.1.4). It became obvious that the capacity of the two pumps was still not high enough to enable the required flow rates at larger heights.

In order to further study the observed large flask pair differences in the CO₂ mixing ratio (see figure 3.7) a laboratory experiment was carried out to qualify the exchange rate for both flasks under flushing and filling conditions. It could be shown that the removal of the conditioner gas is in fact more efficient from the first flask than for the second. When combining the information on exchange rates, mixing ratios of the conditioner gas and the flow rates noticed during the flights a rough estimate of the residual conditioner gas in the sampled flasks is obtainable.

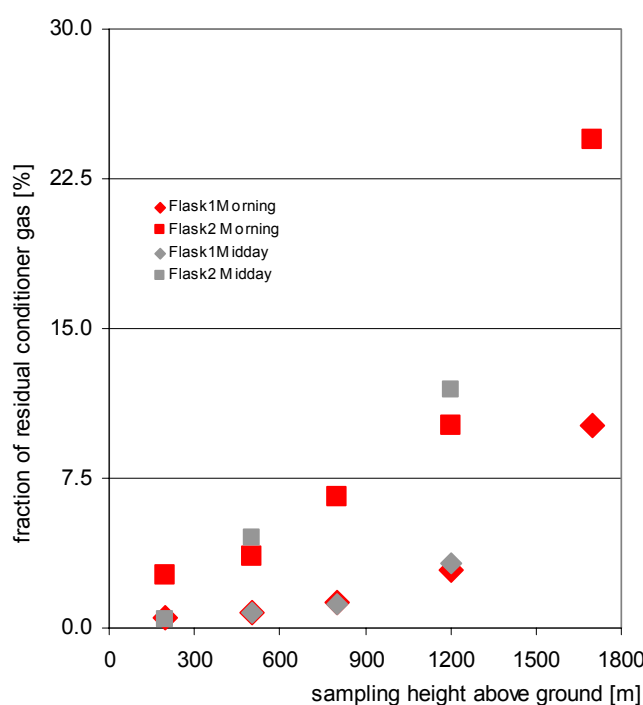


Figure 3.7.

Fraction of residual conditioner gas inside the flasks after flushing 4 minutes and sampling 2 minutes. Morning and midday flight on 10 May 2001 above the agricultural site Gebesee. Uppermost level sampled only during the morning flight.

3.2.2. Conclusions of the first laboratory experiments and test flights

The most important findings of the test flights and the laboratory experiments are:

- Flask pair differences, as frequently found are reflecting at least 1) the occurrence of high mixing ratio variability on small spatial scales and 2) effects of insufficient flow rates.
- Mixing ratio changes between flights of one day, are to large extend due to air mass changes
- The differences of flight samples to those from the ground are related to 1) different footprint sizes, 2) failures of the calibration standards and 3) errors made during individual measurements and originating from deficiencies of the sampling system.

At least two modifications were needed: the flask sampling system had to be improved and, even more crucial, assumptions of the CBL approach were not satisfied under certain weather conditions.

Regarding the sampling and the flight strategy the focus has to be a lower sampling height and a flight pattern for the entire vertical profile under strict GPS guidance.

3.3. Modified Flight Sampling System

3.3.1. Adjustment of the flow rate and tests regarding effects of the drying reagent on the CO₂ mixing ratio

September - December 2001

Since the Spain summer campaign the new 'Flight Sampling Unit' was operational. Because of still recognizable impairments and to test the modifications further laboratory experiments were carried out. Their goal was an improved flushing and exclusion of potential problems caused by the chemical drying agent.

3.3.1.1. Exchange characteristic

Intention was to determine the exchange rate for two flasks arranged in a line, at typical pressure and flow rate of the modified sampling unit. Therefore six flask pairs, filled with a gas mixture of known composition, were flushed with synthetic air for time intervals of different duration from 0 to 16 minutes. The individual flasks were subsequently analysed by gas chromatography for the mixing ratios of CO₂ and N₂O, displayed in figure 3.8.

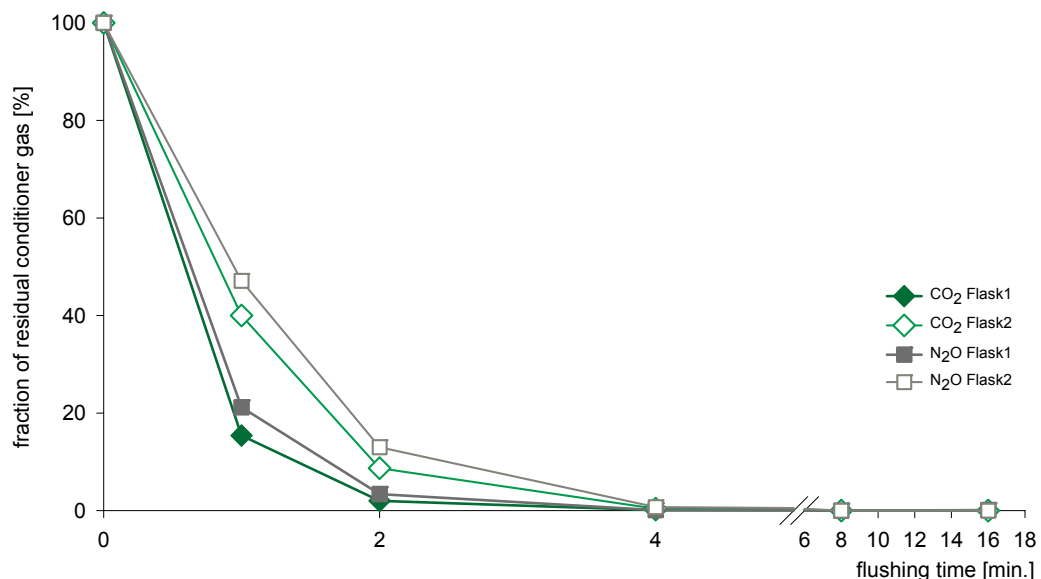


Figure 3.8. Laboratory experiment: Fraction of residual conditioner gas inside the flasks as a function of flushing time. Air was analyzed for the mixing ratios of CO₂ and N₂O

A difference between the first and the second flask became obvious regarding the exchanged fraction of the conditioner gas. The residual CO₂ mixing ratio after one

minute was 15.4 % in Flask1, but 40.0 % in Flask2. After four minutes still small fractions of 0.1 %, respectively 0.4 % were left. Unexpected was the reduced removal rate of N₂O from both flasks. Responsible for this might be gas specific behaviours, like surface interactions, but until now no studies have been carried out regarding such processes.

3.3.1.2. Influence of the drying medium on the carbon dioxide mixing ratio

In particular due to the sensitivity of the oxygen isotope to liquid water it is necessary to dry the sampled air at least to a dew point below 2°C [GEMERY et al. 1996]. The sampling unit is therefore equipped with a stainless steel coalescence filter and a tube filled with the chemical drying agent magnesium perchlorate [Mg(ClO₄)₂]. For the flask pair differences in mixing ratios also [Mg(ClO₄)₂] might be responsible because of pressure dependent adsorption and desorption.

Focus of the first experiment was to study, whether there is any effect. The examination was done under flight-typical pressure conditions with air of known composition from a tank, but with different time frames for flushing and sampling. Additionally a reference flask pair was flushed and filled with a constant rate of 2 l min⁻¹ for 20 minutes at reduced initial pressure.

From the results of the analysis, as shown in table 3.3., a pressure dependency could be confirmed: under high pressure conditions, which are associated with the flushing procedure, an adsorption of CO₂ occurs. When reducing the inside pressure, by a lowering of the flow rate, the CO₂ is slowly desorbed again.

Therefore the chemical drying tube was located behind the mass flow controller and the restriction valve was replaced by a ‘pre-pressure-controller’. Though this compartment was configured to provide stable pressure conditions.

Table 3.3. Comparison of gas mixing ratios of CH₄, CO₂ and N₂O before and after passing a drying tube filled with magnesium perchlorate.

flasks in front of the Mg(ClO ₄) ₂ column						flasks behind the Mg(ClO ₄) ₂ column			
1	1845.1	364.0	318.1	flushing		1844.8	362.4	318.2	5
3	1846.0	364.1	318.4	4	2	1844.8	362.4	318.0	7
9	1844.3	364.1	318.4	flushing		1844.9	364.0	318.4	13
11	1845.0	364.1	318.4	0	30	1842.8	364.1	318.5	15
17	1843.4	364.2	318.2	flushing		1844.6	362.7	318.2	22
19	1844.2	364.0	318.4	3	3	1846.3	362.4	318.1	23
25	1845.9	364.0	318.2	flushing		1845.5	363.4	318.4	27
27	1847.2	364.2	318.3	2	10	1843.1	363.3	318.3	29
flask No.	CH ₄ [ppb]	CO ₂ [ppm]	N ₂ O [ppb]	flow period in min.		CH ₄ [ppb]	CO ₂ [ppm]	N ₂ O [ppb]	flask No.
Mean	1845.1	364.1	318.3			1844.6	363.1	318.2	
Std.Dev.	1.2	0.1	0.1			1.2	0.7	0.2	

Flow rates: for flushing 10 l / min.; for filling 2 l / min.

The improvements were tested by placing the drying tube either in front of the mass flow controller, or within the pressure stabilized compartment. In addition reference flasks were sampled directly behind the gas tank. The first configuration resulted in a reduced CO₂ mixing ratio, but the results from the pressure-stabilized system showed values in the range or even slightly higher as obtained from the reference measurements.

3.3.2. Comparison of the different sampling systems

January 2002

Due to the influence of the drying reagent on the CO₂ mixing ratio an additional laboratory experiment was conducted, in order to investigate the individual behaviours of the different sampling units. The results are listed in table 3.4.

In a large storage room the basic and the modified flight sampling system, the ground sampling unit and a reference set up without drying compartment were operated concurrently. The first test sampling was performed with all systems simultaneously. In a second test the sampling was carried out solely with the new flight system, but with modified flushing and sampling periods. Finally in a third test combined sampling was executed again. The aim was to compare the results from the basic flight system and the modified flight unit, which was operated without the drying section. For the detailed system configurations and the experiment protocol see Appendix A5.

Although the experiment was performed inside a wide-sized, non public room to avoid disturbances by air mass exchanges, an increase of the CO₂ mixing ratio during the sampling period occurred. This increase has to be taken into account when interpreting the data, because the sampling durations were different for the individual systems (for instance 10 minutes 'Ground reference unit' and 2 minutes 'Flight sampling system'). The same trend is also recognizable for the individual flask pairs, where, except one case, the first flask contains higher CO₂ mixing ratios than the second flask. These records are contrary to the former observations from the real flight samplings, where in most cases higher values were measured in the second flask.

The high differences for CH₄ and CO₂ obtained from the reference and from the flight system with the modified flushing rate might be caused by an insufficient flushing procedure. Even if the flow rate was determined to be high enough to exchange the air inside the flasks at least four times, the second flask contained still residuals of the conditioner gas.

By the comparison of the flight system with and without the drying section no significant differences could be found. The range of the discrepancies, which were recorded also for the ground sampling unit and, in particular for the basic flight system, are clearly below the amount of change that was monitored throughout the

period of the complete experiment. Also the increase of the mixing ratio, observed in the first flasks, might be related to this general shift. Also the discrepancy between the flasks sampled with the old system in the third test might be interpreted as an indication for spatial CO₂ variability even inside a closed room without distinct CO₂ sources.

Table 3.4. Results of the experiment comparing the diverse sampling units
(indicated in red are outliers excluded from the analysis)

Flask Code	System	p [bar]	CH ₄ [ppb]	CO ₂ [ppm]	N ₂ O [ppb]
E 230-27	Modified Flight System	2.25	2138.7	586.5	324.2
E 217-27	Modified Flight System	2.25	2140.9	586.1	324.3
E 218-27	Ground Reference Unit	2.21	2140.9	591.2	324.3
E 265-27	Ground Reference Unit	2.18	2138.3	590.7	324.2
E 248-27	Basic Flight System	2.00	2141.5	588.1	324.2
E 231-27	Basic Flight System	2.01	2142.7	587.9	324.3
E 250-27	Reference	2.08	2141.2	586.6	324.2
E 239-27	Reference	2.08	2135.1	579.7	324.2
Mean			2140.6	588.2	324.2
Std.Dev.			1.6	2.1	0.0
E 233-27	Modified Flight System	2.25	2136.5	588.8	324.2
E 273-27	Modified Flight System	2.25	2126.5	576.8	324.4
E 257-27	Modified Flight System; without drying	2.25	2141.6	598.5	324.1
E 251-27	Modified Flight System; without drying	2.25	2141.7	598.2	324.1
E 237-27	Basic Flight System	2.01	2141.3	598.5	324.0
E 235-27	Basic Flight System	2.01	2139.2	599.6	324.1
E 263-27	Reference	2.05	2137.7	595.8	324.1
E 261-27	Reference	1.88	2125.1	579.5	324.2
Mean			2140.3	598.1	324.1
Std.Dev.			1.8	1.4	0.0

The difference in the N₂O mixing ratios observed between the sampling systems seems not to be caused by the configurations. As a general decrease of the N₂O mixing ratio can be recognized during the test period it is most likely that this might be also the main cause for the variability between the systems (see for reference the test documentation with the time schedule in Appendix A5).

For the modified flight sampling unit no significant influence of the [Mg(ClO₄)₂] on the CO₂ mixing ratio could be recognized any more. However, an effect on the mixing ratio of H₂ could be identified from the data obtained by the later field campaigns when H₂ was implemented regularly in the analytical scheme. This has to be taken into account for the interpretation of the results.

Table 3.5. Compendium of the system configurations and of the analysed flask sample parameters for all flights

<i>Test flights Germany</i>		Configuration of the Flight Sampling System	Spectrum of analyses	Surface sampling
Hainich	10/2000	Conventional system		No
Hainich	01/2001	Conventional system: - PVC pipes replaced by decarbon tubing		No
Gebesee & Hainich	02/2001	Modified system (test configuration): - inlet tube with enlarged diameter, - vertical drying column, - continuous operation under final pressure, - twin-pump system	CO ₂ , CH ₄ , N ₂ O, delta ¹³ C, delta ¹⁸ O	No
Gebesee	05/2001			No

<i>RECAB field campaigns</i>		Configuration of the Flight Sampling System	Spectrum of analyses	Surface sampling
Valencia (Spain)	06/2001	Modified system: - More powerful pump, - Additional coalescing filter,	CO ₂ , CH ₄ , N ₂ O, delta ¹³ C, delta ¹⁸ O	Yes
Thuringia (Germany)	07/2001	- Replacement of the Gelman plastic filter by a stainless steel particle filter		(Yes)
Uppland (Sweden)	08/2001			Yes
Valencia (Spain)	12/2001			Yes
The Netherlands	01/2002	Modified system: - Implementation of an electronic pressure controller and establishment of pressure stabilized compartment	CO ₂ , CO, CH ₄ , H ₂ , N ₂ O, SF ₆ , delta ¹³ C, delta ¹⁸ O	Yes
Lazio (Italy)	06/2002			Yes
The Netherlands	07/2002			Yes
SPA ¹³ CE (Hainich, Germany)	08/2002			Yes

3.4. Summary of the modifications and assessment of the improvements

Modifications of the system have been carried out also during the first RECAB flight campaigns until November 2001, when with the Valencia winter experiment the finally configured system could be used. For an overview of the development and the use of the individual system configurations see table 3.5. References to laboratory experiments and further modifications and tests during the campaigns are given in chapter 4. ‘RECAB field experiments’ and chapter 5. ‘Discussion’.

Assessment of the improvements

The modifications resulted in significant improvements with respect to the data collection. In particular the unification of the sampling process by the continuously operation under final pressure condition at all levels throughout the entire profile and the implementation of the documentation, which was not possible with the former flight sampling system used by the MPI-BGC, established direct comparability of individual samplings. An overview of the realized improvements is given in table 3.6.

Even if the problems with the chemical drying agent could be solved with respect to the CO₂ mixing ratio, a systematic impairment seems to continue for hydrogen. Since H₂ was used only as an additional tracer for anthropogenic contaminations, the importance for the carbon investigation is limited, when keeping these problems for data interpretation in mind. Nevertheless it has to be pointed out, that there are still some smaller problems which have to be removed in further examinations.

Table 3.6. Improvements realized by the new 'Flight Sampling Unit'

Parameter	Modification	Result
Material	<ul style="list-style-type: none"> ▪ replacement of all synthetics by stainless steel parts and Decabon® tubing 	<ul style="list-style-type: none"> ▪ prevention of surface reactions and diffusion
Drying units	<ul style="list-style-type: none"> ▪ change to a vertical orientation of the drying tube ▪ rearrangement of the drying tube inside the pressure stabilized compartment ▪ implementation of an additional coalescing filter 	<ul style="list-style-type: none"> ▪ efficient removal of the residual air humidity
Operating pressure	<ul style="list-style-type: none"> ▪ construction of a dual outlet system with similar restrictions ▪ adaptation of pump capacity ▪ establishment of a pressure stabilized compartment for drying tube and sampling flasks 	<ul style="list-style-type: none"> ▪ uninterrupted operation and continuous air stream through tubing and pump ▪ constant operation under final pressure conditions ▪ avoidance of processes at the flask surfaces caused by pressure variations ▪ unification of the sampling procedure for all flight levels
Documentation	<ul style="list-style-type: none"> ▪ recording of the operation status in log files 	<ul style="list-style-type: none"> ▪ Provision of information for comparison with online data

A detailed comparison of the system configuration and the operation scheme of the initial and the modified sampling units is given in Appendix A2 and on the CD-ROM.

4. RECAB FIELD EXPERIMENTS

JUNE 2001 – AUGUST 2002

The field campaigns served two interests: Firstly, data acquisition with respect to the regional carbon budgets, the prior aim of the RECAB project. Secondly, performance of specific experiments to test and evaluate technical modifications and subsequent adaptation of the investigation strategy.

To achieve both goals this chapter is divided into two sections. The first part will focus on the intentions and the observations of the field campaigns in chronological order. Following on these will be regionally interpreted, by examining specific aspects.

Table 4.1. Schedule of the RECAB field campaigns and nomenclature of the sampling locations

Region	Period	Flight Profile Sites	Ground Reference Sites	Flight Days
Valencia (Spain)	06/2001	Rice, Orchard, Mare	Rice, Orchard	6
Thuringia (Germany)	07/2001	Hainich, Gebesee	Hainich	5
Uppland (Sweden)	08/2001	Norunda, Florarna	Florarna (Swamp, Forest)	7
Valencia (Spain)	12/2001	Rice, Orchard, Macchia, (Mare)	Rice, Orchard, Macchia, Highway	6
The Netherlands	01/2002	Forest, Maize, Cabauw	Loobos, Maize, Marshland	5
Lazio (Italy)	06/2002	Tuscania, Orvinio	Roccarespampani, Orvinio (Meadow, Valley)	2.5
The Netherlands	07/2002	Forest, Maize, Cabauw	Maize, Marshland	3
SPA ¹³ CE (Hainich, Germany)	08/2002	Hainich, (Holzland)	Hainich	3.5

The complete data sets, the descriptions of the studied areas and notes about the flight operations, as well as a picture collection for each region, respectively campaign, can be found in the documentation folders on the CD-ROM.

4.1. Data Acquisition and Observations

4.1.1. Valencia Summer Experiment

17 June – 7 July 2001

First experiment with the modified flight sampling system

The first field campaign using the modified flight sampling system took place in a coastal zone with intensive agriculture south of Valencia (Spain).

The main foci of the investigation were CO₂ mixing ratio variations and the identification of contributions by individual sources and sinks. Further, additional air samples were taken for the first time at ground level in an apricot orchard during night and day, as well as in the rice field area around noon.

Profile flights were carried out above an area dominated by orchards of citrus and apricot plants and above a plain with wetland rice cultivation. An overview of the observed trace gas mixing ratios and the delta¹³C values at lowest flight level and within the free troposphere is given in table 4.2.

	CO ₂ [ppm]	CO [ppb]	CH ₄ [ppb]	N ₂ O [ppb]	H ₂ [ppb]	SF ₆ [ppt]	delta ¹³ C [%]
Lowest Level	360 - 380	/	1802 - 1919	318 - 323	/	/	-7.746 - -8.638
Free Troposphere	364 - 379	/	1764 - 1966	316 - 326	/	/	-7.940 - -8.335

Heights LL and FT:

100 – 150 m / 1500 – 2000 m

Number of flight days: 6

Number of profile sites: 2

Table 4.2. Range between the maxima and minima of the mixing ratios and the delta¹³C values obtained from the flask sampling during the summer campaign (17 June to 7 July 2001) in the Valencia region.

Ground level samples were taken at one day around noon within the rice fields and two times, on 3 July before sunrise and on 5 July at noon, inside an apricot orchard. Figure 4.1 presents the data from the orchard samplings.

The height of the trees was approximately 3.5 m. During the night of 2 July the plot was flooded for watering; high soil moisture was still recognizable the night after this flooding event. However, when taking the samples on 5 July the top soil was completely dry again.

Obvious are the high values during night time below the canopy top. This steep gradient does not occur during day time. Instead, a rather stable value of the mixing ratio can be observed throughout the entire profile for all gas species. However, a difference can be recognized because of the increasing N₂O mixing ratio from the morning to midday sampling, which is in contrast to the CH₄ mixing ratio changes.

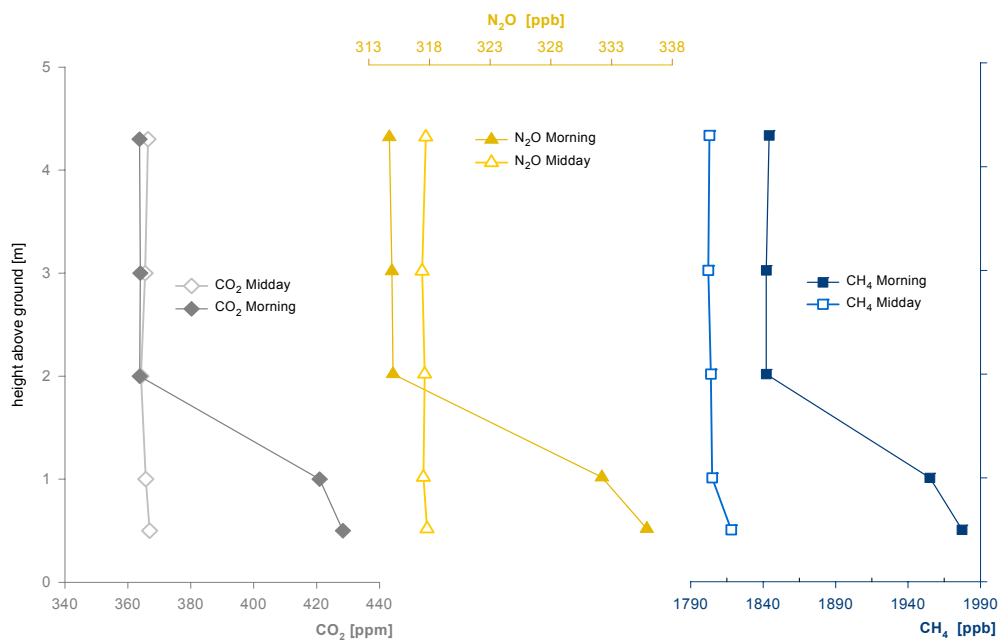


Figure 4.1. Mixing ratios of CO_2 , N_2O and CH_4 from samples taken inside the apricot *Orchard* (Valencia / Spain) before sunrise (3 July 2001) and around noon (5 July 2001).

Representing the flight activities, two consecutive days are presented in figure 4.2. At both sites the CO_2 decrease is highest near the ground, whereas the upper profiles differs from each other: the profiles from the rice fields are characterised by an increase of the mixing ratio sampled around the 500 m level, which is stable until the afternoon (not shown). On the other hand a CO_2 increase within the profiles above the orchards can be recognized for the sample levels 1000 and 1500 m between the morning and the midday flight.

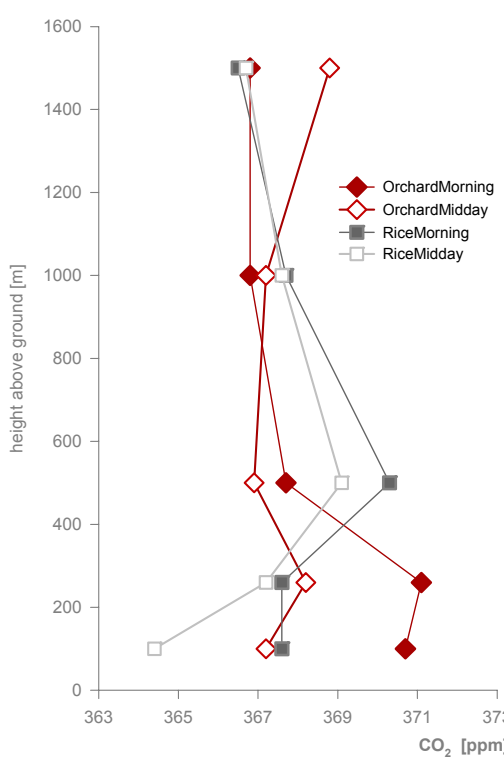


Figure 4.2.

CO_2 mixing ratios from sampling flights performed above the ‘Orchard site’ (Valencia / Spain) on 3 July 2001 (around 8:00 and 11:00 UTC) and the rice field area on 4 July 2001 (around 9:00 and 12:00 UTC).

4.1.2. Thuringia Summer Experiment

15 July – 2 August 2001

The flight investigation took place around the Hainich and the Gebesee sites in Thuringia / Central Germany (for description of the region see also chapter 3.1.1.). An overview of the observed trace gas mixing ratios and the delta¹³C values at lowest flight level and within the free troposphere is given in table 4.3.

	CO_2 [ppm]	CO [ppb]	CH_4 [ppb]	N_2O [ppb]	H_2 [ppb]	SF_6 [ppt]	$\delta^{13}\text{C}$ [%]
Lowest Level	355 - 403		1815 - 1981	316 - 328			-7.736 - -9.720
Free Troposphere	356 - 364		1781 - 1882	314 - 319			-7.710 - -7.850

Heights LL and FT: 90 – 340 m / 1800 – 2500 m Number of flight days: 5 Number of profile sites: 2

Table 4.3. Range between the maxima and minima of the mixing ratios and the delta¹³C values obtained from the flask sampling during the Thuringia summer campaign (15 July to 2 August 2001).

Figure 4.3. presents the CO₂ mixing ratios, obtained from the flights carried out above the agricultural field site ‘Gebesee’ (23 July; morning flight: 9:00 UTC, afternoon flight: 16:00 UTC) and around the Hainich Tower (24 July 2001; morning flight: 7:30 UTC, afternoon flight 16:00 UTC).

For the ‘Gebesee’ data the high mixing ratios sampled during the morning flights near the ground and the steep gradient to the samples taken at the higher levels are obvious. Contrary to the ‘Gebesee’ data lower CO₂ mixing ratios with an only slight difference between morning and afternoon samples were observed at the lower levels above the ‘Hainich’. Remarkable is the increasing difference of morning and afternoon samples up to the free troposphere.

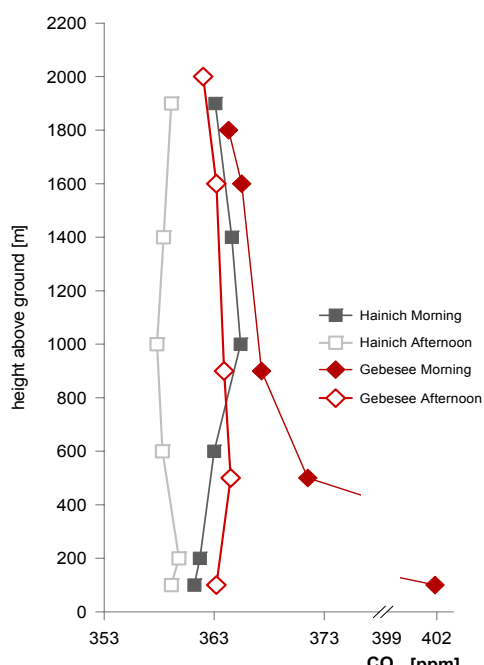


Figure 4.3.

CO₂ mixing ratios from flights performed above the agricultural site 'Gebesee' and above the 'Hainich' forest (Germany).

Notice the interrupted scale on the x-axis.

4.1.3. Uppland Summer Experiment 11 August – 9 September 2001

Implementation of additional trace gas analyses

Extensive agriculture and urban settlements are of only minor importance at the most northern RECAB field site. Boreal forests and wetlands are the major landcover types.

Since it became obvious in previous campaigns that advection is a major factor affecting the budgeting strategy, the need to include more gases into the analysing scheme was anticipated. In addition a reduced height of the lowest flight level was desirable, to find the influences of local sources or sinks.

The flask analysis was therefore carried out for additional trace gases. For most of the samples from 19 August 2001 onwards mixing ratios became available for CO, H₂ and SF₆.

The emphasis of the investigations was on the diurnal variation of the CO₂ mixing ratio and on the comparison of two different, but characteristic major land units of the study region - the forest site at Norunda and the Florarna wetland area. Further, special attention was paid to the vertical profiles at Florarna, focussing on the contributions of the swampy and the wooded parts on a daily time scale. Ground reference data were obtained by measurements and sampling inside the forest and within the open swamp, using the new mobile mast.

An overview of the observed trace gas mixing ratios and the delta¹³C values at lowest flight level and within the free troposphere is given in table 4.4.

	CO ₂ [ppm]	CO [ppb]	CH ₄ [ppb]	N ₂ O [ppb]	H ₂ [ppb]	SF ₆ [ppt]	delta ¹³ C [%]
Lowest Level	350 - 380	100 - 134	1807 - 1889	316 - 319	415 - 474	4.83 - 5.07	-7.077 - -8.536
Free Troposphere	354 - 364	96 - 122	1783 - 1869	316 - 321	452 - 492	4.78 - 5.01	-7.364 - -7.955

Heights LL and FT: 60 - 90 m / 1980 – 2440 m Number of flight days: 7 Number of profile sites: 2

Table 4.4. Range between the maxima and minima of the mixing ratios and the delta ¹³C values obtained from the flask sampling during the Swedish summer campaign (11 August to 9 September 2001).

As examples for the flight profiles the results from samplings around the Norunda Tower on the 19 August and above the Florarna wetland on the 30 August are presented in figures 4.4. and 4.5. At both locations, however more distinct at the Florarna site, a decrease of the CO₂ mixing ratio can be recognized during the day, while the ¹³C isotope ratio is increasing.

Contrary to the development of the CO₂ mixing ratio CO increases during the day at the Florarna site and at the Norunda location. At Norunda a clear jump up between the midday and the afternoon flight was observed, even for the sample level within the free troposphere.

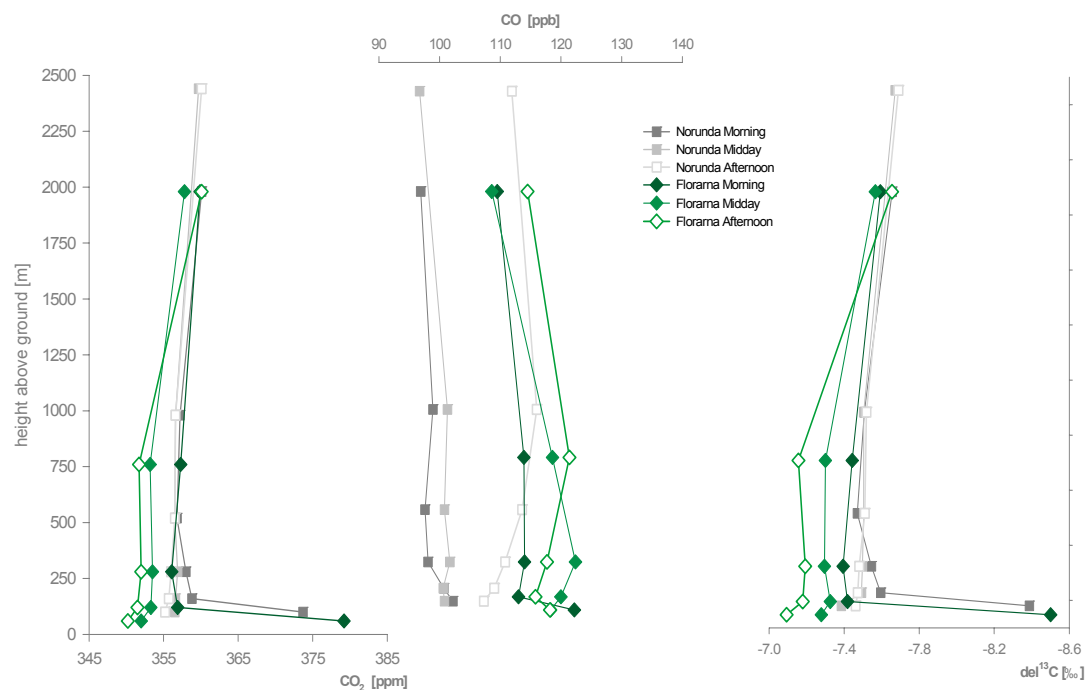


Figure 4.4. CO₂ and CO mixing ratios and delta ¹³C values from the flight profiles around the *Norunda* Tower on 19 August 2001 and above the *Florarna* nature reserve on 30 August 2001 (Uppland / Sweden).

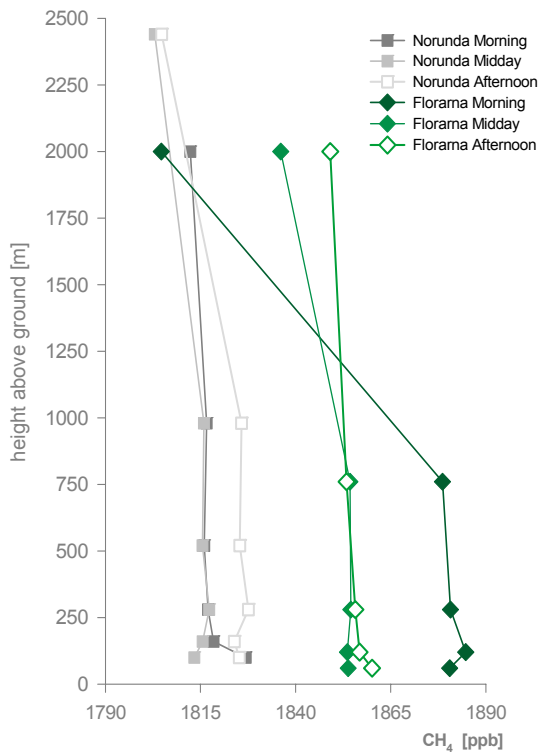


Figure 4.5.
CH₄ mixing ratios from the flight profiles around the *Norunda* Tower on 19 August 2001 and above the *Florarna* nature reserve on 30 August 2001 (Uppland / Sweden).

As seen before from the flight samples also the data from the ground reference samplings (see figure 4.6.) are indicating a CO₂ decrease associated with an increase of the ¹³C isotopes during the day (particularly observed at the open swamp). Additionally these data are showing an increase of the CO mixing ratio between the samplings from morning and midday, whereas the results from the samples taken within the forest are characterised by a slight decrease.

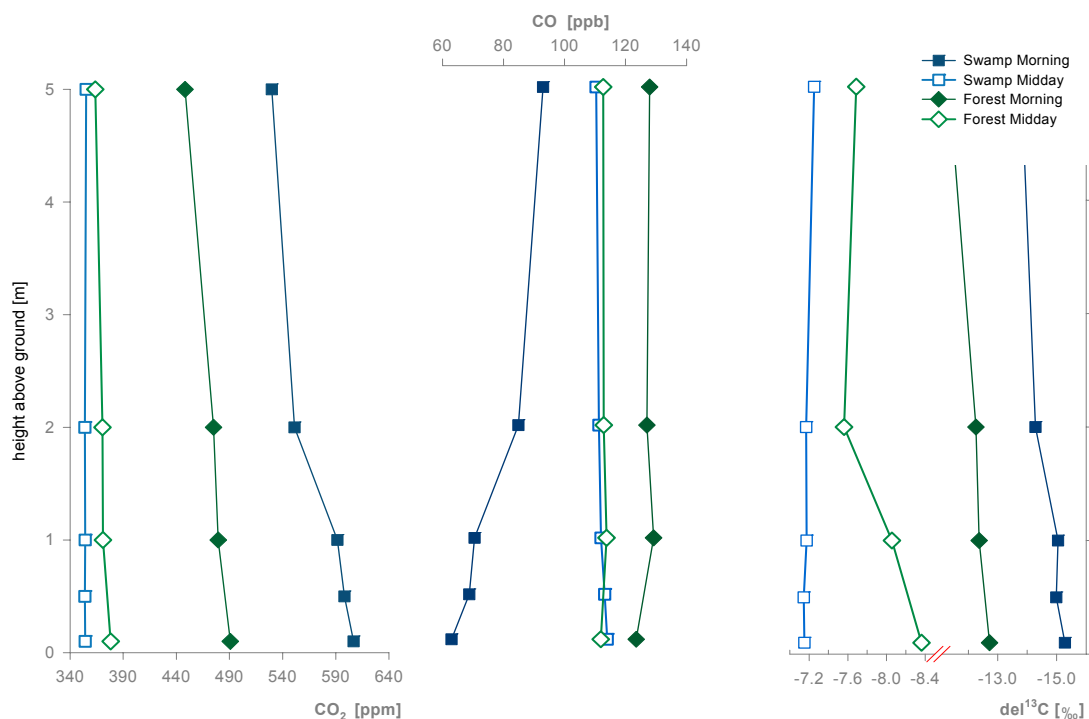


Figure 4.6. Ground reference samples taken at the *Florarna* nature reserve (Uppland / Sweden) within the open swamp (Morning 30, Midday 29 August 2001) and inside a wooded area (Morning 6, Midday 5 September 2001). Shown are the mixing ratios of CO₂ and CO and the delta¹³C values.

From the results two problems were identified: beside a frequent missing of the still shallow CBL during the morning flight flask pair differences appeared again. A systematic disturbance seemed to be likely, since most frequently the higher CO₂ mixing ratio was detected in the second flask. The chemical drying agent and an insufficient flushing rate were identified as the probable sources of the error and studied in laboratory experiments until the next campaign took place (see chapter 3.2.2.).

4.1.4. Valencia Winter Experiment 16 November – 15 December 2001

Final configuration of the modified flight sampling system

Since air mass changes caused by the diurnal land-sea-wind circulation had to be expected similar as in summer, one focus of the investigation was the more distinct identification of the influence of advection. For this purpose the ground reference unit, enhanced by a wind vane, was first installed for several days within the rice fields. Later on ground level sampling was carried out in order to obtain specific source characteristics at the citrus orchard and beside a highway.

Due to the fact that the study sites were affected strongly by several disturbances, like point sources, advection and the high rate of urbanization, additional sampling and measurements should be carried out on a remote site. Investigations were therefore also performed at a mountain plateau, covered by macchia, the typical shrub vegetation community common around the Mediterranean Sea.

A further aim of the investigations was to obtain information, whether transformation processes or systematic differentiations occur between the flight samples and the data obtained from the ground reference examinations. For this experiment the rice field site provided the best conditions; because of the wide open area without obstacles and urban settlements low level flights could be realized.

An overview of the observed trace gas mixing ratios and the delta¹³C values at lowest flight level and within the free troposphere is given in table 4.5.

	CO ₂ [ppm]	CO [ppb]	CH ₄ [ppb]	N ₂ O [ppb]	H ₂ [ppb]	SF ₆ [ppt]	delta ¹³ C [%]
Lowest Level	371 - 389	148 - 273	1830 - 1958	318 - 320	394 - 483	4.85 - 8.05	-8.215 - -9.087
Free Troposphere	366 - 373	110 - 202	1793 - 1851	318 - 323	439 - 480	4.85 - 5.18	-7.997 - -8.286

Heights LL and FT: 6 - 46 m / 825 – 1000 m Number of flight days: 6 Number of profile sites: 3

Table 4.5. Range between the maxima and minima of the mixing ratios and the delta¹³C values obtained from the flask sampling during the Valencia winter campaign.

Figure 4.7 presents the results from profile flights carried out on two consecutive days above the rice fields and from one day at the remote mountain site. The profiles at the rice field site are characterised by a decrease of the CO₂ mixing ratio and by delta¹³C values becoming less negative at all sample levels from the morning to the midday flight. However, for the CO mixing ratio 5 July, midday, at highest sampling level, an increase occurred.

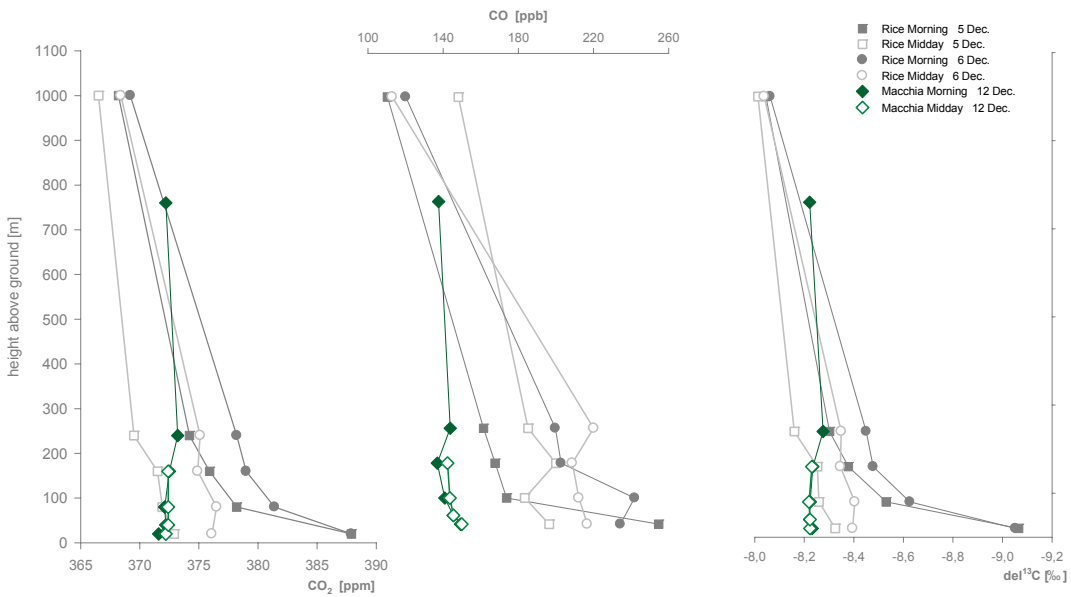


Figure 4.7. Mixing ratio profiles from the Spanish winter experiment (16 November to 15 December 2001) above the *Rice* field area and at the remote mountain site ‘Cortes de Pallás’ (labelled ‘Macchia’). Shown are the CO₂ and CO mixing ratios and delta ¹³C values.

The profiles from the mountain site are very similar in the morning and at noon. But it has to be mentioned that because of technical problems the morning flight started 3 hours later than the morning flights above the rice field area.

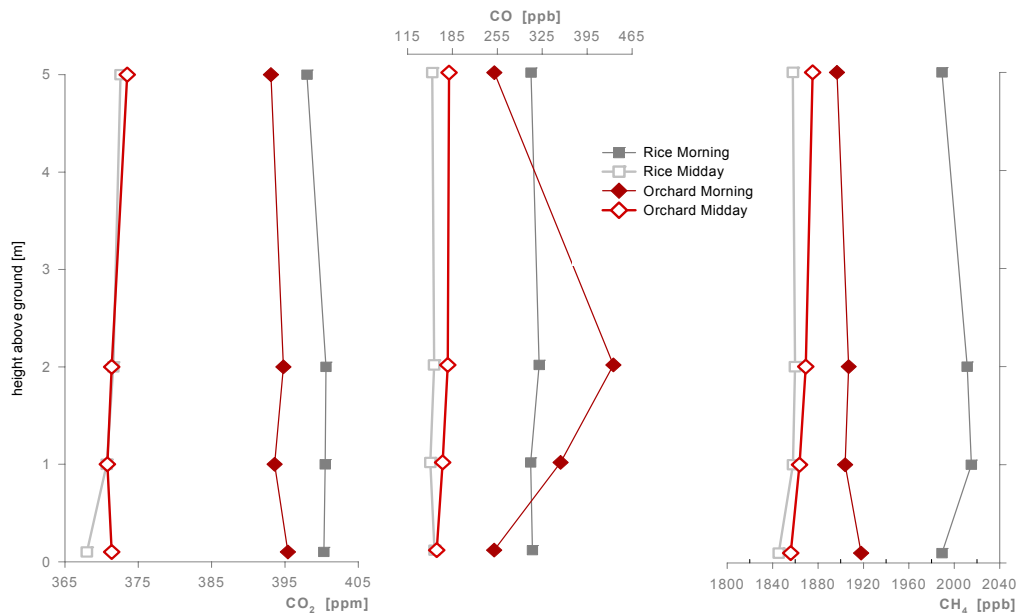


Figure 4.8. Mixing ratios of CO₂, CO and CH₄ from samples taken at the *Rice* field location and inside a citrus *Orchard* (Morning: 3 December 2001, Midday: 30 November 2001; Valencia / Spain).

Ground reference samples were taken at four different sites: Figure 4.8. presents the results from the rice field location and a citrus orchard, whereas figure 4.9. shows the sampling results from the remote mountain site and close to the highway.

For the rice and the orchard location a decrease of the CO₂ mixing ratio can be observed for the samples from before sunrise to around noon. This tendency can be recognized also for the other trace gas species (see data tables for reference). Remarkable are also the increase of the CO mixing ratio within the orchard and the high CH₄ mixing ratio at the rice field site in the morning.

Figure 4.9. compares the data from the ground reference samplings at the remote mountain site and beside a highway near Valencia. Remarkable are the high mixing ratios of CO₂ and CO in particular at the surface level near the highway, which is also associated with a low ¹³C isotope presence. In contrast the mountain site samplings are characterised by clearly less negative delta ¹³C values and lower CO₂ and CO mixing ratios. A slight decrease of the mixing ratios can be recognized until noon, which is associated with an increase of the relative fraction of the ¹³C isotope.

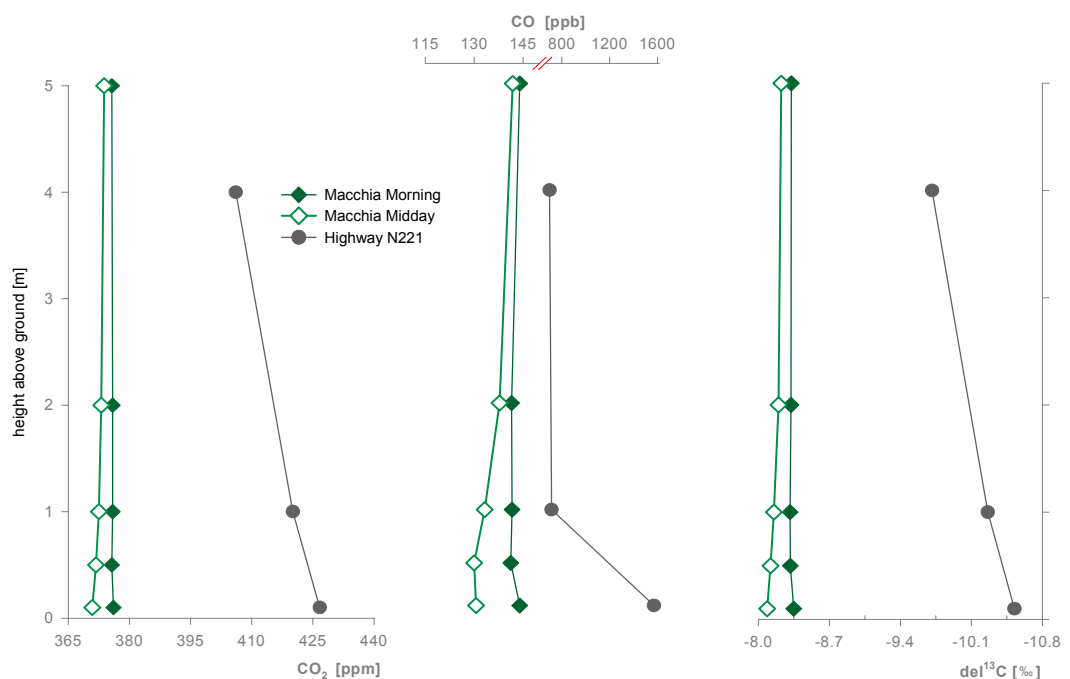


Figure 4.9. Results of the samples taken at the ‘Macchia’ remote mountain site and close to the ‘Highway N221’ (Valencia / Spain). Shown are the mixing ratios of CO₂ and CO and the delta¹³C values.

4.1.5. The Netherlands Winter Experiment

14 January – 10 February 2002

Test of the improved sampling strategy

Very intensive agriculture and a high level of urban sprawl are characteristic for the field site in the central part of The Netherlands.

Specific Intentions

From the results of the earlier campaigns it had become obvious that not only the instrumentation threatened the scientific goal but also changing air masses. With respect to the basic aim of the project – the estimation of a regional carbon budget and the qualification and quantification of sources and sinks – the suitability of the chosen approach is questionable. On one hand, it is fundamental for the identification of different contributions to the final budget that the characteristics of the individual sources and sinks should be distinguishable from each other. Therefore a background mixing ratio has to be found, from which contamination events and the carbon fluxes directed in- or outside the regional pool could be determined.

Another important question was to identify the sites and sampling heights which are characteristic for the entire region to be described.

One reaction to accommodate these requirements was to implement the ground reference unit for finding the trace gas characteristics of the major land classes. A second attempt focused on the proper flight sampling strategy itself: accomplished by the integration of an adapted investigation approach.

FLIGHT AND SAMPLING STRATEGY

Aim of the new strategy is to get additional information with respect to transformation processes due to the exchange of the local air mass by advection. The basic idea is to combine local results from sampling above characteristic land use classes with data representing the regional scale as a whole, by carrying out flights along a transect orientated at the prevalent wind direction. Compared to the common strategy, of measuring one vertical profile around a central point of the study region, the implementation of the new attempt is more complicated. The idea was to sample three individual sites across the study region, following a line from west to east: marshland, agricultural land and forest.

VARIABILITY OF THE WIND

An additional attempt focused on better wind field information. Because of air mass changes with unknown origin most frequently the sampled air probes are not useable for budgeting. Therefore, in a test mode vertical profiles should also include the wind vector.

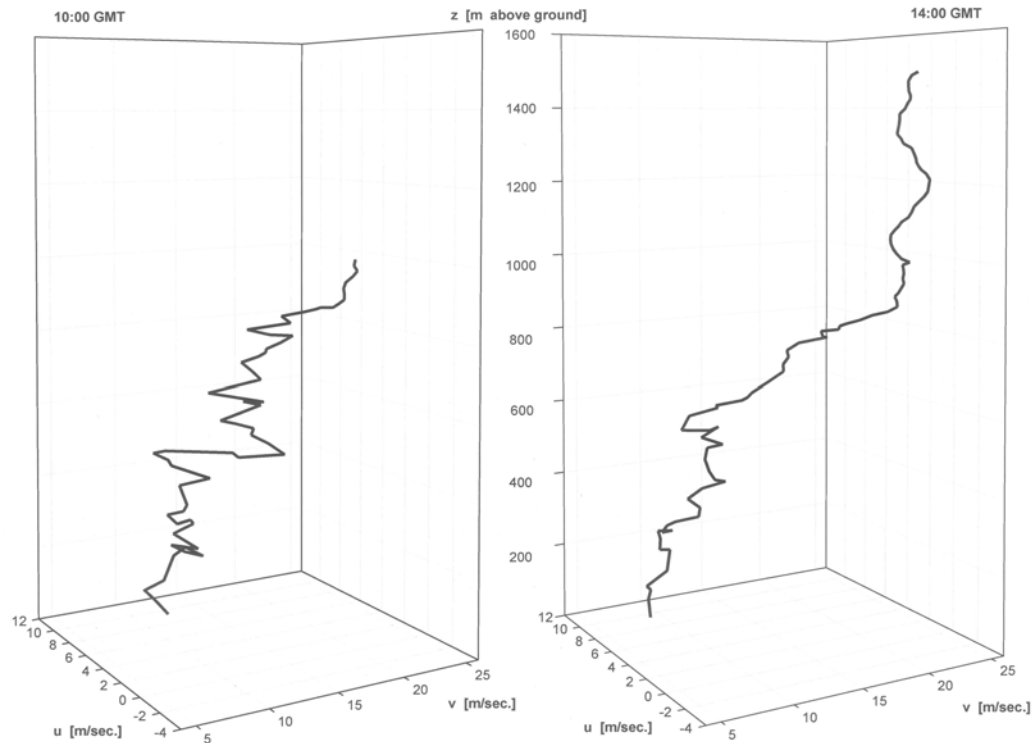


Figure 4.10. Wind velocities in u- and v-direction recorded by the MFP 'Sky Arrow' during the combined flight section above the Forest site on 29/01/ 2002 (The Netherlands).

Data from GIOLI, B. & B. DE MARTINO

Unstable conditions were predominant during the complete campaign. In particular a very inconsistent wind field at the spatial as also at the temporal scale became obvious, as documented by the records of the MFP when performing the combined vertical profiles (see figure 4.10.).

An overview of the observed trace gas mixing ratios and the delta¹³C values at lowest flight level and within the free troposphere is given in table 4.6.

	CO ₂ [ppm]	CO [ppb]	CH ₄ [ppb]	N ₂ O [ppb]	H ₂ [ppb]	SF ₆ [ppt]	delta ¹³ C [%]
Lowest Level	378 - 396	165 - 346	1859 - 2126	318 - 321	514 - 631	4.92 - 7.15	-8.390 - -9.465
Free Troposphere	372 - 379	126 - 203	1807 - 1846	318 - 319	505 - 559	4.82 - 5.18	-8.127 - -8.489

Heights LL and FT:

60 m / 915 m

Number of flight days: 5

Number of profile sites: 3

Table 4.6. Range between the maxima and minima of the mixing ratios and the delta¹³C values from the flask sampling during the winter campaign in The Netherlands.

The two flights presented in figure 4.11 were performed on 2 February 2002. All three sites were sampled uninterrupted, starting with the ‘Marsh’ location (north of the Cabauw Tower; morning: 10:00 UTC, midday: 14:20 UTC), followed by the ‘Maize’ site (morning: 10:50 UTC, midday: 15:10 UTC) and finished at the ‘Forest’ (morning: 11:30 UTC, midday: 16:00 UTC; here only the two lowest heights were sampled, caused by the flight time capacity of the aircraft). Obvious are the decrease of the CO₂ mixing ratio and the shift of the delta¹³C to less negative values between both flights through the entire profile, whereas the CO mixing ratio at the lowest two sample levels increased. The highest reduction of the CO₂ mixing ratio in the lower atmosphere was observed at the ‘Marsh’ site. For all trace gases the values measured within the free troposphere were lower than the mixing ratios sampled beneath.

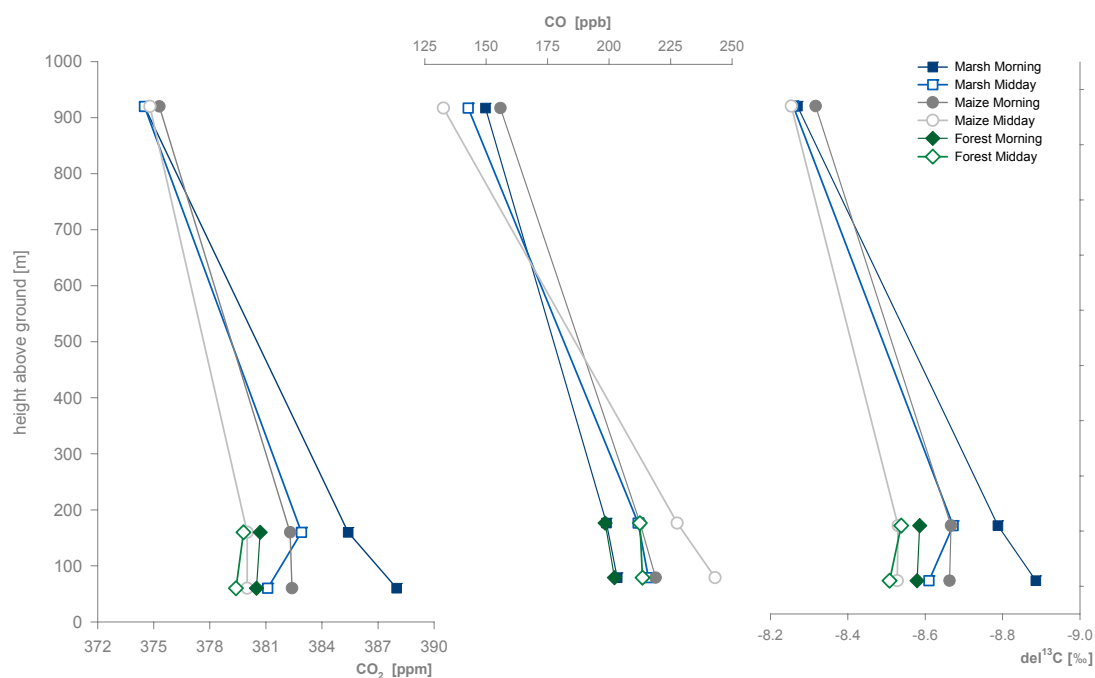


Figure 4.11. CO₂ and CO mixing ratios and delta¹³C values from profile flights on 2 February 2002 above the ‘Marsh’ [Cabauw], the ‘Maize’ and the ‘Forest’ site (The Netherlands).

Additional ground reference measurements and samplings were carried out at all three different land use types. Results from the flask sampling performed at the ‘Marsh’ location and within the forest nearby the ‘Loobos Fluxnet Tower’, a few kilometres north-east of the ‘Maize’ reference site are displayed in figure 4.12.

Morning samples at the forest site were taken on two different days (4 and 6 February 2002), both around 6:40 UTC. Midday sampling took place on 5 February around 13:00 UTC. Samples at the 'Marsh' site were performed on 6 (midday) and 7 February 2002 (morning) at the same local time as at the forest location.

A large difference of the CO₂ mixing ratio and the delta¹³C values between the morning and midday data at the 'Marsh' site is obvious. On the other hand the decrease nearest the surface, observed during the day, is smaller in the forest than the difference that can be recognized between the samples taken in the morning of the 4 and the 6 February 2002.

Compared with the data from the flights similar behaviour is obvious, reflecting in particular the tendency of a decreasing CO₂ mixing ratio and an increase of the ¹³C isotopes during day time.

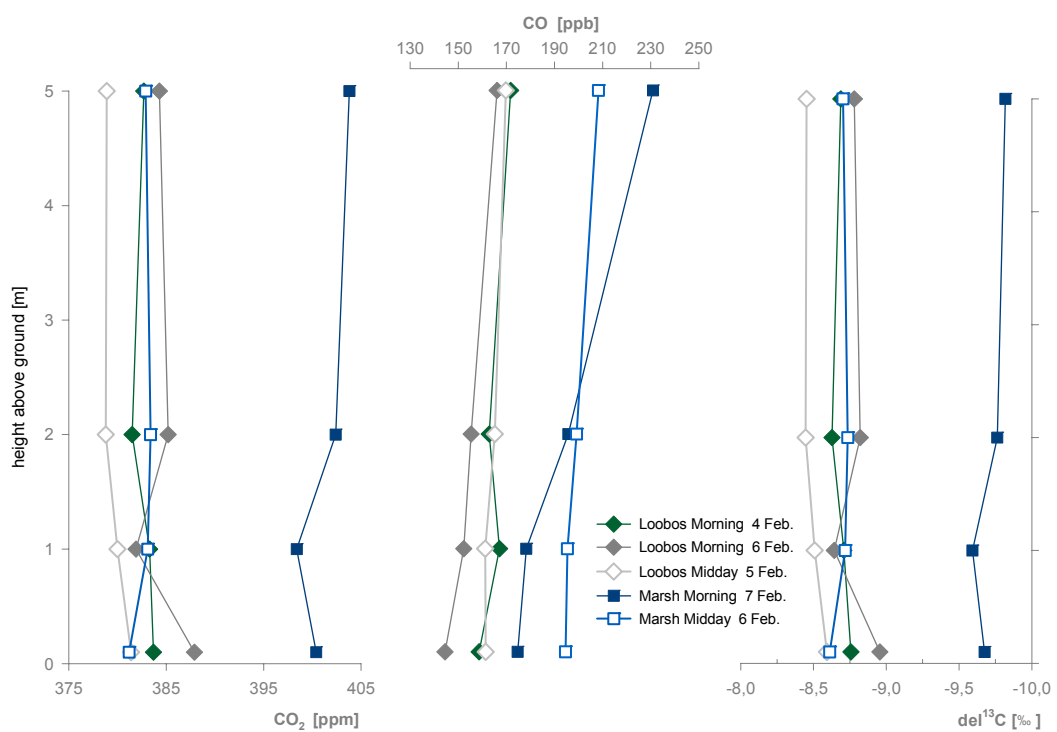


Figure 4.12. CO₂ and CO mixing ratios and delta¹³C values from ground reference samplings carried out in a forest nearby the 'Loobos Tower' and within the 'Marsh' area north of the Cabauw Tower (The Netherlands).

4.1.6 Lazio Summer Experiment

27 May – 27 June 2002

The experiment took place in the northern part of the Lazio region, Italy. Mostly forested mountain ridges and intense agriculture in the plains west of the mountains are characteristic for this study area.

A specific goal of this campaign was to proceed with the ‘transect approach’ (see chapter 5.4.2.). Additionally the examination should be extended by studies regarding the development of distinct layers [MUSCHINSKI & WODE 1998]. To accomplish this it was aimed to sample at an isolated site, where during night time a clear stratification of layers from different origin would occur. Therefore flights were carried out within and above a bowl-shaped valley near the settlement of Orvinio.

Observations

Because of several technical problems flights could be performed on two days only in the morning and in the afternoon. Thus only singular events have been investigated. An overview of the observed trace gas mixing ratios and the delta¹³C values at lowest flight level and within the free troposphere is given in table 4.7.

	CO ₂ [ppm]	CO [ppb]	CH ₄ [ppb]	N ₂ O [ppb]	H ₂ [ppb]	SF ₆ [ppt]	delta ¹³ C [%]
Lowest Level	366 - 410	130 - 369	1796 - 1884	318 - 320	542 - 670	5.16 - 5.76	-7.775 - -9.840
Free Troposphere	373 - 375	101 - 682	1778 - 1801	317 - 318	534 - 1056	5.03 - 5.15	-8.124 - -8.209

Heights LL and FT: 50 - 80 m / 3000 m Number of flight days: 2.5 Number of profile sites: 2

Table 4.7. Range between the maxima and minima of the mixing ratios and the delta¹³C values obtained from the flask sampling during the airborne campaign in the Lazio region (27 May to 27 June 2002).

Figure 4.13. presents the flight profiles from both locations. For the CO₂ mixing ratio at the two lowest levels a decrease is recognizable between the morning and the midday flight, distinct particularly at the Orvinio location, associated with a relative increase of the ¹³C isotope fraction. For CO no clear decrease is visible. Instead, a very high CO mixing ratio was found above the mountain site, as well as a large difference between the morning and the midday flight at both locations within the free troposphere. A diurnal variation of the CO₂ mixing ratio and the delta¹³C values becomes also obvious by the ground reference samples, however a differentiation between both sites is not so clear as for the flight data.

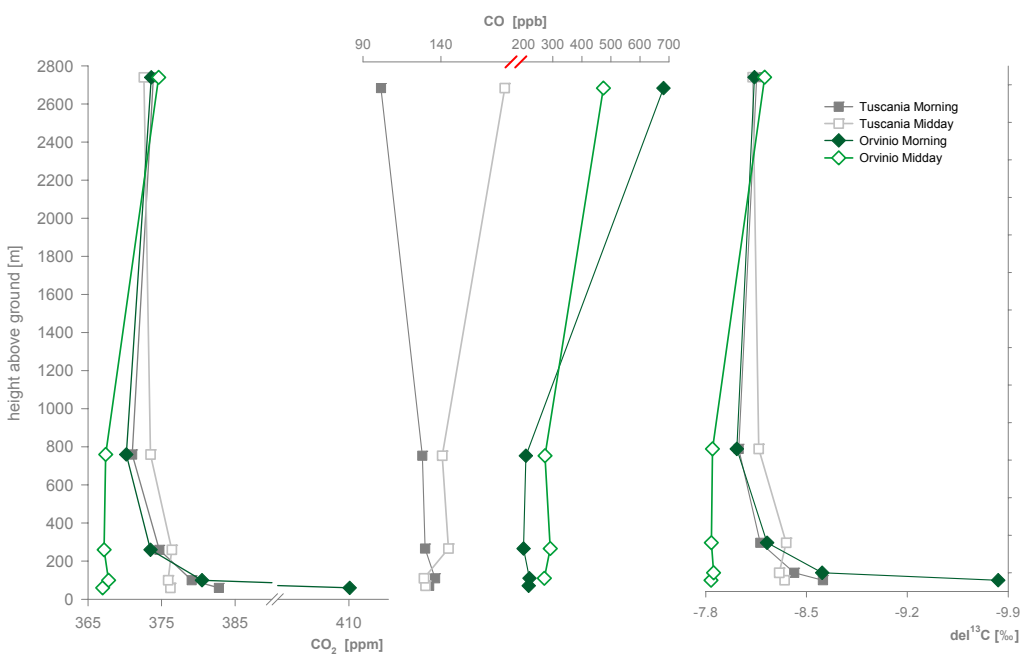


Figure 4.13. CO₂ and CO mixing ratios and delta¹³C values obtained from the profile flights performed at the 'Tuscania' [Roccarespampani] site on 15 June and above the remote mountain location 'Orvinio' on 18 June 2002 (Lazio / Italy).

The highest values could be observed closest to the ground (see figure 4.14.). Contrary to the general behaviour of CO₂ and delta¹³C at the mountain site the CO increased strongly from the morning to the midday sampling; but a distinct jump upwards was observed for the 1 m samplings in CO₂ and delta¹³C.

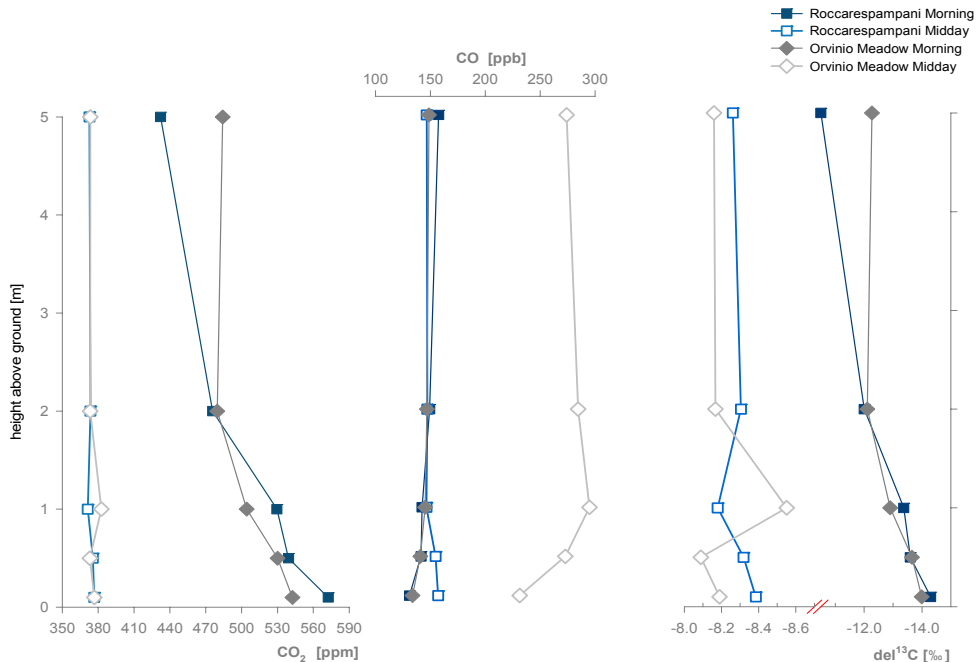


Figure 4.14. Ground reference samples taken beside the tower at the 'Roccarespampani' forest site and above a Meadow within the valley of 'Orvinio' (Lazio / Italy). Shown are CO₂ and CO mixing ratios and the delta¹³C for samples taken before sunrise (Morning) and around noon (Midday).

4.1.7 The Netherlands Summer Experiment **Enhancement of the improved sampling strategy**

10 – 28 July 2002

Main emphasis was to improve the enhanced ‘transect approach’ sampling strategy (see ‘The Netherland Winter Experiment’), that aims to combine the quantification and qualification of the most important sources and sinks with the carbon budget synopsis for the entire region. Also specific attention was given to a comparison of the winter and summer results, in particular with respect to differences of the mixing ratios and the responsible processes.

Observations

An overview of the observed trace gas mixing ratios and the delta¹³C values at lowest flight level and within the free troposphere is given in table 4.8.

	CO ₂ [ppm]	CO [ppb]	CH ₄ [ppb]	N ₂ O [ppb]	H ₂ [ppb]	SF ₆ [ppt]	delta ¹³ C [%]
Lowest Level	359 - 403	132 - 264	1855 - 2166	319 - 327	561 - 684	5.16 - 5.66	-7.536 - -9.566
Free Troposphere	364 - 370	113 - 151	1776 - 1819	318 - 319	556 - 649	5.13 - 5.31	-7.716 - -8.041

Heights LL and FT: 60 m / 1700 - 1800 m Number of flight days: 3 Number of profile sites: 3

Table 4.8. Range between the maxima and minima of the mixing ratios and the delta¹³C values obtained from the flask sampling during the summer campaign in The Netherlands (10 to 28 July 2002).

An example for the flight profiles is given in figure 4.15 for the 15July above the marshland north of the Cabauw Tower and near to the ‘Maize’ reference site at around 8:00 UTC at the ‘Maize’ site and at 9:00 UTC at the ‘Cabauw’ location, as well as at 12:45 UTC (‘Maize’) and at 13:50 UTC (‘Cabauw’).

Except for the two lowest morning sample levels at the ‘Maize’ site only slight differences can be recognized in the profiles of the CO₂ mixing ratio and the delta¹³C values. But contrary to these parameters great variability is obvious for CO. Remarkable is a clearly reduced mixing ratio sampled at the level of 915 m height above the ‘Maize’ location, and a decrease between the morning and the midday sampling within the free troposphere.

Ground reference sampling was again carried out inside and above a maize field (18 July; 4:00, 11:00 and 15:30 UTC), at the same location as in winter for the marshland north of the Cabauw Tower (28 July; 4:00, 12:00 and 16:30 UTC).

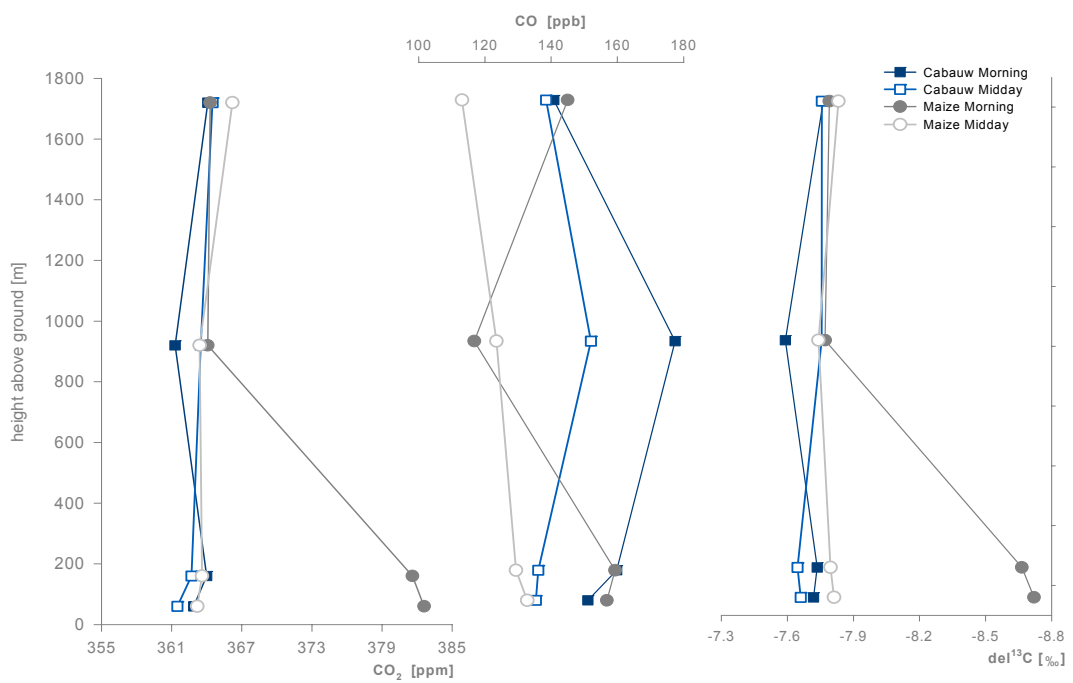


Figure 4.15. CO₂ and CO mixing ratios and delta¹³C values from profile flights on 15 July 2002 above the marshland north of the Cabauw Tower and over the agricultural site nearby the 'Maize' ground reference location (The Netherlands).

The results in figure 4.16 point to very high mixing ratios of CO₂ and CO combined with a low ¹³C isotope fraction for the morning at the marshland site. At both locations during day time CO₂ mixing ratios decreased while the fraction of the ¹³C isotope increases. Thereby the highest ¹³C values were recorded nearest to the surface over the marshland around midday.

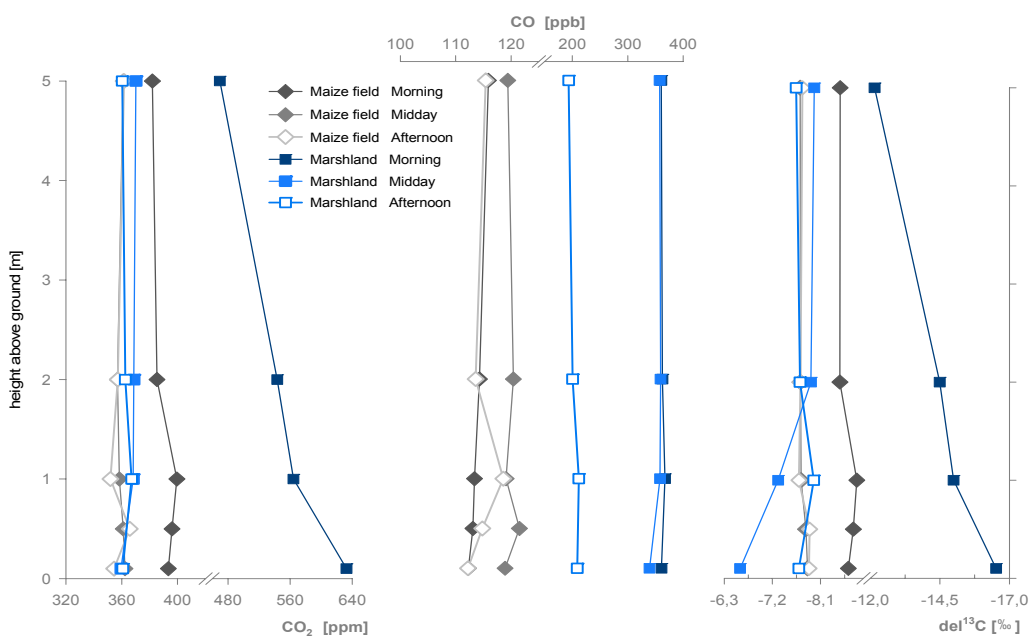


Figure 4.16. Mixing ratios of CO₂ and CO and delta¹³C values inside the Maize field on 18 July 2002 and on 28 July 2002 above the meadow site Marshland (The Netherlands).

4.1.8. SPA¹³CE Thuringia Summer Experiment Combined ground level and flight investigations

6 – 15 August 2002

During the first two weeks of August an intensive measurement activity focussing on different scales has taken place in and over the Hainich National Park.

Aim of the SPA¹³CE (Soil Plant Atmosphere ¹³C Exchange) experiment was to monitor the isotope characteristics from the microbiological level up to the regional and continental scale over a period of several days. Within the project vertical profiles of mixing ratios were measured above the Hainich on the 6, 14 and 15 August 2002 twice a day.

Table 4.9. Weather conditions recorded at the Hainich Tower 14 and 15 August 2002
(Temperature at 2 m height, wind velocity and direction at the top of the tower)

	Temperature [°C]		Wind velocity [m/s]		Wind direction
	Max.	Min.	Max.	Min.	
14 August 2002	19.5	14.4	4.1	1.3	WNW
15 August 2002	22.8	16.8	2.8	0.8	N

The experimental strategy was, to jointly analyse for several ecosystem levels with the intention to obtain insight into the isotopic composition at different spatial scales. Therefore a basic need was to close the gap between the tower and the flight measurements, which could be achieved by lowering the lowest flight level to the height of the uppermost tower platform (see also the investigation carried out during the ‘Valencia Winter Experiment’, chapter 4.1.4. and 4.2.2.).

An overview of the observed trace gas mixing ratios and the delta¹³C values at lowest flight level and within the free troposphere is given in table 4.10.

	CO ₂ [ppm]	CO [ppb]	CH ₄ [ppb]	N ₂ O [ppb]	H ₂ [ppb]	SF ₆ [ppt]	delta ¹³ C [%]
Lowest Level	362 - 373	90 - 144	1797 - 1877	319 - 321	510 - 538	5.18 - 5.50	-7.559 - -8.125
Free Troposphere	364 - 371	66 - 135	1748 - 1849	318 - 319	522 - 535	5.07 - 5.61	-7.822 - -7.972

Heights LL and FT: 60 m / 1500 m Number of flight days: 3.5 Number of profile sites: 2

Table 4.10. Range between the maxima and minima of the mixing ratios and the delta¹³C values during the SPA¹³CE experiment performed on 6, 14 and 15 August 2002 above the Hainich and from a singular flight on 9 August 2002 for the ‘Holzland’ site south-east of Jena.

Quite similar results for the CO₂ mixing ratios and the delta¹³C values were obtained by the comparison of the concurrently performed tower and flight

samplings. For the first time the gap could be closed and a direct upscaling was possible from the local to the regional scale.

Additional emphasize of the flight investigations was to monitor the gas mixing ratios and isotope composition on consecutive days. A detailed study of the vertical profile structure, with respect to the rate of mixing, was one more specific aim. Another focus was on to examinations of the vertical structure of the CBL with respect to mixing processes.

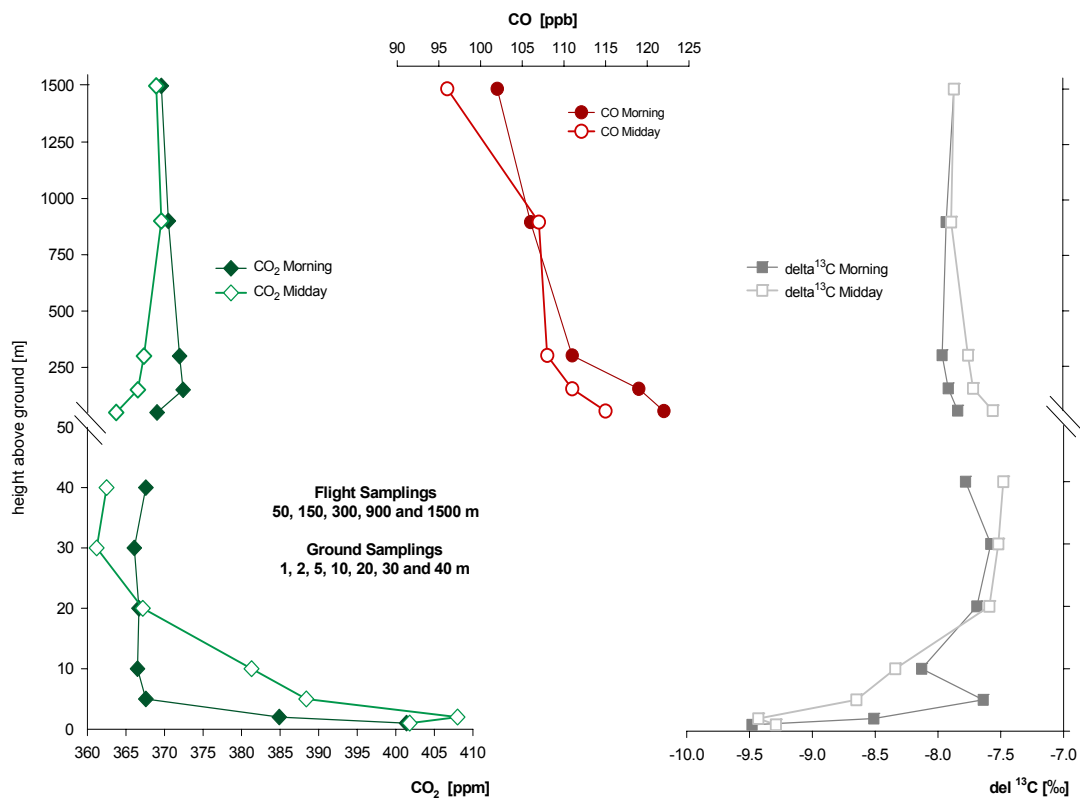


Figure 4.17. Profiles of CO_2 and CO mixing ratios and $\text{delta}^{13}\text{C}$ values on 15 August 2002 from ground level to the free troposphere at the *Hainich* (Germany). Near surface samplings were carried out by A. Knohl.

Observations

The results from both the flight and groundbased samplings, performed simultaneously on 15 August 2002, are presented in figure 4.17. Firstly, it should be recognized that the profiles taken by the tower and by the flight samplings for the same height level correspond very well. From the 30 m level upwards both profiles show a distinct decrease of the CO_2 mixing ratio during the day while the relative fraction of the ^{13}C isotope is increasing. A remarkable observation from the

flight profile is the stability of the CO₂ mixing ratio and of the delta¹³C values with increasing height, starting from the 150 m level, whereas the CO mixing ratio decreases significantly between both samplings as well as with increasing height. In contrast to the observations made on this day data from the day before and from 6 August differ strongly regarding the mixing ratios and the delta¹³C values. Stratification and the presence of distinct layers during the whole day were observed on all days (see figures 4.28. and 4.29.).

4.2. Interpretation of the Results

To reach the primary goal of RECAB, the characterisation of the different study regions, the structure of this section follows the division into different zones.

From the first analysis of trace gas mixing ratios it became obvious that frequently the fundamental assumptions for the CBL budgeting are not met even after major modifications of the sampling system and of the sampling strategy. Therefore, the results will be interpreted now in a more qualitative way

Southern Europe

4.2.1. Valencia Summer Experiment

17 June – 7 July 2001

The high night time values of CO₂, CH₄ and N₂O observed in the ground reference samples (see figure 4.2) might be caused on one hand by the occurrence of stratification within the canopy. On the other hand, an enhanced activity of soil related processes, resulting from higher soil moisture, is most likely. Reduced microbial activity, caused by the drying of the soil, and forced mixing by turbulence during day time should effect a decreasing of the mixing ratios on 5 July 2001. Contrary to this assumption the N₂O profile shows an increase of the mixing ratio, which can be explained by an exchange of local air by air that has passed recently irrigated orchards. Since all apricot trees of the orchard were trimmed between both sampling events the CO₂ uptake was less than the days before.

A decrease of the CO₂ mixing ratio from the morning to the midday flights was detectable at both locations: For the rice field data a significant contribution by vertical mixing can be excluded. Because of the large variability seen for the entire profile a combination of CO₂ uptake by plants and advection of CO₂ poor marine air seems most probable.

The effect of a mesoscale circulation becomes evident when inspecting the CO₂ mixing ratio at the highest flight level, where an increase is obvious between the morning and the midday flights. In the morning the inflow of marine air in the upper branch of the night time circulation is reflected, while during midday air originates from inland, as in the late morning hours the night time off shore wind was replaced by a flow directed to the inland at the surface.

Under such conditions a budget estimate is not possible, since the air masses are rather independent because of their different origin and evolution.

Since the air mass exchange also affects the uppermost level it is dangerous to use this 'free troposphere sample' as a background value for the budgeting.

Even though the modified sampling unit worked well the anticipated improvements regarding a reduction of the flask pair deviation by adapting the sampling flow rate could not be fully achieved. Most probable reasons for this remaining difference are the heterogeneity of the land use and, in particular, strong trace gas point sources because of biomass burning scattered around the orchards. Because of these major local disturbances a regional characterisation with respect to the carbon budget cannot be accomplished by flask sampling.

4.2.2. Valencia Winter Experiment 16 November – 15 December 2001

By analysing the results from flight and near surface sampling the presence of a mesoscale circulation scheme, however less developed than in summer, can be detected. Remarkable are the high mixing ratios above the rice fields at the lowest flight level, probably due to an outflow towards the sea - bearing air of urban origin. In contrast the data from the remote mountain site are characterised by only slight variability, which might be representative for 'undisturbed' rural conditions. A minimal plant activity is recognizable from the CO₂ mixing ratio and the delta¹³C values near to the ground: a slight CO₂ increase during night, coming along with more negative delta¹³C values. That the flight profiles are showing no clear signal might also be caused by the late time of the morning flight. Compared with the other sampled locations the site could be characterised as a remote area, only slightly changed by human activities. Because of this distinct character it could provide representative background data for typical mediterranean vegetation.

A remarkable feature of the near surface reference air samples in the orchard is the CO increase below and inside the still foliated canopy of the trees. Since this behaviour is only recognizable for CO probable is the capture of a smoke plume from the biomass burning around this sampling spot. That the CO₂ mixing ratio is

less affected might be caused by enhanced values from soil respiration captured in a layer close to the ground, which masks the increase in the next upper levels.

The elevated CH₄ mixing ratio found at the rice field site during night time is reflecting the contribution of methanogenic bacteria, which were still active in the mud.

From the enhanced sampling near to the surface, in particular from the activity close to the highway, additional information could be obtained with respect to advection processes. By comparison of the individual signals from the reference sites a strong change in air mass characteristics became evident. Data from the sampling close to the highway exemplifies the fossil fuel contribution (see figure 4.9).

Around the reference tower in the rice field site lowest level flights (<10 m above ground) could be performed. By closing the gap to the near surface measurements the comparison of the reference samples with the flight samples became possible, as well as an estimation of effects caused by using different sampling equipment and schemes. Results from the near surface sampling and from airborne samples taken at lowest flight level are displayed as 'Keeling plot' in figure 4.18. The source signal was calculated to be -25.5 ‰, which is in the typical range for C3 vegetation.

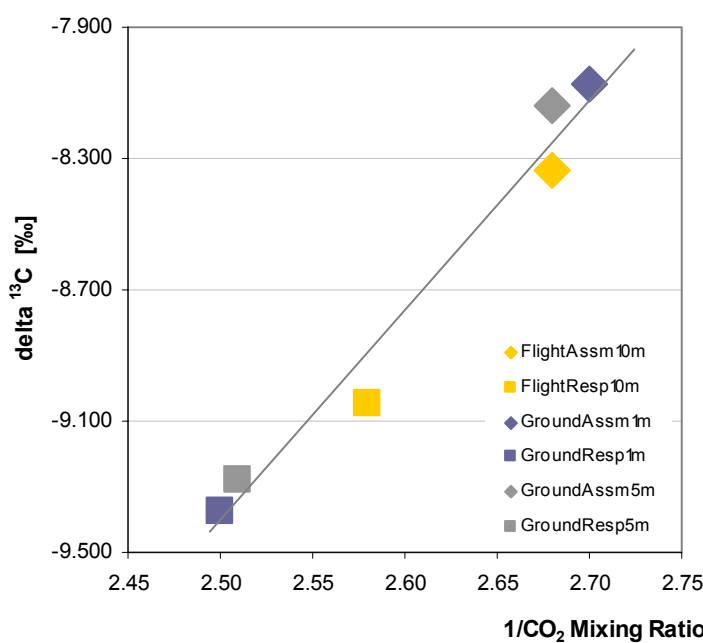


Figure 4.18.

delta¹³C and CO₂ mixing ratios sampled at two heights by the ground reference unit and from the lowest flight level above the Rice field site (Valencia / Spain).

Source -25.5 ‰, R² = 0.9714

Taking into account that the airborne samples were taken delayed, shortly after sunrise, and that the flight data are representing a larger area – the track around the tower was approximately 1000 x 1000 m, with slightly different surface conditions like water cover, plant density, etc. - the results from both systems agree very well (see for further description also in the documentation folder figures 5 and 6, and the flight scheme).

Additionally the very shallow stable layers in the morning, containing the mixture of the upwind emission sources, could be sampled.

Because the effect of air mass exchange by advection becomes more efficient with increasing altitude a budget which bases solely on the CO₂ mixing ratio and the delta¹³C values obtained from the flight samplings might underestimate the contribution by plant activity. Thus only by the combination of flight and additional ground level measurements and air samplings the mandatory information can be achieved.

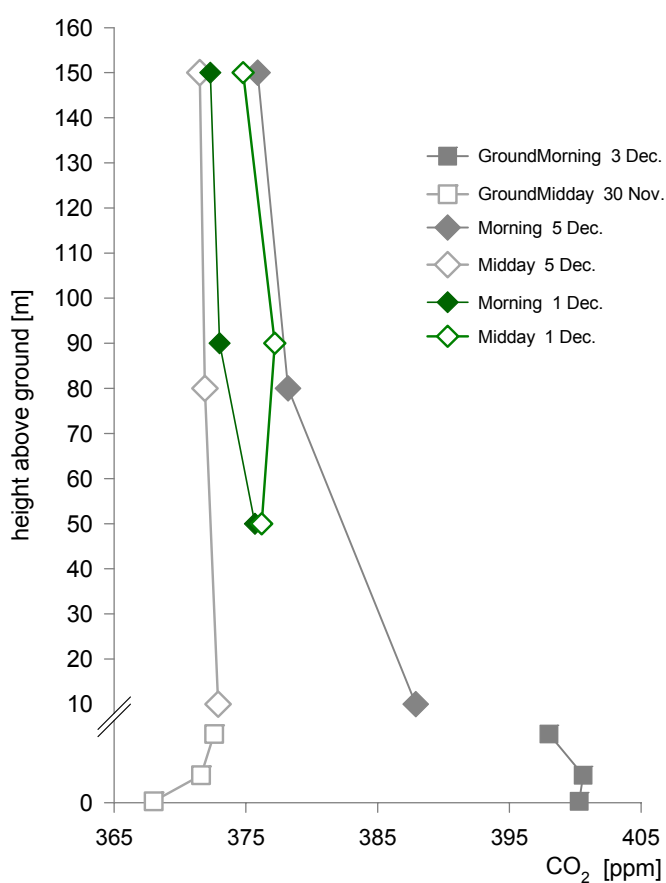


Figure 4.19.

CO₂ mixing ratios from flask samples at ground level and from two different flight days above the Rice field site (Valencia / Spain).

The lowest flight level above ground was on 1 December 50 m, which could be reduced down to 10 m on 5 December.

4.2.3.1. Lazio Summer Experiment

27 May – 27 June 2002

Although profiles could be taken only on one day each for both locations interesting observations were made: For both sites a well developed change of the CO₂ mixing ratio was recorded. When comparing the data from the samplings close to the ground only slight differences in the mixing ratios of CO₂ and delta¹³C became obvious. In contrast the results from the flights are clearly different between both locations. The main reason was the relative small extension of the Roccarespampani forest, which contributed only little to the flight profile. Regarding the differences obtainable at both profile locations it has to be taken into account that at the mountain site the meadows and the forest at the ridges were still assimilating, whereas most of the agricultural areas around the Roccarespampani forest had just been harvested or ploughed.

Of special interest are the observed high CO mixing ratios at the mountain site. Especially one ‘stable layer’ could be identified by the free troposphere sample, indicating that the CBL was covered by a significantly different air mass. From the analyses and by the comparison of the trace gases and the delta¹³C values (see figures 4.13. and 4.20.) this air mass could be identified as one with exceptional composition: the covariance of low SF₆, but high CO and H₂ mixing ratios indicates as most probable source smoke from a forest fire (see also 4.2.3.3 ‘Back Trajectory Calculations’).

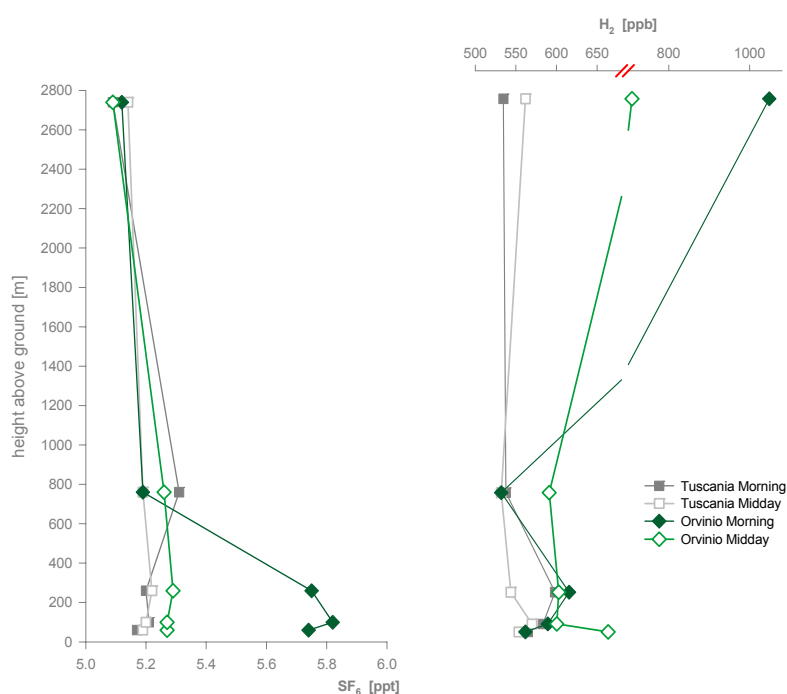


Figure 4.20.

SF₆ and H₂ mixing ratios obtained from flight profiles over the ‘Tuscania’ site on 15 June and above the remote mountain location ‘Orvino’ on 18 June 2002. (Lazio / Italy)

An increase of the mixing ratios is also recognizable during daytime at the lower levels, which will be affected by entrainment of the contaminated air.

A high diurnal variability could be also observed within the free troposphere at the 'Tuscania' flight location; however the difference through the entire profile is less developed than at the mountain site. In consequence the suitability of the free troposphere samples to provide background data has to be checked individually.

One further remarkable result from the near surface sampling at the 'Orvinio' site was the increase of the CO mixing ratio during day time, associated with a clear upward jump of the CO₂ mixing ratio and the delta¹³C value obtained from the flasks sampled at 1 m height. During the period of sampling a meadow was mowed in a few hundred meters distance. Probably the samples were contaminated by advected exhausts of the tractor.

The development of a stable, i.e. stratified layer is conceivable from the comparison of the reference and the flight data: the lowest flight level reflects the characteristics of the meadows, whereas the results from the next upper sample heights indicate air from the forested slopes (not shown; see the data table in the documentation folder). This suggests that a first nocturnal boundary layer was covered by at least one more air mass draining downhill from the ridges. The layer structures inside the valley were dissolved during day time, most probably from circulation driven by thermal convection and overflows over the ridges.

A comparison of the results from Italy with the summer campaign in the Valencia region is problematic: in Italy both locations were sampled only on one day and the background values from the free troposphere are affected by forest fire smoke. On the other hand the results from the campaign in Spain are as well unique, because of the influence from local biomass combustion and the sea breeze circulation.

4.2.3.2. Inverse Studies

One RECAB goal was to use the field data for modelling studies. Modelling in this thesis offers the opportunity to present two aspects: 1) the use of models for the spatial assignment of source areas, and 2) the evaluation of model results by multiple tracer analyses. For example, which uncertainties occur when using only CO₂ data as input parameter for the interpretation of modelling? The answer can be with a mesoscale dispersion model.

Since it became obvious from the multiple tracer analyses, that often distant source areas and formation processes seems to be responsible for the trace gas mixing ratios, a second case study presents modelling including back trajectory calculations.

4.2.3.2. Mesoscale Dispersion Model

High resolution calculations were performed by GORKA PÉREZ-LANDA from the CEAM in Valencia using the mesoscale model MM5. Therefore a potential source was defined in Milano (45°46' N / 09°16'E, source height 50 m above ground) from which 100.000 particles were released continuously during the simulation intervals (from 2002/06/15 03:30 UTC to 2002/06/18 13:00 UTC). The model calculated u, v, w and turbulence, thus taking into account variances of wind velocity and Lagrangian autocorrelations. The spread of the particles was simulated with the Langevin equation.

Figure 4.21 displays the dispersion of polluted air from Milano over a period of three days. On June 17 the plume arrives at the location of the flight profile, i.e. Milano might have contributed. However, from the interpretation of the multiple tracer analyses an influence by biomass burning might be more likely than a contamination by urban or industrial provenance: In particular the relative low SF₆ mixing ratios and the delta¹³C value are indicating a rural source, and the CO data point to a fire in the smoldering stage (see figures 4.13. and 4.20.).

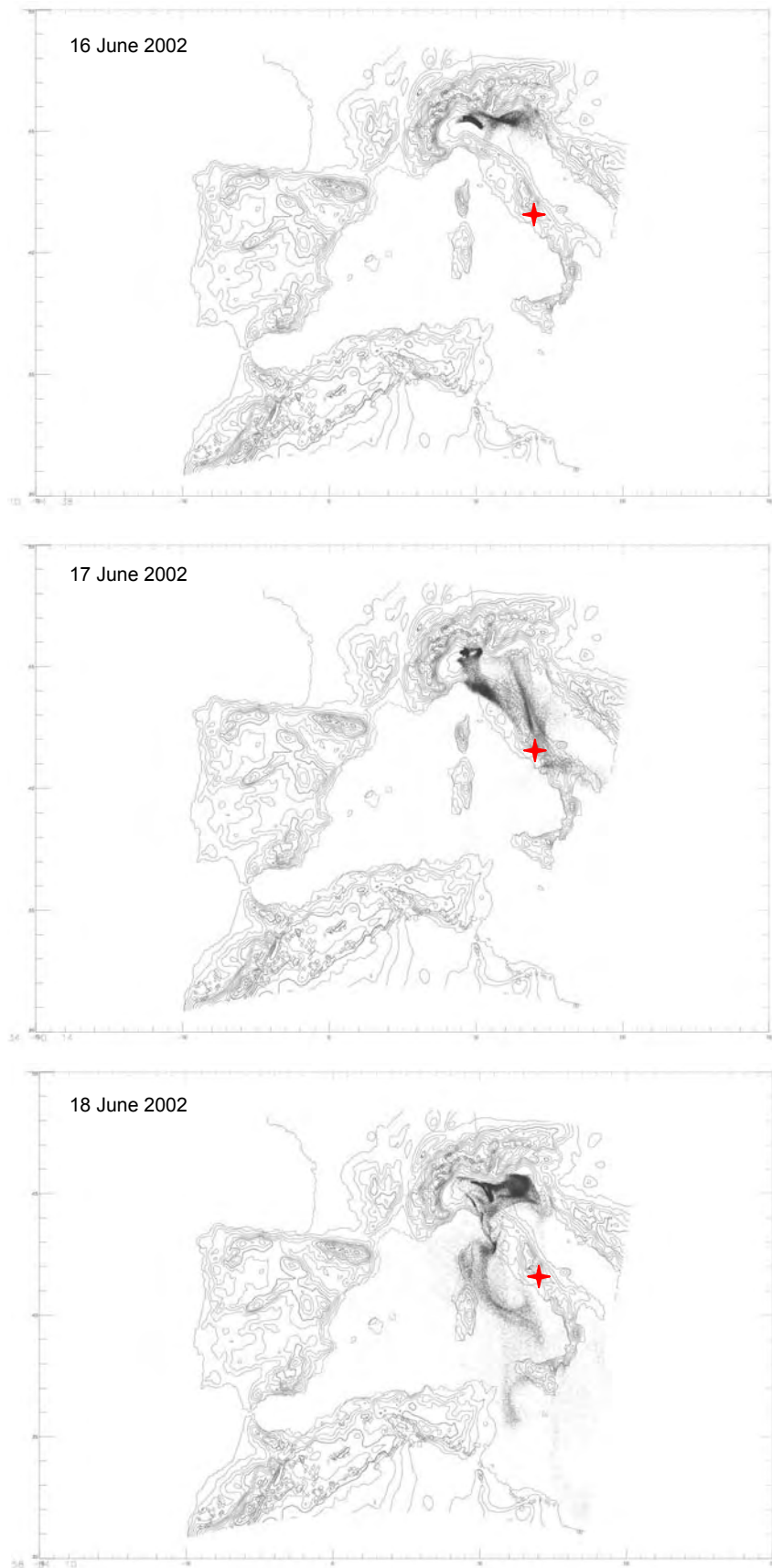


Figure 4.21.

Modelled dispersion of polluted air released continuously at the location of Milano (Italy).

The images are representing the positions of the particles on 16, 17 and 18 June 2002 at 4:30 UTC.

Profile site is indicated by the red star.

Modelling by GORKA PÉREZ-LANDA, CEAM

4.2.3.3. Back Trajectory Calculations

From the multiple tracer analyses as a source of the air sampled on 18 June 2002 at the 'Orvinio' site a wild fire event seems to be most probable. To narrow down suitable source areas back trajectories were calculated for the day before and the actual day the flask samples were taken.

The model revealed some interesting information: the occurrence of long range transport with a rapid crossing of the Atlantic Ocean is described by all model runs (see figures 4.22. and 4.23.) The backward calculation for a detection on 17 June 2002 at 14:30 UTC agrees with the pathways described by STOHL et al. [2003] for observations made in the context of the rapid transport of air masses by so called 'meteorological bomb' events.

Since long range transport of air masses from North America to Europe have been described before [FORSTER et al. 2001] specific attention was given to this process. In a recent publication even the circulation of forest fire smoke around the entire globe is presented [DAMOAH et al. 2004]. The trajectories for June 17 (21:30 UTC) and 18 June 2002 (11:30 UTC) cross the Atlantic within the free troposphere.

From the MODIS fire observation database [<http://rapidfire.sci.gsfc.nasa.gov>] and the Web Fire Mapper Archive [<http://maps.geog.umd.edu/maps.asp>] wildfire events within the period and the spatial range of the 'particle pathways' could be identified on the east coast of the US as well as along the path in Canada (see the documentation of the 'Lazio Summer Campaign' on the CD-ROM).

Even if the time period between the assumed uptake of air from a smoke plume and the detection or sampling at the Italian mountain site comprises several days the origin of the sampled air from wild fires in the boreal areas of Canada and/or from the east coast of the US are most likely (see also figure 5.2.). Because of the clean air conditions at the heights the trajectories passed over the ocean one can assume that no major transformation happened on the way across the Atlantic (see figure 4.23.). This is reflected also by the composition of the air samples, which are indicating an origin from a remote site or the habitation during an extended time period without significant contact to anthropogenic activity (see figures 4.13. and 4.20.).

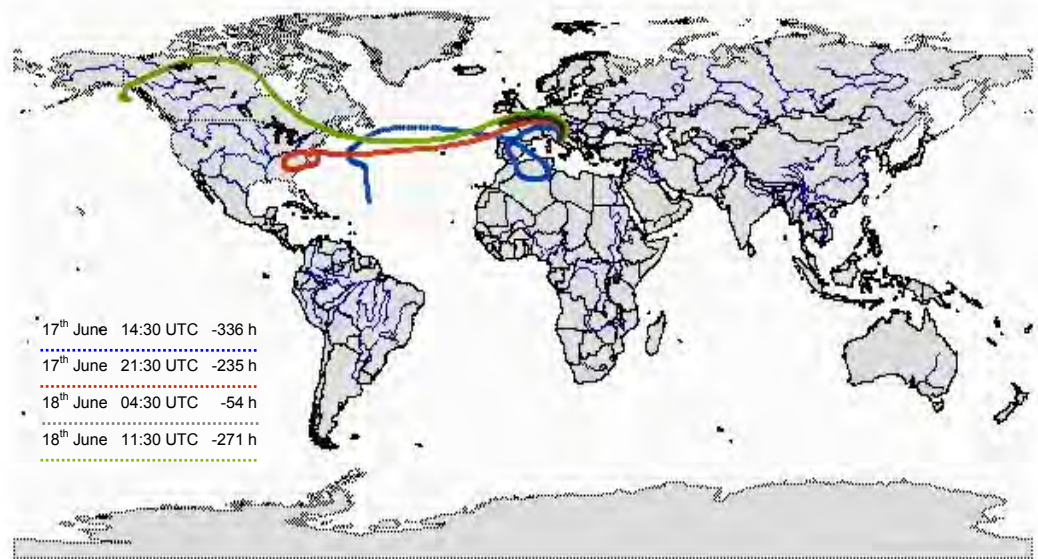


Figure 4.22. Back trajectories of air particles for a receiving point at the 2750 m sampling level above the Italian mountain study location 'Orvinio' (Lazio / Italy) using the 'HYPSPLIT' particle model [DRAKLER & HESS, 2002]. Assumed detections would be on 17 June at 14:30 and 21:30 UTC, 18 June at 11:30 UTC as also for the real sampling event at 04:30 UTC 18 June 2002. The total hours running backwards are indicated for each curve.

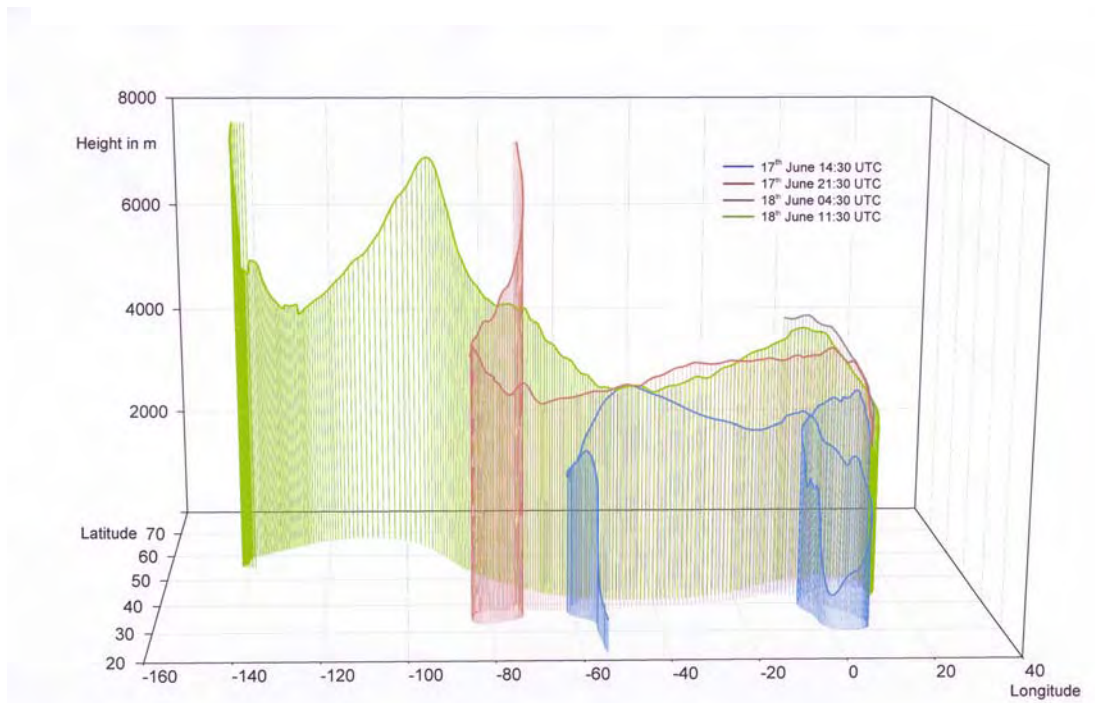


Figure 4.23. Same back trajectories as in figure 4.22. Displayed are the tracks and the heights.

Modelling by MARCUS SCHUMACHER, MPI-BGC

Northern Europe

4.2.4. Uppland Summer Experiment

11 August – 9 September 2001

Even if the samples were taken two weeks after the investigations performed around the Norunda Tower, close to the end of the growing season, the data from the Florarna wetland site reflect higher diurnal amplitudes of the CO₂ mixing ratio. The plant activity can be clearly identified by the related isotope values, which are reflecting nearly perfectly the discrimination of the heavier ¹³C isotope during assimilation (see data table in the documentation folder).

Another remarkable observation was the increase of the CO mixing ratios during day time. One possible explanation could be the conversion of CH₄ via formaldehyde to CO and H₂ (see reaction chain: 2.1.2.11 → 2.1.2.15a). However, because of the trend of the CH₄ mixing ratio (high night time values decreased until noon and then increased again in the afternoon) a CO production dominated by this formation seems unrealistic. A second process could be the conversion of VOCs, in particular since no indication of a source from traffic exhausts or biomass burning could be found via comparisons with the CO₂ mixing ratio or delta¹³C. Because a precursor of CO₂ is produced by the CO formation a more intense discussion of the observations will follow in chapter 5.2. (see figures 5.16 and 5.17).

Regarding all RECAB study regions the Uppland area provided the most homogeneous land use structure. Characteristics are the low rate of urbanisation and the absence of strong point sources, as found within the other campaign areas. Therefore only small disturbances by horizontal advection might be assumed. Nevertheless, the most likely explanation of the rapid CO increase at the Norunda site from midday to afternoon (see figure 4.4.) seems to be an exchange of the air mass by advection. But an identification of the origin is limited since high resolution wind field information is not available for the individual flight levels, nor were additional ground level reference samplings carried out for characteristic trace gas compositions and isotope ratios.

The intention of the sampling above two different typical land use units, the coniferous forest at Norunda and the Florarna wetland site, was to investigate the probability to detect the effects of individual sources and sinks.

A differentiation between the forest and the wetland location becomes clearly obvious from the CO₂ / delta¹³C ratios (see figure 4.24.) and the CH₄ mixing ratios. Because of the activity of methanogenic bacteria higher CH₄ mixing ratios have to be expected in swampy areas, which were confirmed by the flask samplings (see figure 4.5.).

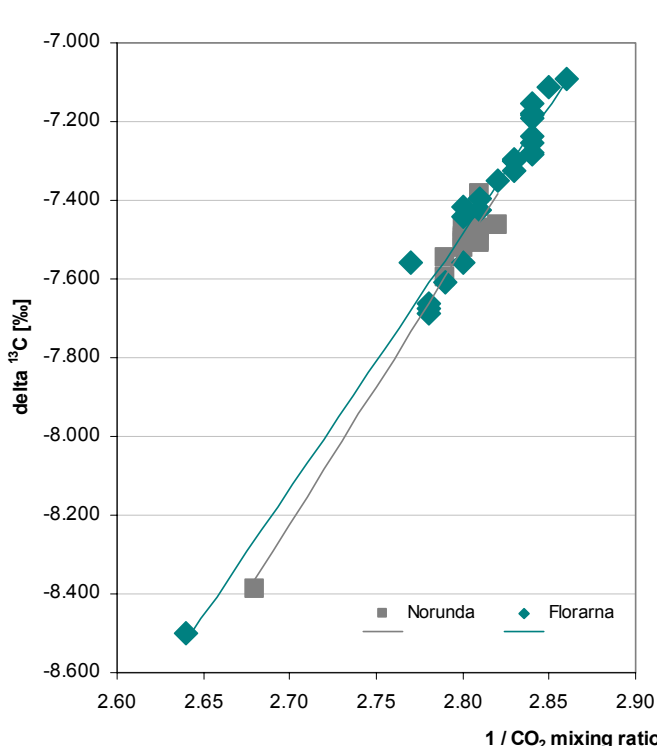


Figure 4.24.

Comparison of the *Norunda* site and the *Florarna* location (Uppland / Sweden) by the individual ratios of delta¹³C and the inverse CO₂ mixing ratios.

Norunda -27.2‰, R² = 0.9667
Florarna -25.6‰, R² = 0.9691

Flights performed at the *Norunda* site on 19 August, above the *Florarna* wetland on 29 and 30 August and 1 September 2001

With respect to the identification of individual contributions a closer examination was carried out at the Florarna site. At the ground level flask sampling was performed before sunrise and in the early afternoon to obtain distinct signals dominated by respiration and photosynthetic activity respectively, once within the open swamp and two times inside a wooded area. The afternoon sampling coincided with the flight activity, to get most actual data for the comparison of ground and flight samples and to minimize the potential of daily variations. Such variability was observed from the two investigations executed inside the wooded area (see also figure 4.25.). The differences seem to be mainly related to

temperature, humidity and in particular more stable conditions, caused by the reduced intensity of solar irradiance: during the cooler and rainy day higher CO₂ mixing ratios were recorded, correlated with more negative delta ¹³C values, indicating that the respiration rate exceeded assimilation.

Regarding the comparison of both ground level locations in particular the fact that the data from the open swamp reflecting a higher uptake, even if the vegetation (mostly sedges) was already in an advanced stage of senescence, seems to be surprising. A hypothesis to explain this observation is that the samples taken within the open swamp might rather be reflecting a contribution from the surrounding forests. But only the night time samples could be clearly related to the vegetation unit of the individual location; CH₄ mixing ratios up to 6600 ppb over the swamp versus maxima ~ 1900 ppb inside the wooded area (see data table in the documentation folder) speak against it.

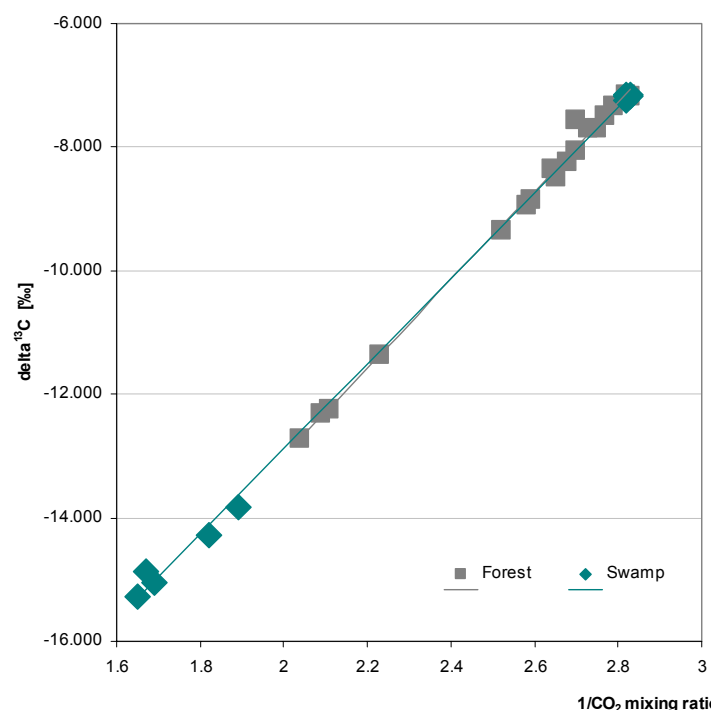


Figure 4.25.

Ratios of delta ¹³C and inverses CO₂ mixing ratios from the ground level investigations at the *Flororna* site (Uppland / Sweden) inside the wooded area and within the open swamp area.

The differing sources of CO₂ are indicated by the slightly different linear regression intercepts.

Forest -27.3‰, R² = 0.9956
Swamp -26.7‰, R² = 0.9989

However, since during day time higher wind velocities were recorded than during the night horizontal transport which affected the day time samplings could not be excluded. Also when taking the other trace gases into account no clear differentiation between the wooded part and the open swamp is possible.

Despite the large uncertainty an interpretation of the different values for both sites is attempted. Regarding the relation of inverse CO₂ and delta¹³C the wetland samples seemed to be affected by different sources than the ones from the wooded part, which are characterised by slightly more negative delta¹³C (see figure 4.25). This relation is nearly equal to the one obtained from the flights above the forest around the Norunda tower. However, the expected mixed signal from wetland and forest was not reflected by the Florarna flight samplings; instead a source characterised by a less negative value seemed to be dominant (see also figure 4.24.), which could not be identified from the available observations.

From the comparison of the ground and the flight data two conclusions can be obtained: (1) although the lowest flight level was at 50 m above ground (30 – 40 m above the canopy) the morning flights did not sample the boundary layer. (2) The measurements are affected by advection even in this rather homogeneous terrain.

Central Europe

4.2.5. Thuringia Summer Experiment

15 July – 2 August 2001

When comparing the results from both locations in particular the higher mixing ratios at the 'Gebesee' site became obvious. Especially the morning sample taken at the lowest level is surprising, since for two reasons a smaller difference to the data from the 'Hainich' should be expected: Because most of the crops in the surrounding area of Gebesee were just in the stage of maturity a weaker signal reflecting plant activity might be assumed. And, since the sampling at the 'Hainich' was performed nearly one and a half hours earlier the contribution from respiration should be more distinct at that site. A probable explanation could be that at the 'Gebesee' site an air plume of urban origin was sampled, released with the starting thermal mixing from the stable nighttime boundary layer. In addition a further contribution by horizontal transport might be possible. Advection seems in general not negligible since related variations were observed by the diurnal samplings also for the other trace gases. Similar conclusions may be drawn from the 'Hainich' flights. For the rather small decrease of CO₂ mixing ratios between midday and afternoon the vegetation seems not to be responsible, since no signs related to a reduction of the photosynthetic activity were observed. The comparison of the gas and isotope ratios indicates that the variability might be rather a result from advection, masking the photosynthetic activity by the replacement of the rural local air by air of more urban origin.

Because of the unknown degree of disturbances the flask samples did not allow a budgeting.

4.2.6 The Netherlands Winter Experiment 14 January – 10 February 2002

The observed development of the CO₂ mixing ratio and the delta ¹³C values during day time, as already presented in figure 4.11, point to a contribution by plant activity although such an effect of the vegetation seems not to be realistic in winter. Data obtained from ground level and from the profile flights over marshland reflect a tendency, which can not be explained by the activity of the sparse grass cover. More likely is that the area was affected by urban influences. This can be seen from the CO₂, the delta ¹³C and the CO data of the samples taken at 5 m height in the morning which are indicating products related to combustion processes. Since the sampling was performed a few hundred meters away from any settlements, advection must be an important parameter regarding the transport of contaminations from sources located upwind.

The relevance of advection as a major interfering parameter becomes also obvious from the shape of the flight profile. Lower mixing ratios of CO₂ and CO, as well as a reduced amount of the ¹³C isotope were sampled in the free troposphere, compared to the ones taken within the CBL. Additionally a decrease can be recognized between the morning and the midday samples, which becomes particularly distinct for the CO mixing ratio. The most probable explanation is air exchange, whereby air of marine origin became more dominant.

When comparing the data from all flight days a high variability is recognizable also from day-to-day (see figure 4.26). By correlating the different tracers a rough differentiation of the origin of the sampled air masses might be possible, whereby the clearest signal for air with an oceanic character can be seen in the data from the morning flight on the 3^t January.

Because of the observed day-to-day variability the determination of a background value from the samples taken within the free troposphere was impossible.

'Contaminations' caused by air mass changes might frequently not be identified.

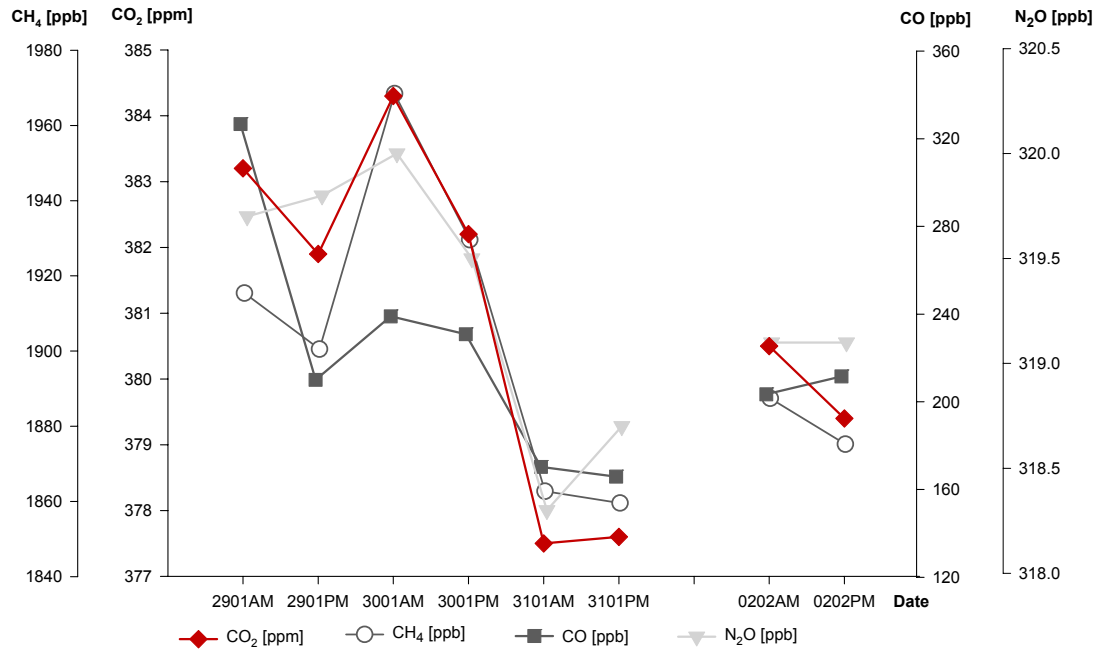


Figure 4.26. Mixing ratios of CH_4 , CO_2 , CO and N_2O obtained from the flask samples executed on the 29, 30, 31 January and the 2 February 2002 above the *Forest* site at lowest flight level (The Netherlands).

Additionally, due to the highly variable wind conditions each profile has its own characteristics. The results from the flights over the same area cannot be classified. And since wind direction was never really stable during a complete flight day, the ‘transect approach’ could not be defined either.

Regarding the technical improvements, which were realized since the previous campaigns concerning flask pair differences, no systematic tendency, indicating a further influence of the $[\text{Mg}(\text{ClO}_4)_2]$, could be observed anymore. The remaining differences are in the range of the expected and observed small scale variability.

When comparing the results obtained from the flight profiles and the ground reference investigations, shown in figures 4.15. and 4.16., a discrepancy between both locations and between the ground and the flight samples taken at the individual sites becomes obvious. Contrary to the clear signals related to the plant activity identified by the ground samples, only a small signal can be detected in the flight results. Regarding the Cabauw data one explanation might be the late hour of the morning sampling: a contribution of air from the residual layer of the previous day might be entrained by vertical mixing. And the CO₂ uptake during assimilation should be already effective. In this case one has to expect significantly decreased CO₂ mixing ratios around noon, since the photosynthetic activity and turbulent mixing processes are assumed to be most effective during the middle of the day. Since such a clear signal was not found it is likely that the signals obtained from the flight profile are masked by an air mass change between the morning and the midday samplings, which could be confirmed also by the variations of the CO mixing ratios. In this context the data of the samples taken at the 915 m level above the 'Maize' location must be interpreted as the signal of an isolated layer with a distinctly different origin.

The large differences between both sites, which became obvious from the ground reference samples, are reflecting clearly the different local land use characters. In particular, the relative high CO ratios obtained from the marshland samples might mirror more pronounced anthropogenic influences (close distance to major agglomerations) than for the maize field.

Sampling approach

An important question resulting from the local observations was to identify the sites and sampling heights which are characteristic for the entire region to be described. In theory the regional carbon budget should be estimated by a) the summation of the individual contributors or b) the measurement of an air column containing a well mixed average of them. Consequently the analysis of the entire air column of the flight profile should lead to the identical result as the one got from the

estimation obtained from the spatially weighted contributions of the local sources and sinks.

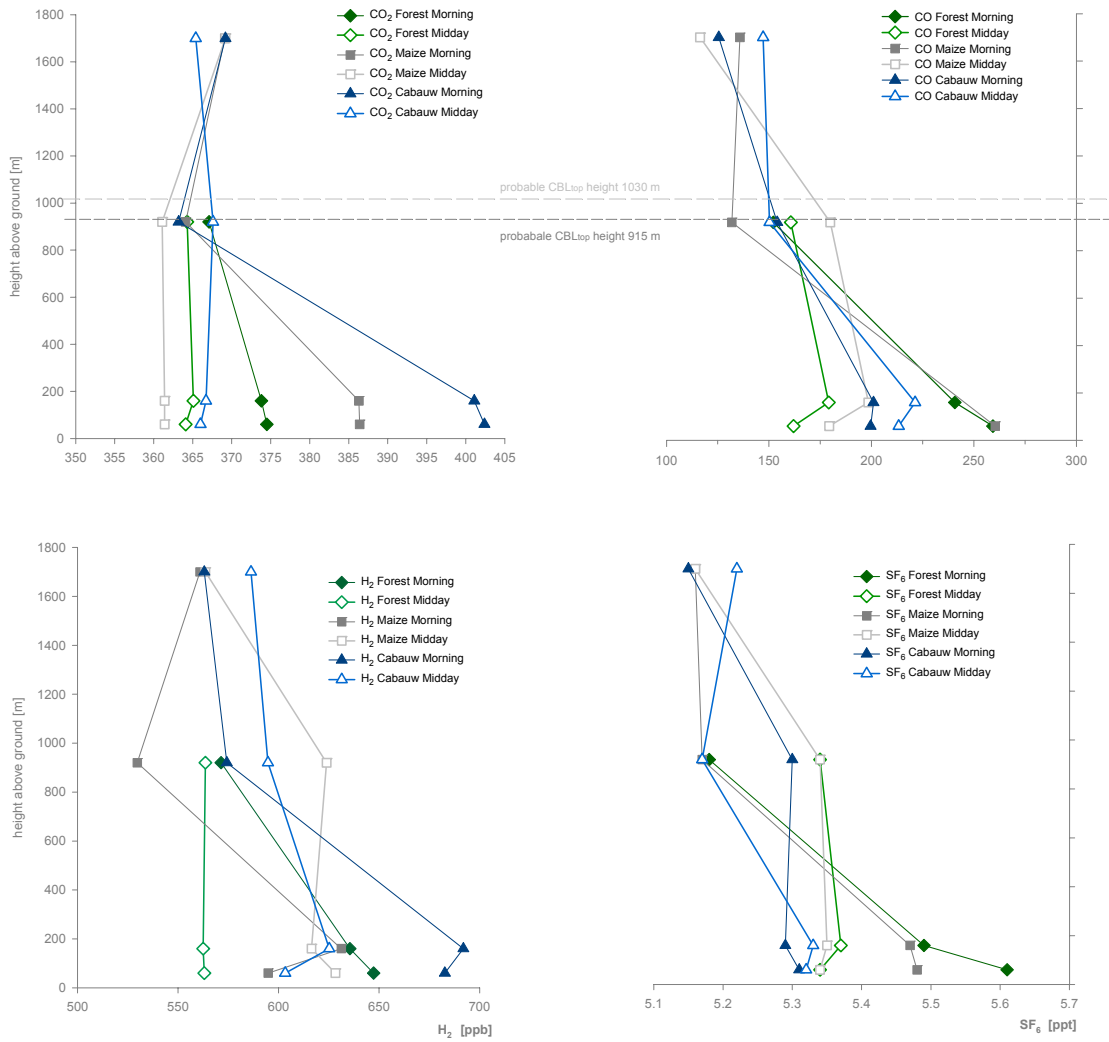


Figure 4.27. Summary of the CO₂, CO, H₂ and SF₆ gas mixing ratios obtained from the profile samplings performed on 27 July 2002 above the three different study sites (The Netherlands).

In particular differences among the sub-regional territories became obvious for the morning flights by the comparison of the individual profile sites (see figure 4.27). From the signatures of the lower level samples the main land classes could be well differentiated, as well as a continuous homogenization with increasing height was observed. But at no altitude a blending height was identified, that could be labelled as 'representative' for the entire region. Thus the question has to be answered

how important is the selection of the individual profile site is with respect to the budget of a larger area.

To substantiate these conclusions the results from the 27 July 2002 may be taken for example. In order to obtain the regional surface fluxes from the observed diurnal mixing ratio differences in the CBL profile, the fluxes for the individual profile sites were calculated with a simple budget equation:

$$F_{CO_2} = \frac{d(CO_2)_m}{dx} \frac{dx}{dt} \rho_m h \quad [4.1.]$$

F_{CO_2} is the flux density at the surface, expressed as micromoles per square meter per second. By inserting h (the height of the CBL top) combined with a mean wind velocity $\bar{u} = 2.4 \text{ m s}^{-1}$ to obtain dx / dt , the spatial extension of the study region is defined. ρ_m is the mean molar density of the air.

Exemplary surface fluxes and the regional extensions for the three different study sites were calculated for two CBL top heights:

Table 4.11. Estimated CO₂ surface fluxes calculated for two different CBL top heights on 27 July 2002 at the field sites in The Netherlands

Site	CBL _{top} height = 1030 m	CBL _{top} height = 915 m
	flux ($\mu\text{mol} / \text{m}^2 \text{s}$)	flux ($\mu\text{mol} / \text{m}^2 \text{s}$)
Forest	-7.08	-6.53
Maize	-11.16	-10.29
Cabauw	-23.82	-22.36

The advection distances between the morning and afternoon flights were 51.8 km (CBL_{top} height = 1030 m) and 48.5 km (CBL_{top} height = 915 m), respectively.

For comparison: the fluxes measured by eddy-correlation on 27 July 2002 at the Cabauw Tower were -9.7 $\mu\text{mol} / \text{m}^2 \text{s}$ in the morning and -10.4 $\mu\text{mol} / \text{m}^2 \text{s}$ around noon.

Since the determination of the CBL top height from the measured and derived gradients of humidity f and potential temperature Θ is difficult, one has to take into account that an uncertainty with respect to the quality of the calculated fluxes exists.

For instance the range of the top heights obtained and used by the different groups in RECAB for 27 July 2002 varied between 955 m and 1500 m.

When comparing the data, in particular the absolute values observed at the Forest and at the Cabauw site, some results are significantly different from the expected ones. The calculated flux at Cabauw seems to be unrealistically high, whereas the Forest value appears to be too low.

The question arises: *what* affects the observed ‘fluxes’? Can the fluxes be attributed to surface processes or are they mainly caused by variations of the air mass origin. Both cases are seriously affecting the budgeting process and the investigation strategy.

Two explanations seem most probable.

(1) The local conditions are represented to a larger extent than assumed so far. If the local ground conditions are dominating the composition of the entire profile, the selection of the sampling site would have the most crucial importance for the investigation, since the ground has to be representative for the whole region.

(2) Changing environmental conditions, resulting in air mass changes, is a key factor. If air mass changes are predominant, affecting smaller scales than covered by the spatial range of the individual profile sites, the sample sites can no longer be directly compared, because of the different background shifts.

Regarding this conclusion of dominating environmental conditions, confirmed by the high variability of wind velocity and direction, the CBL budgeting approach is impossible.

Disturbances, caused by wind direction variability, are the main restriction for the application of the ‘transect approach’. Even if the stretch of the study sites was orientated along the main wind direction, individual short term changes of wind direction occurred at the different sampling levels. Therefore changing by lateral advection affected the samples at the different sites. Thus each profile, respectively each sample level, appears to be completely independent and will not

be representative for the regional air mass. Caused by the insufficient knowledge of the environmental conditions, like advection, CBL height, etc. no direct regional budget estimation is possible with profiles measured above a single site.

However, in spite of all difficulties, some results could be obtained regarding the comparison of the winter and the summer investigations. The elevated CO₂ and CO mixing ratios observed within the free troposphere are reflecting the higher contribution of fossil fuel consumption in winter. Also from the lower level samples a differentiation of diverse sources and sinks between summer and winter flights became obvious. Caused by the high night time respiration of the vegetation, no significant difference could be observed during the morning hours in summer, in contrast to the afternoon samples which are characterised by a clear reduction of CO₂ mixing ratios caused by plant activity.

4.2.8.1. SPA¹³CE Thuringia Summer Experiment 6 – 15 August 2002

Because of the opportunity to verify all improvements and adaptations in combination with high precision ground level investigations the SPA¹³CE experiment was highly suitable regarding a final assessment of the methodology. Additional information could also be obtained from cooperation with the modelling department of the MPI-BGC (CHRISTIAN RÖDENBECK).

From the profiles of figure 4.17 a good agreement of the data obtained by the tower sampling and the sampling performed with the flight unit becomes obvious, i.e. there was no affection due to the different technical equipment and no discrepancy regarding the observed spatial scales. With respect to the CO₂ mixing ratio and the delta¹³C values both reflected the expected diurnal tendencies and amounts. A remarkable observation from the tower sampling is the occurrence of significantly higher CO₂ mixing ratios correlated with more negative delta¹³C values beneath the beech canopy from the samples taken around midday, which indicates both a high assimilation activity and contribution also from soil respiration. On the other hand the CO₂ decrease and the relative increase of the ¹³C isotope within and above the canopy reflect a change from predominating respiration to a sink by CO₂ uptake. In particular for the midday observation the influence of local sources, the soil respiration, and of local sinks, the canopy, becomes obvious.

The combination multi tracer flask samples and continuous profiles allowed the further investigation of the sampling strategy and the budgeting approach: the effects of advection for diurnal and day-to-day time scales and the occurrence of stable stratification.

DAY-TO DAY VARIABILITY

A clear differentiation could be made between both days by the analysis and interpretation of the air samplings. 14 August 2002 was characterised by averaged gas mixing ratios close to the global mean values, which suggests, that the air mass was less affected by terrestrial sources but rather likely of maritime origin. Contrary to these results the data of 15 August 2002 show a conspicuous increase of all trace gas mixing ratios, wherefrom an increasing influence of

anthropogenic sources can be derived. The variation of the CO mixing ratios exceeds with more than 30 % from day-to-day even the relatively high diurnal variation by a factor ten. Suggested by the CO₂ and delta¹³C ratio (see figure 4.9) a contribution of biological, respectively plant activity can be identified. Thus the air mass sampled on 15 August is of terrestrial origin.

14.08. 15.08.				14.08. 15.08.				Midday → Morning		
CO ₂	368.1	370.2	2.1	0.57	H ₂	527.5	536.3	8.8	1.66	
[ppm]	371.9	370.2	-1.7	-0.46	[ppb]	527.1	536.3	9.2	1.75	Morning
	368.1	367.1	-1.0	-0.27		527.5	531.7	4.2	0.80	Midday
	-3.7	-3.0	[ppm]			0.4	-4.5	[ppb]		
	-1.00	-0.82	[%]			0.08	-0.85	[%]		
14.08. 15.08.				14.08. 15.08.				Midday → Morning		
CO	85.1	111.7	26.6	31.26	SF ₆	5.18	5.32	0.14	2.70	
[ppb]	87.8	111.7	23.9	27.22	[ppt]	5.19	5.32	0.13	2.50	Morning
	85.1	108.9	23.8	27.97		5.18	5.26	0.08	1.54	Midday
	-2.7	-2.8	[ppb]			-0.01	-0.06	[ppt]		
	-3.13	-2.47	[%]			-0.10	-1.13	[%]		

Table 4.12. Summary of the means from the entire profile for CO₂, CO, H₂ and SF₆ gas mixing ratios sampled on 14 and 15 August 2002 above the *Hainich* (Thuringia / Germany). The variability in between the days expressed in percent is related to the relative mixing ratio change of the samples from 15 August (terrestrial) to the sampling at the same time the day before (marine character). Likewise the differences are calculated between the results of the midday flight on 14 and the morning flight on 15 August.

To asses the effect of an air mass change on surface flux estimates specific calculations were carried out with equation 4.1 for CO₂ and for hypothetical fluxes of CO, H₂ and SF₆ [SF₆ has no terrestrial sinks!].

Table 4.13. Calculated fluxes for CO₂ and CO, H₂ and SF₆ from the flight data of 14 and 15 August 2002 above the *Hainich* (Thuringia / Germany) using equation 4.1.

14.08.	15.08.	14.08.	15.08.	14.08.	15.08.	14.08.	15.08.
-20.0	-16.2	-14.6	-15.2	2.2	-24.4	-0.05	-0.32
CO ₂ [$\mu\text{mol} / \text{m}^2 \text{s}$]		CO [$\text{nmol} / \text{m}^2 \text{s}$]		H ₂ [$\text{nmol} / \text{m}^2 \text{s}$]		SF ₆ [$\text{pmol} / \text{m}^2 \text{s}$]	

On 14 and 15 August 2002 ‘fluxes’ with negative notations (excluding H₂ on August 14 2002) can be recognized, whereby for all gases except CO₂ a higher

decrease is indicated on 15 August 2002. This observation might be in conflict with the carbon budgeting: In particular air mass change is indicated by

- 1) the observed increase of H₂ and the nearly steady mixing ratio of SF₆ in the afternoon on 14 August 2002, and by the
- 2) decrease between the morning and the midday sampling on 15 August 2002.

With respect to the carbon budgeting it has to be assumed, that the origin - and thus the mixing ratio - of the sampled CO₂ also have changed. Thus an unknown fraction of the 'calculated' fluxes might come from outside the region.

Specific studies were initiated in order to get additional information about the exchange processes caused by the day-to-day variability and to verify the origin of the air masses with a transport model (see sub chapter 4.2.8.2; 'Adjoint of a Transport Model'). More specific multiple tracer analyses are also presented in chapter 5.2. 'Variability – Air Mass Change'.

STRATIFIED LAYERS

Following theory stratified layers shall be coupled to stable thermodynamic conditions and should therefore normally be expected in the early morning hours, during winter or at the CBL top. Also during midday flights on both days the presence of isolated layers within the profiles was documented by the continuous CO₂ measurements (see figure 4.28). Discontinuities of the mixing ratio occurred, for example during the midday flight on 15 August within the small height range between 170 and 270 m; from 366.1 ppm to 361.5 ppm and up again to 366.4 ppm. Relating this small scale vertical variability to the variation of the diurnal cycle of CO₂, which is ~3 ppm, a high uncertainty regarding the representativeness of the individual flask samples becomes obvious.

Differences between the online CO₂ measurements and the results from the flask sampling can be recognized in particular at the lowest flight level, due to the identified small scale variability. This direct comparison of the data from both systems became possible with the modifications of the sample system by the implementation of the coupled record documentation (see chapter 3.4 , table 3.6).

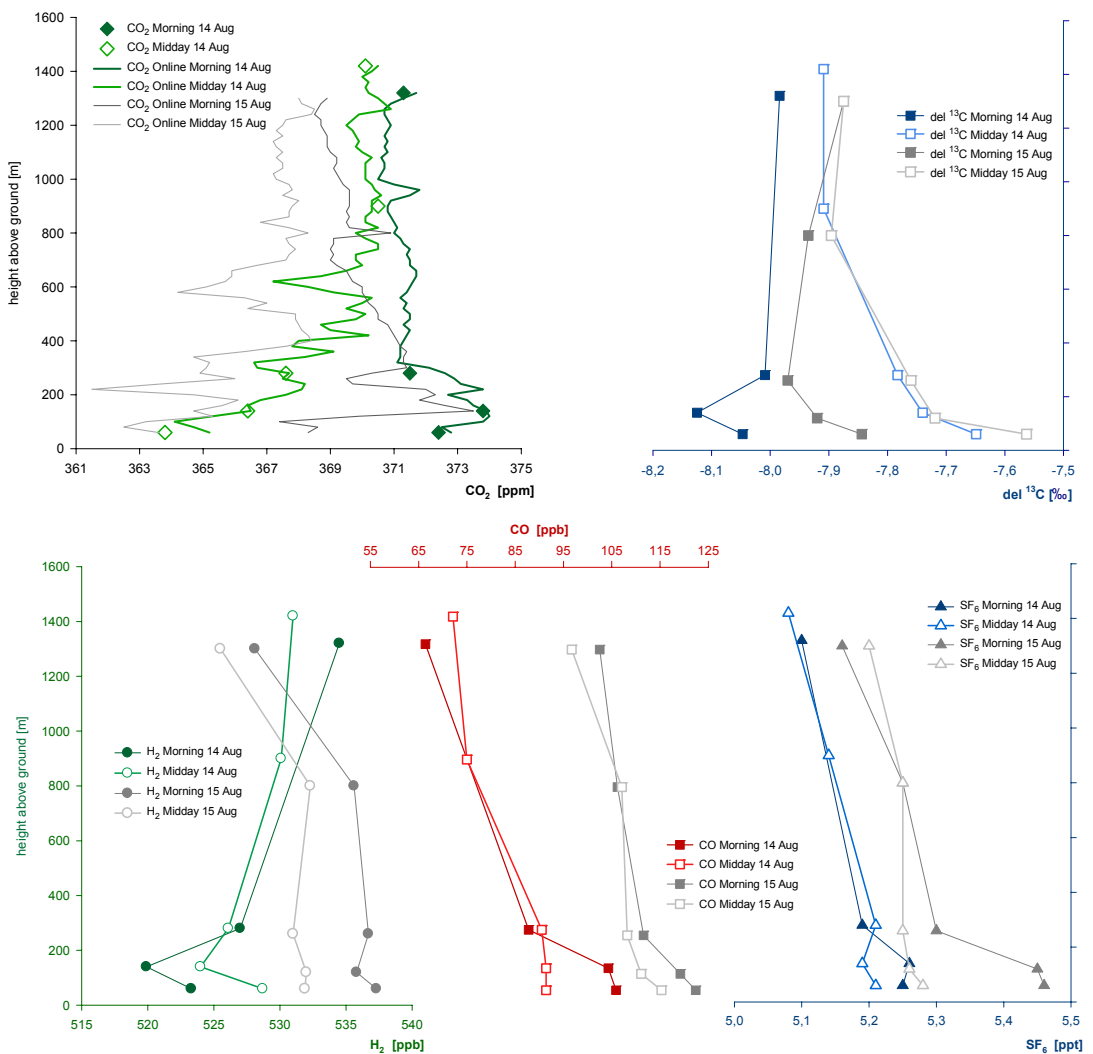


Figure 4.28. Mixing ratios of CO_2 , CO , H_2 , SF_6 and $\delta^{13}\text{C}$ in CO_2 from the samples above the Hainich (Thuringia / Germany) on 14 and 15 August 2002. The CO_2 plot also contains the mixing ratio profiles obtained by the continuous system. Although small scale variability differences between the online results and the flask data can be expected (in particular near to the ground) an acceptable agreement could be achieved by the improved sampling system.

The online system adds valuable information regarding the CO_2 profile that allows to identify of stratified layers and the description of the direct environmental conditions when taking the air samples.

From the occurrence of stratification uncertainties arises, which are not only crucial for discrete sampling approaches. Regarding the significance for flask sampling two aspects could be separated: 1) depending on the level the samples are taken the difference in the mixing ratios between both flights might change significantly.

2) If the layers are characterised by different source areas and formation processes random biases regarding the signal interpretation may be provoked (see for instance chapter 5.2. ‘Signal shift’).

Figure 4.29 presents the profile data from the flights performed on 14 August 2002. Indicated by the red symbols are notional samples ‘taken’ at different levels adapted to the continuous CO₂ profile records. When calculating CO₂ fluxes for both cases, the real and the assumed flask sampling, large discrepancies appear. The notional CO₂ morning mixing ratios are 0.3 ppm higher, at midday 1.6 ppm lower compared with the real sampled data. This results in an assumed CO₂ flux of -23.29 μmol m⁻² s⁻¹ versus -12.99 μmol m⁻² s⁻¹ calculated from the real flask data – which is only 55% of the hypothetical amount.

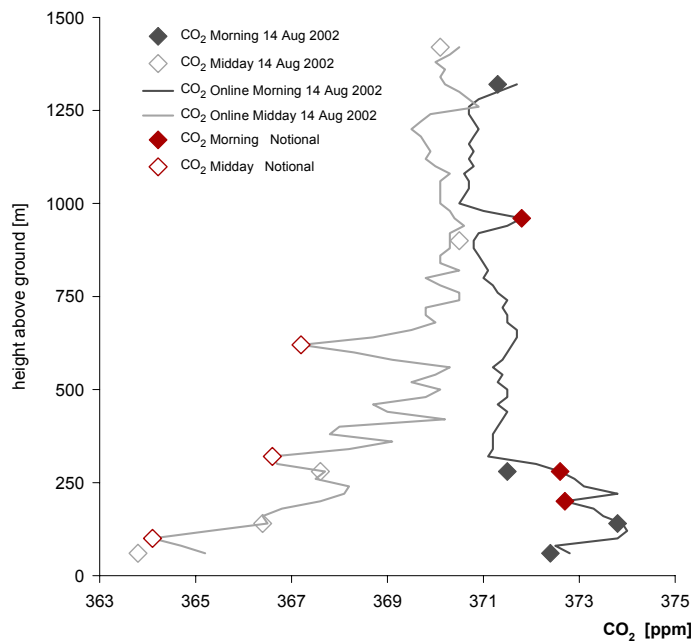


Figure 4.29.

CO₂ mixing ratios recorded by the online system (greyish lines) and obtained from flask sampling (greyish symbols) on 14 August 2002 during the flights over the Hainich (Germany). Red symbols are hypothetical samples ‘taken’ at different levels adapted to the continuous records, used for the estimation of the error potential regarding flask sampling in stratified air masses.

If the layers are caused by diverse source areas and formation processes, and transported to the profile site by advection, each of them has to be taken as an independent contribution, which even might be in no way associated with the regional surface flux. Therefore, also from a continuously profile surface fluxes cannot be derived.

With respect to the characterisation of the individual layers multiple tracer analyses will be a useful tool. However, for the required in-flight detection of the layers the

implementation of further continuous systems, at least of an additional CO sensor, is mandatory.

INTERACTIONS CAUSED BY TOPOGRAPHY

Because of the simultaneous observation of horizontal advection and the presence of stratified layers a further aspect might have to be taken into account.

The Hainich location is characterised by a steep slope to the Werra valley in the west (200 m level difference), the barrier of Harz Mountains (Brocken 1142 m) and Thüringer Wald (Großer Finsterberg 944 m) north and respectively south of the Hainich. It can be assumed that due to the orographical situation an aerodynamic, undulated pattern is initiated. By the establishment of this stationary wavelike structure an attenuation of convective processes at the troughs can be assumed. One consequence might be the conservation of stratification. Additionally, the establishment of an irregular 3 dimensional flow field may partially explain the occurrence of the frequent small scale variability and the differences between the tower and flight measurements during the first flights over the Hainich (see chapter 3.1.3.) and the transect flights described by GIOLI et al. [2004].

4.2.8.2. Inverse Study

Because of the wide range of the observed mixing ratios even nationwide influences seems to be quite probable. Our intention was to verify the assumption of a crucial contribution by advection and to get an estimate of the disturbance.

Adjoint of a Transport Model

To evaluate the observed different gas compositions spatial contribution probabilities were calculated by an adjoint of the TM3 global 3D atmospheric tracer transport model, supported by CHRISTIAN RÖDENBECK from the MPI-BGC.

Calculated were the individual grid box contributions to the CO₂ mixing ratio increase (indicated in ppm), that would be observed corresponding to an assumed tracer flux of 10⁶ mol s⁻¹ (see figure 4.30.) For an estimate of the amount that is directly related to anthropogenic interferences the investigation was combined with data base information of CO₂ emissions from fossil fuel consumption. Therefore the sensitivities were weighted with the spatial distribution of the fossil fuel emissions, obtained from the EDGAR data base. The plots are showing the contribution in ppm of the individual grid boxes, which would be recognized at the observation site (see figure 4.31).

The proposition, that the air mass measured on 15 August 2002 is of a different, more terrestrial origin, seems to be proven, since the transport function identifies also a relative high number of terrestrial cells with high potential to contribute to the measured results. A high input from the grid box located at the central UK industrial region might agree well with the observed rapid change of the gas mixing ratios (see table 4.12 and figure 4.28). On the other hand the model does not reflect the direct surroundings of the profile site properly regarding the sampling level above the CBL top. Because the resolution of the vertical structure is relatively coarse in the model, a capping inversion will not be taken accurately into account. This may explain the overestimation of the boxes which are connected directly to the measurement point.

However, regarding an estimation of the contributions from remote sources by long range transport the model provides helpful information. On the other hand the results from the gas and the isotope analyses and their interpretation can provide probable information with respect to model evaluations.

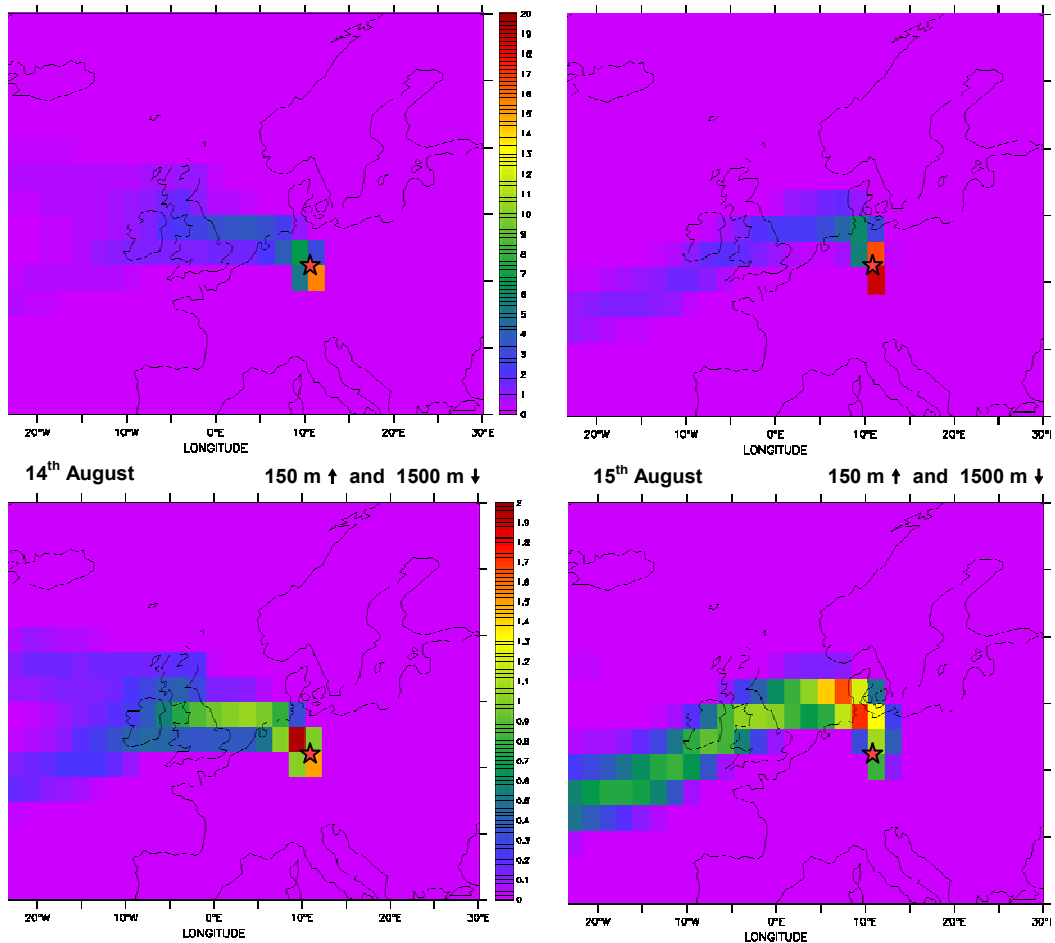


Figure 4.29. Contributed mixing ratio increases which would be measured corresponding to the assumed tracer flux at each grid box. The calculations are related to the sampling flights at 10:45 UTC on 14 and 15 August 2002.

Modelling by CHRISTIAN RÖDENBECK, MPI-BGC

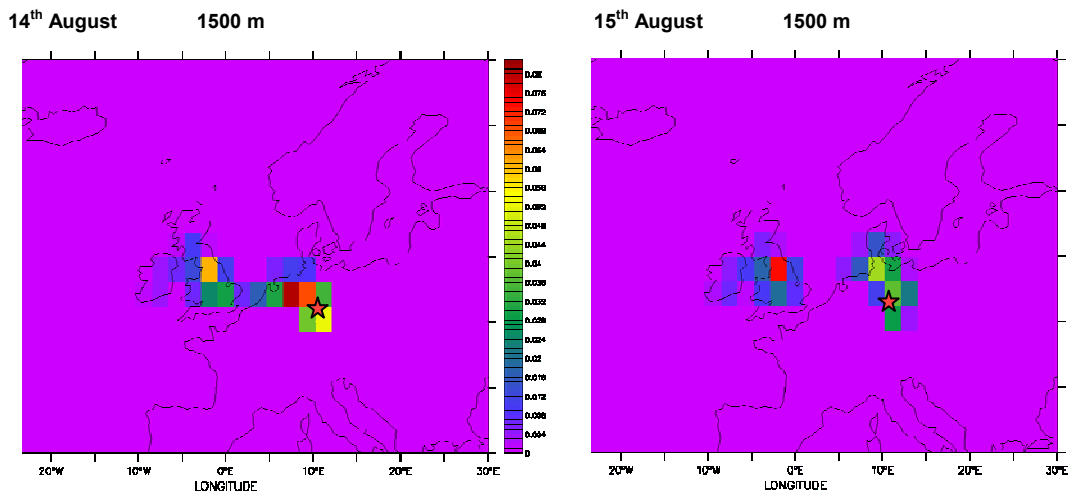


Figure 4.30. Individual contribution of each grid cell with respect to the fossil fuel emissions as estimated from the EDGAR inventory to the mixing ratio at the profile location. (Site is indicated by the red star) Modelling by CHRISTIAN RÖDENBECK, MPI-BGC

5. DISCUSSION

Objective of this chapter is a more thorough discussion of the results obtained from multiple tracer analyses and their potential for carbon budgets.

It is structured into four parts, focussing on specific subjects: 1) characterisation and comparison of the RE CAB study regions by multiple tracer analyses, 2) examination of theoretical and conceptual aspects, 3) summary of the methodological experiences, and 4) the benefits derived by the establishment of the ground reference sampling unit and – as the resulting consequence of the findings - the enhanced understanding from the sophisticated flight investigation strategy.

The field campaign results will be interpreted and discussed first for each study region individually. Then exemplified findings, concerning specific topics with respect to the budgeting, will be presented in more detail. Then some general effects regarding theoretical and conceptual aspects will be discussed, leading to a conclusion with respect to the applicability of the CBL-budget approach for studies based on flask sampling. Before the enhanced investigation strategy will be scrutinized, the most important impairments regarding the practicability of airborne CBL studies are concisely presented.

For the development of the sampling unit several experiments were carried out in the laboratory, during test flights and RE CAB campaigns. Cross references will be given with respect to the observations which initiated the laboratory experiments, and to the perceptions derived from the flights. A summary of the modifications and an assessment of the improvements was already given in chapter 3.4 (pages 56 ff.), directly connected to the discussion of the related laboratory experiments.

Also the adaptations of the flight and sampling strategy were motivated by campaign observations. Linkages between causes and effects are pointed out.

5.1. Comparison of the Study Regions using Multiple Tracer Data

Emphasis of this section is to discuss the results of the RECAB field campaigns presented in chapters 4.1. and 4.2. by using multiple tracer analyses and to evaluate the potential of multiple tracer studies using real field data. The first part of the section discusses the potential with respect to specific processes.

With the integration of CO, SF₆ and H₂ into the analysis scheme three additional trace gases with distinct different characteristics became available (since the campaign in Sweden in 2001). CO and H₂ should be used as tracers for CO₂ that originated from combustion processes, whereas SF₆ was related to the identification of urban, in particular of industrial contributions.

By the interpretation of the multiple tracer data some of the affecting processes could be compiled. However, a general problem of flask sampling analyses becomes also obvious: uncertainties due to the low amount of data.

5.1.1. CO₂ / delta¹³C and CO₂ / CO relationships

CARBON DIOXIDE AND ISOTOPIC SIGNATURE

Individual sources and sinks, like for example plants, are characterised by a specific CO₂ / delta¹³C relationship, where the signal caused by the ¹³C discrimination during the assimilation activity has its pendant in the value obtained from the respired air. When analysing air samples: The more uniform and the larger the sources and sinks are, the clearer is the observable signal. Thus a high correlation coefficient will reflect a mostly homogeneous area, whereas variable contributions from different sources might cause a weak relationship (see figure 5.1).

An important factor is the concurrent seasonality of determining processes. During summer low CO₂ mixing ratios and less negative delta¹³C values can be observed, because of high assimilation activity and low contributions from fossil fuel consumption (in particular from heating). Contrary conditions occur in winter time (see figures 5.3 and 5.16).

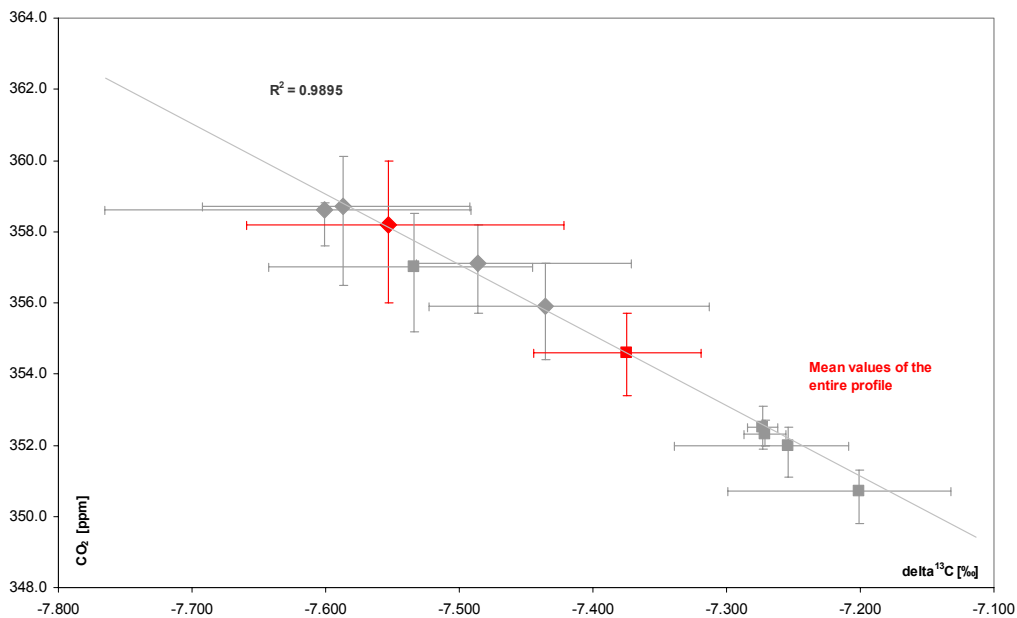


Figure 5.1. CO_2 / $\delta^{13}\text{C}$ ratios obtained from the samples collected over *Florarna* on 29 and 30 August and on 1 September 2001 (Uppland / Sweden). A linear fit through the data points is applied. The range of the mixing ratio during all days is indicated by the bars for CO_2 and $\delta^{13}\text{C}$ respectively. Morning flight data are plotted as diamonds, the midday results as solid squares.
Because of the delayed morning sampling on 1 September the obtained lowest level variances are not directly comparable. The 60 m morning data were therefore excluded. (likewise in figure 5.16)

Likewise the released CO_2 from fossil fuel consumption is characterised by distinct CO_2 / $\delta^{13}\text{C}$ ratios depending on fuel types (see table 5.1).

At least a differentiation of the diverse RE CAB study regions should be derivable. Results from CO_2 / $\delta^{13}\text{C}$ correlation analyses are more specifically discussed under seasonal and latitudinal aspects in subsection 5.1.2.1.

Table 5.1. $\delta^{13}\text{C}$ signature of different carbon sources

Source type	$\delta^{13}\text{C} [\text{\textperthousand}]$	Location	Reference
Coal	- 24.1	The Netherlands	TANS 1981
Petroleum	- 26.5	The Netherlands	TANS 1981
Natural Gas	- 41.0 (mean)	The Netherlands	MEIJER et al. 1996
	- 29.0	Groningen Gas Field (The Netherlands)	TANS 1981
	- 54.3	City Gas Net Krakau (Poland)	FLORKOWSKI et al. 1997
Light Methane (from methanogenic sources)	- 110.0		HOEFS 1996

COMBUSTION PROCESSES

Besides the information obtained from the correlation of CO₂ and the isotopic ratio additional information is contained in the relationship between CO₂ and CO especially on combustion processes. Since the ratios of CO₂ and CO released from combustion processes are depending mainly on fire temperature, material and the kind of burning a differentiation of individual sources is possible. In smoldering stages, which is often a characteristic of biomass burning, CO release is significantly increased compared to a combustion with an open flame (see chapter 2.1.2.2. 'Carbon Monoxide'). If the source processes could be identified a first estimation of the added CO₂ can be achieved. With respect to the identification of contributions from fossil fuel consumption the additional implementation of ¹⁴C into the analyses scheme would be desirable.

From the agricultural (named 'Maize') site in The Netherlands CO₂ and CO data are available from the winter and the summer campaign (see table 5.2). Most obvious is that in particular the CO₂ and CO mixing ratios of the midday samplings (indicated in red colour) vary much between summer and winter time. The variability of the mixing ratios between the days of the individual campaigns is much higher for CO than for CO₂; but the range of the CO mixing ratio is even highest in summer time. This might be an effect of different seasonal synoptic conditions.

Table 5.2. Mixing ratio variability from the flight samplings performed at the profile site around the maize field ground reference in the central Netherlands.

	Mixing ratio					Range between days	
	Morning	Midday	Difference	-		Morning	Midday
CO ₂ [ppm]	374.1	362.4	-11.7	-3.13 %		Summer	3.4
	378.7	377.4	-1.3	-0.34 %		Winter	4.5
	4.6	15.0				Difference	2.9
CO [ppb]	176.8	153.7	-23.1	-13.07 %		Summer	91.2
	176.7	169.1	-7.6	-4.30 %		Winter	44.3
	-0.1	15.4				Difference	61.5

Results obtained at the Italian mountain site (see chapters 4.1.6 and 4.2.3) allow identification of another source. Because of the SF₆ mixing ratios, which are not elevated, an anthropogenic dominated source area might be excluded.

Compared to terrestrial surfaces the oceans are characterised by a lower activity regarding combustion processes and anthropogenic emissions. Additionally, because of the low activity the gas composition can be conserved even during long range transports.

Thus, by the observed multiple tracer mixing ratios a contribution from far away from the study region could be identified (see also the discussion in chapter 4.2.3.3. 'Back Trajectory Calculations', p 88ff.).

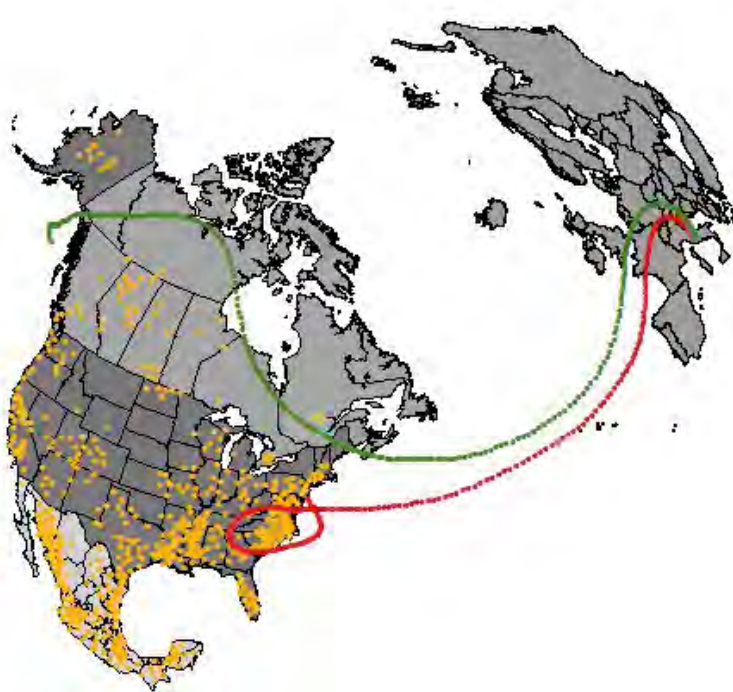


Figure 5.2.

Fires detected by the MODIS sensor between 4 to 18 June 2002. Back trajectories of air particles calculated from a receiving point at the 2750 m sampling level above the 'Orvino' location (Lazio / Italy) on 17 June 2002 21:30 UTC (red) and on 18 June 2002 11:30 UTC (green).

5.1.2. Comparison of the study regions

With respect to the aims of the RECAB project, the ‘qualification and quantification of sources’ and the ‘carbon budgeting of regional scales’, multiple tracer analyses are also providing basic information. Because of the characteristic composition of the air and due to the characteristic relationship of the individual trace gases regional and seasonal behaviours can be distinguished: the nature of the source and its type, the annual cycle and the geographical location.

SEASONAL VARIATIONS AND LONGITUDINAL DIFFERENCES

5.1.2.1. Seasonal Variations

At the Hainich site flights have been performed in 2000, 2001 and 2002 during July and August (see table 5.3.) from which conclusions might be drawn regarding the range of the inter annual variability. A strong diurnal variation could be observed in 2001, while during the other years the CO₂ variability is depressed to one third of the values documented in 2001. But high variations of the mixing ratios between the days were recorded during all campaigns. A corollary of this observation is that there is a high ‘potential of uncertainty’ resulting from the limited number of available flight data for the analyses, which has to be considered for the interpretation.

Table 5.3. Interannual and daily variability at the *Hainich* site (Thuringia / Germany)

Values obtained by integration over the entire profile; Summer flights 2000 - 2003

CO ₂ [ppm]	Mixing ratio			Range between days	
	Morning	Midday	Difference	Morning	Midday
362.,7	360.8	-1.9	2000	0.7	0.4
364.6	360.0	-4.6	2001	2.0	4.0
368.6	367.2	-1.4	2002	6.8	5.6
5,9	7,2		Difference		

As expected the observed absolute CO₂ mixing ratios were higher during winter time than in summer (see table 5.4). Responsible for this observation are mainly three factors: the absence of the CO₂ uptake by assimilation, the enhanced fossil

fuel emissions caused by the heating period and the higher accumulation rate within the shallower developed boundary layer in winter time.

Table 5.4. Averaged seasonal data from flights performed above the Hainich and Gebesee sites during 2000 – 2002 (Thuringia / Germany)

Only samples taken below 1500 ft altitude are included

	August	October	January	May
CO₂ [ppm]	364.3	377.5	384.3	375.3
CH₄ [ppb]	1844.7	1893.5	1874.6	1851.5
N₂O [ppb]	319.3	319.0	318.5	319.4
delta¹³C [%]	-7.783	-8.147	-8.826	-8.449
delta¹⁸O [%]	-0.139	-1.343	-1.878	—

The link between the contributions of CO₂ sources and sinks, the uptake during assimilation in summer time and the elevated fraction originating from fossil fuel combustion in winter, becomes obvious by a correlation analysis (see figure 5.3.). Regarding the diurnal cycle of the mixing ratio higher values occur during the photosynthetic active period. This can be attributed to a predominance of the assimilation over the respiration rate. It is also caused by the deeper CBL during day time in summer leading to stronger dilution of CO₂ from night time respiration.

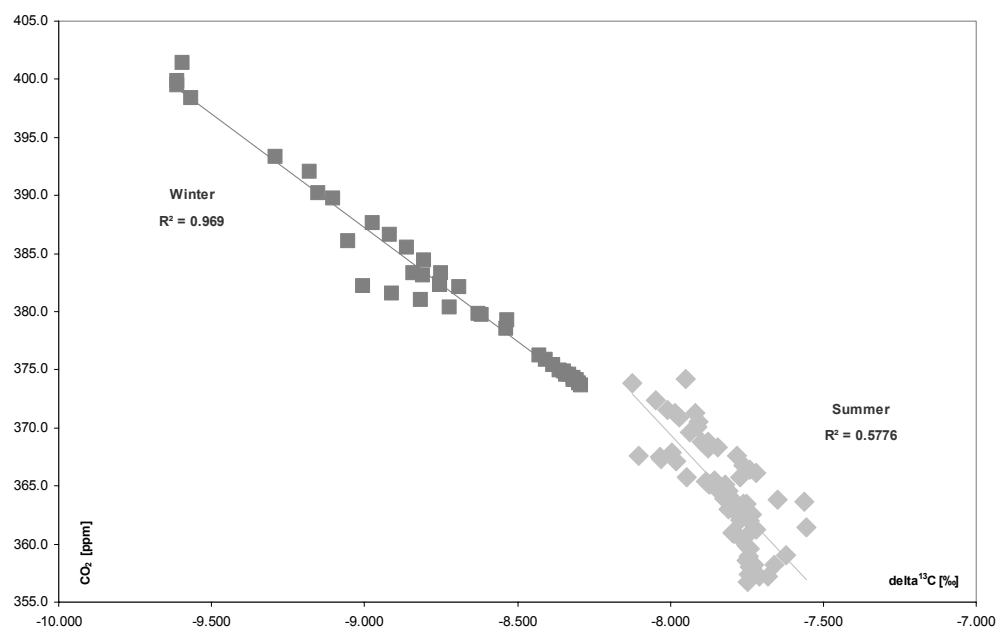


Figure 5.3. CO₂ / delta¹³C relation obtained from samples above the Hainich (Thuringia / Germany) during summer (light grey diamonds) and winter (dark grey squares) flights. Linear fits through the data points are applied. The discrimination for winter is -19.567‰ and for summer -28.099‰.

From the comparison of the seasonal results, as listed in table 5.4., a clear differentiation between summer and winter time is obvious. But when examining the data with respect to the CO₂ / delta¹³C relation some problems become evident. The R² values do not reflect the expected situation, that the correlation in summer and winter time should be nearly equal. During summer different biological sources, like plant and soil respiration are contributing to the CO₂ inventory. In winter the CO₂ originates from manifold strong anthropogenic contributors with a wide range of isotopic signatures (see table 5.1.). During the winter flights the contribution from fossil fuel emissions is high, obvious from the observations made on the flight to / from and at the study site. Thus a less depleted ¹³C signal should be expected, whereas from the flask samples a clearly enhanced ¹³C value compared to the summer data is derived (-19.567 ‰ winter time vs. -28.099 ‰ summer time).

Because of the insufficient characterisation, with respect to dynamic processes within the atmosphere, no definite estimation of the subsidence and free troposphere advection is possible. The most likely explanation is that the flask sampling during winter time was above the CBL within the lower free troposphere where the air is less affected by neighbouring surface processes. Additionally, because of the shallower CBL regional signals might be covered by local contributions (the 'regional rectifier'). A problem regarding the performance of flight sampling during winter arises: Due to aviation safety regulations the requested minimum flight altitude for low level samplings is not feasible.

An annual cycle can also be observed for the soil related processes, like the production of N₂O (see table 5.4). Since mainly microorganisms are responsible for the nitrogen conversion the reaction is strictly depending on the environmental conditions. The activity is affected therefore by soil moisture and soil temperature. Particularly at the beginning of the farming season fertilization increases the availability of nitrogen. Therefore highest N₂O mixing ratios were recorded in spring and summer time, whereas, caused by the reduced microbiological activity, lowest values were obtained during winter.

The discrepancies between the expected and the observed behaviour of the CO₂ and delta¹³C relationship are also recognizable from the comparison of summer- and winter-data obtained from the flights in The Netherlands (see figure 5.4). Less uniform relative ratios of CO₂, delta¹³C and CO exist in summer. Especially prominent are two values; the one located close to the CO axis and the one close to the CO₂ axis. The first reflects the conditions of a sample taken during a morning flight: with high values of CO₂ and very high ones for CO, coming along with a low amount of delta¹³C. From the CO₂ and CO values a contribution from combustion processes might be suggested, but also the delta¹³C a shows air enriched with the heavier isotope. Contrary to this unclear source the second conspicuous data point, calculated from a midday sample, gets an univocal source classification. High CO₂ and delta¹³C values combined with a low amount of CO are representative for respiration air originating from a rural area.

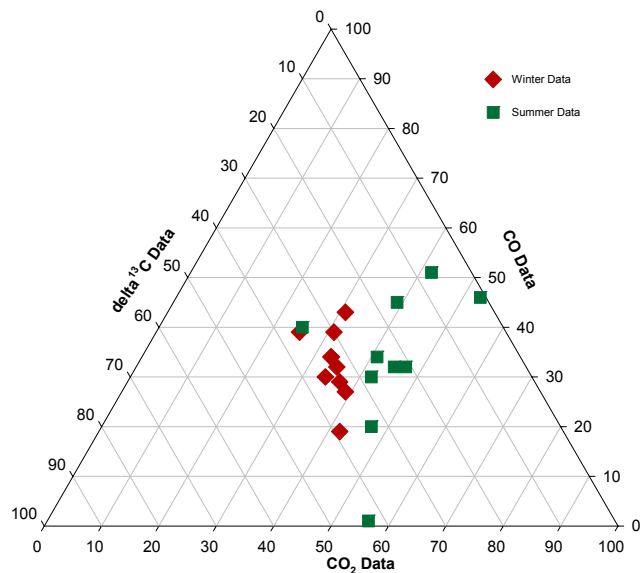


Figure 5.4. Relative composition of CO₂, CO and delta¹³C from flask samples taken in the free troposphere during the summer and the winter experiment in 'The Netherlands'. Displayed are data from morning and midday flights above the *Maize* and the *Cabauw* site. For the discussion of the data see the text above. Scale base for the gas species and the isotope values are defined by the observed ranges of both campaigns (see also Appendix A6).

Cabauw / Maize	CO ₂ [ppm] 360.0 → 380.0	CO [ppb] 116.0 → 166.0	delta ¹³ C [%] -7.750 → -8.500
----------------	--	---------------------------	--

5.1.2.2. Longitudinal Differences

Likewise of specific interest was the comparison of the areas belonging to same latitudinal zones within Europe. Since there are no significant data available from the Italian campaign to carry out a southern Europe examination, a longitudinal analysis was only practicable for the central European study sites 'Thuringia' and 'The Netherlands'.

Table 5.5. Averages of the CO₂ mixing ratios observed above the *Hainich* (Thuringia / Germany) and at the 'Maize' study area (The Netherlands) during the winter and summer campaigns.

	CO ₂ mixing ratios [ppm]		
	Summer	Difference	Winter
Hainich (Thuringia)	364.3	20.0	384.3
'Maize' (The Netherlands)	368.3	9.8	378.1

With respect to CO₂ the most obvious difference between the areas can be seen in the amplitude of the annual cycle, whereas the simple mixing ratio mean is quite similar for both regions (see table 5.5). Because the Dutch area is even more urbanized than Thuringia, one should expect in particular for the winter season a slightly different result. An explanation for the observation might be given by the geographical conditions. Since the location of The Netherlands is less continental than the German study area the influence of air from marine origin is significantly higher (see also table 5.6). Because westerly and south-westerly winds are dominant for both regions a differentiation can be expected following the individual footprints. Thus the air masses sampled at the more continental 'Hainich site' should be transformed while passing over the land surface. Thereby, in summer time the CO₂ mixing ratio will be more and more reduced due to assimilation by plants, whereas during the winter the air might collect successively the released exhausts on their way eastwards.

More difficult is the situation when analysing the CO and SF₆ relationship of the summer data. Figure 5.5 presents the results from flights performed above the marshland site in The Netherlands in July 2002 and the data from the flights carried out above the Hainich during the SPA¹³CE experiment on 14 August 2002,

the day identified by multiple tracer comparisons (see figures 5.12. and 5.13.) and the modelling studies (see figure 4.30.) to be characterised by an air mass which has passed before also the Dutch area. When comparing the data displayed in figure 5.5 significantly higher CO, and slightly elevated SF₆ mixing ratios are observed at the marshland site.

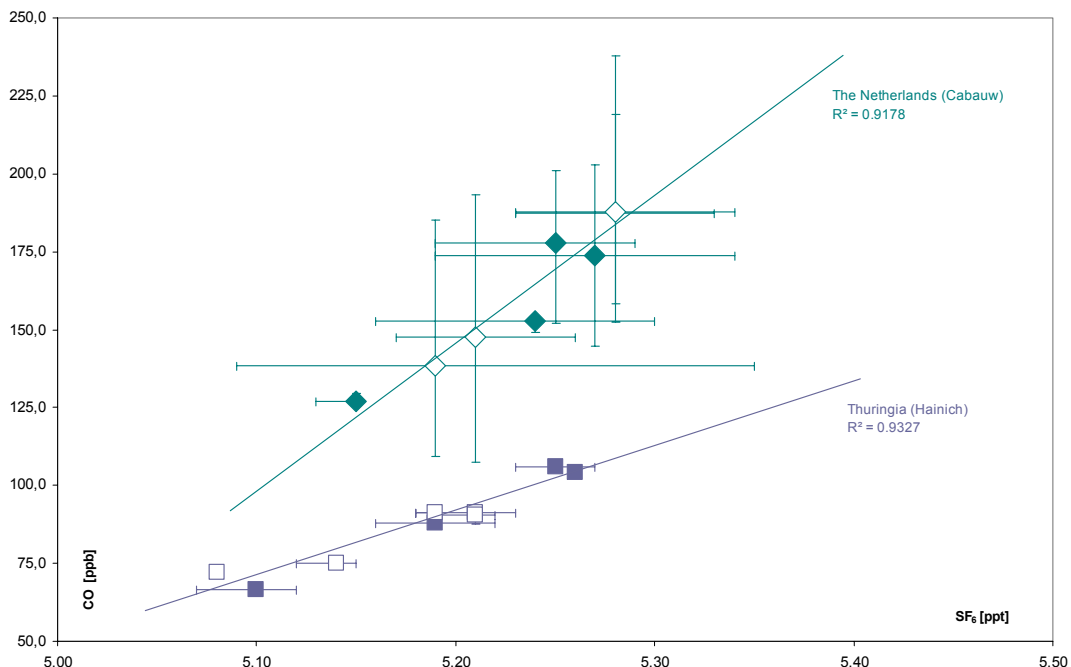


Figure 5.5. CO / SF₆ ratios obtained from the flask samples at the *Cabauw* site (diamonds) during The Netherlands Summer Experiment on 16 and 27 July 2002 and above the *Hainich* (squares) during the SPA¹³CE Experiment on 14 August 2002 (Thuringia / Germany). Indicated are the individual flight levels for morning (solid symbols) and midday (open symbols) flights respectively. For both sites a linear regression was calculated.

The range of the observed maximum and minimum mixing ratios are indicated by the bars for SF₆ and CO. Notice that for the Hainich samples the range reflects the variance of the paired flasks, but for the Cabauw samples the range of two days. For CO the variance of the Hainich results is less than the symbol size.

As a reference possibly representative for both locations CO data from the marine background station ‘MACE HEAD’, Ireland (for location see figure 5.6.) can be taken. For June an average mixing ratio 103.21 ppb is reported, for August 118.97 ppb, respectively [data from CMDL CCGG]. Thus, lower mixing ratios should be expected from the samplings carried out at the Dutch marshland site. Therefore the question arose: Which fraction of the observed signal is contributed by regional

sources and which might be an effect of long range transport or chemical transformation?

The difference between the reference and the observed marshland data are indicating an importance of regional sources. Somewhere in between both sites the probable source area should be located. Since the data obtained from the flights performed above the Hainich on 15 August 2002 (which were characterised to be affected by passing across the UK) are not reflecting similar CO mixing ratios as observed at the marshland, a source located close to The Netherlands might be likely. A contribution from CH₄ conversion, originating from methane emission from tidelands, gas fields and marshlands also seems possible.

Regarding the differences between the Dutch and the German observations dilution processes might be of some importance. But when comparing the effects on SF₆ and CO: for the reduction of CO the contribution of additional processes has to be expected. A probable reaction could be the oxidation to CO₂, which seems to be reflected by the high variance of sources contributing to the summer CO₂ signal as presented in figure 5.3.

DIFFERENTIATION ALONG THE NORTH – SOUTH TRANSECT

5.1.2.3. Latitudinal Differences

The ‘RE CAB study regions’ can be differentiated by latitudinal criteria in three zones: the Uppland area within the northern band, the Valencia and the Latium sites defining the southern part and the Dutch and the German locations in between. When determining the individual sites one has to take into account that the composition of the air might be affected by different and locally specific processes, whereby a direct comparison focusing only on singular effects might be critical. Thus an influence by polluted air from industry is more characteristic and representative for a highly industrialized area as for a remote place. On the other side, CO formation from VOCs is more likely at a forest site, than within highly urbanized areas. Since it became obvious that local interferences are hindering a regional characterisation (see the analysis of the summer campaign in ‘The Netherlands’), the comparison of the zones considers only data from the upper profiles. On the other hand the free troposphere data will as well not reflect the real ‘regional’ characters but more information of the entire zonal band the study site is belonging to.

Since the campaigns were not performed simultaneously CO₂, CH₄ and delta¹³C data from the atmospheric research station MACE HEAD, Ireland (53°20’N / 9°54’W) are presented as an ‘independent relation frame’ (see figure 5.6). A distinct seasonal signal reflecting probably the contribution of assimilation from the CO₂ and delta¹³C data can be recognized, which seems to be congruent with the hypothesis regarding the effect of the time delay of the individual campaigns (see table 2.4, p. 22). But a similar distinct seasonality could not be observed for CH₄. However, it should be taken into account that the data do not offer a real and objective basis for comparisons, since the data themselves are affected by impairments. In this context the question about the significance of time delays seems to be of importance, in particular with respect to the reflection of signals from plant activity (see therefore chapter 5.2.). The influence of vegetation underlies per se inherent constraints – on a temporal basis and as well regarding spatial dynamics, following the progression of the phonological status from the south to north. Another aspect might be the spatial frame of synoptic processes,

on that account the comparability of the individual campaign regions with the reference station might be limited. Thus the 'Mace Head' data should not be taken noncritical as calibration values, but as additional hyper-regional information.

Comparing the results from the flask samplings of the summer campaigns a significant north-south gradient becomes obvious (see figure 5.6.). The CO₂ mixing ratios and isotope composition are reflecting the effect of the vegetation at the Swedish locations, while the results from central and southern Europe are characteristic for more urbanized areas. Intermediate values are obtained from the central sites. As expected from the natural environment, since potential sources like swamps are wide spread in Scandinavia, highest CH₄ mixing ratios were measured at the northern location.

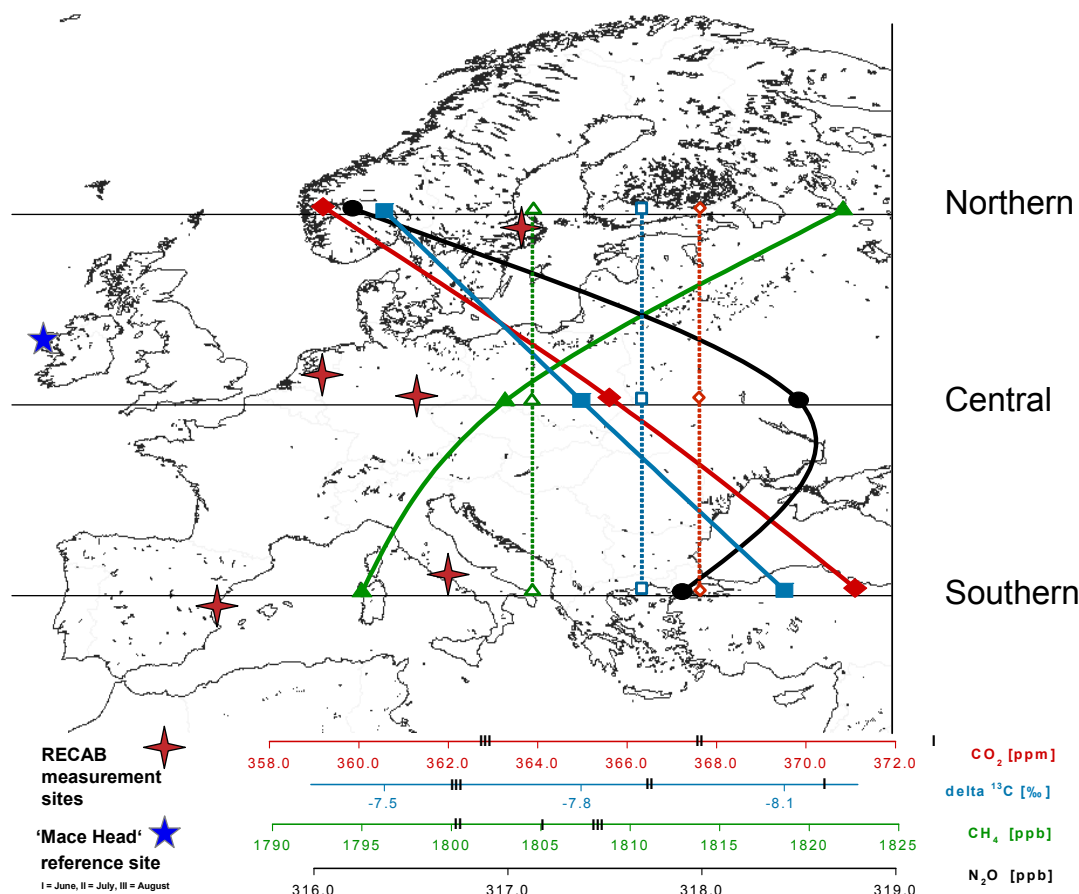


Figure 5.6. Summer campaigns: Averaged values of the measured mixing ratios of CO₂ (diamonds), CH₄ (triangles), N₂O (circles) as well as the $\delta^{13}\text{C}$ in CO₂ (squares) for the three European zones. Only data sampled within the free troposphere have been taken, to avoid perturbations by local contaminations. By the open symbols the mean values calculated for the 'background reference site' MACE HEAD are indicated. On the individual mixing ratio axis the monthly means are marked [2001 / 2002; Data from CMDL CCGG].

Regarding the N₂O mixing ratio a different gradient is being observed. The highest values occur in Central Europe. This can be related to the formation process of N₂O, which is primarily released from moderately moist soils. At the southern locations very dry conditions inhibited microbiological activity, whereas in the northern parts the soils were partly less drained. The higher percentage of agricultural areas and the potentially additional input of nitrogen by fertilizing might also be a contributing factor for the enhanced values which were observed at the Central European sites.

During winter time only the locations in The Netherlands, in Germany and in Spain were sampled (see table 5.6). Contrary to the summer data the lowest CO₂ mixing ratios were measured at the Valencia site. The reduced values in the southern part are reflecting the still active vegetation, since the weather was fine when the campaign took place and the temperatures were above 15°C. Therefore also emissions from heating were reduced, compared to Central Europe, where the temperatures were lower (The Netherlands: about 10°C, Germany: below 0°C).

Table 5.6. Comparison of the mixing ratios obtained from the winter campaign flights in Central Europe (Thuringia and The Netherlands) and in Southern Europe (Valencia). Samples were taken within the free troposphere.

	CO ₂ [ppm]	δ ¹³ C [‰]	CH ₄ [ppb]	N ₂ O [ppb]
Thuringia	380.6	-8.553	1841.1	317.8
The Netherlands	375.7	-8.331	1827.3	318.4
Central (Average)	378.2	-8.442	1834.2	318.1
Valencia	368.3	-8.072	1808.0	318.1

That a part of the differences between the German and the Dutch region might also be attributed to the temperature discrepancy becomes in particular obvious from the N₂O data, reflecting the inhibition of the microbiological activity in the frozen German soils. In addition a significant contribution of the differences can be attributed to longitudinal effects, as described earlier in the context of the seasonal variations.

Figure 5.7 presents the relationship between CO₂ and delta¹³C obtained from flights carried out above the marshland in The Netherlands and the rice fields in Spain. Distinctly higher CO₂ mixing ratios and more negative delta¹³C values were observed at the Dutch region. From the data source discrimination characteristics of -27.454‰ (The Netherlands) and -24.546‰ (Spain) can be calculated, pointing to a stronger impact of anthropogenic emissions and reduced assimilation in The Netherlands.

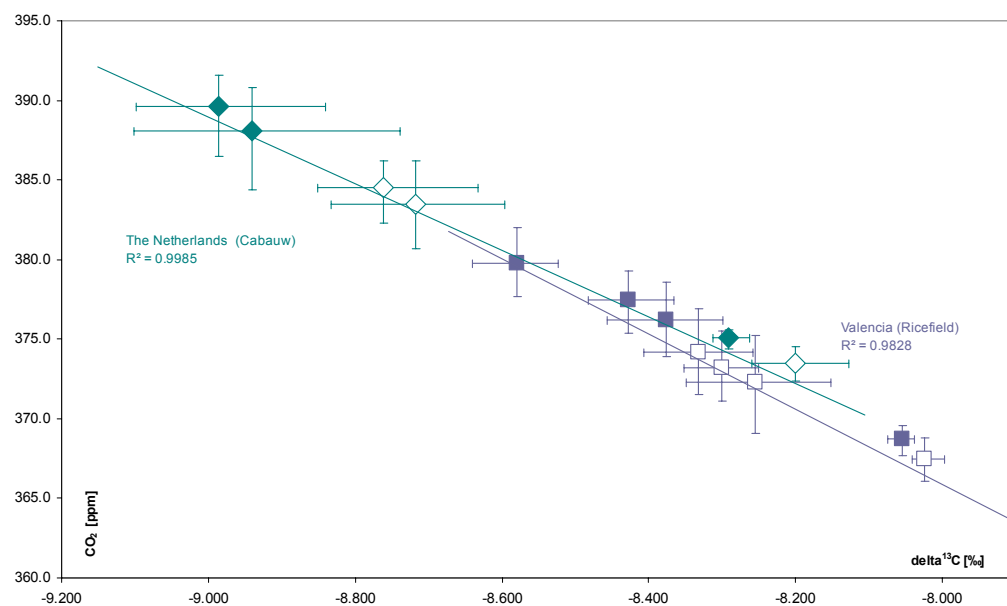


Figure 5.7. CO₂ / delta¹³C relation obtained from samples taken at the Cabauw site (green diamonds) during The Netherlands Winter Experiment on 30 January 2002 and 2 February 2002 and from the Rice field site (blue squares) during the Valencia Winter Experiment on 5 and 6 December 2001 for morning (solid symbols) and midday (open symbols) flights, respectively.

The differentiation of both study regions by a differing CO₂ and delta¹³C relation is also reflected in figure 5.8, which adds CO information. The solid symbols represent samples taken within the CBL and open ones the free troposphere. Besides the wide range of the CO fraction at both locations a high variability of the tracer relation in the Spanish ‘free troposphere’ is obviously caused by contributions from different sources. Local contamination is indicated by the outliers sampled within the CBL. Thus affections are important which are not comparable with a budgeting of the regional scale.

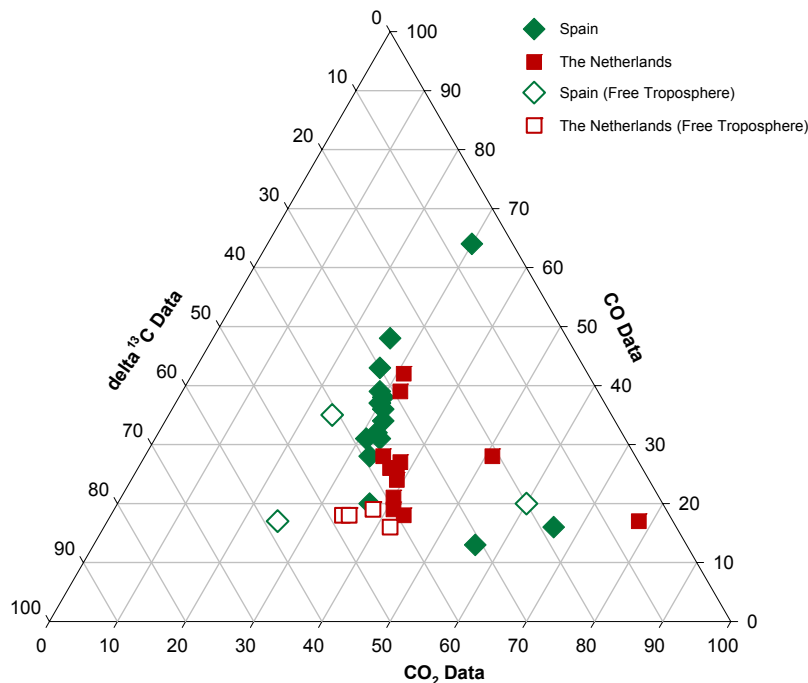


Figure 5.8. Relative composition of CO₂, CO and delta¹³C from flask samples taken during the winter experiments in Spain (*Rice field*) and The Netherlands (*Forest and Maize*). The results presented in this figure are discussed in the text section above. Scales for the CBL are defined by the observed ranges of the individual campaigns, but for the 'Free Troposphere' by both experiments (see also Appendix A6):

	CO ₂ [ppm]	CO [ppb]	delta ¹³ C [%]
Forest / Maize (The Netherlands)	373.0 → 383.0	127.5 → 247.5	-8.250 → -8.700
Ricefields (Spain)	364.0 → 374.0	105.0 → 225.0	-8.000 → -8.450
Free Troposphere	367.5 → 379.5	110.0 → 170.0	-8.030 → -8.480

5.2. Theoretical and Conceptual Aspects

A basic idea of the budget approach is to use the difference in the mixing ratio obtained from two measurements as a measure to calculate fluxes. Thus the environmental conditions at both sample times should be identical.

5.2.1 TIME DEPENDENCE

When analysing biological contributions to mixing ratio changes CBL and vegetation dynamics have to be taken into account. These dynamics as a function of solar irradiance are intensively discussed in the literature [DENNING et al. 1995, BAKWIN et al. 1998, DENNING et al. 1999, STEPHENS et al. 2000]. In this study it affects mainly the diurnal and seasonal comparisons. In summer both parameters are negatively correlated. When CO₂ mixing ratios reduced through assimilation by plants CBL height reaches its maximum during its yearly cycle. In contrast, in winter the shallower CBL accumulates the respiration CO₂.

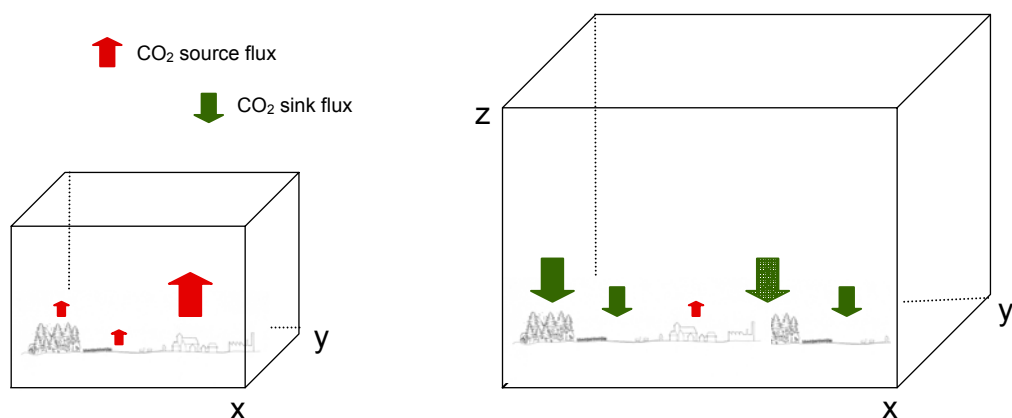


Figure 5.9. Scheme for the time dependence of CBL height and carbon source/sink activity. The left box presents the situation dominant for winter and night time, characterised by a shallow CBL. The right one a summer day near noon. An extended CBL height comes along with high CO₂ uptake by vegetation and low anthropogenic emissions.

The vertical dilution affects not only near surface measurements but also data from continuous profiles. Beyond this effect another phenomenon affects the budgeting

approach. Since the CBL is defined as a nearly closed integration chamber, also the varying spatial dimension of the monitored area needs to be considered.

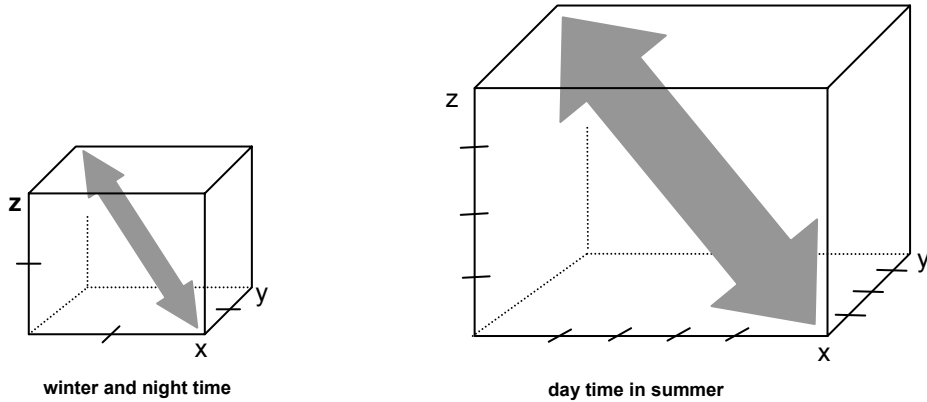


Figure 5.10. Relationship between CBL height and extension of the footprint. On the left a shallow CBL with a small footprint area is presented typical for winter and night time conditions. The situation for a summer day is shown by the right box, where an extended CBL height enlarges the 'footprint'. The dimension of the source area is indicated by the arrow size.

The influencing region on a summer afternoon will be much larger than on a winter morning. The spatial extent of the influencing *region* may vary from nearly local, to regional, to continental, and occasionally even to global scale. Accordingly each concentration profile describes different areas. Because of this relationship between temporal and spatial extension one might define this effect as a 'regional rectifier'.

In this context the uncertainty arose how to fix the flight levels, in particular for the first morning flights. It could be shown that frequently the residual air from the day before was sampled instead of a shallow CBL, missing a major portion of respiration. To sample morning air from a larger area a compromise had to be found: On one hand a sampling height as low as possible was required, to gain information from the CBL reflecting the respiration character. However, the flight time had also to be chosen as late as possible, to sample air of an extended CBL column, representing a regional area. In consequence during summer the starting time had to be fixed with sunrise, which is also the earliest time permitted by the aviation regulations. During winter the starting time was scheduled around two hours after sunrise.

VARIABILITY - AIR MASS CHANGE

By the multiple tracer analyses air with distinctly different compositions could be identified between repeated samplings at one location. Because of the forced rapid changes of the mixing ratios the samplings were most frequently not comparable. The consequence of this was that fluxes and budget calculations for the study regions could not be achieved.

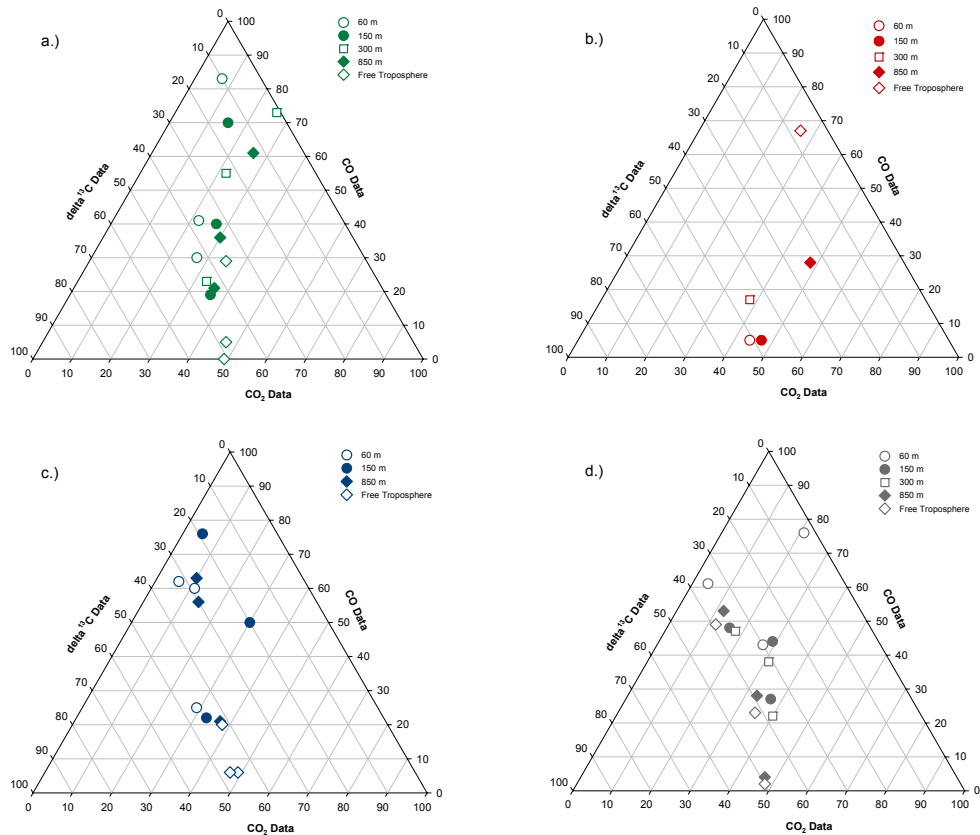


Figure 5.11. Relative composition of CO_2 , CO and $\delta^{13}\text{C}$ from flask samples taken at a) Florarna (Uppland / Sweden), b) Tuscania (Lazio / Italy), c) 'Maize' (The Netherlands) and d) Hainich (Thuringia / Germany; SPA ^{13}CE experiment). Scale basis for each gas species and the isotope values are defined by the observed ranges of the individual campaigns:

	CO_2 [ppm]	CO [ppb]	$\delta^{13}\text{C}$ [%]
Florarna (Sweden)	349.0 → 359.0	106.0 → 136.0	-7.035 → -7.635
Tuscania (Italy)	369.0 → 379.0	125.0 → 185.0	-8.100 → -8.400
Maize (The Netherlands)	360.0 → 370.0	105.0 → 205.0	-7.550 → -8.050
Hainich (SPA ^{13}CE , Germany)	361.5 → 371.5	70.0 → 130.0	-7.550 → -7.950

Variability of air composition as well as of individual gas mixing ratios could be observed according to several aspects: on a spatial basis, e.g. by stratified sampling levels, by different locale profile sites within the study regions and by the diverse regions (see figure 5.11, Appendix A6), on a temporal basis, exemplified by rapid and diurnal changes or by variations on a day-to-day, a seasonal or an inter annual time scale.

Day-to-day Variability

On two consecutive days of the SPA¹³CE experiment different air masses could be observed. A classification to probable source areas could be achieved from multiple tracer analyses and modelling investigations (see also chapters 4.2.8.1. and 4.8.2.2.).

Figure 5.12 presents the CO and SF₆ mixing ratios from both days (solid symbols 14 August 2002, open symbols 15 August 2002; green: morning data, blue: data from midday flights).

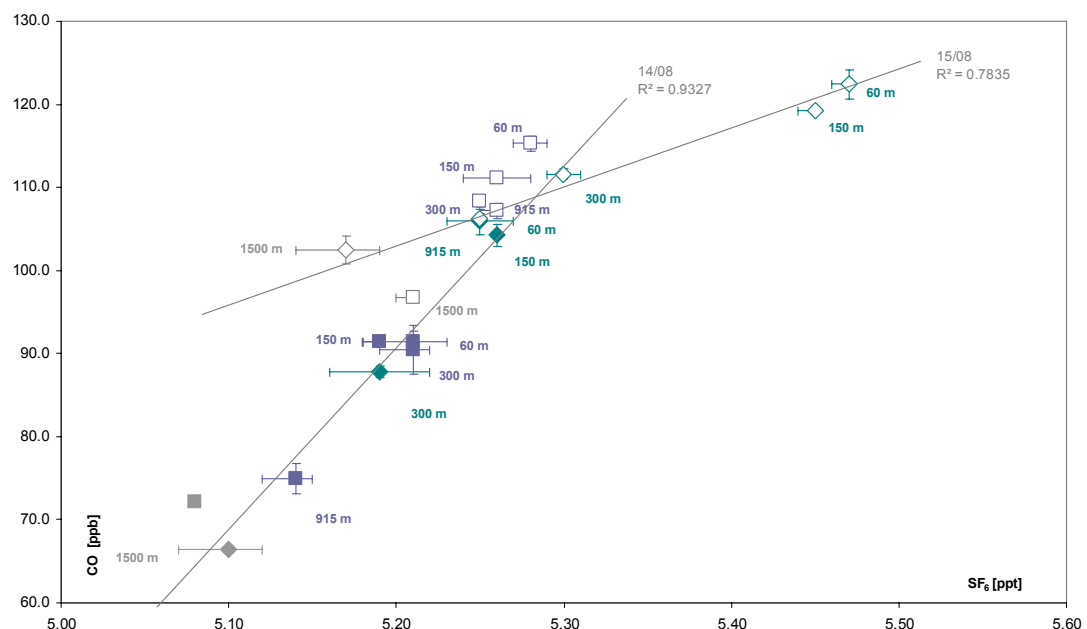


Figure 5.12. CO / SF₆ relation obtained from the flask samplings performed during the SPA¹³CE experiment on 14 and 15 August 2002 above the Hainich (Thuringia / Germany). The flight levels are indicated by green diamonds for morning flights (solid 14, open 15 August 2002), and blue squares for midday data. A linear regression was calculated for both days. The bars for SF₆ and CO indicate the paired flasks.

A higher mixing ratio of both trace gases is clearly noticeable on 15 August 2002. As the formation of SF₆ is related to anthropogenic activity and CO production occurs during combustion processes and from conversion of biogenic precursors a significantly higher contribution from terrestrial sources is reflected by the data. Also the lower explained variance compared with the results from the 14 August suggests the input from several different sources.

An equal finding can be obtained from the analysis of the relationship between the CO₂ mixing ratio and the delta¹³C values, while a lower R² suggests a contribution from several different sources on 15 August 2002. This day a lower CO₂ mixing ratio is associated with slightly more negative delta¹³C values. For 14 August 2002 a discrimination of about -25.649 ‰ can be calculated, against a discrimination of about -26.846 ‰ for 15 August 2002 which might reflect an increased input from fossil fuel consumption and assimilation activity.

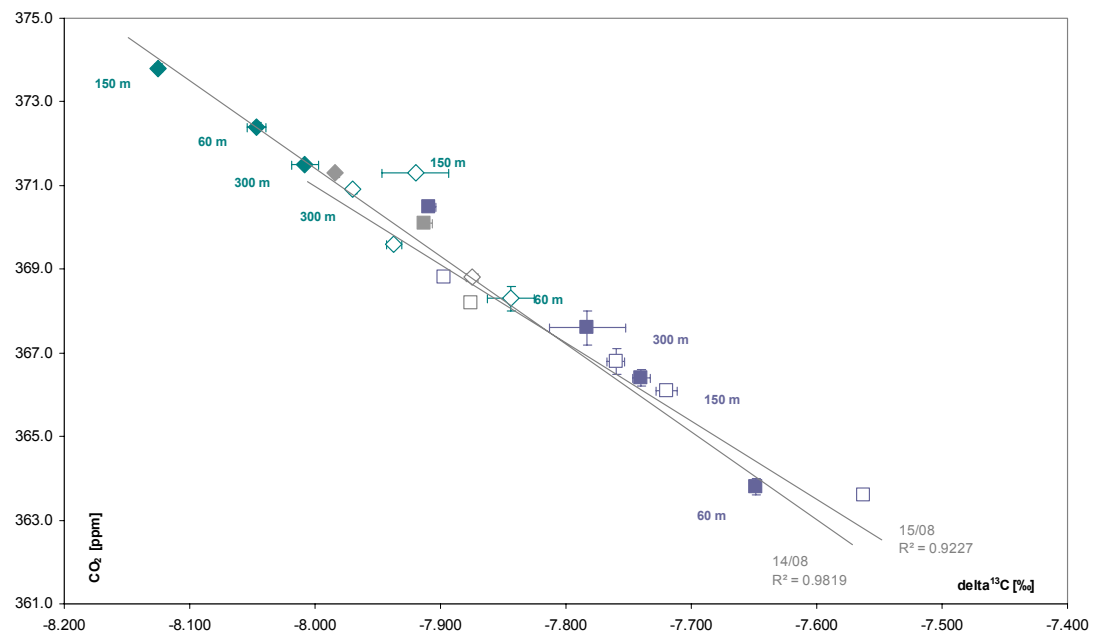


Figure 5.13. Mean mixing ratios of CO₂ and delta¹³C from each flight level and of the entire profiles from the flights performed within the SPA¹³CE experiment above the Hainich study site (Thuringia / Germany) on 14 and 15 August 2002.

Morning results are shown as green diamonds (solid 14, open 15 August 2002), the midday data as blue squares. Linear regressions were calculated for both days. Discrimination values are: 14/08/2002 (-25.649 ‰) and 15/08/2002 (-26.846 ‰). The error bars are indicating the range of the mixing ratios between paired flasks.

These differences were also confirmed by ground level sampling (see figure 4.17). However, since advection affects the entire profile, a disturbance and concealment of the canopy contribution by air mass change can not be excluded. It is, therefore still difficult to distinguish which part of the signal is of local origin and which can be assigned to air mass change because of advection.

Local Characteristics - Land-Sea-Wind Circulation

Beside the identification of exchange processes on a day-to-day time scale, which was achieved by using multiple tracer data, the detection of disturbances within a diurnal cycle became also possible. The affection by periodical circulation schemes shall be demonstrated on the basis of the results from the Valencia field experiments.

Due to its geographical location at the shore of the Mediterranean Sea a distinct diurnal land-sea-wind circulation scheme can be observed. During day time the terrestrial surface is heated stronger by solar irradiance. This is in conjunction with convection above the land and a draft directed downwards creates an onshore wind. In contrast during the night, the warmer water body causes an offshore wind. The resulting wind is collaterally affected due to the local topography. Within the valleys directed orthogonal to the Mediterranean Sea an amplification is induced.

Figure 5.14 presents the CO / SF₆ relationship during two days of the winter campaign. A clear difference between morning (green diamonds) and midday data (blue squares) becomes obvious. In particular for the midday results distinctly higher SF₆ and slightly elevated CO mixing ratios can be recognized.

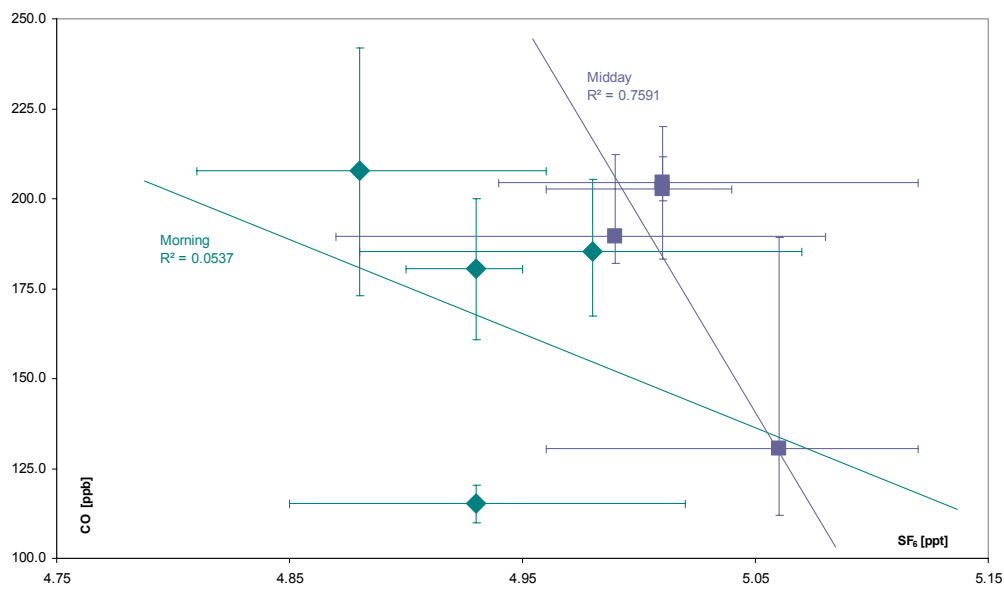


Figure 5.14. CO / SF₆ relation obtained from flask sampling above the Rice field site at the Valencia Winter Experiment (Spain) on 5 and 6 December 2001. Indicated are the individual flight levels for morning flights (green diamonds) and midday flights (blue squares) flights. For both dates a linear regression was calculated.

The range of the observed maximum and minimum mixing ratios is indicated by the bars for SF₆ and CO.

From this a classification of the source origin can be achieved: the relatively high SF₆ mixing ratios observed by the midday data indicate a contribution from anthropogenic sources. Also, the slightly elevated CO mixing ratios point to a terrestrial influence. Emissions from human activity contribute to the air mass while floating inland. In contrast, the morning samples were performed in the downdraft which takes air of marine origin inland.

This exchange process can also be seen from the relationship between the CO₂ mixing ratio and the delta¹³C values. Results from the ground level samplings are presented in subchapter 5.4.1. (see figure 5.21).

Since the effects caused by advection or by local events frequently exceeded the expected amount of the natural provoked values, the process of air mass change must be taken into account. This means that the geographical location in particular has to be considered, because of the effects forced by topography (see also chapter 4.2.8.1., pages 107f) and diurnal circulation schemes.

'SIGNAL SHIFT' – EFFECTS OF TIME DELAYED DETECTION

The interaction of temporal and spatial components determines an additional aspect that has to be taken into account. This was examined by the Swedish flight profiles from 30 August 2001.

Figure 5.15 displays the three profiles sampled during the day, showing within the CBL the typical diurnal cycle with an uptake of CO₂ by the vegetation. In contrast, the 'background' data from the free troposphere presented a distinct change in the afternoon when a significant increase of the CO₂ mixing ratio was observed, concomitant with a relative depletion of the ¹³C content. By ascribing this variation to air mass change caused by advection, two reasons for the composition of the afternoon signal have to be discussed: 1) the air originates from a different, urban source area, or 2) the air originates from a different source area, but of the same land use type. The change observed by the afternoon data will then be an effect of different formation processes, i.e. the sample represents a respiration signal.

When assuming that the afternoon sample is characterised by respiration one can replace the morning sample by this data. Consequently, the other two data sets can also be exchanged to adapt the free troposphere signal to the profiles obtained from the CBL, leading to the substitution scheme: afternoon (real) → *morning (notional)*, morning becomes *midday* and midday becomes *afternoon*.

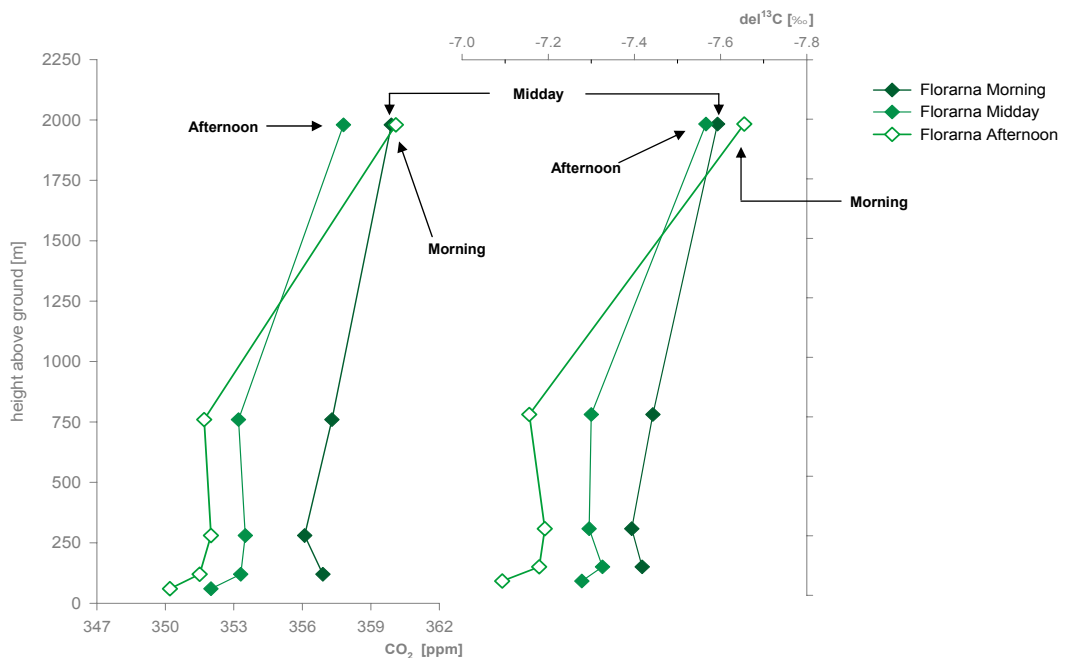


Figure 5.15. Time delayed detection of ‘formation specific’ CO₂ and delta¹³C signals observed on 30 August 2001 above the Florarna site (Uppland / Sweden). The afternoon sample taken in the free troposphere shows a composition typical for respiration. For description of the calculation and shifting scheme see text.

Estimating the order of a probable uncertainty regarding flux calculations from a comparison between the real observed data and the data set with the adapted classification the following can be said: the depletion of CO₂ during the day obtained from the observation can be mentioned to be -3.1 ppm versus a rate of -4.9 ppm derived from the changed classification, equivalent to flux rate differences like $-16.8 \text{ } \mu\text{mol m}^{-2} \text{ s}^{-1}$ to $-26.5 \text{ } \mu\text{mol m}^{-2} \text{ s}^{-1}$. This means that a calculation based on the *observed* profile will underestimate the hypothetical, but rather plausible, value by about 40%. Relating this result to the uptake of carbon by vegetation, a further brief calculation gives an indication regarding the sensitivity of inventories. Within the period of a growing season (defined here by a time frame of 100 days with 8 hours per day uptake by vegetation) a flux of

$1\mu\text{mol m}^{-2} \text{s}^{-1}$ is equivalent to a carbon uptake of about $350 \text{ kg ha}^{-1} \text{ season}^{-1}$. For instance, the net annual carbon fixation of European forests studied by the CarboEurope project ‘Forest Carbon Nitrogen trajectories’ (FORCAST) is in the main between 3 and $6 \text{ t C ha}^{-1} \text{ a}^{-1}$ [MUND, *personal communication*].

By the occurrence of the combination of temporal driven processes and advection, which itself has a time depending component, crucial uncertainties might be provoked. Thus one also has to take this relationship into account when analysing effects provoked by reactions between gases and removal depending on deposition processes.

CH₄ AND VOC CONVERSION

Even at the Swedish site, characterised by a land cover of less heterogeneity and a low contamination potential, a high variability of the mixing ratios could be observed (see table 5.7). Beside the enforced changes due to air mass replacement by advection, modifications can also be caused by chemical reactions between certain compounds. For some of the observed trace gases transformation is even the major terrestrial sink – or on the other side a not negligible source.

Table 5.7. Relative change of the mixing ratios observed above the *Florarna* site (Uppland / Sweden) on 30 August 2001
 (expressed in percent from morning to midday, from midday to afternoon and from morning to afternoon flights respectively; calculated from data sampled within the entire CBL column)

	CH ₄	CO ₂	CO	SF ₆	H ₂
Morning → Midday	-0.02	-2.51	+3.45	-0.61	+0.07
Midday → Afternoon	+2.96	-0.45	-1.26	+1.43	-1.13
Morning → Afternoon	+2.80	-3.04	+2.16	+0.81	-1.07

In addition to combustion processes, CO can also be produced by the conversion of CH₄ and from VOCs. The destruction of CH₄ depends mainly on the reaction with the OH radical (see reaction chain 2.1.2.11 ff.). Because of the very high CH₄ mixing ratio occurring at the wetland site and due to the percentage of CO formation described from CH₄ conversions to be about 20% (see table 2.1), a probable contribution by this pathway has to be quantified. Figure 5.16 presents

the correlation between CH₄ and CO mixing ratios, suggesting a principal relationship ($R^2 = 0.6629$).

Based on the samplings carried out at the Florarna site CH₄ conversion rates were calculated using different reaction coefficients (uniform 298K and 760 Torr) and concentrations for OH.

Because of the observed variability within the diurnal time frame (see for instance table 5.7) and on a day-to-day time scale (indicated by the bars in figures 5.1., 5.16 and 5.17), averages from the three days of morning and midday flights were used for the estimations (see table 5.8).

Table 5.8. Averaged mixing ratios used for calculation of the conversion rates

	Morning	Midday	Difference
CH ₄	1872.0 ppb	1864.3 ppb	-7.7 ppb
CO	115.9 ppb	121.8 ppb	+5.9 ppb
CO ₂	358.4 ppm	352.1 ppm	-6.3 ppm

The rate of the destroyed CH₄, i.e. of the formed CO, varied between 198 ppt h⁻¹ (with $k = 4.9 \cdot 10^{-15} \text{ cm}^3 \text{ molecules}^{-1} \text{s}^{-1}$ [WARNECK 2000] and OH_{conc.} = $6 \cdot 10^6 \text{ mol cm}^{-3}$) and 558 ppt h⁻¹ (with $k = 8.4 \cdot 10^{-15} \text{ cm}^3 \text{ molecules}^{-1} \text{s}^{-1}$ [Atkinson 1989] and OH_{conc.} = $1 \cdot 10^7 \text{ mol cm}^{-3}$). During the period between both flights of about 5 hours the total of the transformed CH₄ can be assumed to be in the order of ~ 1ppb to 2.8ppb. These amounts explain 13 – 36% of the observed CH₄ depletion, but 17 – 47% of the formed CO.

A second chemical formation of CO, with a contribution of about 20% in the same order as reported for CH₄ (see table 2.1), is the oxidation of volatile organic compounds (VOCs). VOCs originate mainly from biogenic processes (see table 5.9), in which emissions from foliage represent the primary source. The two prominent classes are monoterpenes, which originates mostly from coniferous species, and isoprene, released substantially by deciduous plants and as well as from wetlands [JANSON and DE SERVES 1999].

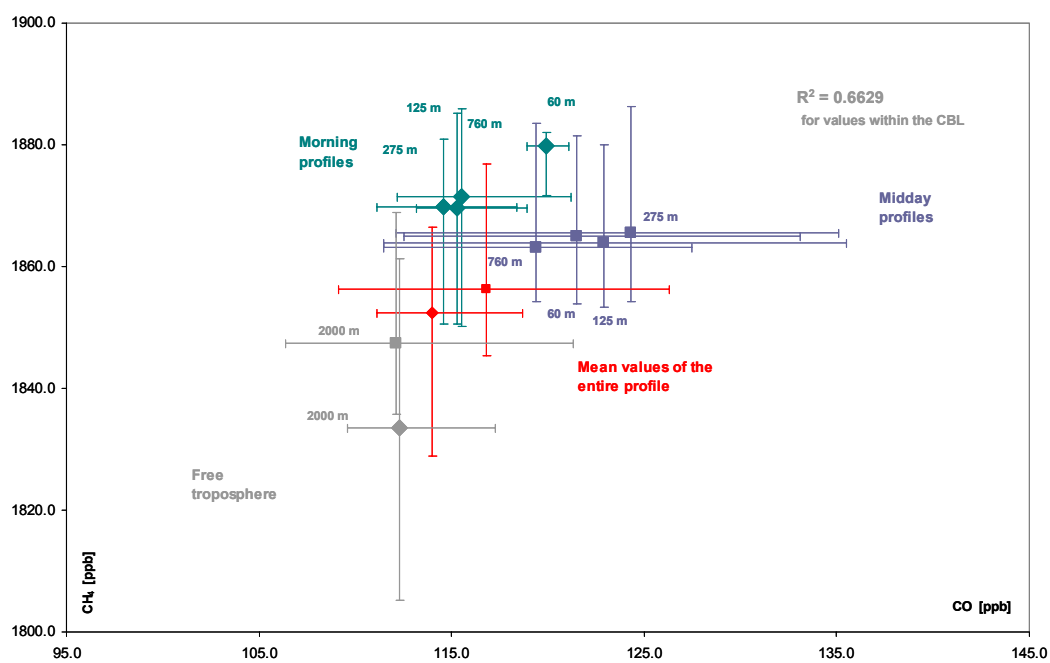


Figure 5.16. CH_4 / CO relation from samples above the *Florarna* nature reserve (Uppland / Sweden) on 29 and 30 August and 1 September 2001. Indicated are the means for the individual flight levels for morning (solid diamonds) and midday (solid squares) flights, and of the entire profiles. Ranges of the mixing ratios during all days are indicated by the bars for CH_4 and CO. For the calculation of the explained variance only samples taken within the CBL are considered, with the exception of the morning 60 m data, which were excluded (see also figure 5.1).

Because the reaction rate of OH radicals with VOCs is much higher than with CH_4 , and high VOC mixing ratio occurs in the boreal zone during summer, a relevant contribution by this pathway can be assumed. It is, however, difficult to give an estimate, since VOCs were not part of the analytical scheme of RECAB. The calculation is, therefore, only a rough indication for this formation way.

Table 5.9. Summary of Global emissions of Hydrocarbons and Other Organic Volatiles from Various Sources
(from Warneck 2000)

Anthropogenic Sources	Emission rate (Tg/a)
Petroleum related and chemical industry	36 – 62
Natural gas	2 - 14
Organic solvent use	8 - 20
Biomass burning	25 – 80
Total anthropogenic sources	71 - 175

Biogenic Sources	Emission rate (Tg/a)
Emissions from foliage	
Isoprene	175 – 503
Monoterpenes	127 – 480
Other organic compounds	510
Grassland	< 26
Soils	< 3
Ocean waters (light alkanes and alkenes)	2.5 - 6
Ocean waters (C ₉ – C ₂₈ alkanes)	< 26
Total biogenic sources	815 - 1530

But measurement results from this region are available from the 'BIPHOREP project' (*Biogenic VOC emissions and photochemistry in the boreal regions of Europe*).

Studies focussing on VOC emission and transformation were performed around the Norunda field site (Sweden) and at different regions in Finland in 1996 and 1997. For the calculation of a supposable CO formation from VOCs data were used adapted to mixing ratios reported by LAURILA et al. [1999] for the 'Mekrijärvi' field site in south-east Finland. According to the isoprene emissions from wetlands reported by JANSON and DE SERVES [1999], a VOC mixing ratio of 750 ppt propylene-equivalent [CHAMEIDES et al. 1992] is assumed.

With a reaction rate $k = 2.6 \cdot 10^{-11} \text{ cm}^3 \text{ molecules}^{-1} \text{ s}^{-1}$ [Atkinson 1989] and OH_{conc.} = $1 \cdot 10^7 \text{ mol cm}^{-3}$ a VOC destruction results of about 700 ppt h⁻¹. When this fraction is projected over a period of 5 hours, similar to the CH₄ transformation, a depletion of about 3500 ppt is obtained. PAULSON AND SEINFELD [1992] calculate a CO yield from isoprene oxidation to be in the order of 3.4 CO per molecule of isoprene, which leads to a CO formation of about 11.9 ppb. However, one has to take into account that the reaction is limited by the replenishment of VOCs, i.e. the total CO formation will decrease with time. Nevertheless, by the consumption of the pool, which takes about 1 hour of time, 2.4 ppb CO will be formed, that is approximately 40 % of the observed 5.9 ppb.

When using CO as a tracer for CO₂ formed by combustion processes to identify particularly anthropogenic contributions, a determination of the individual sources of CO is mandatory. If conversion from CH₄ and VOCs is neglected, which

contribution to CO formation can be assumed to be in sum about 60 to 100 % at the Florarna site, an overestimation of CO₂ input from anthropogenic sources seems to be quite probable. However, a probable affection by advection becomes again evident, because conversion can not explain solely the observed changes of the CH₄ mixing ratio.

Since CO formation happens from manifold sources via several reactions and with variable formation efficiencies [NOVELLI et al. 1998, WOTAWA et al. 2001], a realistic identification and assessment of different sources is not achievable with the current equipment. It would, therefore, a desirable improvement to implement continuous CO recordings and, if possible, to include situ measurements of VOCs and OH into the analytic scheme.

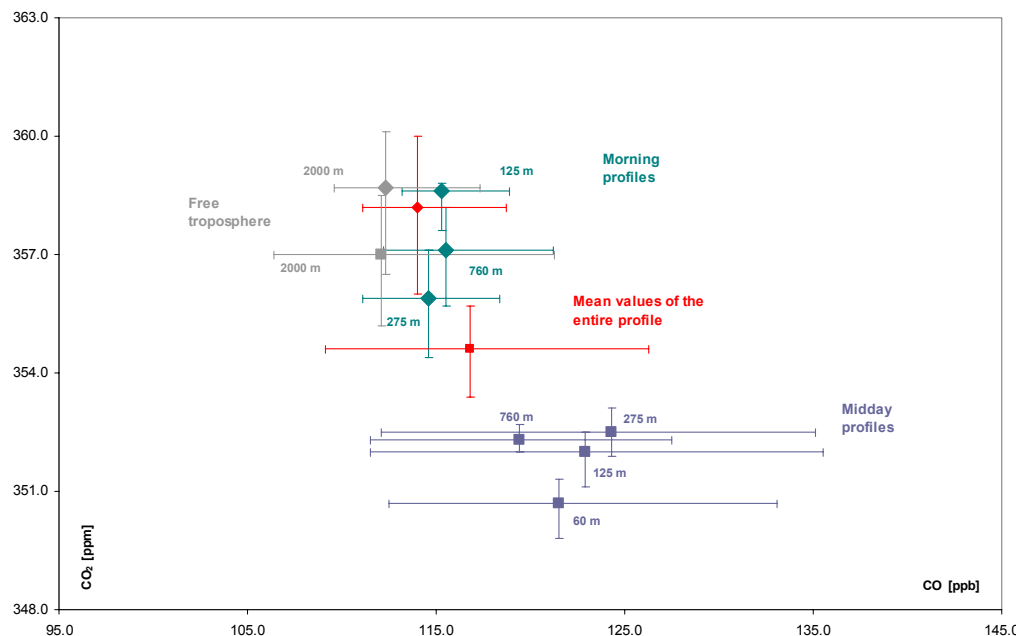


Figure 5.17. Mean mixing ratios of CO₂ and CO from each flight level (excluding 60 m morning flight height, as mentioned in figure 5.9.) and means of the entire profiles from flights above the *Florarna* ground reference sites on 29 and 30 August and 1 September 2001 (Uppland / Sweden). Morning results are shown as solid diamonds, midday data as solid squares. The bars for CO₂ and CO indicate the range of the mixing ratios throughout all days. For comparison with results from the Hainich study area see also figure 5.18.

It also has to be taken into account that CO itself is a precursor, since it is oxidised by OH to CO₂ (see reaction formula 2.1.2.1.). Regarding the amount of carbon derived by this way from global estimates (see table 2.1.) a contribution in the order of 0.6 – 1.1 PgC/a has to be expected, i.e. a fraction of 0.5 – 0.9 % related to

the postulated C flux between land and atmosphere of about 120 PgC/a [HOUGHTON et al. 2001].

Contrary to the conversion reaction described for CH₄, the mixing ratio of CO is not higher than the formation product, but much smaller than that of CO₂. Thus, significance with respect to an increase of the CO₂ mixing ratio seems unlikely. From a calculation (with CO = 120 ppb, $k = 2.4 \cdot 10^{-13} \text{ cm}^3 \text{ molecules}^{-1}\text{s}^{-1}$ [WARNECK 2000] and OH_{conc.} = $1 \cdot 10^7 \text{ mol cm}^{-3}$) results a CO₂ yield of 1 ppb h⁻¹, i.e. 5 ppb during 5 hours observation period. Based on the observed depletion this additional input would effect a minor underestimation of the CO₂ flux; the difference between a calculated surface flux including the supplementary CO₂ yield and the one unaccounted for this affection is in the order of 2 %.

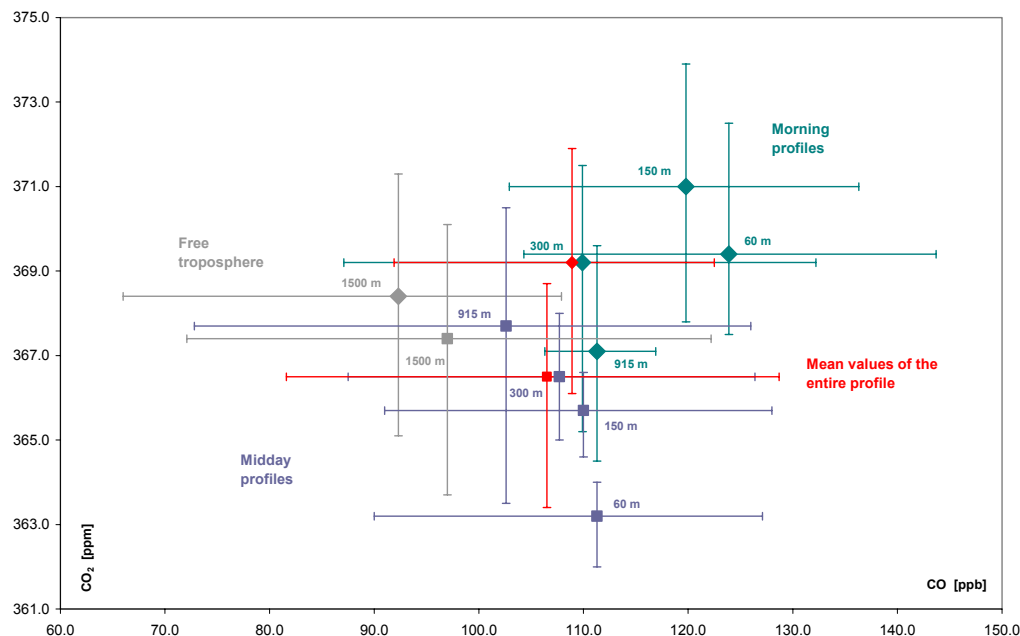


Figure 5.18. Mean mixing ratios of CO₂ and CO from each flight level and means of the entire profiles from flights above the Hainich study site within the SPA¹³CE experiment on 6, 14 and 15 August 2002 (Thuringia / Germany). Morning results are shown as solid diamonds, midday data as solid squares. The range of the mixing ratios covering all days is indicated by the bars for CO₂ and CO.

APPLICABILITY OF THE ‘CBL-BUDGET APPROACH’

From the analysis of the flight data it becomes obvious that fundamental assumptions of the ‘CBL budget approach’ (like linearity, see chapter 2.1.3.) are most frequently not prevalent.

The ‘CBL budget approach’ is bases on the hypothesis that the changes within the observed air column are completely explainable by the monitored fluxes. The influence of the subsidence should thereby be calculated from meteorological observations, or rather from results of reanalyses obtained from NCEP (National Centers for Environmental Predictions; USA). Furthermore, the contribution of entrainment should be assessable by the definition of individual CBL top heights for each profile. The heights are estimated from the curves of the potential temperature \varTheta and the relative air humidity f , respectively, and the specific humidity q . Finally, it is assumed that horizontal advection is negligible.

From the field observations it has turned out that in particular the last two assumptions are not met. It was frequently not possible to determine the CBL top height from the profile data of \varTheta and f (see figure 5.19.).

The fact that the CBL column is mainly affected by horizontal advection became obvious by the observed high temporal variability of the non-active trace gas mixing ratios. That the conditions of the ‘region’ are much more affected by large scale influences than expected is indicated by the random shift of the trace gas composition observed even in the free troposphere, which should also be used as background reference.

Another crucial error assumption became obvious by the high variability of the mixing ratios on small spatial scales and by the occurrence of stable stratification within the CBL. On average, the CBL is mixed less efficiently by convective processes than expected (see chapter 4.2.3.8. and figure 5.19.).

Likewise in this context, an additional uncertainty is caused by the temporal inconsistency of the transported air with respect to the direction and the speed at the individual levels. Thus, 3D field descriptions of the mixing ratios and the wind speed are needed in order to calculate properly the entrainment and the budget [VILÁ-GUERAU DE ARELLANO et al. 2004].

Related to these findings it turned out that profiles performed above only a single site were not able to provide representative data for the entire study region (→ The Netherlands field campaigns, chapters 4.2.6. & 4.2.7.).

When using the ‘fixed-mass’ budgeting approach (which neglects horizontal advection), LAUBACH & FRITSCH [2002] have quoted the error estimates to be 10-20% for CO₂. In fact the margin of error resulting from the interferences might be in the same order of magnitude than the expected signal from the processes that should be quantified - or even exceeds this. In particular, the rapid replacement of local air by air masses of quite different origin prevents regional flux- and budget estimations. In one case the probable error resulting from day-to-day variability due to advection (14 to 15 August 2002, SPA¹³CE experiment) is assumed to be approximately 50% of the expected diurnal cycle.

Because of stratification, with mixing ratio differences several magnitudes higher than the value of the expected diurnal depletion, no realistic estimation of the error potential of this source can be given. On the other hand, exemplified by the flight on 15 August 2002, a range up to 130% might be not unrealistic.

As expected, the sum of all errors make useful estimates unacceptable.

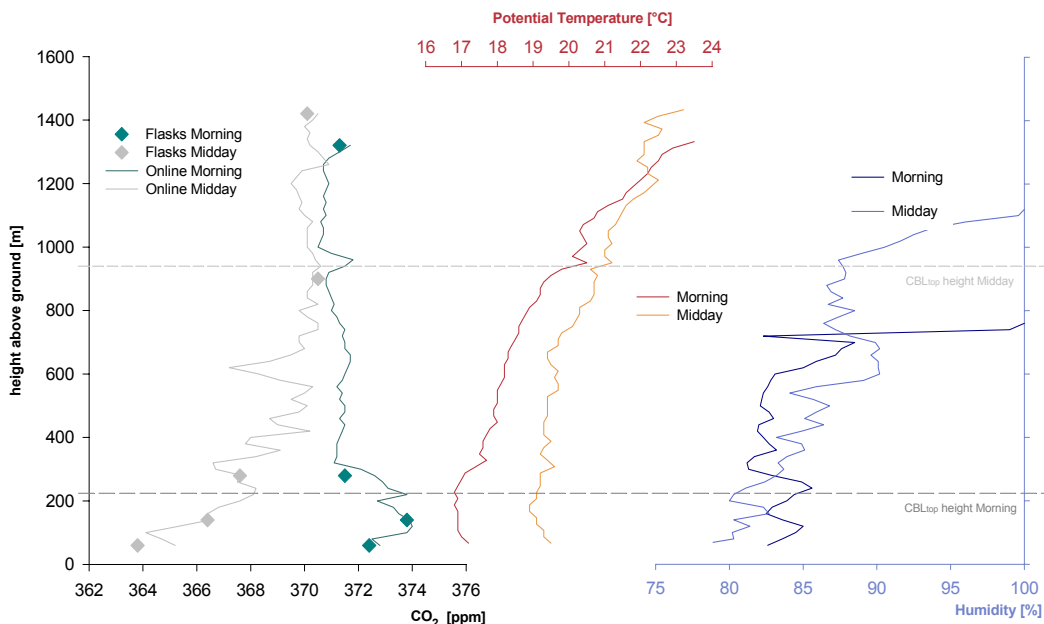


Figure 5.19. Profiles of potential temperature, relative humidity and CO₂ mixing ratios obtained from Licor online measurements and flask samplings. Shown are also the CBL_{top} heights derived from the profiles of θ and f . Flights were performed above the Hainich around 8:00 and 12:30 UTC on 14 August 2002.

5.3. Summary of Methodological Experiences

Multiple tracer analyses emerged to be an important approach regarding carbon investigations in the lower troposphere. Compared with previous CBL studies, mandatory information for the characterisation of the sampled air became available by implementing multiple tracer comparison examinations. Thus, for this study basic information could be obtained with respect to the verification of the underlying theories and the practised strategies, in particular the identification of most critical impairments. The multiple tracer analyses were also essential for the interpretation of the data regarding the characterisation and comparison of the RECAB study regions.

As a basic finding it should be noted: Which *spatial* and *temporal* character is represented by the air of the individual flasks is definitively determined by the instantaneously prevalent conditions of the sampled volume. Thus the '*where and when*' of the sampling has a major influence on the results of the budget calculation.

Systematic errors caused by the sampling unit were minimised by the development of a new construction scheme (see chapters 3.2. ff.). By the establishment of a ground reference unit additional information became available regarding the identification of affecting impairments (discussed in the following chapter 5.4). Regarding the characterisation of the sampled air, fundamental information has been obtained by comparison- and correlation-studies focussing on the trace gas composition and the delta¹³C fraction. Benefit with respect to the effects caused by advection could also be achieved from the combined approaches with modelling studies.

Diverse sources of uncertainty could be identified by the multiple tracer analyses. But most importantly, a quantification of the disturbing potentials could not be achieved because of the low amount of data.

However, by the examination of data from the field experiments some calculations were performed, which give at least an impression regarding the magnitude of uncertainty. Variability in the order of ~50% regarding the expected diurnal effect by assimilation uptake due to the affection by advection was described for the

SPA¹³CE experiment (p 103ff.). Because of improper definition of the CBL_{top} height, flux discrepancies of about 8% were pointed out from the summer campaign in The Netherlands (p 99f.). Provoked by time delayed detection of the signals due to transport processes, a difference of ~ 40% between observed and notional values was calculated (p 134f.). The error potential due to stratification, exemplified by summer time profiles taken above the Hainich, was in the order of ~50% (p 106ff.). Another process, affecting primarily the CO₂ / CO ratio used as one parameter to determine the contribution of anthropogenic sources to the CO₂ signal, was analysed on data basis from the Swedish experiment. Due to conversion processes arose an uncertainty with respect to the CO fraction of about 60 – 100% (p 135ff.). LAUBACH & FRITSCH quote the error estimate for CO₂ to be 10 – 20% when using their ‘fixed mass approach’; neglecting all of the listed processes above except the uncertainty from the determination of the CBL_{top} height. Finally, there are more processes whose contribution could not be sufficiently estimated, like the affection by contaminations (see for instance chapter 4.2.1., p 80).

As a corollary with respect to the applicability of the ‘CBL-budget concept’ it has to be concluded that several fundamental parameters could not be determined as precisely as necessary. In addition to this, uncertainties were caused by temporal and spatial inconsistencies (see chapter 5.2.). As a result it appears that the common experimental strategy based on the ‘CBL-budget approach’ does not seem to be optimal for estimating the carbon balance on a regional scale.

As a consequence a new sampling strategy was developed whose design considers critical impairments like advection, alteration and local effects (discussed in detail in chapter 5.4.). However, the capability of the enhanced examination scheme could not finally be determined because of technical problems and insufficient equipment.

IDENTIFIED IMPAIRMENTS

Application of regional ‘CBL Budgeting Studies’ – Spatial and temporal aspects

- *mismatching of scales and ‘regional rectifier’:* The extension of the represented area, which is defined by the height of the well mixed CBL, does not match the spatial extension of the ‘region’ to be studied. Additionally, the CBL height is highly variable, which depends mainly on solar irradiance. As a consequence to this, the extension of the study region is also not constant. A well developed CBL may provide information even from continental scales in summertime, whereas a shallow winter CBL will reflect rather local contributions. *(Chapters 4.2.3.1., p 84ff., 5.2., p 127ff.)*
- *air mass exchange / background shift:* Significant modifications of the gas composition are caused by advection. Advection is, therefore, one dominant parameter which affects to large extent the calculation. In consequence: a reliable quantification of the carbon balance was impossible to achieve by using the available equipment.
(Chapters 4.2.6., p 95ff., 4.2.8.1., p 102ff., 5.2., p 127ff.)
- *small scale variability:* The high variability of the tracer mixing ratios, effected by various source and sink types and activity, as well as insufficient turbulent mixing, provokes distinct differences on small scales (horizontal, as well as vertical stratification) which are a main source of uncertainty with respect to the sampling strategy, the data interpretation and the budgeting.
(Chapter 3.1.2., p 43ff.)
- *turbulent mixing:* Because of the most frequently observed insufficient turbulence within the CBL, the development of a ‘regional average mix’ was not achieved. Instead, the establishment and persistence of stratification was recorded quite often. *(Chapter 4.2.8.1., p 105ff.)*
- *wind profile inconsistence:* Highly variable temporal and spatial conditions of wind direction and velocity were observed. Which means that exchange processes might occur rapidly, separately and independent at the

individual profile layers. From the analysis data provided by the weather services this behaviour can not be estimated sufficiently.

(*Chapter 4.1.5., p 70f.*)

- *contaminations:* Particularly in cases of insufficient turbulent mixing contaminations from local sources may affect the measurements in a serious way. Even in the free troposphere pollution plumes could be observed.

(*Chapters 3.1.2., p 44ff., 4.2.3.1., p 84ff., 5.1.1., p 113ff.*)

- *conversion:* Possible modifications of the CO / CO₂ ratios due to conversion reactions (CH₄, VOCs), which can not be verified with the available equipment.

(*Chapter 5.2., p 135ff.*)

- *determination of the CBL top height:* The proper determination of the CBL height, which is necessary for the budget and flux calculations, is frequently not possible from the available measurement data. Since it can be assumed that the CBL top is not a plain structure, a determination by solely vertical profiles is critical. Additional investigations by soundings will offer a suitable solution.

(*Chapters 4.2.7., p 100ff., 5.2., p 141ff.*)

- *lack of basic information:* Pre-flight information about the CBL structure for the determination of the sampling heights, with respect to the occurrence of distinct different layers, was not available.

Data Potential

- *data quantity:* The flight studies provided only a limited number of data. Because of the observed high variability and the missing of real replications of the measurements, the quantity of the data sets is not sufficient for reliable characterisations of the study site, nor for an estimate regarding the representation capability of the data for the studied region.

It also has to be taken into account that the CO₂ flux is no linear process but an effect of complex interactions, for instance the relationship of ambient CO₂ mixing ratio, temperature and vapour pressure, irradiance for the carbon uptake by assimilation.

(*Chapter 2.1.4., p 28ff.*)

- *insufficient number of observed parameters:* Lack of observed parameters, like the 3-dimensional wind field (with needed high resolution regarding the small scale variability) and the absence of continuous measurements of additional trace gas species (in particular CO). This information would at least be necessary for back tracking investigations regarding the source identification and for the data interpretation in general.
- *not comparable environmental conditions:* Since the experiments could not be executed concurrently and under similar conditions (for example the weather situation, the status of the vegetation, the day length) these basic uncertainties have to be taken into account regarding a direct comparison.
- *unrepresentative conditions:* Frequently, the campaigns were performed under environmental conditions, which were not characteristic for a long year average ('The Netherlands' winter experiment, 'Italy' summer campaign).

Technical Conditions

- *sampling and measurement instrumentation:* Problems due to the affections caused by the chemical drying reagent on H₂ continue to exist, as well as investigations with respect to probable interferences on the delta¹⁸O ratios, and a mismatch of the online CO₂ mixing ratio data with laboratory measurements.
- *performance of the flight operation:* Due to the required weather conditions and because of aviation regulations, sampling flights can only be performed during limited time frames and within specific areas.

5.4. Enhanced Investigation Strategy

From the observations it became obvious that the dynamical behaviour of the CBL and its structure are frequently not developed as expected. A corollary of the observations was that further examinations had to verify the basic assumptions with respect to their validity. Following these findings the investigation concept was modified by a) the regular implementation of ground reference measurements and sampling and b) by the adaptation of the flight strategy.

5.4.1. Implementation of Ground Reference Measurements and Sampling

In contrast to the practised scheme, the establishment of an independent reference seemed to be imperative in order to carry out the flight measurements as more or less self-contained studies. Additionally, a more specific estimation of the contribution from local surface processes seemed to be mandatory.

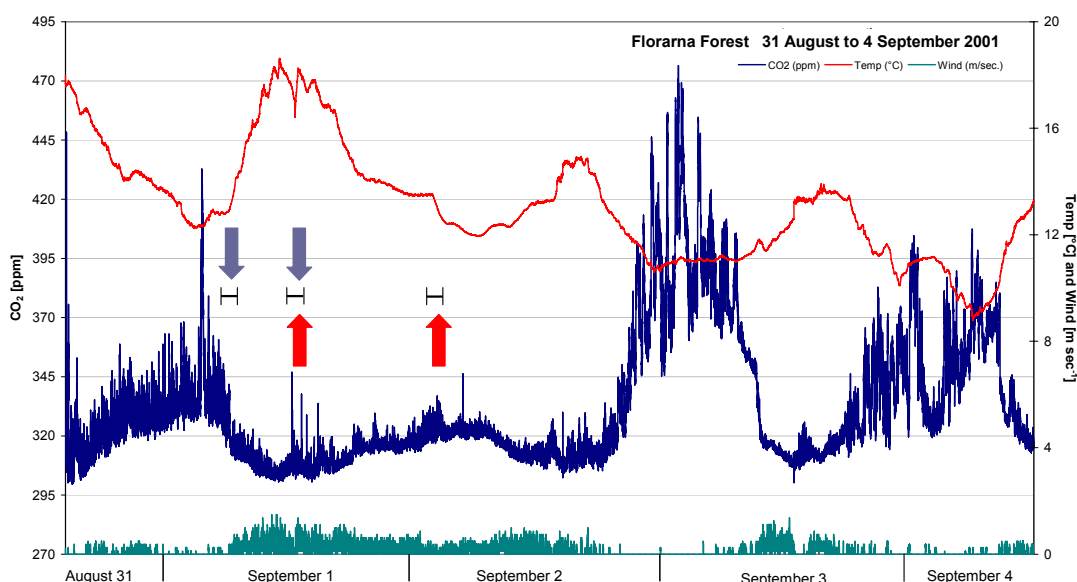


Figure 5.20. Continuous measurement records taken at the wooded site within the *Florarna* nature reserve (Uppland / Sweden) by the mobile ground reference unit from late afternoon on 31 August 2001 [16:00 UTC] until midday on 4 September 2001 [11:30 UTC]. Indicated by the black bars are periods when flask sampling were performed simultaneously ; blue arrows specify flight sampling events, red arrows near surface samplings respectively.

For this reason the ground reference unit was developed, recording continuously meteorological and eco-physical parameter, as well as the CO₂ mixing ratio and to provide the opportunity of flask sampling (for system description see 2.2.1.3., Appendix A2 and the documentation folder on the CD-ROM). A major requirement

for the construction was to obtain a low-cost system designed for the autonomous utilisation even in unapproachable terrain. A configuration was established that can be, in case of need, handled by only one person. Because of its low cost, several systems might be integrated in the investigation scheme observing different profile sites concurrently.

The aim of this construction was to associate the flight data with the activity of the regional ecosystems. Figure 5.20 presents data obtained by the ground reference system at a remote site in Sweden. Indicated are, beside the records of CO₂ mixing ratio, air temperature and wind speed, the periods when profile flights and ground reference samples were taken. The graphs clearly show the relevance of the environmental conditions and the ecosystem behaviour. For instance, the carbon uptake is not a linear but quite a complex process. The efficiency of the uptake depends inter alia on the ambient CO₂ mixing ratio, temperature and vapour pressure, the amount of the photosynthetic active radiation (PAR), etc. (see chapter 2.1.4., p 28f.).

Another example with respect to the benefit of the additional information is presented in figure 5.21. The results shown are from the winter campaign in Spain, illustrating the range of the observed differences regarding the CO₂ mixing ratio and the related delta ¹³C values: on the one hand the anthropogenic contributions are obvious, when comparing the results from the sampling next to the highway with the samples originating from the remote mountain field site. On the other hand, the influence of advection can be recognized from the night time ¹³C signal observed at the rice field site and within the orchard.

Caused by a land-sea-wind circulation, contaminated air from the highway and the urban settlements was transported by offshore winds to the orchard and the rice field site. Chapter 5.2. 'Variability – Air Mass Change' focus mainly on the flight results. A detailed description of the exchange scheme is given in figures 9 and 10 in the documentation folder on the CD-ROM.

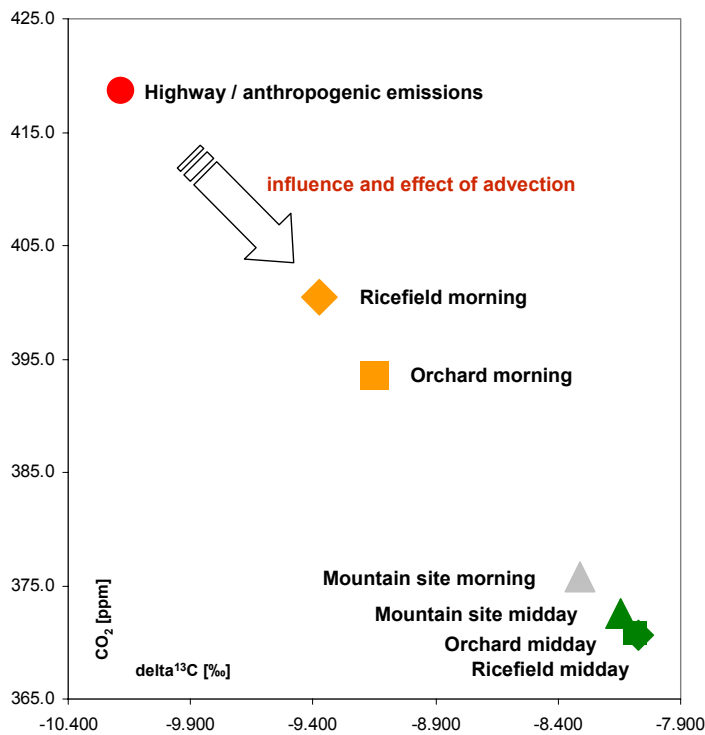


Figure 5.21.

Characteristic signatures of different land use classes, i.e. CO_2 sinks and sources (Valencia / Spain; December 2001). The effect of advection is indicated by the night time data from the rice field and the orchard (plant) site – which are reflecting in fact a *mixed* signal with main contributions originating from anthropogenic sources.

The experiments presented in chapters 3.2. (p 48ff.) and 4.2.2. (p 81f.) showed, that both sample systems, the modified flight sampling system and the ground reference unit, are compatible, which is a basic need regarding the real linkage of the flight profiles to the surface processes we are interested in.

Due to the importance of the data obtained by the ground reference system it is an integral feature within the ‘Transect approach’.

5.4.2 Adapted Flight Investigation Strategy – ‘Transect Approach’

As could be shown in the previous sections the applicability of the CBL-budget concept is subject to a high potential of uncertainty, primarily due to environmental conditions like advection and the mixing status of the boundary layer (see chapters 5.2. and 5.3.). Adjustments, for instance the implementation of a footprint (*‘Transportfunktion’*) feature for the vicinity of the sample location, as discussed by FRITSCH [2003], will fail, since the effective processes are still missed. The utilization of eddy-correlation data from local tower measurements, for calibration and quality control, provides only an apparent reference because these observations are also affected by the processes which shall be excluded (see findings from the SPA¹³CE experiment, chapter 4.2.8.).

The limitation due to the required environmental conditions is also a problem that affects the applicability of Lagrangian attempts. As described for example by SCHMITGEN et al [2004] the experiment performed in the ‘Landes des Gascogne’ region (France) was designed as a quasi ‘one-process-orientated’ study, focussing on the CO₂ uptake by a forest. The premise for detecting a significant decrease of the CO₂ mixing ratio due to the uptake by assimilation is the ability to persecute an air mass for a period above a certain land surface. Thus the practicability is bound to dedicated regions, and to definite weather conditions – which were prevalent only at one of four flight days during the experiment.

As a conclusion one has to challenge to what extent results from both approaches, biased to exceptional situations, can reflect a representative character of a region.

In consequence, with the ‘Transect approach’ an improved investigation concept was developed which takes the most important impairments into account.

The idea is based on the sampling of vertical profiles, above the most representative land classes during each flight, but also taking advection and further forced modifications of the air within the ‘regional’ scaled column into consideration. Thus the results should be obtained from a combination of

- a) the local source and sink activity, derived from the lowest level samplings,
- b) the ‘regional’ average from the samples taken through the entire profile
- c) a ‘quasi-Lagrangian’ attempt to assess the individual modifications.

- d) Additionally ground level reference investigations with flask sampling, continuously CO₂ measurements and recording of meteorological and eco-physical parameter aiming the linkage to the surface processes.

The hypothesis is that a regional representative can be obtained from a combination of successively executed profiles at multiple characteristic locations along a line of the prevailing wind direction, with a ‘chronosequence’ of these individual source signals. Thus the intention of taking the advection explicitly into account was to minimize the random background shift at the profile sites and to get information about changes caused by other modifying processes.

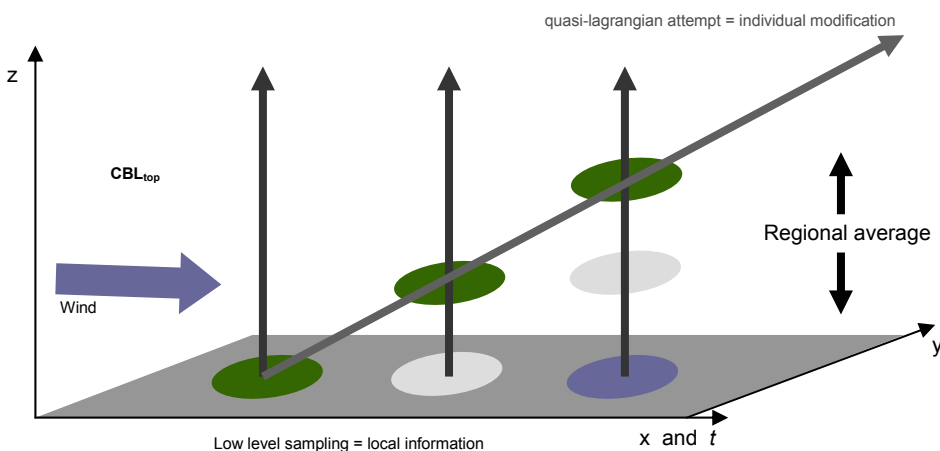


Figure 5.22. Scheme of the ‘Transect Approach’. The profile sampling follows the stretch of the wind. Sampling is performed above various typical land use classes: local information will be obtained from the low level samples, as well as from additional ground level reference investigations. At the following profile sites the ground signal should be found again at higher altitudes but already with a modified character (quasi-Lagrangian attempt). By the entire profile at the end of the transect the regional average should be represented. An estimation of the diurnal effects and of affections from advection has to be achieved from the results of the replicated flights during the day.

Another aim was to assess and minimise the uncertainties that are caused by the environmental conditions. Even if there is still no direct information available to estimate the amounts entering the investigation column, a significant enhancement might be achievable when implementing a ‘semi Lagrangian’ monitoring attempt. Thus the attempt of the ‘transect approach’ can be seen as a fusion of the originally intended Eulerian consideration with a simple Lagrangian treatment.

Figure 5.2. represents the relationships of CO and SF₆ data obtained from flask sampling within the CBL during the Dutch summer experiment. Displayed are the results of the morning flights performed above the most western site (Cabauw, marshland – blue triangles) and the more easterly location (Maize – greyish squares) and by the red outlined squares the midday results from the 900m sampling level. On 16 July 2002 north-west winds occurred, on 27 July 2002 south westerly wind direction was dominant.

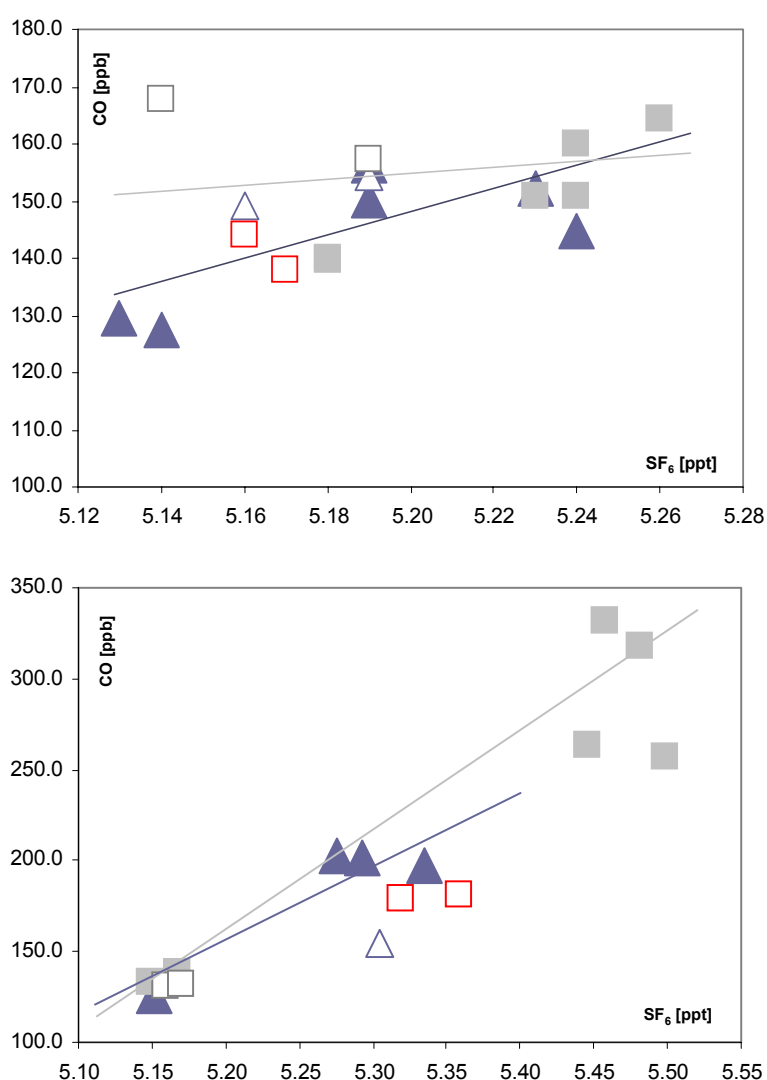


Figure 5.8.

Relationship of CO and SF₆ mixing ratios from flask sampling performed during the summer campaign in The Netherlands on 16 July (upper panel) and 27 July 2002 (lower panel).

Displayed are data from the morning flights within the CBL above the Cabauw (blue triangles) and at the Maize location (grey squares). By the red outlined squares the results from the midday sampling at the 900m level at the Maize site are indicated. The 900m samples from the morning flights are also shown by outlined symbols. Linear fits through the data points are applied

When analysing the results from the morning profiles at both locations with regard to an attribution of the maize midday data, it becomes obvious that a better correlation with the character of the air identified in the morning at the Cabauw site, than with the air sampled in the morning at the maize site, is present. This

observation suggests that the intended following of a local signal could be achieved.

Associated with the investigation strategy was the application of the modified flight sampling unit. In this context the most important enhancement has to be seen in the operation mode, to flush and sample under final pressure combined with an adjustable flow rate. Adapted to the aircraft speed ‘average way lengths’ for the flask samples can be defined. With a flight speed above ground of 140 km/h and a sampling flow rate of 3 l min^{-1} the passed distance during the period the volume of a flask exchanges once is about 1600 m. Since the two flasks are arranged in line one can obtain two individual samplings representing each 1600 m, which combined averages a way length of about 3200 m. Additional information is provided by the comparison of the individual flasks, since the differences reflect the presence of small scale variability. However, one might obtain ex poste a rough impression of the amount – but an estimation regarding the scales of the variability is still unsolved.

UNCERTAINTIES

Also this examination concept is still forced by restrictions, as could be derived from the flights performed in The Netherlands (see chapters 4.2.6. and 4.2.7.). Air mass changes in particular may affect the sampling, caused by the variability of the wind direction and an associated probable lateral advection. Also the definition of the transect basics, for example its orientation, is difficult especially in highly urbanized areas.

Where and when to sample are most crucial decisions, determining the results. To accommodate this uncertainty pre-sampling information regarding the scale of variability should be obtained by in-flight high frequency measurements. Further improvements are needed, like the documentation of the CBL structure which also has relevance regarding the requested additional information for the model calculations.

6. CONCLUSIONS

This study has demonstrated the appropriateness of multiple tracer analyses and proposed an enhanced investigation strategy that overcomes the highlighted impairments of previous approaches. Further, this study has also established the validity of using multiple tracer analyses for the study of the carbon cycle. It turned out that multiple tracer analyses are not only an adequate tool – but that multiple tracer analyses are of rather basic importance for investigations focussing on the carbon cycle.

6.1. Relevance of the Results

The budgeting of dynamic systems implies in principle great uncertainties. It becomes in particular problematic when assumptions turn out to be unrealistic and fundamental parameter can not be determined sufficiently. In this study problems with respect to regional carbon budgets are identified, caused by complex interactions of different processes. Frequently, inefficient vertical mixing is accompanied by rapid horizontal air mass changes. Due to the relation between transport distance and time the simultaneous occurrence of air originating even from opposite formations is not uncommon. On account of this, one finds in the CBL large temporal and spatial variability on a small scale. Thus the '*where and when*' of the measurements is a crucial parameter. Further, since the flows entering and leaving the '*CBL column*' can not be determined properly, a demarcation of the spatial unit '*region*' is difficult. Due to these impairments regional budgets from profile flights are prevalently impossible.

Also, surface observations are subject to the effects described for the airborne investigations. By linking the flight sampling to near surface measurements it was proven that changes caused by advection and entrainment are effective through the entire profile. When the relationship between transport velocity and kinetic of the surface-atmosphere interactions, defined by Taylor's hypothesis, are exceeded, or when air mass change occurs by vertical transport, a rapid alteration of the footprint from local to larger scales is unavoidable.

By combining modelling studies with the results from multiple tracer analyses, mutual benefit can be obtained. Transport models provide helpful information for the identification of most probable source regions. On the other hand, these field measurements provide data which help to validate processes simulated in the models.

6.2. Perspectives

Benefits were obtained by enhancements focussing on sampling system and investigation strategy. However, the linking between local investigations and continental studies could not be achieved. But, highly accurate information with respect to the *actual local* situation became available by flask sampling combined with continuous measurements. Thus, the goal of advanced studies should be a catenation with continuous near surface multiple tracer analyses. Most suitable might be a combined approach of tall tower and airborne studies. Benefits from the airborne investigations will be obtained through aircraft mobility, in particular from sampling the ‘dynamic background’ within the free troposphere, and from additional samplings at several distributed locations within and outside the tower’s footprint area, realising the new *transect approach* sampling strategy.

A major problem of the RECAB project was the study area itself. Because of its heterogeneity the appearance of processes was quite complex. But knowledge about these conditions is mandatory for an application.

Thus, when go on to scale up source regions, a simple study area, i.e. a more homogeneous landscape, has to be chosen. And, before trying to get a budget number, more basic information has to be obtained: It became obvious that the structure and dynamics of the lower atmosphere are not understood well enough for such calculations. Regarding the occurrence of stratification, as well as for the study of the CBL dynamic in general, the implementation of 3-dimensional high frequency wind field measurements is mandatory. Further enhancements should be achieved by additional ground-based soundings (SODAR) for the description of the CBL top height.

Large homogeneous regions like Siberia are of particular interest, because in northern boreal regions with wetland areas and permafrost soils two highly sensitive land classes are dominant where, due to the anticipated climatic changes, additionally CH₄ and CO₂ contributions have to be expected. Additionally, the conversion of CH₄ and VOC has to be taken into account, since an estimation of CO formation is a basic requirement when using CO as tracer for combustion derived CO₂.

In order to meet the requirements for such investigations, an enhanced instrumentation and additional continuous profile measurements of an advanced gas spectrum (CO, CH₄, OH and stable isotopes in CO₂; by gas chromatography and tuneable-diode-laser-mass spectroscopy) are necessary. With respect to a division of contributions from fossil fuel consumption and biomass burning it is desirable to analyse individual air samples also for ¹⁴C.

Finally, modelling approaches should be an integrative part of the studies. On the one hand, forecast models should be used to facilitate the setup of the experiments. And on the other hand, information about transport and transformation processes need to be modelled to narrow down possible source areas.

*... 'There are more things in heaven and earth, Horatio,
Than are dreamt of in your philosophy.'*

HAMLET ACT I, SCENE 5

7. SUMMARY

Great capability was ascribed in this study to multiple tracer analyses as a tool for the interpretation and characterisation of air samples. The potential and capability of multiple tracer analyses was examined by focussing on processes and environmental conditions, based on data obtained from air sampling performed within the EU project RECAB (Regional assessment and modelling of the carbon balance in Europe). The motivation for the study was the need to close the gap between local and continental/global scales.

Because of the significance of the observations particular focus was given to the experimental investigations. Due to the findings of prior test flights and from results obtained by the RECAB field campaigns, specific laboratory experiments were carried out to evaluate the appropriateness of the ‘CBL-budget approach’, that was proposed for the estimations of the regional carbon budgets.

Since the campaigns provided on the one hand data from the regular profile flights, but were used on the other hand for enhanced experiments and validation studies, the observations and the interpretation of the results are pointed out more explicitly.

From field data and specific laboratory experiments, severe impairments were identified, regarding the appropriateness of the technical equipment and the validity of fundamental assumptions about the CBL behaviour.

It was found that basic assumptions of the current strategy did not reflect the real conditions, primarily because of insufficient perception about the dynamics and the structure of the CBL.

Additionally, it turned out that with the ‘up scaling’, besides the extension of the spatial aspect – from the leaf level to the region, an importance is attributed to the complex interactions of spatial and temporal processes. A change of the spatial scale is directly connected to an adjustment of the time factor and vice versa. With this in mind, the coupled factors of horizontal advection and entrainment have to be mentioned. This also includes air from the free troposphere, as well as the influence of gas phase reactions with respect to the trace gas composition of the air samples.

Because of the identified impairments, the aim of the RECAB project – The qualification and quantification of carbon budgets within regions – could not be achieved as desired. Instead, mandatory requirements to improve investigations were specified and initiated: e.g. a new configured system for flask sampling, a ground reference unit were designed, and an enhanced investigation strategy was developed, focussing on flight and ground level studies.

Concluding the findings their relevance and their transformability to related studies have been evaluated. Finally, the requirements and potential foci for advancement measurements were discussed, which should perform the enhanced investigation strategy combined with ground-based continuous multiple tracer analyses.

8. ANNEXES

A1 ABBREVIATIONS and CONVERSION OF UNITS

CBL	Convective Boundary Layer
CEAM	Centro de Estudios Ambientales del Mediterráneo Foundation
CMDL	Climate Monitoring and Diagnostics Laboratory
ECD	Electron Capture Detector
FID	Flame Ionization Detector
GC	Gas Chromatograph
GIS	Geographic Information System
GPS	Global Positioning System
IRMS	Isotope Ratio Mass Spectroscopy
knts	knots
LPD	Lagrangian Particle Dispersion
MFP	Mobile Flux Plane
MPI-BGC	Max-Planck-Institut für Biogeochemie
MSL	Mean Sea Level
NBL	Nocturnal Boundary Layer
NCEP	National Centers for Environmental Prediction
NMCHs	Non Methane Hydro Carbons
ppb	parts per billion
ppm	parts per million
ppt	parts per trillion
RGA	Reduction Gas Analyzer
RECAB	REgional assessment and modelling of the CArbon Balance in Europe
UTC	Universal Time Coordinate
VOCs	Volatile Organic Compounds

Conversion Factor

1 m	3.2808 ft	1 ft	0.3048 m
1 m s ⁻¹	0.5148 knts	1 knts	1852 m h ⁻¹

A2 EQUIPMENT

Instrument Description – Configuration of sampling units

Flight sampling unit: ½“ Decabon® tube (length 650 cm) from wing tip to pump (KNF N 145.1.2.AVE) – ¼“ steel tube outlet – 3-way-valve (Swagelok; 1 – pump out, 2 – sample unit, 3 – cockpit) – ¼“ Decabon® tube (all lines within the sample unit) - coalescing filter (stainless steel NUPRO FC Series [Swagelok] with 0.3 micron filter [GE-15K-FC-03]) – massflow controller (Bronkhorst F201C-FACB22-V [flushing rate ~10.5 l min⁻¹, sampling rate 3.0 l min⁻¹ at 2 bar abs.]) – vertical drying column (stainless steel) with Mg(ClO₄)₂ [~ 70 g] as binder medium (Fluka Chemika) – particle filter (stainless steel NUPRO FC Series [Swagelok] with 0.3 micron filter [GS-15K-FC-03]) – unidirectional restrictor valve (Swagelok) – mechanical flow controller (only for control purpose, Krohne 0/232939.2) – 3-way-valve (Swagelok; 1 – in, 2 – out →sample unit, 3 – out →restriction outlet 1 bar rel. [Swagelok RL4 (0.7-15bar)]) – analog manometer (Empeo, NR63.14 0-2.5 bar) – sample flasks (1 l bor-silicate 3.3 glass flasks [Schott], with two valves [Glas Expansion, Australia] sealed with Teflon® PFA O-rings, prefilled with calibration gas of known trace gas mixing ratios [2 bar abs.] - in and out fixed by ½" Cajon Ultratorr shafts (Swagelok) – pressure controller (Bronkorst P702C-FAC-22-V; restriction 2 bar abs.)

Original flight sampling unit: ½“ Teflon® tube (length 650 cm) from wing tip to horizontal drying column (stainless steel) with Mg(ClO₄)₂ [~ 65 g] as binder medium (Fluka Chemika) – ¼“ Teflon® tube (all lines within the sample unit) – particle filter (Gelman, 1.0 micron) – pump (KNF N 814 KNDC) – unidirectional restrictor valve (Swagelok) – sample flasks (1 l bor-silicate 3.3 glass flasks [Schott], with two valves [Glas Expansion, Australia] sealed with Teflon® PFA O-rings, prefilled with calibration gas of known trace gas mixing ratios [2 bar abs.] - in and out fixed by ½" Cajon Ultratorr shafts (Swagelok) – 3-way-valve (Swagelok; 1 – in, 2 – out →flushing, 3 – out →sampling); *for flushing:* – mechanical flow controller (Krohne 0/232939.2) – outlet *for sampling:* – analog manometer (Empeo, NR63.14 0-2.5 bar) – restriction outlet 2 bar abs (TAVCO, 2391244-8-3)

Ground sampling unit: ½“ Decabon® tube from mast to pump unit (two pumps in row: KNF N 828 KNDC & KNF N 814 KNDC) – ¼“ Decabon® tube (all lines within the sample unit) – horizontal drying column (stainless steel) with Mg(ClO₄)₂ [~ 65 g] as binder medium (Fluka Chemika) – particle filter (Gelman, 0.3 micron) – mechanical flow controller (Krohne 0/232939.2) – unidirectional restrictor valve (Swagelok) – analog manometer (Empeo, NR63.14 0-2.5 bar) – sample flasks (1 l bor-silicate 3.3 glass flasks [Schott], with two valves [Glas Expansion, Australia] sealed with Teflon® PFA O-rings, prefilled with calibration gas of known trace gas mixing ratios [2 bar abs.] - in and out fixed by ½" Cajon Ultratorr shafts (Swagelok) – restriction outlet 1 bar rel. (Swagelok RL4 (0.7-15bar))

A3 Configuration of analytical instrumentation

Gas Chromatograph [GC]: flasks with sampled air connected with Cajon Ultratorr fittings to $\frac{1}{16}$ " stainless steel capillaries – drying tube ($\frac{1}{4}$ ", 2 g Mg(ClO₄)₂) – sample standard selection valve (8 Port Valco multiposition valve: EMTCSD8UWE) –

GAU1 (FID for CH₄ and CO₂, ECD₁ for N₂O):

linked to first GC injection valves [**FID line**]: Valco two-position valve (ET6C10UWE) – flushing sample loops FID 2.2 ml – connected via sample loop separation valve (ET6C4UWE) to second GC injection valve [**ECD₁ line**] (ET6C10UWE) – ECD sample loop: 5 ml – sample flow rate regulated by mass flow controller (MKS 1179A) - GC columns (FID/ECD): Hayesep Q 6 ft x $\frac{1}{8}$ " (pre-col) and Porapak Q 12 ft x $\frac{1}{8}$ " (main col) - ECD line: methanizer bypass valve (EHC4WE) – methanizer (Agilent Nickel Catalyst Assembly Part No G1580-61020) – ECD

FID line: FID

GAU2 (RGA for CO and H₂, ECD₂ for SF₆):

Linked to first GC injection valve [**RGA line**] (ET6C10UWE) – flushing sample loop RGA 1 ml – connected to second GC injection valve [**ECD₂ line**] (ET6C10UWE) – ECD sample loop 25 ml – sample flow rate regulated by mass flow controller (MKS 1179A) - GC columns (RGA): 3 ft x $\frac{1}{8}$ " glass beads , 3 ft x $\frac{1}{8}$ " molecular sieve - RGA; GC columns (ECD₂): Hayesep Q 6 ft x $\frac{3}{16}$ " (pre-col) and Hayesep Q 10 ft x $\frac{3}{16}$ " (main col) - ECD₂ bypass valve (ETC4UWE) – ECD

GC oven temperatures: FID 60°C; ECD₁ 50°C; RGA (pre col) 72 °C,
RGA (main col) 105 °C; ECD₂ 80°C

Detector temperatures: FID 200°C; ECD₁ 385°C; RGA 270 °C; ECD₂ 385°C

Carrier and detector gases:

FID carrier gas: Helium 5.0 (Messer Griesheim purified with VICI Helium purifier HP2), 30 ml/min; FID detector gases: H₂ (H₂ generator Whatman 75-83) 33 ml/min; air (Messer Griesheim FID-Mix = 60 % N₂, 40 % O₂) 220 ml/min; makeup (He 5.0) 15 ml/min
ECD₁: Argon (95%) - Methane (5%) 30 ml/min (Messer Griesheim „ECD-Gas“, purified with Supelco high capacity gas purifier)

RGA: synthetic air 30 ml/min (Messer Griesheim, purified with Molecular Products: Sofnocat 423)

ECD₂: Argon (95%) - Methane (5%) 100 ml/min (Messer Griesheim „ECD-Gas“, purified with Supelco high capacity gas purifier)

For a more detailed description see: Jordan, A. and W. A. Brand (2002)

IsotopeRatioMassSpectrometer [IRMS]: flasks with sampled air – $\frac{1}{2}$ " Cajon Ultratorr adaptor – $\frac{1}{8}$ " stainless steel line - 32 Port Valco multiport valve; 16 probe lines (two for working standard, one for reference gas, 13 for sampled air) each second port blind for evacuating lines before admitting next sample →

BGC-Air-Trap: massflow controller (MKS; 60 ml/min, 330 mbar) – Trap1 [water vapour; $\frac{1}{4}$ " & $\frac{1}{8}$ " double wall stainless steel, -70°C dry ice/ethanol – valve1 for evacuating] – valve2 (for isolating Trap2) → Trap2 [CO₂ and N₂O; $\frac{1}{4}$ " & $\frac{1}{8}$ " double wall stainless steel / gold, -196°C liquid nitrogen], out freezing and accumulation of CO₂ (needs through passing of ~500 ml sampled air, than closing valve 2 and sucking out the non-condensed air from Trap2; $\frac{1}{4}$ " line connected to Dual Inlet System of the IRMS) – closing valve3 to isolate trap2. Thaw (~ 20min) and release to the Dual Inlet System / changeover valve via a 100 cm long 0.1 mm i.d. capillary, crimped at the end (Upchurch Scientific; USA) → *Finnigan MAT 252 IRMS* [ionization – acceleration and magnetic deflection – capture in Faraday cups – detection]

For a more detailed description see: Werner, R.A., Rothe, M. and Brand, W.A. (2001) and Werner, R.A., and Brand, W.A. (2001)

A4 Instrument Manufacturers

SAMPLE UNITS:

Company Name	Product	Address	Telephon	Email
Serto Jacob GmbH	Decarbon Tube	Kasseler Str. 64-66 34277 Fuldabrück	+49 561 580040	info@serto.de
KNF Neuberger	Pump	Alter Weg 3 79112 Freiburg	+49 7664 59090	info@knf.de
Swagelok Group	Valves, Filters	29500 Solon Road Solon, Ohio 44139 U.S.A	+1 4402484600	
Gelman	Particle Filter	Fisher Scientific Liebigstrasse 16 61130 Niederau	+49 6187 201921	
TAVCO Inc.	Restriction valve Flight sampling unit	20500 Prairie St. Chatsworth, CA 91311 U.S.A.		
Fluka Chemie	Mg(ClO ₄) ₂	Industriegasse 25 9471 Buchs Switzerland	+41 81 7552511	Fluka@Sial.com
Krohne	Mechanical massflow controller	In der Dehne 12 37127 Dransfeld	+49 5502 300762	info@krohne.com
EMPEO - KBM	Manometer	Friedrich-Gauss-Str. 2 53757 Sankt Augustin	+49 2241 41006	empeo-kbm@t-online.de
SCHOTT Glas	Flasks	Hattenbergstrasse 55122 Mainz	+49 6131 664907	info.duran@schott.com
Glas Expansion	Flask valves	167 Camberwell Road Hawthorn Australia	+41 219212931	
Messer Griesheim	Gas (Precondition)	Spezialgase Fütingsweg 34 47805 Krefeld	+49 21513790	

LABORATORY EQUIPMENT:

Company Name	Product	Address	Telephon	Email
Agilent	Gas Chromatograph	Hewlett Packard Str. 8 76337 Waldbronn Germany	+49 7243 6020	germany@agilent.com
CSIRO	Reference gases		http://www.csiro.au	
Fluka Chemie	Mg(ClO ₄) ₂	Industriegasse 25 9471 Buchs Switzerland	+41 81 7552511	fluka@sial.com
Institut für Umweltphysik	intercomparison		http://www.uphys.uni-heidelberg.de	
Max-Planck-Institut für Chemie	comparison		http://www.mpcch-mainz.mpg.de	
Messer Griesheim	Gas (Carrier & Detector)	Spezialgase Füttingsweg 34 47805 Krefeld Germany	+49 21513790	
MKS	Massflow controller	Schatzbogen 53 81829 München Germany	+49 89 4200080	info@mksinst.com
Molecular Products	Sofnocat	Mill End Thaxted Essex CM6 2LT United Kingdom	+44 1371830676	sales@molprod.com
NOAA / CMDL	Reference gases		http://www.cmdl.noaa.gov/ccgg/refgases/stdgases.html	
Swagelok Group	Valves	29500 Solon Road Solon, Ohio 44139 U.S.A	+1 4402484600	
Thermo FinniganMAT	IRMS	Barkhausenstrasse 2 28197 Bremen Germany	+49 42154930	isotope@ThermoFinniganMat.de
Upchurch Scientific	Capillaries		http://www.upchurch.com	
Valco	Valves	Untertannberg 7 6214 Schenkon Switzerland	+41 419256200	info@vici.ch
Westfalen	Working standard gas	Industrieweg 43 48155 Münster Germany	+49 2516950	info@westfalen-ag.de

EXPERIMENTAL SET UPSet up of the modified flight sampling system Ia

½“ Decarbon® tube (length 650 cm) to pump (KNF N 145.1.2.AVE) – ¼“ steel tube outlet – 3-way-valve (Swagelok; 1 – pump out, 2 – sample unit, 3 – cockpit) – ¼“ Decarbon® tube (all lines within the sample unit) - coalescing filter (stainless steel NUPRO FC Series [Swagelok] with 0.3 micron filter [GE-15K-FC-03]) – massflow controller (Bronkhorst F201C-FACB22-V [flushing rate ~10.5 l min⁻¹, sampling rate 3.0 l min⁻¹ at 2 bar abs.]) – vertical drying column (stainless steel) with Mg(ClO₄)₂ [~ 71 g] as binder medium (Fluka Chemika 63102) – partikel filter (stainless steel NUPRO FC Series [Swagelok] with 0.3 micron filter [GS-15K-FC-03]) – unidirectional restrictor valve (Swagelok) - mechanical flow controller (only for control purpose, Krohne 0/232939.2) – 3-way-valve (Swagelok; 1 – in, 2 – out →sample unit, 3 – out →restriction outlet 1 bar rel. [Swagelok RL4 (0.7-15bar)]) – analog manometer (Empeo, NR63.14 0-2.5 bar) – sample flasks (1 l bor-silicate 3.3 glass flasks [Schott], with two valves [Glas Expansion, Australia] sealed with Teflon® PFA O-rings, prefilled with calibration gas of known trace gas mixing ratios [2 bar abs.] - in and out fixed by ½” Cajon Ultratorr shafts (Swagelok) – pressure controller (Bronkorst P702C-FAC-22-V; restriction 2 bar abs.)

Set up of the modified flight sampling system Ib

½“ Decarbon® tube (length 650 cm) to pump (KNF N 145.1.2.AVE) – ¼“ steel tube outlet – 3-way-valve (Swagelok; 1 – pump out, 2 – sample unit, 3 – cockpit) – ¼“ Decarbon® tube (all lines within the sample unit) - coalescing filter (stainless steel NUPRO FC Series [Swagelok] with 0.3 micron filter [GE-15K-FC-03]) – massflow controller (Bronkhorst F201C-FACB22-V [flushing rate ~10.5 l min⁻¹, sampling rate 3.0 l min⁻¹ at 2 bar abs.]) – partikel filter (stainless steel NUPRO FC Series [Swagelok] with 0.3 micron filter [GS-15K-FC-03]) – unidirectional restrictor valve (Swagelok) - mechanical flow controller (only for control purpose, Krohne 0/232939.2) – 3-way-valve (Swagelok; 1 – in, 2 – out →sample unit, 3 – out →restriction outlet 1 bar rel. [Swagelok RL4 (0.7-15bar)]) – analog manometer (Empeo, NR63.14 0-2.5 bar) – sample flasks (1 l bor-silicate 3.3 glass flasks [Schott], with two valves [Glas Expansion, Australia] sealed with Teflon® PFA O-rings, prefilled with calibration gas of known trace gas mixing ratios [2 bar abs.] - in and out fixed by ½” Cajon Ultratorr shafts (Swagelok) – pressure controller (Bronkorst P702C-FAC-22-V; restriction 2 bar abs.)

Set up of the ground sampling unit

½“ Decarbon® tube (length 650 cm) to pump unit (two pumps in row: KNF N 828 KNDC & KNF N 814 KNDC) – ¼“ Decarbon® tube (all lines within the sample unit) – horizontal drying column (stainless steel) with Mg(ClO₄)₂ [~ 66 g] as binder medium (Fluka Chemika 63102) – partikel filter (Gelman, 0.3 micron) – mechanical flow controller (Krohne 0/232939.2) – unidirectional restrictor valve (Swagelok) – analog manometer (Empeo, NR63.14 0-2.5 bar) – sample flasks (1 l bor-silicate 3.3 glass flasks [Schott], with two valves [Glas Expansion, Australia] sealed with Teflon® PFA O-rings, prefilled with calibration gas of known trace gas mixing ratios [2 bar abs.] - in and out fixed by ½” Cajon Ultratorr shafts (Swagelok) – restriction outlet 1 bar rel. (Swagelok RL4 (0.7-15bar))

Set up of the basic flight sampling system

¼“ Decarbon® tube (length 650 cm) to horizontal drying column (stainless steel) with Mg(ClO₄)₂ [~ 69 g] as binder medium (Fluka Chemika 63102) – ¼“ Teflon® tube (all lines within the sample unit) – partikel filter (Gelman, 1.0 micron) – pump (KNF N 814 KNDC) – unidirectional restrictor valve (Swagelok) – sample flasks (1 l bor-silicate 3.3 glass flasks [Schott], with two valves [Glas Expansion, Australia] sealed with Teflon® PFA O-rings, prefilled with calibration gas of known trace gas mixing ratios [2 bar abs.] - in and out fixed by ½” Cajon Ultratorr shafts (Swagelok) – 3-way-valve (Swagelok; 1 – in, 2 – out →flushing, 3 – out →sampling); *for flushing:* – mechanical flow controller (Krohne 0/232939.2) – outlet *for sampling:* – analog manometer (Empeo, NR63.14 0-2.5 bar) – restriction outlet 2 bar abs (TAVCO, 2391244-8-3)

Set up of the reference unit

¼“ Decarbon® tube (length 650 cm) – partikel filter (Gelman, 1.0 micron) – pump (KNF N 814 KNDC) – mechanical flow controller (Krohne 0/232939.2) – sample flasks (1 l bor-silicate 3.3 glass flasks [Schott], with two valves [Glas Expansion, Australia] sealed with Teflon® PFA O-rings, prefilled with calibration gas of known trace gas mixing ratios [2 bar abs.] - in and out fixed by ½” Cajon Ultratorr shafts (Swagelok) – restriction outlet 2 bar abs (TAVCO, 2391244-8-3) – mechanical flow controller (Krohne 0/232939.2)

EXPERIMENT EXECUTION

Location: large storage room (Department ‘Freiland’)

Concurrently operation of all four systems; air was sucked in from one point at the top of the stillage rack.

One complete run was executed with all systems. A solely experiment was afterwards performed operating the modified flight sampling system with altered time intervals for flushing and sampling. Finally one loop was realized with the modified flight sampling system in configuration Ib (without drying compartment), the basic flight sampling system and the reference unit.

Modified flight sampling system:

2 minutes flushing with 10 l min.^{-1} , 2 minutes flushing with 3 l min.^{-1} , 2 minutes sampling with 3 l min.^{-1}

With altered time intervals

4 minutes flushing with 3 l min.^{-1} , 2 minutes sampling with 3 l min.^{-1}

Ground sampling unit:

10 minutes flushing and sampling procedure with 5 l min.^{-1}

Basic flight sampling system:

6 minutes flushing, then sampling until the air pressure within the flasks exceeded 2 bar.; flow rate 2 l min.^{-1}

Reference unit:

6 minutes flushing and sampling procedure with 1.5 l min.^{-1}

A6 Scale Basis for Triplet Calculations *for figures 5.4., 5.8. and 5.11.*

Location	Dates	CO ₂ [ppm]	CO [ppb]	delta ¹³ C [%]
Florarna (Sweden)	Aug 29 & 30, Sep 1 2001	349.0 (\rightarrow 359.0)	106.0 (\rightarrow 136.0)	-7.035 (\rightarrow -7.635)
Tuscania (Italy)	Jun 15 2002	369.0 (\rightarrow 379.0)	125.0 (\rightarrow 185.0)	-8.100 (\rightarrow -8.400)
Maize (The Netherlands)	Jul 15, 16 & 27 2002	360.0 (\rightarrow 370.0)	105.0 (\rightarrow 205.0)	-7.550 (\rightarrow -8.050)
Hainich (SPA ¹³ CE, Germany)	Aug 6, 14 & 15 2002	361.5 (\rightarrow 371.5)	70.0 (\rightarrow 130.0)	-7.550 (\rightarrow -7.950)
<hr/>				
Cabauw / Maize ¹	Jan 30, 31 ¹			
	Feb 2 Jul 16 & 27 2002	360.0 (\rightarrow 380.0)	116.0 (\rightarrow 166.0)	-7.750 (\rightarrow -8.500)
<hr/>				
Forest / Maize (The Netherlands)	Jan 29, 31 Feb 02 2002	373.0 (\rightarrow 383.0)	127.5 (\rightarrow 247.5)	-8.250 (\rightarrow -8.700)
Ricefields (Spain)	Dec 2, 4 - 6 2001	364.0 (\rightarrow 374.0)	105.0 (\rightarrow 225.0)	-8.000 (\rightarrow -8.450)
Free Troposphere	both campaigns	367.5 (\rightarrow 379.5)	110.0 (\rightarrow 170.0)	-8.030 (\rightarrow -8.480)

Basic value (\rightarrow 100% value)

A7 Trace gas mixing ratios and isotopic composition of CO₂ from the RECAB field campaigns for the lowest flight levels and for the free troposphere

Valencia Summer

	CO ₂ [ppm]	CO [ppb]	CH ₄ [ppb]	N ₂ O [ppb]	H ₂ [ppb]	SF ₆ [ppt]	delta ¹³ C [%]
Lowest Level	360 - 380	/	1802 - 1919	318 - 323	/	/	-7.746 - -8.638
Free Troposphere	364 - 379	/	1764 - 1966	316 - 326	/	/	-7.940 - -8.335

Heights LL and FT 100 – 150 m; 1500 – 2000 m Number of flight days 6 Number of profile sites 2

Thuringia Summer

	CO ₂ [ppm]	CO [ppb]	CH ₄ [ppb]	N ₂ O [ppb]	H ₂ [ppb]	SF ₆ [ppt]	delta ¹³ C [%]
Lowest Level	355 - 403	/	1815 - 1981	316 - 328	/	/	-7.736 - -9.720
Free Troposphere	356 - 364	/	1781 - 1882	314 - 319	/	/	-7.710 - -7.850

Heights LL and FT 90 – 340 m; 1800 – 2500 m Anzahl der Flugtage 5 Number of profile sites 2

Uppland Summer

	CO ₂ [ppm]	CO [ppb]	CH ₄ [ppb]	N ₂ O [ppb]	H ₂ [ppb]	SF ₆ [ppt]	delta ¹³ C [%]
Lowest Level	350 - 380	100 - 134	1807 - 1889	316 - 319	415 - 474	4.83 - 5.07	-7.077 - -8.536
Free Troposphere	354 - 364	96 - 122	1783 - 1869	316 - 321	452 - 492	4.78 - 5.01	-7.364 - -7.955

Heights LL and FT 60 – 90 m; 1980 – 2440 m Number of flight days 7 Number of profile sites

Valencia Winter

	CO ₂ [ppm]	CO [ppb]	CH ₄ [ppb]	N ₂ O [ppb]	H ₂ [ppb]	SF ₆ [ppt]	delta ¹³ C [%]
Lowest Level	371 - 389	148 - 273	1830 - 1958	318 - 320	394 - 483	4.85 - 8.05	-8.215 - -9.087
Free Troposphere	366 - 373	110 - 202	1793 - 1851	318 - 323	439 - 480	4.85 - 5.18	-7.997 - -8.286

Heights LL and FT 6 – 46 m; 825 – 1000 m Number of flight days 6 Number of profile sites 2

The Netherlands Winter

	CO ₂ [ppm]	CO [ppb]	CH ₄ [ppb]	N ₂ O [ppb]	H ₂ [ppb]	SF ₆ [ppt]	delta ¹³ C [%]
Lowest Level	378 - 396	165 - 346	1859 - 2126	318 - 321	514 - 631	4.92 - 7.15	-8.390 - -9.465
Free Troposphere	372 - 379	126 - 203	1807 - 1846	318 - 319	505 - 559	4.82 - 5.18	-8.127 - -8.489

Heights LL and FT 60 m; 915 m Number of flight days 5 Number of profile sites 3

Lazio Summer

	CO ₂ [ppm]	CO [ppb]	CH ₄ [ppb]	N ₂ O [ppb]	H ₂ [ppb]	SF ₆ [ppt]	delta ¹³ C [%]
Lowest Level	366 - 410	130 - 369	1796 - 1884	318 - 320	542 - 670	5.16 - 5.76	-7.775 - -9.840
Free Troposphere	373 - 375	101 - 682	1778 - 1801	317 - 318	534 - 1056	5.03 - 5.15	-8.124 - -8.209

Heights LL and FT 50 – 80 m; 3000 m Number of flight days 2.5 Number of profile sites 2

The Netherlands Summer

	CO ₂ [ppm]	CO [ppb]	CH ₄ [ppb]	N ₂ O [ppb]	H ₂ [ppb]	SF ₆ [ppt]	delta ¹³ C [%]
Lowest Level	359 - 403	132 - 264	1855 - 2166	319 - 327	561 - 684	5.16 - 5.66	-7.536 - -9.566
Free Troposphere	364 - 370	113 - 151	1776 - 1819	318 - 319	556 - 649	5.13 - 5.31	-7.716 - -8.041

Heights LL and FT 60 m; 1700 – 1800 m Number of flight days 3 Number of profile sites 3

SPA¹³CE (Thuringia) Summer

	CO ₂ [ppm]	CO [ppb]	CH ₄ [ppb]	N ₂ O [ppb]	H ₂ [ppb]	SF ₆ [ppt]	delta ¹³ C [%]
Lowest Level	362 - 373	90 - 144	1797 - 1877	319 - 321	510 - 538	5.18 - 5.50	-7.559 - -8.125
Free Troposphere	364 - 371	66 - 135	1748 - 1849	318 - 319	522 - 535	5.07 - 5.61	-7.822 - -7.972

Heights LL and FT 60 m; 1500 m Number of flight days 3.5 Number of profile sites 2

9. REFERENCES

- Amiro, B.D. et al.** [1999]: BOREAS flight measurements of forest-fire effects on carbon dioxide and energy fluxes
Agricultural and Forest Meteorology (4), 199-208
- Anderson, B.E. et al.** [1996]: Airborne observations of spatial and temporal variability of tropospheric carbon dioxide
Journal of Geophysical Research-Atmospheres (D1), 1985-1997
- Andreae, M.O. and P. Merlet** [2001]: Emission of trace gases and aerosols from biomass burning
Global Biogeochemical Cycles (4), 955-966
- Andres, R.J. et al.** [1999]: Carbon dioxide emissions from fossil-fuel use 1751-1950
Tellus Series B-Chemical and Physical Meteorology (4), 759-765
- Anthoni, P. et al.** [2004]: Forest and agricultural land use dependent CO₂ exchange in Thuringia, Germany
Global Change Biology (10), 2005-2019
- Atkinson, R.** [2000]: Atmospheric chemistry of VOCs and NO_x
Atmospheric Environment (12-14), 2063-2101
- Atkinson, R.** [1994]: Gas-phase Tropospheric Chemistry of Organic Compounds
American Chemical Society New York, 216p
- Atkinson, R.** [1989]: Kinetic and Mechanisms of the Gas-Phase Reactions of the Hydroxyl Radical with Organic Compounds
American Chemical Society New York, 246p
- Aubinet, M. et al.** [2003]: Horizontal and vertical CO₂ advection in a sloping forest
Boundary-Layer Meteorology (3), 397-417
- Aubinet, M. et al.** [2002]: Estimation of the carbon sequestration by a heterogeneous forest: night flux corrections, heterogeneity of the site and inter-annual variability
Global Change Biology (8), 1053-1071
- Aubinet, M. et al.** [2000]: Estimates of the annual net carbon and water exchange of forests: The EUROFLUX methodology
in: *Advances in Ecological Research*, Vol 30, 113-175
- Bakwin, P.S. et al.** [2003]: Strategies for measurement of atmospheric column means of carbon dioxide from aircraft using discrete sampling
Journal of Geophysical Research Vol. 108, (D16), 4514
- Bakwin, P.S. et al.** [1998]: Measurements of carbon dioxide on very tall towers: results of the NOAA/CMDL program
Tellus Series B-Chemical and Physical Meteorology (5), 401-415
- Bakwin, P.S. et al.** [1998]: Determination of the isotopic (C^{13}/C^{12}) discrimination by terrestrial biology from a global network of observations
Global Biogeochemical Cycles (3), 555-562
- Bakwin, P.S. et al.** [1994]: Carbon-Monoxide Budget in the Northern-Hemisphere
Geophysical Research Letters (6), 433-436

- Baldocchi, D. et al.** [2001]: FLUXNET: A new tool to study the temporal and spatial variability of ecosystem-scale carbon dioxide, water vapour, and energy flux densities
Bulletin of the American Meteorological Society (11), 2415-2434
- Baldocchi, D. et al.** [2000]: On measuring net ecosystem carbon exchange over tall vegetation on complex terrain
Boundary-Layer Meteorology (1-2), 257-291
- Baldocchi, D.** [1997]: Flux footprints within and over forest canopies
Boundary-Layer Meteorology (2), 273-292
- Baldocchi, D. et al.** [1996]: Strategies for measuring and modelling carbon dioxide and water vapour fluxes over terrestrial ecosystems
Global Change Biology (3), 159-168
- Barnes, D.H. et al.** [2003]: Hydrogen in the atmosphere: Observations above a forest canopy in a polluted environment
Journal of Geophysical Research-Atmospheres (D6), art. no.-4197
- Battle, M. et al.** [2000]: Global carbon sinks and their variability inferred from atmospheric O₂ and delta C¹³
Science (5462), 2467-2470
- Beckel, L. and F. Zwittkovits** [1997]: Satellitenbildatlas Europa
 RV-Verlag Berlin, 256p
- Bergamaschi, P. et al.** [2000]: Inverse modeling of the global CO cycle
 1. Inversion of CO mixing ratios
Journal of Geophysical Research-Atmospheres (D2), 1909-1927
- Bergamaschi, P. et al.** [2000]: Inverse modeling of the global CO cycle
 2. Inversion of C¹³/C¹² and O¹⁸/O¹⁶ isotope ratios
Journal of Geophysical Research-Atmospheres (D2), 1929-1945
- Bergamaschi, P. et al.** [1998]: Isotope analysis based source identification for atmospheric CH₄ and CO sampled across Russia using the Trans-Siberian railroad
Journal of Geophysical Research-Atmospheres (D7), 8227-8235
- Bergamaschi, P. et al.** [1998]: Stable isotopic signatures (delta C¹³, delta D) of methane from European landfill sites
Journal of Geophysical Research-Atmospheres (D7), 8251-8265
- Beychok, M.R.** [1994]: Fundamentals of stack gas dispersion
 Beychok Irvine, Calif., VIII, 193p
- Bird, M.I. et al.** [2002]: Soil carbon inventories and C¹³ on a latitude transect in Siberia
Tellus Series B-Chemical and Physical Meteorology (5), 631-641
- Black, T.A. et al.** [1996]: Annual cycles of water vapour and carbon dioxide fluxes in and above a boreal aspen forest
Global Change Biology (3), 219-229
- Blake, N.J. et al.** [1993]: Estimates of Atmospheric Hydroxyl Radical Concentrations from the Observed Decay of Many Reactive Hydrocarbons in Well- Defined Urban Plumes
Journal of Geophysical Research-Atmospheres (D2), 2851-2864

Bolin, B. [1981]: Carbon cycle modelling
Wiley Chichester, XIV, 390p

Borrell, P. and P.M. Borrell [2000]: Transport and chemical transformation of pollutants in the troposphere
Springer XXI, 474p

Bosinger, R. et al. [1988]: Carbon Isotopes in Atmospheric Methane at European Sites
Chemical Geology (1-2), 96-96

Bousquet, P. et al. [2000]: Regional changes in carbon dioxide fluxes of land and oceans since 1980
Science (5495), 1342-1346

Bousquet, P. et al. [1999]: Inverse modeling of annual atmospheric CO₂ sources and sinks 1. Method and control inversion
Journal of Geophysical Research-Atmospheres (D21), 26161-26178

Bousquet, P. et al. [1999]: Inverse modeling of annual atmospheric CO₂ sources and sinks 2. Sensitivity study
Journal of Geophysical Research-Atmospheres (D21), 26179-26193

Bouwman, A. (ed.) [1999]: Approaches to scaling of trace gas fluxes in ecosystems
Elsevier Amsterdam, IX, 362p

Bowling, D.R. et al. [2003]: Critical evaluation of micrometeorological methods for measuring ecosystem-atmosphere isotopic exchange of CO₂
Agricultural and Forest Meteorology (3-4), 159-179

Bowling, D.R. et al. [2001]: Technique to measure CO₂ mixing ratio in small flasks with a bellows/IRGA system
Agricultural and Forest Meteorology (1), 61-65

Bowling, D.R. et al. [2001]: Partitioning net ecosystem carbon exchange with isotopic fluxes of CO₂
Global Change Biology (2), 127-145

Brand, W.A. [1996]: High precision isotope ratio monitoring techniques in mass spectrometry
Journal of Mass Spectrometry (3), 225-235

Bräunlich, M. [2000]: Study of atmospheric carbon monoxide and methane using isotopic analysis
Naturwissenschaftlich-Mathematische Gesamtfakultät, Ruprecht-Karls-Universität Heidelberg, 197p, PhD-Thesis

Brenninkmeijer, C.A.M. and T. Röckmann [1997]: Using isotope analysis to improve atmospheric CO budget calculations
IAEA Symposium on Isotope Techniques Vienna, 69-76

Brooks, J.R. et al. [1997]: Carbon isotope composition of boreal plants: Functional grouping of life forms
Oecologia (3), 301-311

Brost, R.A. and M. Heimann [1991]: The Effect of the Global Background on a Synoptic-Scale Simulation of Tracer Concentration
Journal of Geophysical Research-Atmospheres (D8), 15415-15425

Buchmann, N. et al. [2002]: Predicting daytime carbon isotope ratios of atmospheric CO₂ within forest canopies

Functional Ecology (1), 49-57

Buchmann, N. and J.R. Ehleringer [1998]: CO₂ concentration profiles, and carbon and oxygen isotopes in C-3, and C-4 crop canopies

Agricultural and Forest Meteorology (1), 45-58

Buchmann, N. et al. [1997]: Interseasonal comparison of CO₂ concentrations, isotopic composition, and carbon dynamics in an Amazonian rainforest (French Guiana)

Oecologia (1), 120-131

Buchmann, N. et al. [1996]: Carbon dioxide concentrations within forest canopies - Variation with time, stand structure, and vegetation type

Global Change Biology (5), 421-432

Burk, R.L. & M. Stuiver [1981]: Oxygen isotope ratios in trees reflect mean annual temperatures and humidity

Science (211), 1417-1419

Chameides, W.L. et al. [1992]: Ozone precursor Relationships in the Ambient Atmosphere

Journal of Geophysical Research Vol. 97 (D5), 6037-6055

Chevillard, A. et al. [2002]: Transport of Rn-222 using the regional model REMO: a detailed comparison with measurements over Europe

Tellus Series B-Chemical and Physical Meteorology (5), 850-871

Chevillard, A. et al. [2002]: Simulation of atmospheric CO₂ over Europe and western Siberia using the regional scale model REMO

Tellus Series B-Chemical and Physical Meteorology (5), 872-894

Christensen, T.R. et al. [2000]: Trace gas exchange in a high-arctic valley
1. Variations in CO₂ and CH₄ flux between tundra vegetation types

Global Biogeochemical Cycles (3), 701-713

Ciais, P. et al. [2000]: Regional biospheric carbon fluxes as inferred from atmospheric CO₂ measurements

Ecological Applications (6), 1574-1589

Ciais, P. et al. [1999]: A global calculation of the delta C¹³ of soil respired carbon:
Implications for the biospheric uptake of anthropogenic CO₂

Global Biogeochemical Cycles (2), 519-530

Ciais, P. et al. [1997]: A three-dimensional synthesis study of delta O¹⁸ in atmospheric CO₂ 1. Surface fluxes

Journal of Geophysical Research-Atmospheres (D5), 5857-5872

Ciais, P. et al. [1997]: A three-dimensional synthesis study of delta O¹⁸ in atmospheric CO₂ 2. Simulations with the TM2 transport model

Journal of Geophysical Research-Atmospheres (D5), 5873-5883

Ciais, P. et al. [1995]: A Large Northern-Hemisphere Terrestrial CO₂ Sink Indicated by the C¹³/C¹² Ratio of Atmospheric CO₂

Science (5227), 1098-1102

- Ciais, P. et al.** [1995]: Partitioning of Ocean and Land Uptake of CO₂ as Inferred by Delta-C¹³ Measurements from the NOAA Climate Monitoring and Diagnostics Laboratory Global Air Sampling Network
Journal of Geophysical Research-Atmospheres (D3), 5051-5070
- Cleugh, H.A. and C.S.B. Grimmond** [2001]: Modelling regional scale surface energy exchanges and CBL growth in a heterogeneous, urban-rural landscape
Boundary-Layer Meteorology (1), 1-31
- Cleugh, H.A. et al.** [1998]: Regional-Scale Heat and Water Vapour Fluxes in an Agricultural Landscape: An Evaluation of CBL Budget Methods at OASIS
unpublished manuscript, 44p
- Coleman, D.C. (ed.)** [1991]: Carbon isotope techniques
Academic Press San Diego, XII, 274p
- Conway, T.J. and P.P. Tans** [1999]: Development of the CO₂ latitude gradient in recent decades
Global Biogeochemical Cycles (4), 821-826
- Conway, T.J. et al.** [1994]: Evidence for Interannual Variability of the Carbon-Cycle from the National-Oceanic-and-Atmospheric-Administration Climate- Monitoring-and-Diagnostics-Laboratory Global-Air-Sampling- Network
Journal of Geophysical Research-Atmospheres (D11), 22831-22855
- Conway, T.J. et al.** [1993]: Correlations among Atmospheric CO₂, CH₄ and CO in the Arctic, March 1989
Atmospheric Environment Part A - General Topics (17-18), 2881-2894
- Crawford, T.L. et al.** [1996]: Air-surface exchange measurement in heterogeneous regions: Extending tower observations with spatial structure observed from small aircraft
Global Change Biology (3), 275-285
- Crutzen, P.J. et al.** [1998]: Trace gas measurements between Moscow and Vladivostok using the Trans-Siberian Railroad
Journal of Atmospheric Chemistry (2), 179-194
- Crutzen, P.J. et al.** [1979]: Biomass Burning as a Source of Atmospheric Gases CO, H₂, N₂O, NO, CH₃Cl and COS
Nature (5736), 253-256
- Cullis, C.F. and M.M. Hirschler** [1989]: Mans Emissions of Carbon-Monoxide and Hydrocarbons into the Atmosphere
Atmospheric Environment (6), 1195-1203
- Damoah, R. et al.** [2004]: Around the world in 17 days – hemispheric-scale transport of forest fire smoke from Russia in May 2003
Atmospheric Chemistry and Physics Discussion (4), 1449-1471
- Dargaville, R.J. et al.** [2002]: Evaluation of terrestrial carbon cycle models with atmospheric CO₂ measurements: Results from transient simulations considering increasing CO₂, climate, and land-use effects
Global Biogeochemical Cycles (4), art. no.-1092
- Day, T.A. et al.** [2002]: Temporal patterns in near-surface CO₂ concentrations over contrasting vegetation types in the Phoenix metropolitan area
Agricultural and Forest Meteorology (3), 229-245

- Denmead, O.T. et al.** [1996]: Boundary layer budgets for regional estimates of scalar fluxes
Global Change Biology (3), 255-264
- Denning, A.S. et al.** [1999]: Can a strong atmospheric CO₂ rectifier effect be reconciled with a "reasonable" carbon budget?
Tellus Series B-Chemical and Physical Meteorology (2), 249-253
- Denning, A.S. et al.** [1999]: Three-dimensional transport and concentration of SF₆ - A model intercomparison study (TransCom 2)
Tellus Series B-Chemical and Physical Meteorology (2), 266-297
- Denning, A.S. et al.** [1996]: Simulations of terrestrial carbon metabolism and atmospheric CO₂ in a general circulation model 2. Simulated CO₂ concentrations
Tellus Series B-Chemical and Physical Meteorology (4), 543-567
- Denning, A.S. et al.** [1996]: Simulations of terrestrial carbon metabolism and atmospheric CO₂ in a general circulation model 1. Surface carbon fluxes
Tellus Series B-Chemical and Physical Meteorology (4), 521-542
- Denning, A.S. et al.** [1995]: Latitudinal Gradient of Atmospheric CO₂ Due to Seasonal Exchange with Land Biota
Nature (6537), 240-243
- Derwent, R.G. et al.** [2002]: Continuous observations of carbon dioxide at Mace Head, Ireland from 1995 to 1999 and its net European ecosystem exchange
Atmospheric Environment (17), 2799-2807
- Desjardins, R.L. et al.** [1997]: Scaling up flux measurements for the boreal forest using aircraft-tower combinations
Journal of Geophysical Research-Atmospheres (D24), 29125-29133
- DeWekker, S.F.J.** [1995]: The behaviour of the convective boundary layer height over orographically complex terrain
Department of Meteorology, Wageningen Agricultural University, 130p, MSc-Thesis
- Dobbie, K.E. et al.** [1999]: Nitrous oxide emissions from intensive agricultural systems: Variations between crops and seasons, key driving variables, and mean emission factors
Journal of Geophysical Research-Atmospheres (D21), 26891-26899
- Dolman, A.J. et al.** [2002]: The carbon uptake of a mid latitude pine forest growing on sandy soil
Agricultural and Forest Meteorology (3), 157-170
- Draxler, R.R. and G.D. Hess** [2002]: Description of the hysplit_4 modelling system
Air Resource Laboratory, NOAA, 27p
- Ebel, A. et al.** [1997]: Tropospheric modelling and emission estimation
Springer Berlin, XXIV, 440p
- Ehleringer, J.R. et al.** [2002]: Stable isotopes and carbon cycle processes in forests and grasslands
Plant Biology (2), 181-189

- Ehleringer, J.R. et al.** [2000]: Carbon isotope ratios in belowground carbon cycle processes
Ecological Applications (2), 412-422
- Ehleringer, J.R. and C.S. Cook** [1998]: Carbon and oxygen isotope ratios of ecosystem respiration along an Oregon conifer transect: preliminary observations based on small-flask sampling
Tree Physiology (8-9), 513-519
- Ehleringer, J.R. et al.** [1997]: C-4 photosynthesis, atmospheric CO₂ and climate
Oecologia (3), 285-299
- Ehman, J.L. et al.** [2002]: An initial intercomparison of micrometeorological and ecological inventory estimates of carbon exchange in a mid-latitude deciduous forest
Global Change Biology (6), 575-589
- Elkins, J.W. et al.** [1996]: Airborne gas chromatograph for in situ measurements of long-lived species in the upper troposphere and lower stratosphere
Geophysical Research Letters (4), 347-350
- Engelen, R.J. et al.** [2002]: On error estimation in atmospheric CO₂ inversions
Journal of Geophysical Research-Atmospheres (D22), art. no.-4635
- Etheridge, D.M. et al.** [1998]: Atmospheric methane between 1000 AD and present: Evidence of anthropogenic emissions and climatic variability
Journal of Geophysical Research-Atmospheres (D13), 15979-15993
- Falge, E. et al.** [2002]: Seasonality of ecosystem respiration and gross primary production as derived from FLUXNET measurements
Agricultural and Forest Meteorology (1-4), 53-74
- Farquhar, G.D. et al.** [1993]: Vegetation Effects on the Isotope Composition of Oxygen in Atmospheric CO₂ (Response to Vol 363, Pg 439, 1993)
Nature (6444), 368-368
- Farquhar, G.D. et al.** [1993]: Vegetation Effects on the Isotope Composition of Oxygen in Atmospheric CO₂
Nature (6428), 439-443
- Farquhar, G.D. et al.** [1989]: Carbon Isotope Discrimination and Photosynthesis
Annual Review of Plant Physiology and Plant Molecular Biology 503-537
- Fessenden, J.E. and J.R. Ehleringer** [2002]: Age-related variations in delta C¹³ of ecosystem respiration across a coniferous forest chronosequence in the Pacific Northwest
Tree Physiology (2-3), 159-167
- Flanagan, L.B. et al.** [1999]: Spatial and temporal variation in the carbon and oxygen stable isotope ratio of respired CO₂ in a boreal forest ecosystem
Tellus Series B-Chemical and Physical Meteorology (2), 367-384
- Flanagan, L.B. and J.R. Ehleringer** [1998]: Ecosystem-atmosphere CO₂ exchange: interpreting signals of change using stable isotope ratios
Trends in Ecology & Evolution (1), 10-14
- Flanagan, L.B. et al.** [1997]: Discrimination against (COO)-O¹⁸-O¹⁶ during photosynthesis and the oxygen isotope ratio of respired CO₂ in boreal forest ecosystems
Global Biogeochemical Cycles (1), 83-98

- Flanagan, L.B. et al.** [1996]: Carbon isotope discrimination during photosynthesis and the isotope ratio of respired CO₂ in boreal forest ecosystems
Global Biogeochemical Cycles (4), 629-640
- Flesch, T.K.** [1996]: The footprint for flux measurements, from backward Lagrangian stochastic models
Boundary-Layer Meteorology (3-4), 399-404
- Florkowski, T. et al.** [1997]: Isotopic composition of CO₂ and CH₄ in a heavily polluted urban atmosphere and in a remote mountain area
IAEA Symposium on Isotope Techniques Vienna, 37-48
- Forster, C. et al.** [2001]: Transport of boreal forest fire emissions from Canada to Europe
Journal of Geophysical Research-Atmospheres (D19), 22887-22906
- Francey, R.J. et al.** [1999]: A 1000-year high precision record of delta C¹³ in atmospheric CO₂
Tellus Series B-Chemical and Physical Meteorology (2), 170-193
- Francey, R.J. et al.** [1999]: A history of delta C¹³ in atmospheric CH₄ from the Cape Grim air archive and antarctic firn air
Journal of Geophysical Research-Atmospheres (D19), 23631-23643
- Francey, R.J. et al.** [1999]: High precision long-term monitoring of radiatively active and related trace gases at surface sites and from aircraft in the southern hemisphere atmosphere
Journal of the Atmospheric Sciences (2), 279-285
- Francey, R.J. et al.** [1998]: Atmospheric carbon dioxide and its stable isotope ratios, methane, carbon monoxide, nitrous oxide and hydrogen from Shetland Isles
Atmospheric Environment (19), 3331-3338
- Freibauer, A.** [2002]: CarboEurope - A cluster of projects to understand and quantify the carbon balance of Europe
CarboEurope European Office, 24p
- Fritsch, H.** [2003]: Ableitung regionaler Flusswerte von Wärme, Wasserdampf und Kohlendioxid
University of Hamburg, 139p, PhD-Thesis
- Fuentes, J.D. et al.** [2000]: Biogenic hydrocarbons in the atmospheric boundary layer: A review
Bulletin of the American Meteorological Society (7), 1537-1575
- Fung, I. et al.** [1997]: C¹³ exchanges between the atmosphere and biosphere
Global Biogeochemical Cycles (4), 507-533
- Gemery, P.A., M. Trolier and J.W.C. White** [1996]: Oxygen isotope exchange between carbon dioxide and water following atmospheric sampling using glass flasks
Journal of Geophysical Research (D9), 14,415-14,420
- Gerbig, C. et al.** [2003]: Toward constraining regional-scale fluxes of CO₂ with atmospheric observations over a continent: 1. Observed spatial variability from airborne platforms
Journal of Geophysical Research Vol. 108 (D24), 4756

- Gerbig, C. et al.** [2003]: Toward constraining regional-scale fluxes of CO₂ with atmospheric observations over a continent: 2. Analysis of COBRA data using a receptor-oriented framework
Journal of Geophysical Research Vol. 108 (D24), 4757
- Gerbig, C. et al.** [1999]: An improved fast-response vacuum-UV resonance fluorescence CO instrument
Journal of Geophysical Research (D1), 1699-1704
- Gerbig, C. et al.** [1996]: Fast response resonance fluorescence CO measurements aboard the C-130: Instrument characterization and measurements made during North Atlantic Regional Experiment 1993
Journal of Geophysical Research (D22), 29229-29238
- Gioli, B. et al.** [2004]: Comparison between tower and aircraft-based eddy correlation fluxes in five regions of Europe
Submitted to Global Change Biology
- Gioli, B. and B. de Martino** [2002]: Wind profile data obtained by the MFP 'Sky Arrow'
personal communication
- Gloor, M. et al.** [2001]: What is the concentration footprint of a tall tower?
Journal of Geophysical Research-Atmospheres (D16), 17831-17840
- Gloor, M. et al.** [2000]: Optimal sampling of the atmosphere for purpose of inverse modeling: A model study
Global Biogeochemical Cycles (1), 407-428
- Gloor, M. et al.** [1999]: A model-based evaluation of inversions of atmospheric transport, using annual mean mixing ratios, as a tool to monitor fluxes of nonreactive trace substances like CO₂ on a continental scale
Journal of Geophysical Research-Atmospheres (D12), 14245-14260
- Goulden, M.L. et al.** [1996]: Measurements of carbon sequestration by long-term eddy covariance: Methods and a critical evaluation of accuracy
Global Change Biology (3), 169-182
- Graedel, T.E. and P.J. Crutzen** [1993]: Atmospheric change
 Freeman New York, XIII, 446p
- Granier, C. et al.** [2000]: The impact of natural and anthropogenic hydrocarbons on the tropospheric budget of carbon monoxide
Atmospheric Environment 34, 5255-5270
- Greco, S. and D.D. Baldocchi** [1996]: Seasonal variations of CO₂ and water vapour exchange rates over a temperate deciduous forest
Global Change Biology (3), 183-197
- Grelle, A. and A. Lindroth** [1996]: Eddy-correlation system for long-term monitoring of fluxes of heat, water vapour and CO₂
Global Change Biology (3), 297-307
- Griffis, T.J. et al.** [2003]: Ecophysiological controls on the carbon balances of three southern boreal forests
Agricultural and Forest Meteorology (1-2), 53-71

- Griffiths, H. (ed.)** [1998]: Stable isotopes – integration of biological, ecological and geochemical processes
 BIOS Scientific Publishers Oxford, XX, 438p
- Groffman, P.M. et al.** [2000]: Evaluating annual nitrous oxide fluxes at the ecosystem scale
Global Biogeochemical Cycles (4), 1061-1070
- Gross, G.** [1993]: Numerical Simulation of Canopy Flows
 Springer Berlin, 167p
- Guderian, R. (ed.)** [2000]: Anthropogene und biogene Emissionen, Photochemie der Troposphäre, Chemie der Stratosphäre und Ozonabbau
Handbuch der Umweltveränderungen und Ökotoxikologie 1A Springer, XXII, 424p
- Guderian, R. (ed.)** [2000]: Aerosol/Multiphasenchemie, Ausbreitung und Deposition von Spurenstoffen, Auswirkungen auf Strahlung und Klima
Handbuch der Umweltveränderungen und Ökotoxikologie 1B Springer, XXII, 516p
- Gurney, K.R. et al.** [2002]: Towards robust regional estimates of CO₂ sources and sinks using atmospheric transport models
Nature (6872), 626-630
- Haase, H.-P.** [1999]: SF₆ als atmosphärischer Tracer: Untersuchungen zur Verteilung von SF₆ in der Troposphäre und der untersten Stratosphäre
Fachbereich Geowissenschaften, Johann Wolfgang Goethe-Universität Frankfurt/Main, 126p, Diploma-Thesis
- Hakola, H. et al.** [2000]: The ambient concentrations of biogenic hydrocarbons at a northern European, boreal site
Atmospheric Environment 34, 4971 - 4982
- Hansen, U. et al.** [1997]: Biogenic emissions and CO₂ gas exchange investigated on four Mediterranean shrubs
Atmospheric Environment 157-166
- Harris, J.M. et al.** [2000]: An interpretation of trace gas correlations during Barrow, Alaska, winter dark periods, 1986-1997
Journal of Geophysical Research-Atmospheres (D13), 17267-17278
- Heimann, M. and S. Körner** [2003]: The Global Atmospheric Tracer Model TM3
 Technical Report 5, MPI-BGC Jena, IV, 131p
- Heimann, M.** [2002]: Foreword - Special issue with manuscripts related to the EUROSIBERIAN CARBONFLUX project
Tellus Series B-Chemical and Physical Meteorology (5), 417-419
- Heimann, M. and T. Kaminski** [1999]: Inverse modelling approaches to infer surface trace gas fluxes from observed atmospheric mixing ratios
 in: *A. F. Bouwman Approaches to scaling of trace gas fluxes in ecosystems* Elsevier Science, 277-295
- Heimann, M. et al.** [1998]: Evaluation of terrestrial Carbon Cycle models through simulations of the seasonal cycle of atmospheric CO₂: First results of a model intercomparison study
Global Biogeochemical Cycles (1), 1-24
- Heimann, M.** [1995]: Atmospheric Chemistry - Dynamics of the Carbon-Cycle
Nature (6533), 629-630

- Heimann, M. (ed.)** [1991]: The global carbon cycle
NATO ASI Series I. Global Environmental Change Springer Berlin, 599p
- Heimann, M. and C. Keeling** [1986]: Meridional Eddy Diffusion-Model of the Transport of Atmospheric Carbon-Dioxide. 1. Seasonal Carbon-Cycle over the Tropical Pacific-Ocean
Journal of Geophysical Research-Atmospheres (D7), 7765-7781
- Hein, R. et al.** [1997]: An inverse modeling approach to investigate the global atmospheric methane cycle
Global Biogeochemical Cycles (1), 43-76
- Higuchi, K. et al.** [2003]: Regional source/sink impact on the diurnal, seasonal and inter-annual variations in atmospheric CO₂ at a boreal forest site in Canada
Tellus Series B-Chemical and Physical Meteorology (2), 115-125
- Hoefs, J.** [1996]: Stable Isotope Geochemistry
Springer Berlin, 201p
- Holland, F. et al.** [1998]: Highly Time Resolved Measurements of OH during POPCORN Using Laser-Induced Fluorescence Spectroscopy
Journal of Atmospheric Chemistry (31), 205-225
- Hollinger, D.Y. et al.** [1998]: Forest-atmosphere carbon dioxide exchange in eastern Siberia
Agricultural and Forest Meteorology (4), 291-306
- Hollinger, D.Y. et al.** [1994]: Carbon-Dioxide Exchange between an Undisturbed Old-Growth Temperate Forest and the Atmosphere
Ecology (1), 134-150
- Horst, T.W. and J.C. Weil** [1992]: Footprint Estimation for Scalar Flux Measurements in the Atmospheric Surface-Layer
Boundary-Layer Meteorology (3), 279-296
- Houghton, J.T. et al.** [2001]: Climate Change 2001, The scientific basis: Contribution of Working Group I to the Third Assessment Report of the IPCC
Cambridge University Press Cambridge, X, 881p
- Houghton, R.A.** [2001]: Counting terrestrial sources and sinks of carbon
Climatic Change (4), 525-534
- Houghton, R.A.** [2000]: Interannual variability in the global carbon cycle
Journal of Geophysical Research-Atmospheres (D15), 20121-20130
- Houghton, R.A.** [1999]: The annual net flux of carbon to the atmosphere from changes in land use 1850-1990
Tellus Series B-Chemical and Physical Meteorology (2), 298-313
- Houghton, R.A.** [1995]: Land-Use Change and the Carbon-Cycle
Global Change Biology (4), 275-287
- Houweling, S. et al.** [2000]: The modeling of tropospheric methane: How well can point measurements be reproduced by a global model?
Journal of Geophysical Research-Atmospheres (D7), 8981-9002

- Houweling, S. et al.** [2000]: Simulation of preindustrial atmospheric methane to constrain the global source strength of natural wetlands
Journal of Geophysical Research-Atmospheres (D13), 17243-17255
- Houweling, S. et al.** [1999]: Inverse modeling of methane sources and sinks using the adjoint of a global transport model
Journal of Geophysical Research-Atmospheres (D21), 26137-26160
- Houweling, S. et al.** [1998]: The impact of nonmethane hydrocarbon compounds on tropospheric photochemistry
Journal of Geophysical Research-Atmospheres (D9), 10673-10696
- Hutjes, R.W.A. (ed.)** [2003]: Regional Assessment and Monitoring of the Carbon Balance within Europe (RECAB) Final report
 Alterra Green World Research, Wageningen *unpublished manuscript*, 298 p
- Janson, R. and C. De Serves** [1999]: Emissions of Biogenic VOCs from Boreal Ecosystems
 in: *Laurila, T. and V. Lindfors: Biogenic VOC emissions and photochemistry in boreal regions of Europe - BIPOREP*
 European Commission; Air Pollution research report No 70, 158 p
- Janson, R.** [1993]: Monoterpene Emissions from Scots Pine and Norwegian Spruce
Journal of Geophysical Research-Atmospheres (D2), 2839-2850
- Janssens, I.A. et al.** [2003]: Europe's terrestrial biosphere absorbs 7 to 12% of European anthropogenic CO₂ emissions
Science (5625), 1538-1542
- Janssens, I.A. et al.** [2001]: Productivity overshadows temperature in determining soil and ecosystem respiration across European forests
Global Change Biology (3), 269-278
- Janssens, I.A. et al.** [2000]: Assessing forest soil CO₂ efflux: an in situ comparison of four techniques
Tree Physiology (1), 23-32
- Jenkin, M.E., S.M. Saunders and M.J. Pilling** [1997]: The tropospheric degradation of volatile organic compounds: a protocol for mechanism development
Atmospheric Environment 31, 81-104
- Jobson, B.T. et al.** [1998]: Spatial and temporal variability of nonmethane hydrocarbon mixing ratios and their relation to photochemical lifetime
Journal of Geophysical Research-Atmospheres (D11), 13557-13567
- Jordan, A. and W. Brand** [2001]: Trace gas measurement and quality assurance at the MPI for Biogeochemistry
11th WMO/IAEA Meeting Tokyo, 140-144
- Kaimal, J.C. and J.J. Finnigan** [1994]: Atmospheric Boundary Layer Flows
 Oxford University Press, 289p
- Kaminski, T. and M. Heimann** [2001]: Inverse modeling of atmospheric carbon dioxide fluxes
Science (5541), U1-U1
- Kaminski, T. et al.** [1999]: A coarse grid three-dimensional global inverse model of the atmospheric transport - 1. Adjoint model and Jacobian matrix
Journal of Geophysical Research-Atmospheres (D15), 18535-18553

- Kaminski, T. et al.** [1999]: A coarse grid three-dimensional global inverse model of the atmospheric transport - 2. Inversion of the transport of CO₂ in the 1980s
Journal of Geophysical Research-Atmospheres (D15), 18555-18581
- Kanakidou, M. and P.J. Crutzen** [1999]: The photochemical source of carbon monoxide: Importance, uncertainties and feedbacks
Chemosphere Global Change Science (1), 91-109
- Kaplan, J.O. et al.** [2002]: The stable carbon isotope composition of the terrestrial biosphere: Modeling at scales from the leaf to the globe
Global Biogeochemical Cycles (4), art. no.-1060
- Kaplan, J.O.** [2001]: Geophysical applications of vegetation modeling
Lund University, 114p, PhD-Thesis
- Kasibhatla, P.S.** [2000]: Inverse methods in global biogeochemical cycles
 American Geophysical Union Washington, DC, VII, 324p
- Kato, S. et al.** [1999]: Stable isotopic compositions of carbon monoxide from biomass burning experiments
Atmospheric Environment (27), 4357-4362
- Keeling, C. and M. Heimann** [1986]: Meridional Eddy Diffusion-Model of the Transport of Atmospheric Carbon-Dioxide. 2. Mean Annual Carbon-Cycle
Journal of Geophysical Research-Atmospheres (D7), 7782-7796
- Keeling, C.D.** [1958]: The concentration and isotopic abundances of atmospheric carbon dioxide in rural areas
Geochimica and Cosmochimica Acta (13), 322-334
- Keeling, R.F. et al.** [1996]: Global and hemispheric CO₂ sinks deduced from changes in atmospheric O₂ concentration
Nature (6579), 218-221
- Kesselmeier, J. et al.** [2002]: Volatile organic compound emissions in relation to plant carbon fixation and the terrestrial carbon budget
Global Biogeochemical Cycles (4), art. no.-1126
- Kesselmeier, J. and M. Staudt** [1999]: Biogenic volatile organic compounds (VOC): An overview on emission, physiology and ecology
Journal of Atmospheric Chemistry (1), 23-88
- Kesselmeier, J. et al.** [1996]: Emission of monoterpenes and isoprene from a Mediterranean oak species Quercus ilex L measured within the BEMA (Biogenic Emissions in the Mediterranean Area) project
Atmospheric Environment (10-11), 1841-1850
- King, G.M.** [1999]: Characteristics and significance of atmospheric carbon monoxide consumption by soils
Chemosphere Global Change Science (1), 53-63
- Kjellstrom, E. et al.** [2002]: Summertime Siberian CO₂ simulations with the regional transport model MATCH: a feasibility study of carbon uptake calculations from EUROSIB data
Tellus Series B-Chemical and Physical Meteorology (5), 834-849
- Klaassen, W. and M. Claussen** [1995]: Landscape Variability and Surface Flux Parameterization in Climate Models
Agricultural and Forest Meteorology (3-4), 181-188

- Klaassen, W.** [1992]: Average Fluxes from Heterogeneous Vegetated Regions
Boundary-Layer Meteorology (4), 329-354
- Kljun, N. et al.** [2002]: A three-dimensional backward lagrangian footprint model for a wide range of boundary-layer stratifications
Boundary-Layer Meteorology (2), 205-226
- Knöhl, A.** [2003]: Carbon dioxide exchange and isotopic signature (^{13}C) of an unmanaged 250 year-old deciduous forest in Central Germany
Biologisch-Pharmazeutische Fakultät Friedrich-Schiller-Universität Jena, 98p, PhD-Thesis
- Knöhl, A.** [2003]: The SPA ^{13}CE Experiment: Tower Investigations
personal communication
- Kolle, O.** [2002]: Eddy-correlation and meteorological measurements at the Hainich tower
personal communication
- Koppmann, R. et al.** [1998]: Measurements of Carbon Monoxide and Nonmethane Hydrocarbons During POPCORN
Journal of Atmospheric Chemistry (31), 53-72
- Kraftfahrt-Bundesamt** [2003]: Kraftstoffverbrauchs- und Emissions-Typprüfwerte von Kraftfahrzeugen mit Allgemeiner Betriebserlaubnis oder EG-Typengenehmigung
13. Ausgabe, Fassung: April 2003, 618p
- Kramm, G. and F.X. Meixner** [2000]: On the dispersion of trace species in the atmospheric boundary layer: a re-formulation of the governing equations for the turbulent flow of the compressible atmosphere
Tellus Series a-Dynamic Meteorology and Oceanography (5), 500-522
- Kuck, L.R. et al.** [2000]: Measurements of landscape-scale fluxes of carbon dioxide in the Peruvian Amazon by vertical profiling through the atmospheric boundary layer
Journal of Geophysical Research-Atmospheres (D17), 22137-22146
- Kuhlmann, A.J. et al.** [1998]: Methane emissions from a wetland region within the Hudson Bay Lowland: An atmospheric approach
Journal of Geophysical Research-Atmospheres (D13), 16009-16016
- Lafont, S. et al.** [2002]: Spatial and temporal variability of land CO₂ fluxes estimated with remote sensing and analysis data over western Eurasia
Tellus Series B-Chemical and Physical Meteorology (5), 820-833
- Lamarque, J.-F. et al.** [2003]: Identification of CO plumes from MOPITT data: Application to the August 2000 Idaho-Montana forest fires
Geophysical Research Letters Vol. 30 (13), 1688
- Langenfelds, R.L. et al.** [2002]: Interannual growth rate variations of atmospheric CO₂ and its delta C¹³, H₂, CH₄, and CO between 1992 and 1999 linked to biomass burning
Global Biogeochemical Cycles (3), art. no.-1048
- Langenfelds, R.L. et al.** [1996]: Improved vertical sampling of the trace gas composition of the troposphere above Cape Grim since 1991
 in: *R. J. Francey, A.L. Dick and N. Derek: Baseline Atmospheric Program Australia 1993* Department of the Environment, Sport and Territories Bureau of Meteorology in cooperation with CSIRO Division of Atmospheric Research, 46-57

- Langmann, B.** [2000]: Numerical modelling of regional scale transport and photochemistry directly together with meteorological processes
Atmospheric Environment (21), 3585-3598
- Langmann, B. and H.F. Graf** [1997]: The chemistry of the polluted atmosphere over Europe: Simulations and sensitivity studies with a regional chemistry-transport-model
Atmospheric Environment (19), 3237-3255
- Laubach, J. and H. Fritsch** [2002]: Convective boundary layer budgets derived from aircraft data
Agricultural and Forest Meteorology (4), 237-263
- Laurila, T. et al.** [1999]: Ozone, VOC and Nitrogen Species Concentrations in Ambient Air in the Boreal Region of Europe
 in: *Laurila, T. and V. Lindfors: Biogenic VOC emissions and photochemistry in boreal regions of Europe - BIPHOREP*
 European Commission; Air Pollution research report No 70, 158 p
- Laursen, K.K. et al.** [1992]: Some trace gas emissions from North American biomass fires with an assessment of regional and global fluxes from biomass burning
Journal of Geophysical Research Vol.97 (D18), 20687-20701
- Law, B.E. et al.** [2002]: Environmental controls over carbon dioxide and water vapour exchange of terrestrial vegetation
Agricultural and Forest Meteorology (1-4), 97-120
- Law, R.M. et al.** [2003]: Data and modelling requirements for CO₂ inversions using high-frequency data
Tellus Series B-Chemical and Physical Meteorology (2), 512-521
- Law, R.M. et al.** [2002]: Using high temporal frequency data for CO₂ inversions
Global Biogeochemical Cycles (4), art. no.-1053
- Law, R.M. and P.J. Rayner** [1999]: Impacts of seasonal covariance on CO₂ inversions
Global Biogeochemical Cycles (4), 845-856
- Law, R.M. et al.** [1996]: Variations in modeled atmospheric transport of carbon dioxide and the consequences for CO₂ inversions
Global Biogeochemical Cycles (4), 783-796
- Lawrence, M.G. et al.** [2003]: Global chemical weather forecasts for field campaign planning: predictions and observations of large-scale features during MINOS, CONTRACE, and INDOEX
Atmospheric Chemistry and Physics 267-289
- Lawrimore, J.H. M. Das and V.P. Aneja** [1995]: Vertical sampling and analysis of nonmethane hydrocarbons for ozone control in urban North Carolina
Journal of Geophysical Research Vol. 100, (D11), 22785-22793
- Leclerc, M.Y. et al.** [2003]: Impact of non-local advection on flux footprints over a tall forest canopy: a tracer flux experiment
Agricultural and Forest Meteorology (1-2), 19-30
- Leclerc, M.Y. et al.** [1997]: Observations and large-eddy simulation modeling of footprints in the lower convective boundary layer
Journal of Geophysical Research-Atmospheres (D8), 9323-9334

- Lehning, M.** [1998]: The regional pollutant budget of the atmospheric boundary layer: Concept, interpretations and observational results
Meteorologische Zeitschrift (3), 112-119
- Lehning, M. et al.** [1998]: Vertical exchange and regional budgets of air pollutants over densely populated areas
Atmospheric Environment (8), 1353-1363
- Lehning, M.** [1996]: Transport Processes and Regional Pollutant Budgets over Topography of Varying Complexity
Swiss Federal Institute of Technology, ETH Zürich, 147p, PhD-Thesis
- Lerdau, M. et al.** [1997]: Controls over monoterpene emissions from boreal forest conifers
Tree Physiology (8-9), 563-569
- Levin, I. et al.** [2002]: Three years of trace gas observations over the EuroSiberian domain derived from aircraft sampling - a concerted action
Tellus Series B-Chemical and Physical Meteorology (5), 696-712
- Levin, I. et al.** [1995]: Long-Term Observations of Atmospheric CO₂ and Carbon Isotopes at Continental Sites in Germany
Tellus Series B-Chemical and Physical Meteorology (1-2), 23-34
- Levin, I. et al.** [1993]: Stable Isotopic Signature of Methane from Major Sources in Germany
Chemosphere (1-4), 161-177
- Levin, I.** [1987]: Atmospheric CO₂ in continental Europe - an alternative approach to clean air CO₂ data
Tellus Series B-Chemical and Physical Meteorology 21-28
- Levy, P.E. et al.** [1999]: Regional-scale CO₂ fluxes over central Sweden by a boundary layer budget method
Agricultural and Forest Meteorology 169-180
- Lin, G.H. and J.R. Ehleringer** [1997]: Carbon isotopic fractionation does not occur during dark respiration in C-3 and C-4
Plant Physiology (1), 391-394
- Lindfors, V., M. Kuhn and W.R. Stockwell** [1999]: Photochemistry of VOCs in the boreal zone
 in: *Laurila, T. and V. Lindfors: Biogenic VOC emissions and photochemistry in boreal regions of Europe - BIPHOREP*
 European Commission; Air Pollution research report No 70, 158 p
- Lindfors, V., J. Rinne and T. Laurila** [1999]: Upscaling the BIPHOREP Results – Regional Biogenic VOC Emissions in the European Boreal Zone
 in: *Laurila, T. and V. Lindfors: Biogenic VOC emissions and photochemistry in boreal regions of Europe - BIPHOREP*
 European Commission; Air Pollution research report No 70, 158 p
- Lindroth, A.** [2002]: RE CAB: Description of the study regions - Uppland (Sweden)
RE CAB 2nd annual scientific report, unpublished manuscript, 55-58
- Lindroth, A. et al.** [1998]: Long-term measurements of boreal forest carbon balance reveal large temperature sensitivity
Global Change Biology (4), 443-450

- Lloyd, C.R.** [1995]: The Effect of Heterogeneous Terrain on Micrometeorological Flux Measurements - a Case-Study from Hapex-Sahel
Agricultural and Forest Meteorology (3-4), 209-216
- Lloyd, J. et al.** [2002]: Seasonal and annual variations in the photosynthetic productivity and carbon balance of a central Siberian pine forest
Tellus Series B-Chemical and Physical Meteorology (5), 590-610
- Lloyd, J. et al.** [2002]: A trace-gas climatology above Zotino, central Siberia
Tellus Series B-Chemical and Physical Meteorology (5), 749-767
- Lloyd, J. et al.** [2001]: Vertical profiles, boundary layer budgets, and regional flux estimates for CO₂ and its ¹³C/¹²C ratio and for water vapour above a forest/bog mosaic in central Siberia
Global Biogeochemical Cycles (2), 267-284
- Lloyd, J.** [1999]: Current perspectives on the terrestrial carbon cycle
Tellus Series B-Chemical and Physical Meteorology (2), 336-342
- Lloyd, J. et al.** [1996]: Vegetation effects on the isotopic composition of atmospheric CO₂ at local and regional scales: Theoretical aspects and a comparison between rain forest in Amazonia and a boreal forest in Siberia
Australian Journal of Plant Physiology (3), 371-399
- Lloyd, J. and G.D. Farquhar** [1994]: C¹³ Discrimination During CO₂ Assimilation by the Terrestrial Biosphere
Oecologia (3-4), 201-215
- Lloyd, J. and J.A. Taylor** [1994]: On the Temperature-Dependence of Soil Respiration
Functional Ecology (3), 315-323
- Logan, J.A. et al.** [1981]: Tropospheric Chemistry - a Global Perspective
Journal of Geophysical Research-Oceans and Atmospheres (NC8), 7210-7254
- Logan, J.A. et al.** [1978]: Global Budgets for Carbon-Monoxide and Nitrogen-Oxides
Transactions-American Geophysical Union (12), 1076-1076
- Mahrt, L.** [1997]: Flux Sampling Errors for Aircraft and Towers.
Journal of Atmospheric and Oceanic Technology (15), 416-429
- Maiss, M. et al.** [1996]: Sulfur hexafluoride - A powerful new atmospheric tracer
Atmospheric Environment (10-11), 1621-1629
- Maiss, M. and I. Levin** [1994]: Global Increase of SF₆ Observed in the Atmosphere
Geophysical Research Letters (7), 569-572
- Makar, P.A. et al.** [1999]: Chemical processing of biogenic hydrocarbons within and above a temperate deciduous forest
Journal of Geophysical Research-Atmospheres (D3), 3581-3603
- Makar, P.A. et al.** [2003]: Speciation of volatile organic compound emissions for regional air quality modeling of particulate matter and ozone
Journal of Geophysical Research-Atmospheres (D2), art. no.-4041
- Marik, T. and I. Levin** [1996]: A new tracer experiment to estimate the methane emissions from a dairy cow shed using sulfur hexafluoride (SF₆)
Global Biogeochemical Cycles (3), 413-418

- Masarie, K.A. et al.** [2001]: NOAA/CSIRO Flask Air Intercomparison Experiment: A strategy for directly assessing consistency among atmospheric measurements made by independent laboratories
Journal of Geophysical Research-Atmospheres (D17), 20445-20464
- Matson, P.A. and R.C. Harriss** [1988]: Prospects for Aircraft-Based Gas-Exchange Measurements in Ecosystem Studies
Ecology (5), 1318-1325
- McGuire, A.D. et al.** [2001]: Carbon balance of the terrestrial biosphere in the twentieth century: Analyses of CO₂, climate and land use effects with four process-based ecosystem models
Global Biogeochemical Cycles (1), 183-206
- Meijer, H.A.J. et al.** [1996]: Isotopic Characterisation of Anthropogenic CO₂ Emissions Using Isotopic and Radiocarbon Analysis
Phys. Chem. Earth (5-6), 483-487
- Menut, L.** [2003]: Adjoint modeling for atmospheric pollution process sensitivity at regional scale
Journal of Geophysical Research-Atmospheres (D17), art. no.-8562
- Miller, J.B. et al.** [2003]: The atmospheric signal of terrestrial carbon isotopic discrimination and its implication for partitioning carbon fluxes
Tellus Series B-Chemical and Physical Meteorology (2), 197-206
- Miller, J.B. and P.P. Tans** [2003]: Calculating isotopic fractionation from atmospheric measurements at various scales
Tellus Series B-Chemical and Physical Meteorology (2), 207-214
- Miller, J.B. et al.** [1999]: Measurement of O¹⁸/O¹⁶ in the soil-atmosphere CO₂ flux
Global Biogeochemical Cycles (3), 761-774
- Miyoshi, A., S. Hatakeyama and N. Washida** [1994]: OH radical-initiated photooxidation of isoprene: An estimate of global CO production
Journal of Geophysical Research Vol.99 (D9), 18779-18787
- Moxley, J.M. and J.N. Cape** [1997]: Depletion of carbon monoxide from the nocturnal boundary layer
Atmospheric Environment (8), 1147-1155
- Mund, M.** [2004]: Carbon budgets of European beech forests (*Fagus sylvatica*) under different silvicultural management.
Georg-August-Universität Göttingen, 198p, PhD-Thesis
- Munger, J.W. et al.** [1998]: Regional budgets for nitrogen oxides from continental sources: Variations of rates for oxidation and deposition with season and distance from source regions
Journal of Geophysical Research-Atmospheres (D7), 8355-8368
- Muschinski, A. and C. Wode** [1998]: First in situ evidence for coexisting submeter temperature and humidity sheets in the lower free troposphere
Journal of the Atmospheric Science (18), 2893-2906
- Nakazawa, T. et al.** [1997]: Aircraft measurements of the concentrations of CO₂, CH₄, N₂O, and CO and the carbon and oxygen isotopic ratios of CO₂ in the troposphere over Russia
Journal of Geophysical Research-Atmospheres (D3), 3843-3859

- Noilhan, J. et al.** [1997]: Defining area-average parameters in meteorological models for land surfaces with mesoscale heterogeneity
Journal of Hydrology (3-4), 302-316
- Novelli, P.C. et al.** [1999]: Molecular hydrogen in the troposphere:
 Global distribution and budget
Journal of Geophysical Research-Atmospheres (D23), 30427-30444
- Novelli, P.C. et al.** [1998]: Distributions and recent changes of carbon monoxide
 in the lower troposphere
Journal of Geophysical Research-Atmospheres (D15), 19015-19033
- Novelli, P.C. et al.** [1998]: An internally consistent set of globally distributed atmospheric
 carbon monoxide mixing ratios developed using results from an intercomparison of
 measurements
Journal of Geophysical Research-Atmospheres (D15), 19285-19293
- Novelli, P.C. et al.** [1992]: Mixing Ratios of Carbon-Monoxide in the Troposphere
Journal of Geophysical Research-Atmospheres (D18), 20731-20750
- Oberlander, E.A. et al.** [2002]: Trace gas measurements along the Trans-Siberian
 railroad: The TROICA 5 expedition
Journal of Geophysical Research-Atmospheres (D14), art. no.-4206
- Ogee, J. et al.** [2003]: Partitioning net ecosystem carbon exchange into net assimilation
 and respiration using (CO₂)-C¹³ measurements: A cost-effective sampling strategy
Global Biogeochemical Cycles (2), art. no.-1070
- Ogunjemiyo, S. et al.** [1997]: Analysis of flux maps versus surface characteristics from
 Twin Otter grid flights in BOREAS 1994
Journal of Geophysical Research-Atmospheres (D24), 29135-29145
- O'Leary, M.H.** [1995]: Environmental Effects on Carbon Isotope Fractionation
 in Terrestrial Plants
 in: *E. Wada et al.: Stable Isotopes in the Biosphere*
 Kyoto University Press, 78-91
- Pataki, D.E. et al.** [2003]: The application and interpretation of Keeling plots in terrestrial
 carbon cycle research
Global Biogeochemical Cycles (1), art. no.-1022
- Paulson, S.E. and J.H. Seinfeld** [1992]: Development and Evaluation of a Photooxidation
 Mechanism for Isoprene
Journal of Geophysical Research Vol.97 (D18), 20703-20715
- Pérez-Landa, G. et al.** [2002]: A study of the dispersion of an elevated plume on complex
 terrain under summer conditions
5th Symposium on Boundary Layers and Turbulence Wageningen,
The Netherlands, 346-349
- Petron, G. et al.** [2002]: Inverse modeling of carbon monoxide surface emissions using
 Climate Monitoring and Diagnostics Laboratory network observations
Journal of Geophysical Research-Atmospheres (D24), art. no.-4761
- Peylin, P. et al.** [2002]: Influence of transport uncertainty on annual mean and seasonal
 inversions of atmospheric CO₂ data
Journal of Geophysical Research-Atmospheres (D19), art. no.-4385
- Peylin, P. et al.** [2001]: Inverse modeling of atmospheric carbon dioxide fluxes - Response
Science (5541), U1-U2

- Peylin, P. et al.** [1999]: A 3-dimensional study of delta O¹⁸ in atmospheric CO₂: contribution of different land ecosystems
Tellus Series B-Chemical and Physical Meteorology (3), 642-667
- Potosnak, M.J. et al.** [1999]: Influence of biotic exchange and combustion sources on atmospheric CO₂ concentrations in New England from observations at a forest flux tower
Journal of Geophysical Research-Atmospheres (D8), 9561-9569
- Prentice, I.C. et al.** [2000]: The carbon balance of the terrestrial biosphere: Ecosystem models and atmospheric observations
Ecological Applications (6), 1553-1573
- Ramonet, M. et al.** [2002]: Three years of aircraft-based trace gas measurements over the Fyodorovskoye southern taiga forest, 300 km north-west of Moscow
Tellus Series B-Chemical and Physical Meteorology (5), 713-734
- Ramonet, M. et al.** [2001]: LSCE/RAMCES-Test: Using Mg(ClO₄)₂ for airborne air sampling (November 2001)
Personal communication and unpublished report, 5p
- Randerson, J.T. et al.** [2002]: Carbon isotope discrimination of arctic and boreal biomes inferred from remote atmospheric measurements and a biosphere-atmosphere model
Global Biogeochemical Cycles (3), art. no.-1028
- Randerson, J.T. et al.** [2002]: A possible global covariance between terrestrial gross primary production and C¹³ discrimination: Consequences for the atmospheric C¹³ budget and its response to ENSO
Global Biogeochemical Cycles (4), art. no.-1136
- Randerson, J.T. et al.** [1997]: The contribution of terrestrial sources and sinks to trends in the seasonal cycle of atmospheric carbon dioxide
Global Biogeochemical Cycles (4), 535-560
- Rannik, U. et al.** [2000]: Footprint analysis for measurements over a heterogeneous forest
Boundary-Layer Meteorology (1), 137-166
- Raupach, M.R.** [1998]: Influences of local feedbacks on land-air exchanges of energy and carbon
Global Change Biology (5), 477-494
- Raupach, M.R. and J.J. Finnigan** [1997]: The influence of topography on meteorological variables and surface-atmosphere interactions
Journal of Hydrology (3-4), 182-213
- Raupach, M.R. et al.** [1996]: Coherent eddies and turbulence in vegetation canopies: The mixing-layer analogy
Boundary-Layer Meteorology (3-4), 351-382
- Raupach, M.R.** [1995]: Vegetation Atmosphere Interaction and Surface Conductance at Leaf, Canopy and Regional Scales
Agricultural and Forest Meteorology (3-4), 151-179
- Raupach, M.R. et al.** [1993]: Inferring regionally averaged surface fluxes of conserved scalars from convective boundary layer budgets
unpublished manuscript, 41p

Raupach, M.R., O.T. Denmead and F.X. Dunin [1992]: Challenges in Linking Atmospheric CO₂ Concentrations to Fluxes at Local and Regional Scales
Australian Journal of Plant Physiology 697-716

Rayner, P.J. and R.M. Law [1999]: The interannual variability of the global carbon cycle
Tellus Series B-Chemical and Physical Meteorology (2), 210-212

Rayner, P.J. et al. [1999]: Reconstructing the recent carbon cycle from atmospheric CO₂, delta C¹³ and O₂/N₂ observations
Tellus Series B-Chemical and Physical Meteorology (2), 213-232

Rayner, P.J. et al. [1996]: Optimizing the CO₂ observing network for constraining sources and sinks
Tellus Series B-Chemical and Physical Meteorology (4), 433-444

Reithmaier, L. [2003]: Application of remote sensing methods for micrometeorological site evaluation
Department for Micrometeorology,
University of Bayreuth, 154p, Diploma-Thesis

Roche, C. [1999]: Interactions biosphère-atmosphère aux échelles locales et composition isotopique (¹³C, ¹⁸O) du CO₂ atmosphérique: application à la Forêt Landaise
Institute Pierre et Marie Curie, Univ. Paris, 202p, PhD-Thesis

Röckmann, T. et al. [2003]: The isotopic fingerprint of the pre-industrial and the anthropogenic N₂O source
Atmospheric Chemistry and Physics 315-323

Röckmann, T. et al. [2002]: Using C¹⁴, C¹³, O¹⁸ and O¹⁷ isotopic variations to provide insights into the high northern latitude surface CO inventory
Atmospheric Chemistry and Physics 147-159

Röckmann, T. [1998]: Measurement and Interpretation of ¹³C, ¹⁴C, ¹⁷O and ¹⁸O Variations in Atmospheric Carbon Monoxide
Naturwissenschaftlich-Mathematische Gesamtfakultät,
Ruprecht-Karls-Universität Heidelberg, 151p, PhD-Thesis

Röckmann, T. et al. [1998]: Mass-independent oxygen isotope fractionation in atmospheric CO as a result of the reaction CO+OH
Science (5376), 544-546

Röckmann, T. and C.A.M. Brenninkmeijer [1997]: CO and CO₂ isotopic composition in Spitsbergen during the 1995 ARCTOC campaign
Tellus Series B-Chemical and Physical Meteorology (5), 455-465

Rödenbeck, C. et al. [2003]: Time-dependent atmospheric CO₂ inversions based on interannually varying tracer transport
Tellus Series B-Chemical and Physical Meteorology (2), 488-497

Ruimy, A. et al. [1996]: The use of CO₂ flux measurements in models of the global terrestrial carbon budget
Global Change Biology (3), 287-296

Rundel, P.W. et al. [1989]: Stable isotopes in ecological research
Springer New York, XV, 525p

- Salvador, R. et al.** [1997]: Mesoscale modelling of atmospheric processes over the western Mediterranean area during summer
International Journal of Environment and Pollution (3-6), 513-529
- Sass, R.L. et al.** [1999]: Exchange of methane from rice fields: National, regional and global budgets
Journal of Geophysical Research-Atmospheres (D21), 26943-26951
- Samuelsson, P. and M. Tjernstrom** [1999]: Airborne flux measurements in NOPEX: comparison with footprint estimated surface heat fluxes.
Agricultural and Forest Meteorology (98-99), 205-225
- Schimel, D.S. et al.** [2001]: Recent patterns and mechanisms of carbon exchange by terrestrial ecosystems
Nature (6860), 169-172
- Schmid, H.P.** [2002]: Footprint modeling for vegetation atmosphere exchange studies: a review and perspective
Agricultural and Forest Meteorology (1-4), 159-183
- Schmid, H.P. and C.R. Lloyd** [1999]: Spatial representativeness and the location bias of flux footprints over inhomogeneous areas
Agricultural and Forest Meteorology (3), 195-209
- Schmidt, H.-L. et al.** [1995]: Non-Statistical Isotope Distribution in Natural Compounds: Mirror of their Biosynthesis and Key for their Origin Assignment
 in: *E. Wada et al.: Stable Isotopes in the Biosphere*
 Kyoto University Press, 17-35
- Schmidt, J. et al.** [1988]: Emission of Nitrous-Oxide from Temperate Forest Soils into the Atmosphere
Journal of Atmospheric Chemistry (1-2), 95-115
- Schmidt, M. et al.** [2001]: Western European N₂O emissions: A top-down approach based on atmospheric observations
Journal of Geophysical Research-Atmospheres (D6), 5507-5516
- Schmidt, M. et al.** [1996]: Carbon dioxide and methane in continental Europe: A climatology and (222)Radon-based emission estimates
Tellus Series B-Chemical and Physical Meteorology (4), 457-473
- Schmitgen, S. et al.** [2004]: Carbon dioxide uptake of a forested region in southwest France derived from airborne CO₂ and CO measurements in a quasi-Lagrangian experiment
Journal of Geophysical Research Vol.109 (D14), D14302
- Schmitt, R. et al.** [1988]: Effects of Long-Range Transport on Atmospheric Trace Constituents at the Baseline Station Tenerife (Canary-Islands)
Journal of Atmospheric Chemistry (4), 335-351
- Scholze, M. et al.** [2003]: Climate and interannual variability of the atmosphere-biosphere (CO₂-C¹³) flux
Geophysical Research Letters (2), art. no.-1097
- Schulte-Bispig, H. et al.** [2003]: Nitrous oxide emission inventory of German forest soils
Journal of Geophysical Research-Atmospheres (D4), art. no.-4132

- Schulze, E.-D. et al.** [2002]: The long way from Kyoto to Marrakesh: Implications of the Kyoto Protocol negotiations for global ecology
Global Change Biology (6), 505-518
- Schulze, E.-D. et al.** [2001]: Global biogeochemical cycles in the climate system
 Academic Press San Diego, 42 S., [48] Bl., S. 43-350
- Schulze, E.-D. et al.** [1999]: Productivity of forests in the Eurosiberian boreal region and their potential to act as a carbon sink - a synthesis
Global Change Biology (6), 703-722
- Schutz, H. et al.** [1990]: Influence of Soil-Temperature on Methane Emission from Rice Paddy Fields
Biogeochemistry (2), 77-95
- Seiler, W.** [1987]: CH₄ Emission from Natural and Anthropogenic Sources
Abstracts of Papers of the American Chemical Society 82-GEOC
- Seiler, W. et al.** [1984]: Methane Emission from Rice Paddies
Journal of Atmospheric Chemistry (3), 241-268
- Seiler, W. and R. Conrad** [1982]: Global Carbon-Monoxide Fluxes - Inappropriate Measurement Procedures
Science (4547), 761-761
- Seiler, W. et al.** [1978]: Influence of Plants on Atmospheric Carbon-Monoxide and Dinitrogen Oxide
Pure and Applied Geophysics (2-3), 439-451
- Shibistova, O. et al.** [2002]: Seasonal and spatial variability in soil CO₂ efflux rates for a central Siberian Pinus sylvestris forest
Tellus Series B-Chemical and Physical Meteorology (5), 552-567
- Shuttleworth, W.J.** [1988]: Macrohydrology - The new challenge for process hydrology
Journal of Hydrology 31-56
- Shuttleworth, W.J.** [1988]: Corrections for the effect of background concentration change and sensor shift in real-time eddy-correlation systems
Boundary Layer Meteorology (3), 167-180
- Sidorov, K. et al.** [2002]: Seasonal variability of greenhouse gases in the lower troposphere above the eastern European taiga (Syktyvkar, Russia)
Tellus Series B-Chemical and Physical Meteorology (5), 735-748
- Singh, S.** [2000]: Trace gas emissions and plants
 Kluwer Academic Publishers, XVI, 328p
- Slanina, S.** [1997]: Biosphere-atmosphere exchange of pollutants and trace substances
 Springer Berlin, XXV, 528p
- Smith, K.A. et al.** [2000]: Oxidation of atmospheric methane in Northern European soils, comparison with other ecosystems, and uncertainties in the global terrestrial sink
Global Change Biology (7), 791-803
- Smolarkiewicz, P.K.** [1983]: A Simple Positive Definite Advection Scheme with Small Implicit Diffusion
Monthly Weather Review (3), 479-486

- Soee, A.** [2003]: The SPA¹³CE Experiment: Ground Investigations
personal communication
- Soegaard, H. et al.** [2003]: Carbon dioxide exchange over agricultural landscape using eddy correlation and footprint modelling
Agricultural and Forest Meteorology (3-4), 153-173
- Soegaard, H. et al.** [2000]: Trace gas exchange in a high-arctic valley
 3. Integrating and scaling CO₂ fluxes from canopy to landscape using flux data, footprint modeling, and remote sensing
Global Biogeochemical Cycles (3), 725-744
- Soegaard, H.** [1999]: Fluxes of carbon dioxide, water vapour and sensible heat in a boreal agricultural area of Sweden - scaled from canopy to landscape level
Agricultural and Forest Meteorology 463-478
- Sogachev, A. et al.** [2002]: A simple three-dimensional canopy - planetary boundary layer simulation model for scalar concentrations and fluxes
Tellus Series B-Chemical and Physical Meteorology (5), 784-819
- Spivakovsky, C.M. et al.** [1990]: Tropospheric OH in a 3-Dimensional Chemical Tracer Model - an Assessment Based on Observations of CH₃CCl₃
Journal of Geophysical Research-Atmospheres (D11), 18441-18471
- Steffen, W. et al.** [1998]: The terrestrial carbon cycle: Implications for the Kyoto Protocol
Science (5368), 1393-1394
- Stephens, B.B. et al.** [2000]: The CO₂ Budget and Rectification Airborne Study:
 Strategies for Measuring Rectifiers and Regional Fluxes
 in: *P. Kasibhatla et al.: Inverse Methods in Global Biogeochemical Cycles*
 Washington AGU, 311-324
- Sternberg, L.S.L.** [1989]: Oxygen and hydrogen isotope ratios in Plant Cellulose:
 Mechanisms and Applications
 in: *P.W. Rundel et al.: Stable isotopes in ecological research*
 Springer New York, 124-141
- Stohl, A. et al.** [2003]: Rapid intercontinental air pollution transport associated with a meteorological bomb
Atmospheric Chemistry and Physics 969-985
- Stohl, A. et al.** [2002]: On the pathways and timescales of intercontinental air pollution transport
Journal of Geophysical Research-Atmospheres (D23), art. no.-4684
- Stohl, A. et al.** [2002]: A replacement for simple back trajectory calculations in the interpretation of atmospheric trace substance measurements
Atmospheric Environment (29), 4635-4648
- Stull, R.B.** [2001]: An introduction to boundary layer meteorology
 Kluwer, reprint Dordrecht, XII, 670p
- Styles, J.M. et al.** [2002]: Estimates of regional surface carbon dioxide exchange and carbon and oxygen isotope discrimination during photosynthesis from concentration profiles in the atmospheric boundary layer
Tellus Series B-Chemical and Physical Meteorology (5), 768-783

- Sugawara, S. et al.** [1996]: Aircraft measurements of the stable carbon isotopic ratio of atmospheric methane over Siberia
Global Biogeochemical Cycles (2), 223-231
- Tans, P.P. and D.W.R. Wallace** [1999]: Carbon cycle research after Kyoto
Tellus Series B-Chemical and Physical Meteorology (2), 562-571
- Tans, P.P.** [1997]: A note on isotopic ratios and the global atmospheric methane budget
Global Biogeochemical Cycles (1), 77-81
- Tans, P.P. et al.** [1990]: Error-Estimates of Background Atmospheric CO₂ Patterns from Weekly Flask Samples
Journal of Geophysical Research-Atmospheres (D9), 14063-14070
- Tans, P.P. et al.** [1989]: Latitudinal Distribution of the Sources and Sinks of Atmospheric Carbon-Dioxide Derived from Surface Observations and an Atmospheric Transport Model
Journal of Geophysical Research-Atmospheres (D4), 5151-5172
- Tans, P.P.** [1981]: ¹³C/¹²C of industrial CO₂
in: *B. Bolin Carbon Cycle Modelling* New York John Wiley, 127-129
- Thom, M. et al.** [1993]: The Regional Budget of Atmospheric Methane of a Highly Populated Area
Chemosphere (1-4), 143-160
- Trolier, M. et al.** [1996]: Monitoring the isotopic composition of atmospheric CO₂: Measurements from the NOAA Global Air Sampling Network
Journal of Geophysical Research-Atmospheres (D20), 25897-25916
- Trudinger, C.M. et al.** [1999]: Long-term variability in the global carbon cycle inferred from a high-precision CO₂ and delta C¹³ ice-core record
Tellus Series B-Chemical and Physical Meteorology (2), 233-248
- Trumbore, S.E.** [1999]: Role of isotopes and tracers in scaling trace gas fluxes
in: *A. F. Bouwman Approaches to scaling of trace gas fluxes in ecosystems* Elsevier Science, 259-274
- Tyler, S.C. et al.** [1997]: Methane oxidation and pathways of production in a Texas paddy field deduced from measurements of flux, delta C¹³, and delta D of CH₄
Global Biogeochemical Cycles (3), 323-348
- Valentini, R. et al.** [2000]: Carbon and water exchanges of two contrasting central Siberia landscape types: regenerating forest and bog
Functional Ecology (1), 87-96
- Valentini, R. et al.** [2000]: Respiration as the main determinant of carbon balance in European forests
Nature (6780), 861-865
- Valentini, R. et al.** [1996]: Seasonal net carbon dioxide exchange of a beech forest with the atmosphere
Global Change Biology (3), 199-207
- Valentini, R. et al.** [1995]: Ecosystem Gas-Exchange in a California Grassland - Seasonal Patterns and Implications for Scaling
Ecology (6), 1940-1952

- Valentini, R. et al.** [1992]: Hydrogen and Carbon Isotope Ratios of Selected Species of a Mediterranean Macchia Ecosystem
Functional Ecology (6), 627-631
- Valentini, R. et al.** [1991]: An Experimental Test of the Eddy-Correlation Technique over a Mediterranean Macchia Canopy
Plant Cell and Environment (9), 987-994
- Vay, S.A. et al.** [1999]: Airborne observations of the tropospheric CO₂ distribution and its controlling factors over the South Pacific Basin
Journal of Geophysical Research-Atmospheres (D5), 5663-5676
- Vilà-Guerau de Arellano, J. et al.** [2004]: The entrainment process of carbon dioxide in the atmospheric boundary layer
submitted to: *Journal of Geophysical Research-Atmospheres* (D5), 5663-5676
- Vöglin, R.** [1992]: Die tageszeitliche Entwicklung der konvektiven Grenzschicht über hügeligem Gelände
Sonderforschungsbereich 210 'Strömungsmechanische Bemessungsgrundlagen für Bauwerke', Universität Karlsruhe, PhD-Thesis
- Walter, B.P. et al.** [2001]: Modeling modern methane emissions from natural wetlands
1. Model description and results
Journal of Geophysical Research-Atmospheres (D24), 34189-34206
- Walter, B.P. et al.** [2001]: Modeling modern methane emissions from natural wetlands
2. Interannual variations 1982-1993
Journal of Geophysical Research-Atmospheres (D24), 34207-34219
- Walter, B.P. and M. Heimann** [2000]: A process-based, climate-sensitive model to derive methane emissions from natural wetlands: Application to five wetland sites, sensitivity to model parameters, and climate
Global Biogeochemical Cycles (3), 745-765
- Warneck, P.** [2000]: Chemistry of the natural atmosphere
Academic Press, 2nd edition, San Diego, Calif., XVII, 927p
- Werner, R.A. et al.** [2001]: Extraction of CO₂ from air samples for isotopic analysis and limits to ultra high precision delta O¹⁸ determination in CO₂ gas
Rapid Communications in Mass Spectrometry (22), 2152-2167
- Werner, R.A. and W.A. Brand** [2001]: Referencing strategies and techniques in stable isotope ratio analysis
Rapid Communications in Mass Spectrometry (7), 501-519
- Wilson, J.D. and B.L. Sawford** [1996]: Review of Lagrangian stochastic models for trajectories in the turbulent atmosphere
Boundary-Layer Meteorology (1-2), 191-210
- Wingenter, O.W. et al.** [1996]: Hydrocarbon and halocarbon measurements as photochemical and dynamical indicators of atmospheric hydroxyl, atomic chlorine and vertical mixing obtained during Lagrangian flights
Journal of Geophysical Research-Atmospheres (D2), 4331-4340
- Winston, G.C. et al.** [1997]: Winter CO₂ fluxes in a boreal forest
Journal of Geophysical Research-Atmospheres (D24), 28795-28804

Winter, R. et al. [1998]: Geo-Satellitenbild-Atlas Deutschland
RV-Verlag München, 239p

Wittenberg, U. et al. [1998]: On the influence of biomass burning on the seasonal CO₂ signal as observed at monitoring stations
Global Biogeochemical Cycles (3), 531-544

Wotawa, G. et al. [2001]: Inter-annual variability of summertime CO concentrations in the Northern Hemisphere explained by boreal forest fires in North America and Russia
Geophysical Research Letters (24), 4575-4578

Yakir, D. and L.D.L. Sternberg [2000]: The use of stable isotopes to study ecosystem gas exchange
Oecologia (3), 297-311

Yakir, D. [1998]: Oxygen-18 of leaf water: a crossroad for plant-associated isotopic signals
in: *H. Griffiths Stable Isotopes - integration of biological, ecological and geochemical processes* BIOS Scientific Publishers, 147-168

Yakir, D. and X.F. Wang [1996]: Fluxes of CO₂ and water between terrestrial vegetation and the atmosphere estimated from isotope measurements
Nature (6574), 515-517

Yakir, D. et al. [1994]: Isotopic Heterogeneity of Water in Transpiring Leaves - Identification of the Component that Controls the Delta ¹⁸O of Atmospheric O₂ and CO₂
Plant Cell and Environment (1), 73-80

Yakir, D. [1992]: Potential Use of O¹⁸ and C¹³ in Cellulose for Estimating the Impact of Terrestrial Photosynthesis on Atmospheric CO₂
Photosynthesis Research (1), 108-108

Yakir, D. et al. [1989]: Isotopic Inhomogeneity of Leaf Water - Evidence and Implications for the Use of Isotopic Signals Transduced by Plants
Geochimica Et Cosmochimica Acta (10), 2769-2773

Yang, P.C. et al. [1999]: Spatial and temporal variability of CO₂ concentration and flux in a boreal aspen forest
Journal of Geophysical Research-Atmospheres (D22), 27653-27661

Zenger, A. [1998]: Atmosphärische Ausbreitungsmodellierung
Springer Berlin, IX, 159p

Zondervan, A. and H.A.J. Meijer [1996]: Isotopic characterisation of CO₂ sources during regional pollution events using isotopic and radiocarbon analysis
Tellus Series B-Chemical and Physical Meteorology (4), 601-612

INTERNET ADDRESSES

CARBIS data base (RECAB)

<http://www.hyd.uu.se/carbis/recab/default.asp>

CarboEurope Cluster

<http://www.bgc-jena.mpg.de/public/carboeur/index.html>

Climate Monitoring and Diagnostics Laboratory

http://www.cmdl.noaa.gov/ccgg/gallery/index.php?pageType=folder&currDir=/Data_Figures

Deutscher Wetterdienst (Klimaarchiv)

<http://www.dwd.de/de/WundK/index.htm>

Deutsches Fernerkundungsdatenzentrum DFD

<http://www.caf.dlr.de/caf/institut/dfd/>

Dundee Satellite Receiving Station

<http://www.sat.dundee.ac.uk/auth.html>

EOS Data Gateway (Landsat ETM+)

<http://edcimswww.cr.usgs.gov/pub/imswelcome/>

FLUXNET Worldwide CO₂ flux measurements

<http://www.daac.ornl.gov/FLUXNET/fluxnet.html>

Global Fire Monitoring Center (GFMC)

<http://www.fire.uni-freiburg.de/>

GLOBAL WEB FIRE MAPS

<http://maps.geog.umd.edu/maps.asp>

Intergovernmental Panel on Climate Change (IPCC)

<http://www.ipcc.ch/>

MODIS Rapid Response System - Fire Monitoring Satellite

<http://rapidfire.sci.gsfc.nasa.gov/gallery/>

NASA Visible Earth (Image Directory)

<http://visibleearth.nasa.gov/>

National Climatic Data Centre (NCEP)

<http://www.ncdc.noaa.gov/oa/ncdc.html>

RECAB homepage

<http://www.biotheon.com/recab>

Umweltbundesamt

<http://www.umweltdaten.de/luft/nir-2002.pdf>

U.S. Greenhouse Gas Emissions Inventories

[http://yosemite.epa.gov/oar/globalwarming.nsf/UniqueKeyLookup/SHSU5BUM9T\\$/File/ghg_gwp.pdf](http://yosemite.epa.gov/oar/globalwarming.nsf/UniqueKeyLookup/SHSU5BUM9T$/File/ghg_gwp.pdf)

Wetterzentrale (Analysekarten)

<http://www.wetterzentrale.de/>

WMO World Data Centre for Greenhouse Gases

<http://gaw.kishou.go.jp/wdcgg.html>

10. ACKNOWLEDGEMENTS

At the ending of a study which emerged over a time period of more than three years thank owes to numerous people who contributed either way to the work.

First, I like to thank Prof. Dr. Martin Heimann. His suggestions and the valuable discussions, especially with respect to atmospheric processes and structural aspects, were inspiring and motivation for the work.

Likewise I am very thankful to Prof. Dr. Hartmut Graßl for his incitation, his cooperation and the unhesitant adaptation of an external PhD-student.

I have to thank Prof. Dr. Jon Lloyd, who had to assume the RECAB project and the supervision in the middle of the project. During this time I got a lot of responsibility, discretionary and the chance even for comprehensive studies and experiments.

Prof. Dr. Ernst-Detlef Schulze had taken over the supervision at interim. I am obliged for discussions about processes and interactions with respect to contributions from ecosystems.

For instructive discussions and for the stable isotope analyses of the flask samples I am grateful to Roland Werner, Michael Rothe and Willi Brand. Additional thanks I owe to Armin Jordan for the trace gas analyses and for his patient collaboration.

Christian Rödenbeck and Manuel Gloor sacrificed a lot of their time to introduce me into the basics of modelling. Christian also provided the adjoint transport model calculations. Thanks for the friendly cooperation.

A great experience was the SPA¹³CE experiment. Thanks to all participants and for the opportunity to be part in this inspiring and enjoyable project.

The Freiland group made the tower data from the Hainich available and assisted several times with additional instruments for the field campaigns.

I deserves thank to my colleagues from the REcab project. On behalf of all participants I acknowledge the project coordinator Ronald Hutjes, and I am grateful to Gorka Pérez-Landa for fruitful discussions about modelling and the provision of the dispersion modelling results and to Beniamino Gioli for the comparison data obtained by the Sky Arrow.

A particular mentioning applies to all colleagues, friends and pilots from Sweden, The Netherlands, Germany, Spain and Italy which tried to achieve the impractical and made the time in the field as pleasant as possible.

Thanks also to Roland von Glasow, who corrected the first draft and gave instructive comments in particular with respect to atmospheric chemistry.

Finally I owe special thanks to Waldemar Ziegler. During all campaigns he was the highly motivated and unfailing fellow who carried every burden without complaining and had to bear my companionship over several weeks under simplest field conditions. I pay my tribute.

The investigations of this study were performed at the Max-Planck Institut für Biogeochemie, Jena, as part of the REcab project (EVK2-CT-1999-00034), funded by the EU Commission under the 5th Framework Programme.

Summer Field Campaign

27 May – 27 June 2002



Summer Field Campaign

27 May – 27 June 2002

Flight profile samplings on 15 June above the Roccarespampani location and on 18 June at the mountain site near Orvinio

Sampling heights: 55, 105, 260, 760 and 2745 m above ground.

Sampling times: Morning flights taken place around 3:40 UTC, midday flights were executed around 13:30 UTC.

Aircraft: Morane Socata 894A, 180 HP. Single engine, propeller clockwise. Four seat low wing airplane. Flight speed during sampling procedure 75 knts (~140 km/h), climbing rate 1 m s^{-1} . Tube inlet mounted at left wing tip, approximately 15 cm beneath the profile bottom, facing downwards to the front

Ground reference samplings: 13 June ‘day time’ [15:30 UTC] and 14 June ‘night time’ [4:30 UTC] at the Roccarespampani site

20 June ‘day time’ [15:30 UTC] and 21 June ‘night time’ [5:30 UTC] above meadows close to the Abbey ruin near Orvinio

21 June ‘day time’ [15:30 UTC] and 22 June ‘night time’ [4:30 UTC] at the Orvinio mountain site located near the rim

Lazio Summer Experiment

27 May – 27 June 2002

To the west the study area is bordered by the Tyrrhenian Sea, the east margin is formed by ridges of the Apennine Mountains. Topography is mostly gentle rolling, but increasing in west-east direction up to 1200 m above MSL.

A stable high pressure cell dominated the weather conditions during the campaign. Caused by clear sky very high air temperatures were observed on all days, which were 5°C above the long year average for this period. Temperature maxima at the ground around noon of about 37°C were reached on most days. During morning hours wind was nearly calm, also in the afternoon wind speed did not exceed 3.5 m sec.⁻¹, mainly from southern and western directions. No precipitation was recorded through the time.

Vertical profile flights were performed at two different sites: above the deciduous forest of Roccarespampani, labelled ‘Tuscania’ (160 m above MSL) and above a mountain site called ‘Orvinio’, with grasslands and meadows surrounded by forests (850 m above MSL). Two flights were planned per day, with sampling at five levels. The uppermost level had to be defined at this great altitude, since an extended increasing of the CBL during day time was expected because of the strong thermal convection.

Additional air samples were collected during night and day time. Near surface measurements were carried out in the Roccarespampani forest, above the meadows of the mountain valley and close to the forested ridge.

Summer Field Campaign

27 May – 27 June 2002

- Title MODIS image of Italy from 25 March 2003 (NASA).
- Figure 1 Aerial photograph of Roccarespampani Forest and its surrounding from 2750 m above ground.
- Figure 2 Location of Roccarespampani reference site from low flight level.
- Figure 3 'Orvinio' mountain site. Central part of the bowl shaped valley from 300 m above ground.
- Figure 4 Photograph taken from the lowest sampling level during the morning flight at the 'Orvinio' location.
- Figure 5 Composite of the ground reference sites.
- Figure 6 Sensors for meteorological measurements mounted on the left wing of the aircraft.
- Figure 7 MODIS Satellite Images of Central Europe; 15 and 18 June 2002 (NASA).
- Figure 8 Fires detected globally by MODIS sensor between 4 and 11, and 11 and 18 June 2002
- Figure 9 Fires detected by MODIS sensor in Northern America between 4 and 18 June 2002



Figure 1 Aerial photograph of the Roccarespampani Forest and its surrounding. The ground reference location is marked by the yellow arrow. Picture taken from highest flight level, 2750 m above ground on 15 June 2002.



Figure 2 Roccarespampani forest, viewing south-west. The location of the ground reference site is marked by the yellow arrow.

Afternoon 15 June 2002



Figure 3 Aerial photograph of 'Orvinio' mountain site. In the foreground the ruin of the abbey. The ground reference site was located close by on the left meadow behind. Flight altitude approximately 300 m above ground, viewing north-west.

Picture: 18 June 2002



Figure 4 Morning sampling flight at the 'Orvinio' mountain site. Picture taken from the lowest flight level on 18 June 2002.



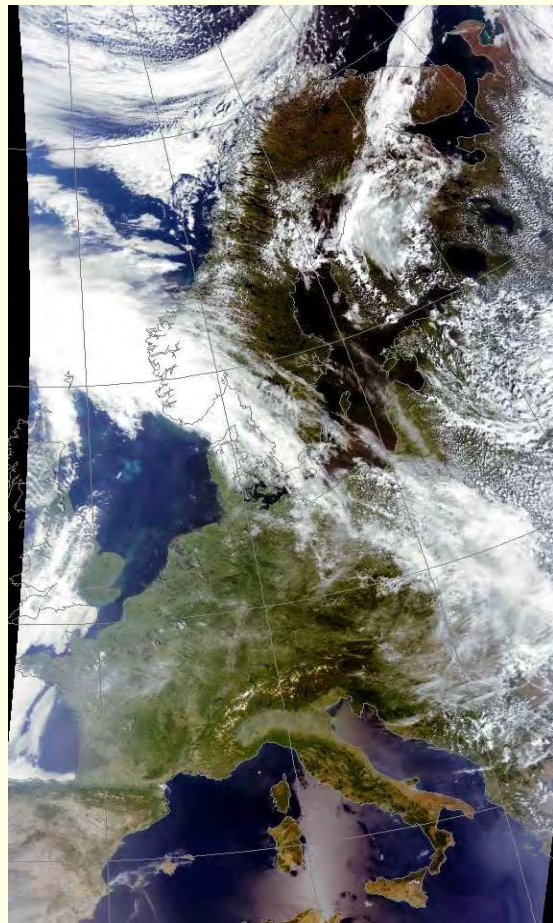
Figure 5 Ground reference sites: Mountain site 'Orvinio Valley' (top left), 'Orvinio Abbey' (right) and detail with sampling inlet at Roccarespampani (bottom left). Pictures: 14, 21 and 22 June 2002



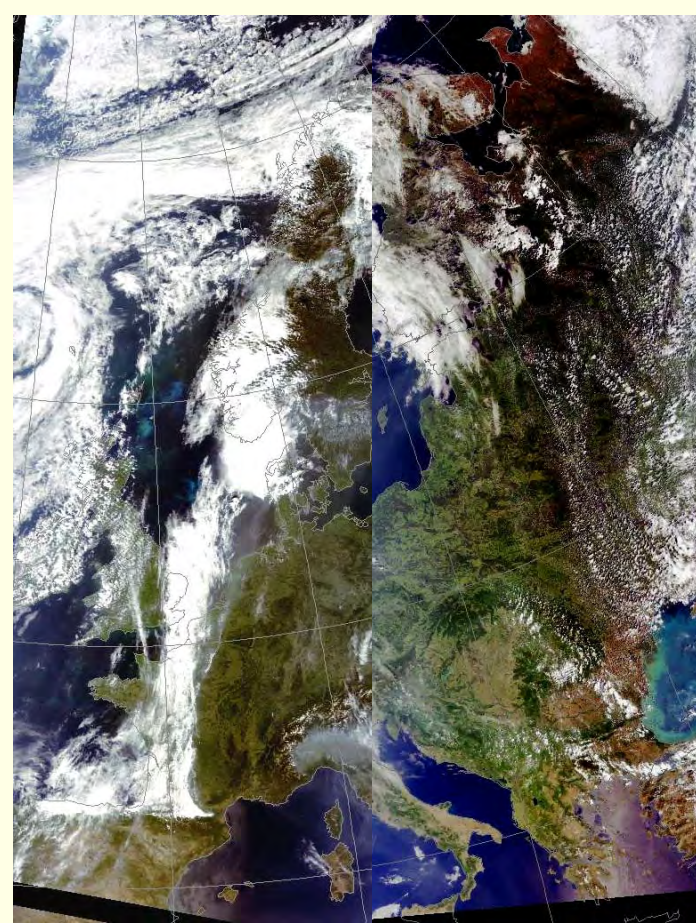
Figure 6 Probes of the online system for meteorological measurements mounted on the left wing.

Approaching the 'Orvinio' profile location for morning sampling.

Picture: 18 June 2002



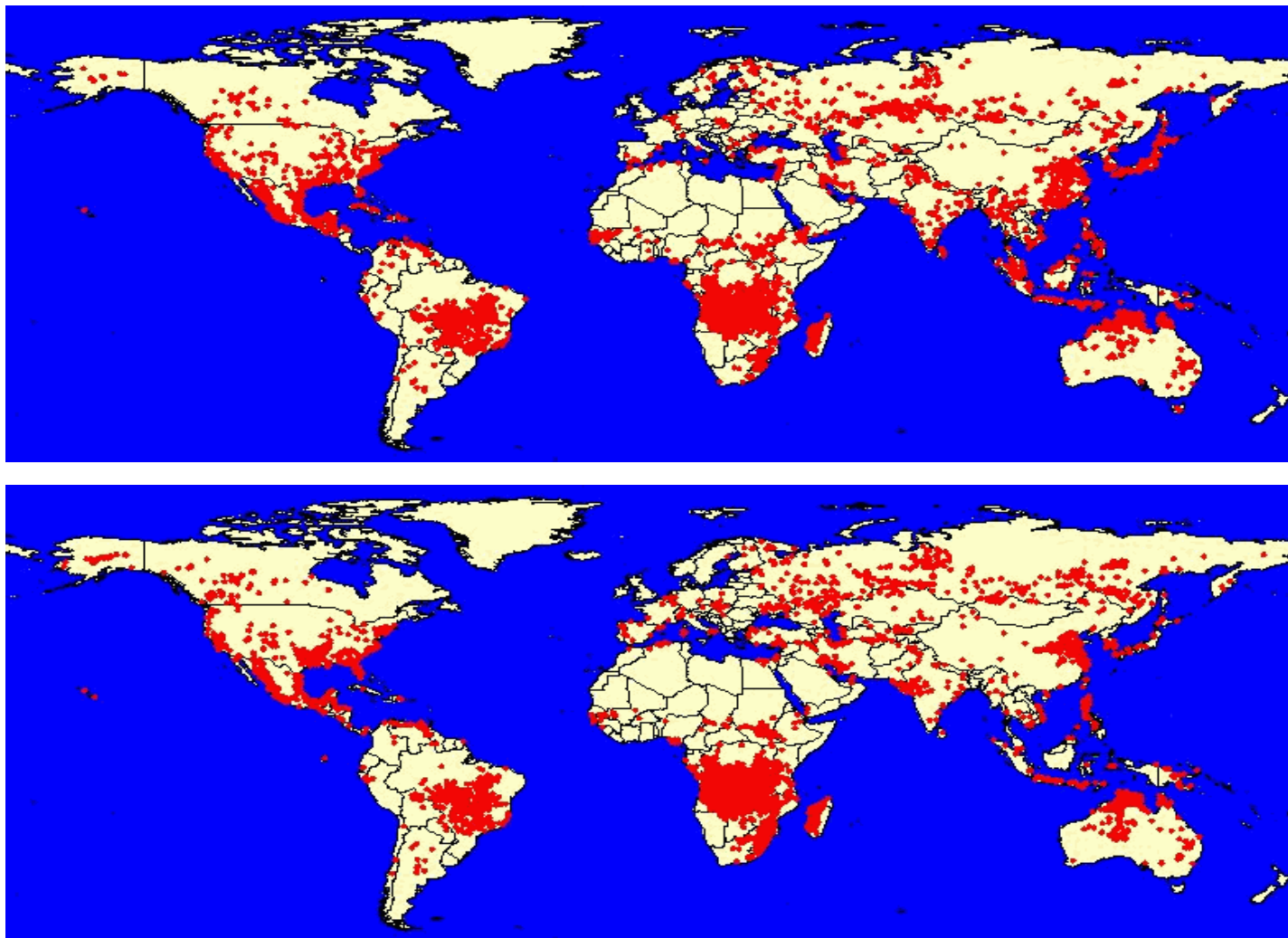
17 June 2002 10:20 UTC



18 June 2002 west 11:04 and east 9:25 UTC

Figure 7 MODIS Satellite Images(from Dundee Satellite Receiving Station:
right panel is a composite of two pictures from consecutive passes)

Satellite: Terra Sensor: MODIS
RGB composite image reprojected (RGB 1,4,3 composite)



upper panel: 4 – 11 June 2002

lower panel: 11 - 18 June 2002

Figure 8 Fires detected by the MODIS sensor between 4 and 18 June 2002
(http://maps.geog.umd.edu/GlobalFires_HTML)

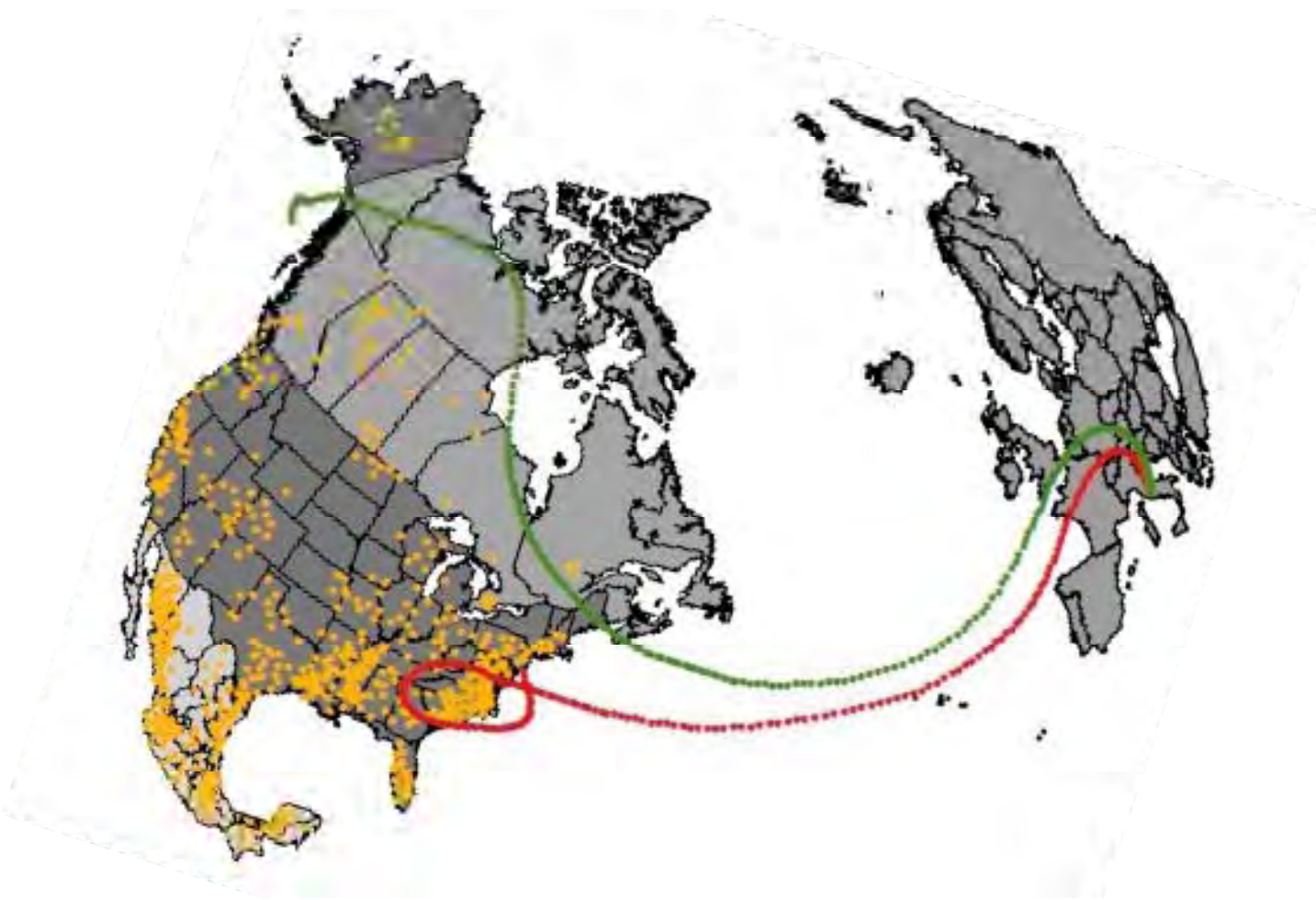


Figure 9 Fires detected by the MODIS sensor between 4 and 18 June 2002 in Northern America
(http://maps.geog.umd.edu/GlobalFires_HTML)

Back trajectories of air particles calculated from a receiving point at the 2750 m sampling level above the 'Orvinio' location on 17 June 2002 21:30 UTC (red) and on 18 June 2002 11:30 UTC (green)

Description of table parameters

date&time (GMT) - date and time the sampling procedure was completed in Greenwich Mean Time

flask code - marking of nameplates for each flask

site - location of the flight pattern, leg length ~2km

Orvi - flight track, mountain site north of the little village of Orvinio;
agricultural area, valley (bowl like)

Tusca - flight track east of Tuscania (Roccarespampani Fluxnet site), oak
forest, agricultural area

ground sampling location

Rocca - Roccarespampani Fluxnet site, oak forest: 42°24.0'N / 011°55.0'E,
178 m a. MSL

Orv-Abt - mountain site, valley bottom nearby ruin of Romanic abbey Santa
Maria del Piano, meadow: 42°08'N / 12°57'E, 682 m a. MSL

Orv-Val - mountain site, slope near the ridge, oak forest:
42°08'N / 12°53'E, 959 m a. MSL

alt (ft) - sampling height in feet above ground

init p. - internal flask pressure at the beginning of the analysis

Mixing ratios

Precision of the analyses

CH₄ [ppb] -	methan mixing ratio in ppb	1.3 ppb
CO₂ [ppm] -	carbon dioxide mixing ratio in ppm	0.08 ppm
N₂O [ppb] -	nitrous oxide mixing ratio in ppb	0.15 ppb
CO [ppb] -	carbon monoxide mixing ratio in ppb	1.0 ppb
H₂ [ppb] -	hydrogen mixing ratio in ppb	5.0 ppb
SF₆ [ppt] -	sulfur hexafluoride mixing ratioin ppt	0.08 ppt

Isotope Ratio

$$d[\$] = (R_{sa}/R_{ref} - 1) \cdot 1000 \quad R_{sa} \text{ and } R_{ref} \text{ are the sample and reference isotope ratios}$$

del ¹³C [\$] - ratio of the carbon 13 isotope and carbon 12 isotope due to the VPDB
isotope ratio scale

del ¹⁸O [\$] - ratio of the oxygen 18 isotope and oxygen 16 isotope due to the
VPDB (gas) isotope ratio scale

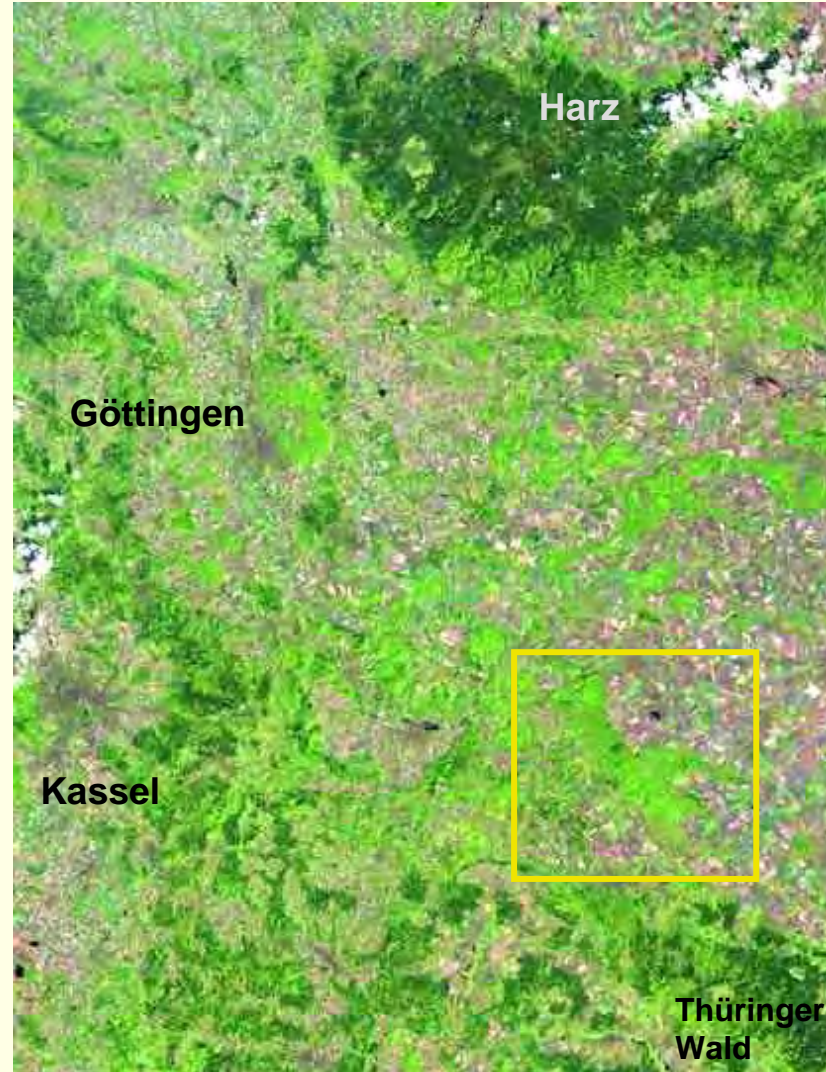
$$\text{Precision of the analyses} \quad {}^{13}\text{C} = 0.012 \$ \quad {}^{18}\text{O} = 0.02 \$$$

date&time [GMT]	flask code	site	alt [ft]	init p.	mixing ratios						isotope	
					CH ₄ [ppb]	CO ₂ [ppm]	CO [ppb]	H ₂ [ppb]	SF ₆ [ppt]	N ₂ O [ppb]	del ¹³ C [%]	del ¹⁸ O [%]
12.06.2002 04:18	J473-01	Orvi	250	1.9	1848.5	380.7	160.9	563.9	5.34	319.4	-8.575	0.403
12.06.2002 04:18	J479-01	Orvi	250	1.9	1848.8	380.4	159.9	561.9	5.36	319.5	-8.574	0.457
12.06.2002 04:30	J470-01	Orvi	450	1.9	1845.2	375.5	161.7	591.9	5.39	319.5	-8.296	0.340
12.06.2002 04:30	J452-01	Orvi	450	1.9	1845.9	376.1	161.9	586.6	5.37	319.4	-8.327	0.278
12.06.2002 04:38	J460-01	Orvi	850	1.9	1846.6	373.9	159.1	600.0	5.41	319.5	-8.223	0.383
12.06.2002 04:38	J450-01	Orvi	850	1.9	1845.8	374.3	158.7	589.8	5.42	319.4	-8.236	0.327
15.06.2002 04:27	J480-01	Tusca	180	1.6	1838.3	382.7	133.6	567.3	5.16	319.3	-8.618	1.054
15.06.2002 04:27	J481-01	Tusca	180	1.6	1851.0	382.8	131.4	562.3	5.17	319.2	-8.610	1.048
15.06.2002 04:35	J453-01	Tusca	350	1.8	1818.6	379.0	136.2	584.0	5.20	319.0	-8.417	1.138
15.06.2002 04:35	J166-01	Tusca	350	1.7	1817.4	379.1	136.3	582.4	5.22	319.1	-8.412	1.144
15.06.2002 04:44	J167-01	Tusca	850	1.8	1802.0	374.7	129.0	598.2	5.20	318.8	-8.179	1.100
15.06.2002 04:57	J448-01	Tusca	2500	1.8	1809.1	370.9	127.9	538.4	5.31	318.8	-8.028	1.056
15.06.2002 04:57	J449-01	Tusca	2500	1.8	1810.8	371.0	128.2	537.0	5.30	318.9	-8.030	1.076
15.06.2002 05:34	J482-01	Tusca	9000	1.8	1778.9	373.9	100.7	533.8	5.07	317.9	-8.160	0.606
15.06.2002 05:34	J454-01	Tusca	9000	1.9	1777.7	373.8	102.5	535.4	5.11	318.1	-8.148	0.616
15.06.2002 14:21	J170-01	Tusca	180	1.7	1797.1	376.1	130.1	552.6	5.19	318.6	-8.348	0.916
15.06.2002 14:21	J168-01	Tusca	180	1.7	1795.9	376.3	130.1	554.5	5.19	318.7	-8.347	0.936
15.06.2002 14:29	J179-01	Tusca	350	1.7	1795.7	375.9	128.9	568.6	5.20	318.7	-8.320	0.939
15.06.2002 14:29	J173-01	Tusca	350	1.7	1795.1	375.9	129.4	571.0	5.20	318.7	-8.302	0.901
15.06.2002 14:38	J180-01	Tusca	850	1.7	1795.3	376.3	145.6	542.8	5.22	318.6	-8.351	0.880
15.06.2002 14:38	J175-01	Tusca	850	1.7	1797.0	376.5	144.2	544.7	5.21	318.5	-8.367	0.895
15.06.2002 14:48	J182-01	Tusca	2500	1.8	1799.2	373.3	140.6	532.2	5.19	318.3	-8.158	1.017
15.06.2002 14:48	J176-01	Tusca	2500	1.8	1798.5	373.6	141.1	532.0	5.19	318.5	-8.177	1.109
15.06.2002 15:21	J177-01	Tusca	9000	1.9	1791.2	372.6	180.1	560.4	5.15	318.0	-8.128	0.681
15.06.2002 15:21	J186-01	Tusca	9000	1.9	1792.4	372.5	181.9	563.1	5.12	318.0	-8.124	0.644
18.06.2002 04:00	J056-01	Orvi	150	1.9	1881.3	410.2	202.5	553.5	5.76	320.1	-9.840	1.141
18.06.2002 04:00	J038-01	Orvi	150	1.9	1884.4	409.9	231.9	569.9	5.71	320.0	-9.822	1.155
18.06.2002 04:17	J055-01	Orvi	350	1.9	1863.5	380.7	196.2	578.9	5.84	320.0	-8.625	1.128
18.06.2002 04:17	J047-01	Orvi	350	1.9	1861.4	380.2	243.0	599.9	5.80	320.1	-8.592	1.179
18.06.2002 04:26	J053-01	Orvi	850	1.9	1846.2	373.5	172.3	609.2	5.74	319.8	-8.224	1.058
18.06.2002 04:26	J043-01	Orvi	850	1.9	1847.0	373.4	206.3	621.5	5.75	320.0	-8.228	1.010
18.06.2002 04:38	J040-01	Orvi	2500	1.8	1821.1	370.1	167.3	573.8	5.45	319.2	-8.008	1.062
18.06.2002 04:38	J041-01	Orvi	2500	1.8	1819.7	370.2	247.9	618.9	5.46	319.1	-8.024	1.113
18.06.2002 05:16	J046-01	Orvi	9000	1.7	1799.7	373.6	682.1	1056.1	5.11	317.1	-8.134	0.494
18.06.2002 05:16	J087-01	Orvi	9000	1.7	1801.1	373.6	680.2	1040.2	5.12	317.0	-8.144	0.496
18.06.2002 14:24	J044-01	Orvi	150	1.9	1806.2	366.8	369.2	670.1	5.27	318.5	-7.832	1.620
18.06.2002 14:24	J045-01	Orvi	150	1.9	1808.0	367.2	348.7	656.8	5.27	318.7	-7.842	1.545
18.06.2002 14:39	J071-01	Orvi	350	1.9	1804.5	367.8	270.8	600.3	5.27	318.7	-7.855	1.472
18.06.2002 14:46	J016-01	Orvi	850	2.0	1803.9	367.0	292.0	603.9	5.29	318.3	-7.831	1.489
18.06.2002 14:46	J019-01	Orvi	850	2.0	1803.9	367.4	290.4	601.6	5.29	318.6	-7.846	1.482
18.06.2002 14:56	J025-01	Orvi	2500	2.0	1803.4	367.3	275.8	592.6	5.27	318.4	-7.843	1.467
18.06.2002 14:56	J021-01	Orvi	2500	2.0	1802.7	367.4	270.9	591.5	5.25	318.6	-7.851	1.495
18.06.2002 15:37	J018-01	Orvi	9000	1.8	1781.0	374.6	468.1	705.8	5.14	317.9	-8.209	0.613
18.06.2002 15:37	J037-01	Orvi	9000	1.8	1783.4	374.6	480.5	712.9	5.03	317.9	-8.208	0.701
18.06.2002 15:57	J059-01	Orvi	150	1.9	1798.9	365.6	141.0	541.5	5.24	318.3	-7.775	1.484
18.06.2002 15:57	J022-01	Orvi	150	1.9	1799.7	365.6	154.8	546.0	5.27	318.4	-7.786	1.564
13.06.2002 15:25	J120-01	Rocca	0.3	2.0	1849.3	375.8	157.1	496.6	5.35	319.8	-8.341	1.581
13.06.2002 15:25	J122-01	Rocca	0.3	2.0	1849.9	377.6	-999	-999	-999	319.8	-8.429	1.619
13.06.2002 15:38	J137-01	Rocca	1.5	2.0	1849.4	375.7	154.6	496.3	5.36	319.7	-8.322	1.397
13.06.2002 15:38	J124-01	Rocca	1.5	2.0	1847.6	375.4	154.9	496.2	5.34	319.6	-8.315	1.377
13.06.2002 16:07	J136-01	Rocca	3.0	2.0	1842.6							

21.06.2002 05:45	J542-01	Orv-Abt	3.0	2.0	1848.4	504.0	145.1	369.0	5.29	319.8	-12.899	0.795
21.06.2002 05:59	J543-01	Orv-Abt	6.0	2.1	1843.4	479.4	146.8	369.7	5.23	319.7	-12.111	1.080
21.06.2002 05:59	J544-01	Orv-Abt	6.0	2.1	1840.5	479.8	146.9	372.4	5.29	319.8	-12.108	1.103
21.06.2002 06:11	J546-01	Orv-Abt	15.0	2.1	1845.2	481.7	149.0	377.4	5.31	319.6	-12.197	0.910
21.06.2002 06:11	J547-01	Orv-Abt	15.0	2.1	1843.2	486.7	148.5	373.4	5.33	319.7	-12.351	0.913
21.06.2002 15:40	J036-01	Orv-Val	0.3	2.0	1807.2	376.0	143.0	503.9	5.26	319.2	-8.284	2.053
21.06.2002 15:40	J549-01	Orv-Val	0.3	2.0	1806.9	373.0	140.6	498.4	5.25	319.1	-8.111	2.039
21.06.2002 15:52	J550-01	Orv-Val	1.5	2.0	1805.6	373.3	139.4	513.8	5.23	319.2	-8.117	1.757
21.06.2002 15:52	J555-01	Orv-Val	1.5	2.0	1803.5	372.6	139.0	511.3	5.25	319.0	-8.091	1.815
21.06.2002 16:06	J557-01	Orv-Val	3.0	2.0	1805.6	370.2	138.3	520.7	5.25	319.2	-7.980	1.698
21.06.2002 16:06	J578-01	Orv-Val	3.0	2.0	1804.7	369.8	139.4	517.5	5.26	319.2	-7.965	1.835
21.06.2002 16:20	J579-01	Orv-Val	6.0	2.0	1807.8	369.7	141.4	520.8	5.27	319.2	-7.971	1.714
21.06.2002 16:20	J580-01	Orv-Val	6.0	2.0	1806.2	369.9	141.1	520.0	5.26	319.2	-7.977	1.785
21.06.2002 16:33	J581-01	Orv-Val	15.0	1.7	1808.4	368.9	139.8	512.0	5.30	319.3	-7.914	2.026
22.06.2002 04:30	J583-01	Orv-Val	0.3	2.0	1829.5	415.1	163.8	453.1	5.34	319.9	-9.994	0.758
22.06.2002 04:30	J584-01	Orv-Val	0.3	2.0	1832.2	413.8	163.9	456.9	5.27	320.0	-9.948	0.767
22.06.2002 04:45	J587-01	Orv-Val	1.5	2.0	1827.4	424.5	160.8	434.1	5.29	319.9	-10.334	0.567
22.06.2002 04:59	J589-01	Orv-Val	3.0	2.0	1832.1	395.2	170.8	496.2	5.29	319.8	-9.203	1.178
22.06.2002 04:59	J585-01	Orv-Val	3.0	2.0	-999	-999	-999	-999	-999	-999	-9.245	1.106
22.06.2002 05:12	J591-01	Orv-Val	6.0	2.0	1836.2	383.2	173.7	514.5	5.37	319.7	-8.641	1.531
22.06.2002 05:25	J592-01	Orv-Val	15.0	2.0	1835.0	375.2	176.5	525.2	5.34	319.8	-8.265	1.709
22.06.2002 05:25	J593-01	Orv-Val	15.0	2.0	1835.9	375.7	176.9	524.7	5.37	319.8	-8.289	1.694

SPA¹³CE – Soil Plant Atmosphere ¹³C Exchange Experiment

29 July – 16 August 2002



SPA¹³CE – Soil Plant Atmosphere ¹³C Exchange Experiment

29 July – 16 August 2002

Participants

N. Buchmann, V. Hahn, A. Knohl, M. Schumacher, U. Seibt, A. Søe (MPI-BGC Jena) and L. Wingate*

Flight profile samplings on 6, 14 and 15 August above the Hainich

(additional on 9 August at Aerocarb [Airborne European Regional Observation of the Carbon Balance] measurement site ‘Holzland’)

Sampling heights: The lowest flight level was following the canopy at a height of almost 8 - 10 m above the treetop. Heights of the other sampling levels were 140, 275, 825 and 1370 m above ground.

Sampling times: Morning flight on 14 August around 8:00 UTC, on 15 August around 7:00 UTC. Midday flights were executed around 10:30 UTC on both days; the flights on 6 August were performed around 7:20 and 12:30 UTC.

Aircraft: Wilga-35, 260 HP. Single 9-cylinder radial engine, propeller clockwise. Four seat shoulder wing airplane. Flight speed during sampling procedure 75 knts (~140 km/h), climbing rate 1 m s⁻¹. Tube inlet mounted at left wing tip, approximately 15 cm beneath the profile bottom, facing downwards to the front

* University of Edinburgh

SPA13CE Thuringia Summer Experiment

Flights 6 – 15 August 2002

Combined ground level and flight investigations

During the first two weeks of August intensive measurement activity of PhD. students from the MPI-BGC had taken place at the Hainich National Park.

Because of foggy conditions in the morning the flights started not at the same time on all days; on 14 August around 8:00 UTC, on 15 August around 7:00 UTC. Midday flights were carried out around 10:30 UTC on both days. The lowest flight level was following the canopy surface at a height of almost 8 - 10 m (see also thesis figure 2.4). Special focus of the study was on the two consecutive days at the end of the experiment.

The synoptic situation of this period was characterized by a low pressure cell that had passed the study area the days before. On the 14 August this cyclone was located over Poland and the Baltic States, moving further on to the south-east. From the Tyrrhenian Sea to Scandinavia a high pressure bridge established, while in the West low pressure cells were moving from the Mid-Atlantic, passing the Orkneys, to the north-east. On both days no precipitation was observed, but in the early morning fog occurred at the valley grounds.

SPA¹³CE – Soil Plant Atmosphere ¹³C Exchange Experiment

29 July – 16 August 2002

- Figure 1 Southern Hainich with marked tower location. View to the East inside the Thuringian Basin.
- Figure 2 Hainich Tower and canopy with shadow of the aircraft..
- Figure 3 Hainich Tower from the ground.
- Figure 4 View from the highest boom mounted on the Hainich Tower above the canopy to the West.
- Figure 5 Small mast beside the main tower used for near ground measurements.
- Figure 6 Branch bag with beech twig for plant related measurements and air sampling.
- Figure 7 Air sampling from branch bags with a similar system as used for the flight samplings during the begin of the RECAB project.
- Figure 8 Soil respiration air sampling.
- Figure 9 Picture of the Hainich Tower taken when passing while sampling at lowest flight level.

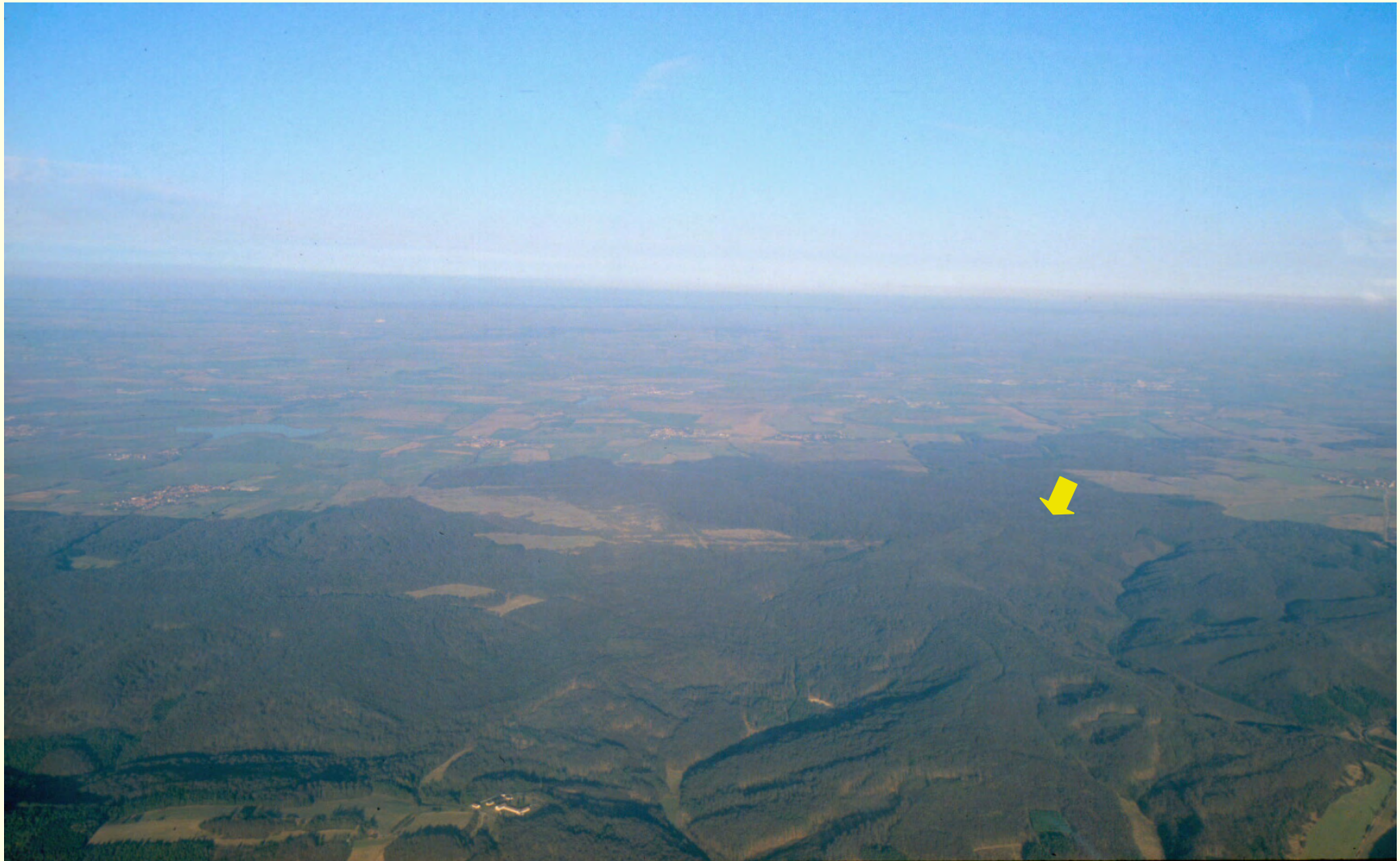


Figure 1 Aerial photograph of the southern Hainich with the tower location (marked by the yellow arrow), viewing to the East inside the Thuringian Basin. Flight altitude approximately 1500 m above ground.

Picture: 16 February 2001



Figure 2 Hainich Tower (height 42 m, treetops around 35 m). Flight altitude approximately ~ 25 m above the canopy. Picture taken at noon on 15 August 2002.



Figure 3 Hainich Tower from the ground. Notice the booms with the measurement equipments and the inlets for air sampling. Surrounding canopy is from ash trees.

Picture: 6 August 2002



Figure 4 View from the Hainich Tower over the canopy to the South. Placed on the boom are the sensors for radiation measurements.

Picture: 6 August 2002



Figure 5 Small mast for near ground measurements close to the main tower (height 3.0 m).

Picture by A. Knohl



Figure 6 Branch bags with enclosed beech twig for direct sampling of air characterized by assimilation and respiration.

Picture: 6 August 2002



Figure 7 Air sampling from branch bags. The configuration of the flask sampling system is similar to the design of the system used at the beginning of the flight investigations.

Picture by A. Knohl



Figure 8 Soil respiration sampling from cylindric sections as visible in the front (right hand site of the sketch book). Filling of small cuvettes for isotopic analyses. Inside the big 'chimney' flask sampling profiles of respired air were carried out.

Picture: 6 August 2002



Figure 9 Hainich Tower (height 42 m, treetops around 35 m). 'Lowest level' sampling altitude approximately 5 - 7 m above the canopy.

Picture at noon on 15 August 2002

PARAMETER/VARIABLE DESCRIPTION

date&time (GMT) - date and time the sampling procedure was completed in Greenwich Mean Time

flask code - marking of nameplates for each flask

site - location of the flight pattern, leg length ~2km

Ground sampling / reference location: *Hainich Tower*

Hainich Fluxnet site, deciduous forest: 51°04.7'N / 010°27.1'E, 439 m a. MSL

alt (ft) - sampling height in feet above ground

init p. - internal flask pressure at the beginning of the analysis

Mixing ratios

		Precision of the analyses
CH₄ [ppb] -	methan mixing ratio in ppb	1.3 ppb
CO₂ [ppm] -	carbon dioxide mixing ratio in ppm	0.08 ppm
N₂O [ppb] -	nitrous oxide mixing ratio in ppb	0.15 ppb
CO [ppb] -	carbon monoxide mixing ratio in ppb	1.0 ppb
H₂ [ppb] -	hydrogen mixing ratio in ppb	5.0 ppb
SF₆ [ppt] -	sulfur hexafluoride mixing ratio in ppt	0.08 ppt

Isotope Ratio

$$d[\$] = (R_{sa}/R_{ref} - 1) \cdot 1000 \quad R_{sa} \text{ and } R_{ref} \text{ are the sample and reference isotope ratios}$$

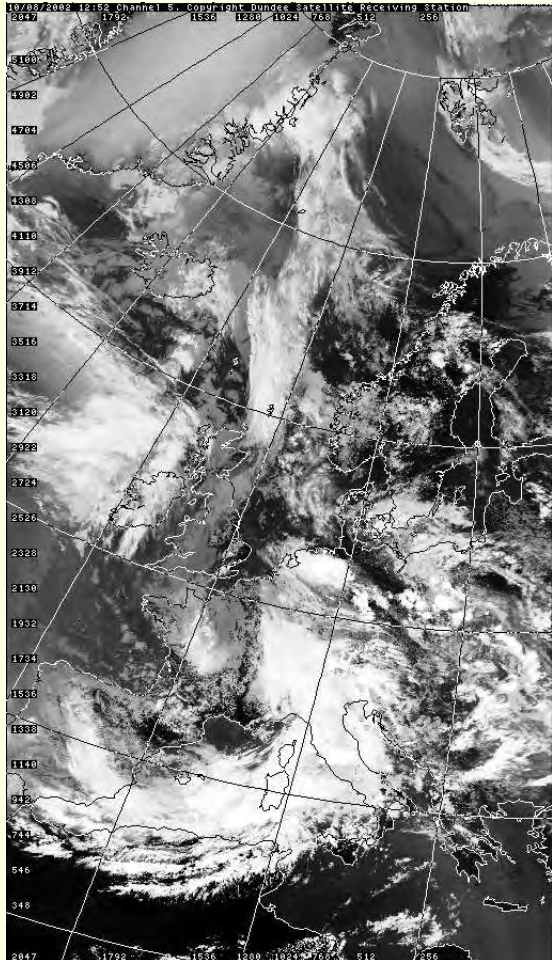
del ¹³C [\$] - ratio of the carbon 13 isotope and carbon 12 isotope due to the VPDB isotope ratio scale

del ¹⁸O [\$] - ratio of the oxygen 18 isotope and oxygen 16 isotope due to the VPDB (gas) isotope ratio scale

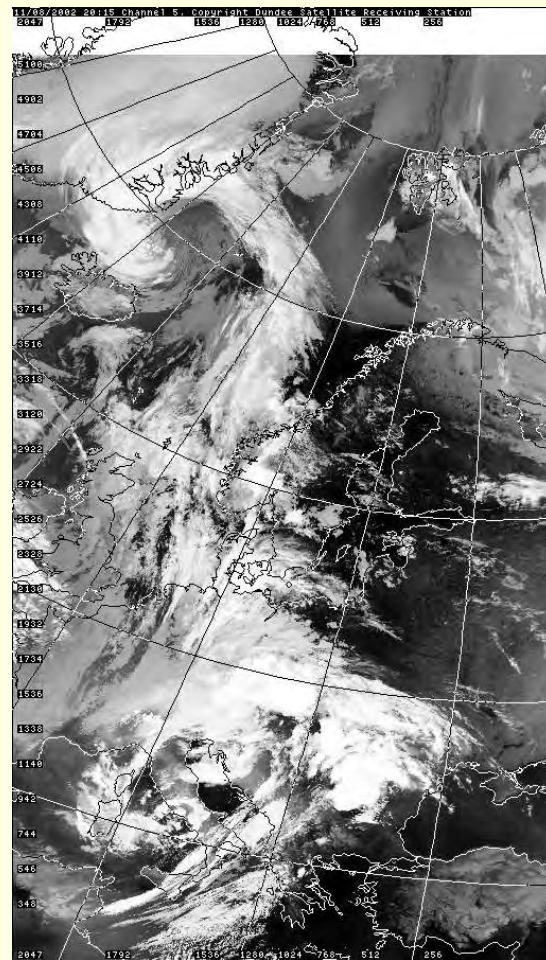
Precision of the analyses $^{13}\text{C} = 0.012 \$$ $^{18}\text{O} = 0.02 \$$

location	alt [m]	collection time (GMT)	mixing ratio			mixing ratio			isotopes [%]		Flask No.
			CH ₄ [ppb]	CO ₂ [ppm]	N ₂ O [ppb]	H ₂ [ppb]	CO [ppb]	SF ₆ [ppt]	del ¹³ C	del ¹⁸ O	
Hainich	60	6.8.02 7:20	1872.8	367.6	319.2	514.1	143.7	5.47	-8.125	-0.252	J233-01
Hainich	60	6.8.02 7:20	1873.4	367.5	319.2	510.0	142.8	5.50	-8.085	-0.197	J220-01
Hainich	152	6.8.02 7:30	1860.3	367.9	319.7	526.1	136.3	5.40	-8.025	-0.297	J215-01
Hainich	152	6.8.02 7:30	1860.9	367.8	319.6	518.5	135.6	5.40	-7.963	-0.161	J219-01
Hainich	300	6.8.02 7:40	1850.4	365.2	318.7	541.1	132.2	5.33	-7.879	-0.545	J207-01
Hainich	300	6.8.02 7:40	1850.8	365.4	318.8	527.1	128.6	5.34	-7.848	-0.273	J208-01
Hainich	915	6.8.02 7:52	1832.7	364.6	318.4	532.8	116.9	5.30	-7.817	-0.719	J209-01
Hainich	915	6.8.02 7:52	1834.4	364.5	318.2	524.0	115.5	5.32	-7.802	-0.530	J214-01
Hainich	1500	6.8.02 8:10									J212-01
Hainich	1500	6.8.02 8:10	1819.7	365.1	317.8	521.5	107.9	5.24	-7.873	-0.398	J211-01
Hainich	60	6.8.02 12:23	1848.6	362.0	318.7	531.7	127.1	5.36	-7.796	-0.004	J022-01
Hainich	60	6.8.02 12:23	1848.6	362.1	318.8	528.8	127.1	5.32	-7.766	0.063	J025-01
Hainich	152	6.8.02 12:31	1848.6	364.6	318.8	533.0	128.0	5.28	-7.841	-0.155	J026-01
Hainich	152	6.8.02 12:31	1850.7	364.7	318.9	522.1	127.3	5.30	-7.831	-0.060	J027-01
Hainich	300	6.8.02 12:39	1847.3	365.0	318.8	532.7	122.0	5.31	-7.814	-0.227	J029-01
Hainich	300	6.8.02 12:39	1848.2	365.1	318.8	524.4	126.4	5.31	-7.826	-0.164	J021-01
Hainich	915	6.8.02 12:50	1845.1	363.5	318.6	531.2	126.0	5.31	-7.798	-0.271	J020-01
Hainich	915	6.8.02 12:50	1846.5	363.8	318.7	523.6	124.9	5.31	-7.788	-0.114	J019-01
Hainich	1500	6.8.02 13:06	1837.7	364.0	318.6	528.3	122.2	5.32	-7.826	-0.309	J018-01
Hainich	1500	6.8.02 13:06	1839.2	363.7	318.6	530.6	122.0	5.30	-7.822	-0.281	J016-01
Holzland	300	9.8.02 12:29	1874.4	362.8	319.9	532.3	145.8	5.84	-7.853	-0.312	J324-01
Holzland	300	9.8.02 12:29	1876.8	363.5	319.9	538.0	148.3	5.89	-7.872	-0.333	J325-01
Holzland	600	9.8.02 12:38	1878.4	366.2	320.1	524.4	145.2	5.88	-7.918	-0.455	J273-01
Holzland	600	9.8.02 12:38	1879.4	367.0	320.1	523.3	146.2	5.90	-7.970	-0.443	J222-01
Holzland	1000	9.8.02 12:48	1871.9	367.5	319.8	521.2	140.9	5.90	-7.931	-0.296	J231-01
Holzland	1000	9.8.02 12:48	1872.3	367.4	320.0	522.0	140.5	6.01	-7.949	-0.316	J224-01
Holzland	1500	9.8.02 13:00	1849.9	367.9	319.2	523.3	134.8	5.61	-7.960	-0.307	J323-01
Holzland	1500	9.8.02 13:00	1849.0	367.9	319.1	523.8	133.1	5.59	-7.972	-0.229	J322-01
Holzland	2000	9.8.02 13:11	1841.6	368.1	318.8	522.0	126.1	5.41	-7.944	-0.180	J218-01
Holzland	2000	9.8.02 13:11	1840.9	368.0	318.8	519.8	126.4	5.40	-7.951	-0.195	J232-01
Holzland	2500	9.8.02 13:27	1848.7	368.1	318.9	521.2	129.2	5.62	-7.970	-0.280	J320-01
Holzland	2500	9.8.02 13:27	1848.0	368.1	318.9	520.8	129.4	5.60	-7.928	-0.213	J275-01
Hainich	60	14.8.02 7:54	1834.1	372.3	319.7	523.2	104.3	5.23	-8.039	0.305	J122-01
Hainich	60	14.8.02 7:54	1838.7	372.5	319.9	523.3	107.4	5.27	-8.054	0.299	J120-01
Hainich	152	14.8.02 8:02	1836.3	373.7	319.9	520.8	102.9	5.26	-8.124	0.260	J334-01
Hainich	152	14.8.02 8:02	1837.1	373.9	319.8	518.9	105.6	5.26	-8.125	0.240	J121-01
Hainich	300	14.8.02 8:11	1793.2	371.5	319.1	527.1	87.1	5.16	-8.019	0.453	J335-01
Hainich	300	14.8.02 8:11	1795.4	371.5	319.0	526.8	88.5	5.22	-7.997	0.417	J330-01
Hainich	1500	14.8.02 8:31	1748.0	371.2	318.4	533.9	66.0	5.07	-7.981	0.691	J331-01
Hainich	1500	14.8.02 8:31	1748.7	371.3	318.5	535.0	66.7	5.12	-7.986	0.727	J332-01
Hainich	60	14.8.02 10:34	1798.9	363.6	319.4	529.5	92.7	5.18	-7.647	0.630	J038-01
Hainich	60	14.8.02 10:34	1796.7	364.0	319.1	527.8	90.0	5.23	-7.651	0.668	J037-01
Hainich	152	14.8.02 10:42	1798.6	366.2	319.3	523.2	91.0	5.19	-7.733	0.544	J031-01
Hainich	152	14.8.02 10:42	1798.0	366.6	319.3	524.8	91.8	5.18	-7.747	0.559	J036-01
Hainich	300	14.8.02 10:50	1792.2	367.2	319.1	526.5	87.5	5.19	-7.752	0.569	J327-01
Hainich	300	14.8.02 10:50	1789.3	368.0	319.1	525.7	93.4	5.22	-7.813	0.532	J326-01
Hainich	915	14.8.02 11:02	1767.0	370.5	318.8	530.0	76.8	5.15	-7.904	0.570	J336-01
Hainich	915	14.8.02 11:02	1765.3	370.5	318.7	530.1	73.1	5.12	-7.913	0.594	J030-01
Hainich	1500	14.8.02 11:20	1754.1	370.1	318.1				-7.918	0.603	J090-01
Hainich	1500	14.8.02 11:20	1755.5	370.1	318.1	531.0	72.1	5.08	-7.907	0.559	J091-01
Hainich	60	15.8.02 6:53	1849.3	368.6	320.8	536.1	120.7	5.46	-7.863	0.567	J099-01
Hainich	60	15.8.02 6:53	1847.7	368.0	320.9	538.4	124.1	5.47	-7.825	0.556	J136-01
Hainich	152	15.8.02 7:01	1847.4	371.3	320.9	535.0	119.3	5.45	-7.947	0.464	J133-01
Hainich	152	15.8.02 7:01				536.7	119.1	5.44	-7.893	0.474	J132-01
Hainich	300	15.8.02 7:09	1829.0	370.9	320.3	536.9	112.2	5.31	-7.968	0.460	J134-01
Hainich	300	15.8.02 7:09	1829.7	370.8	320.1	536.5	111.0	5.29	-7.972	0.446	J124-01
Hainich	91										

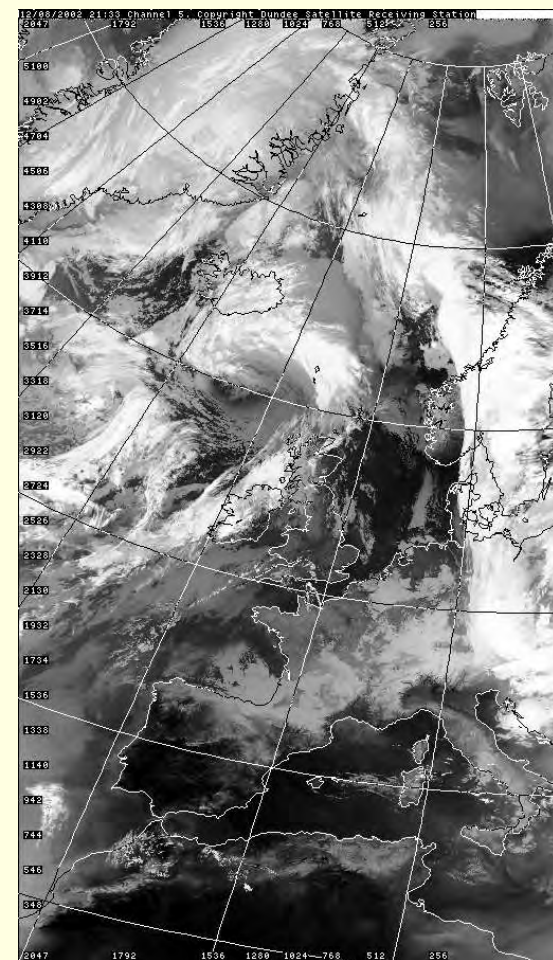
Satellite Images from NOAA 16, AVHRR



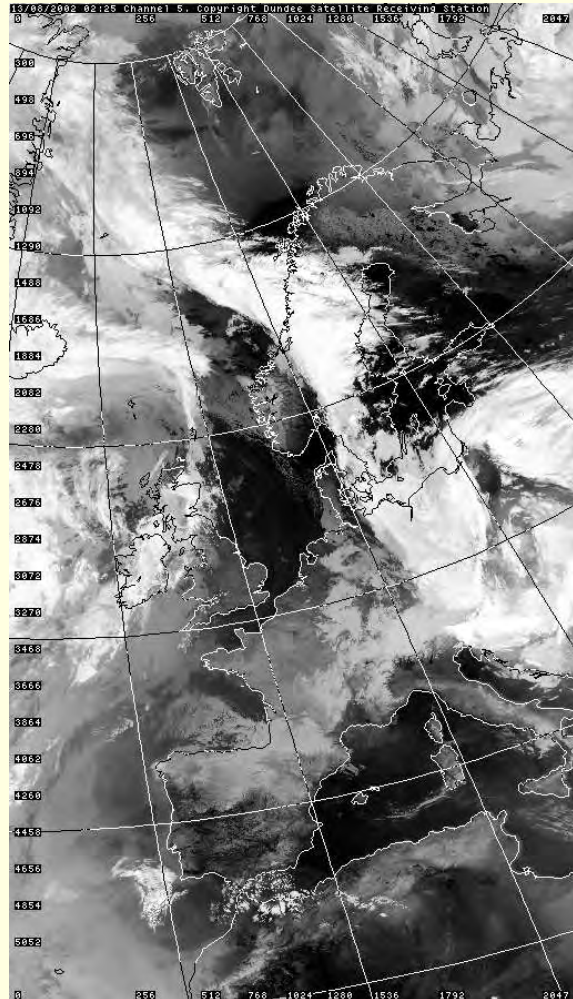
10 August 2002 12:52 UTC



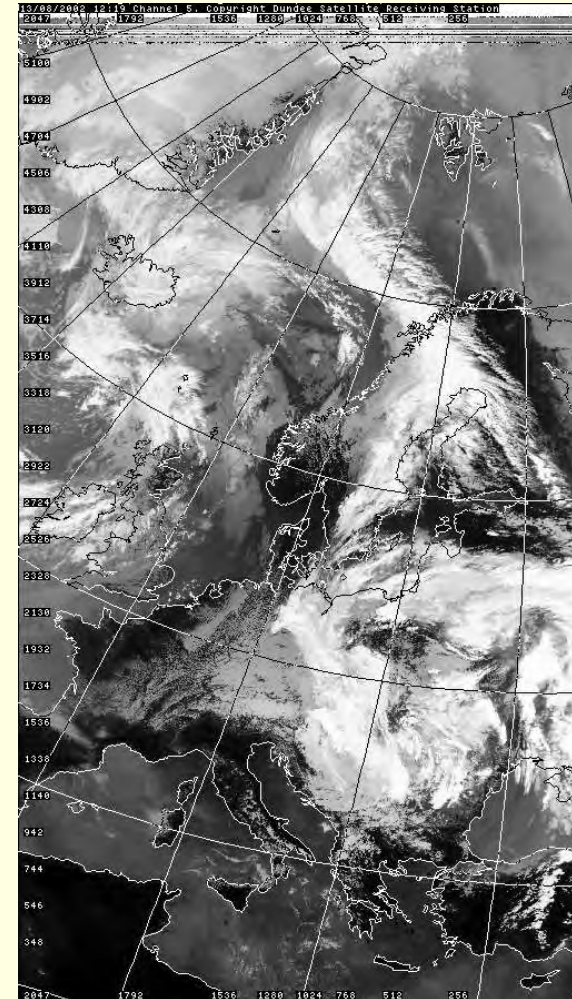
11 August 2002 20:15 UTC



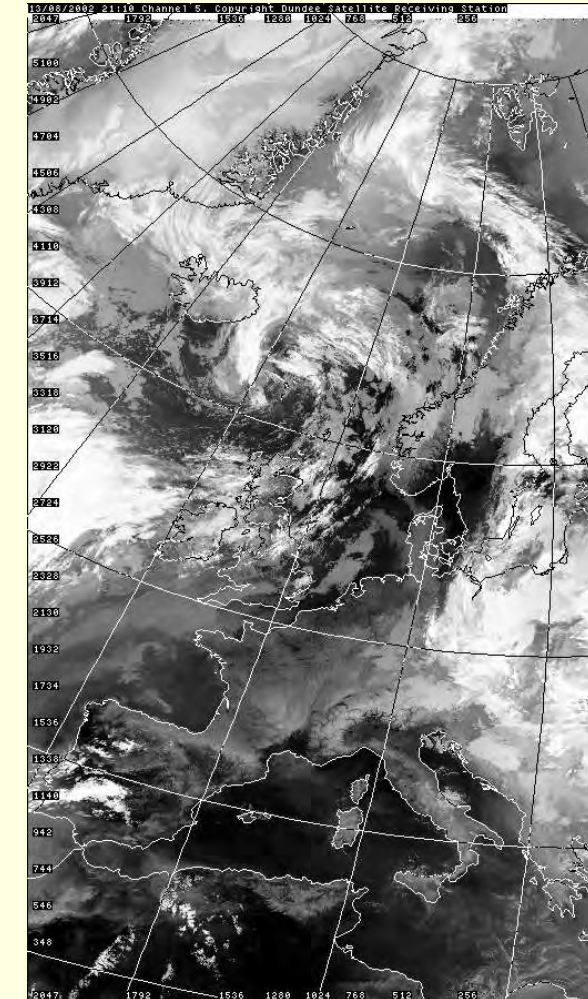
12 August 2002 21:33 UTC



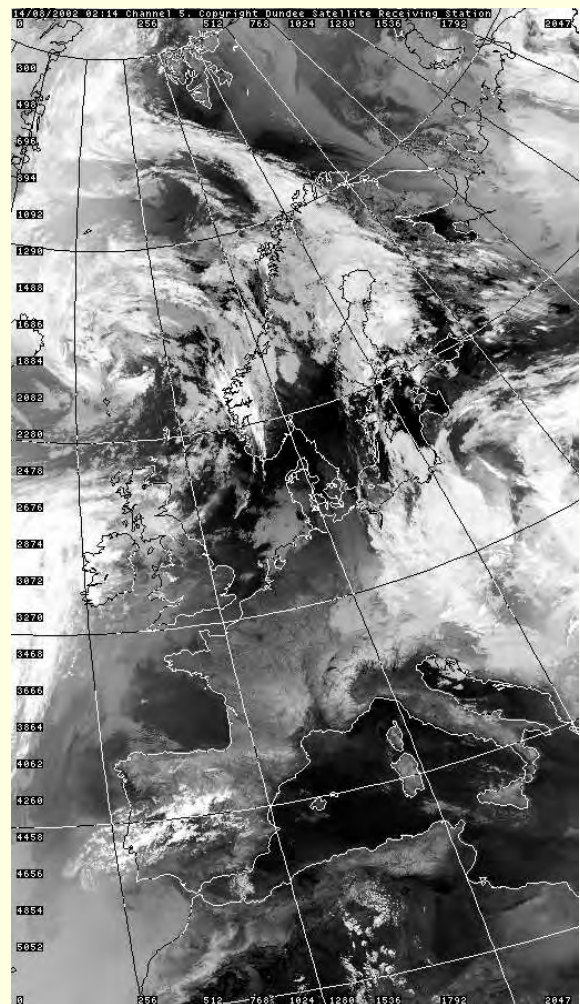
13 August 2002 02:25 UTC



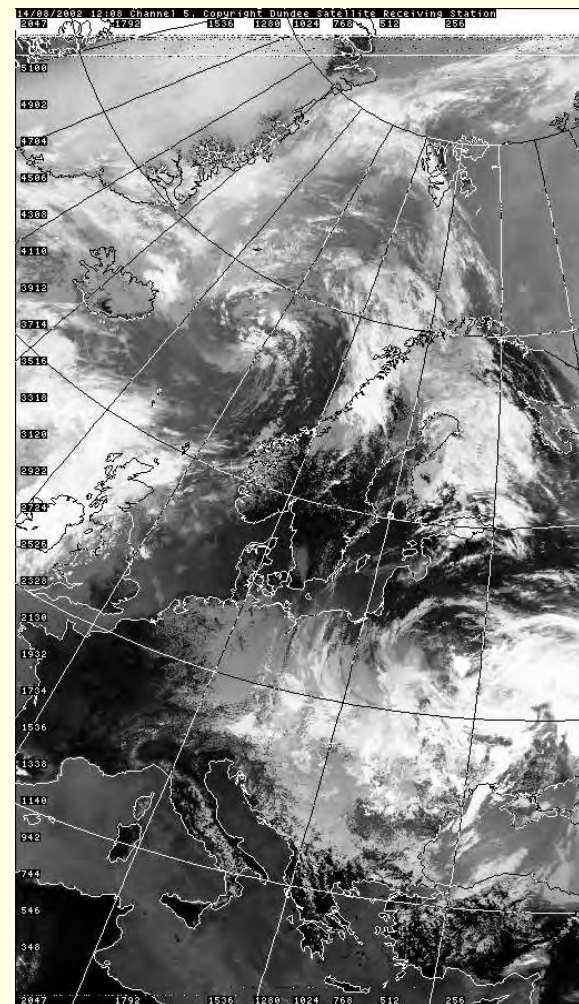
13 August 2002 12:19 UTC



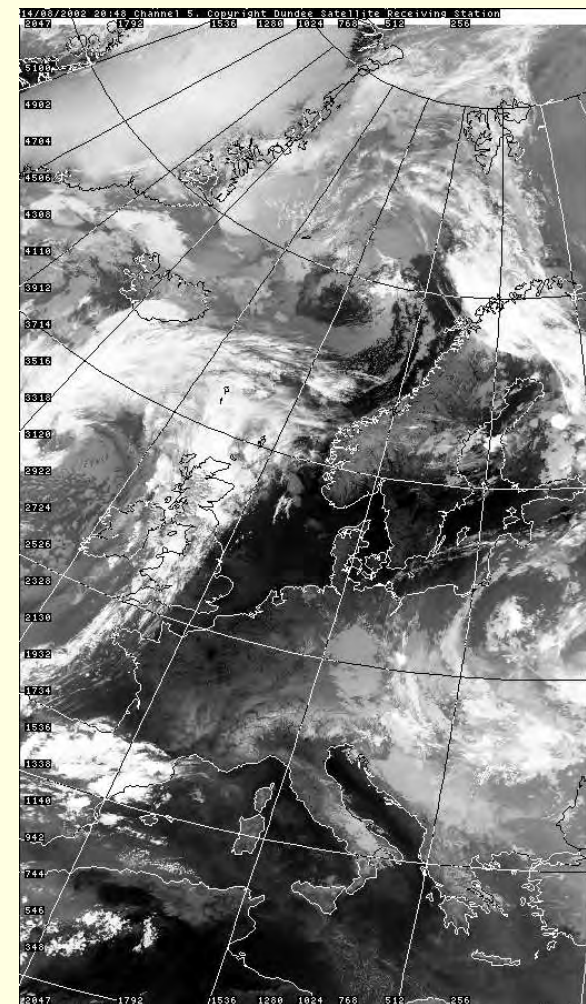
13 August 2002 21:10 UTC



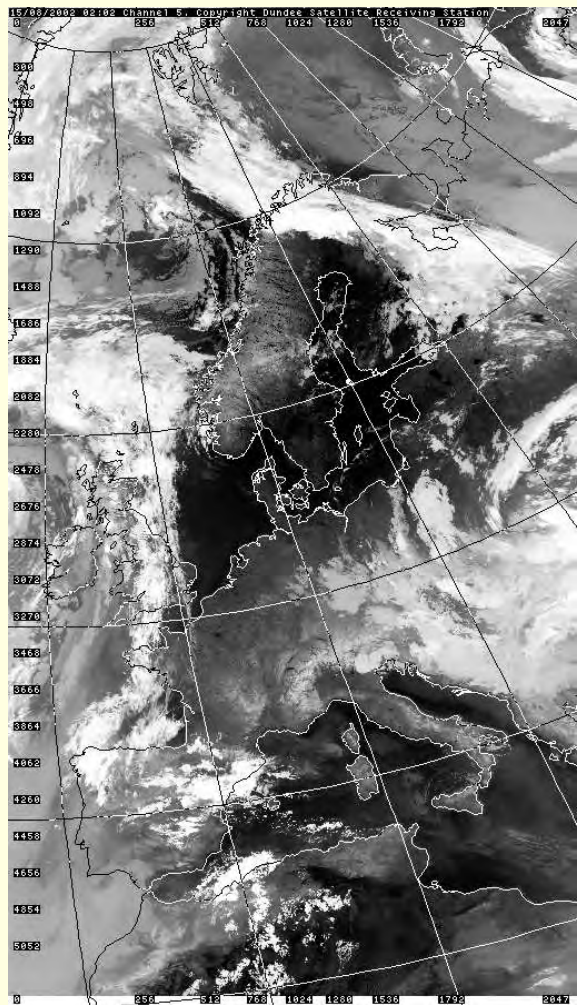
14 August 2002 02:14 UTC



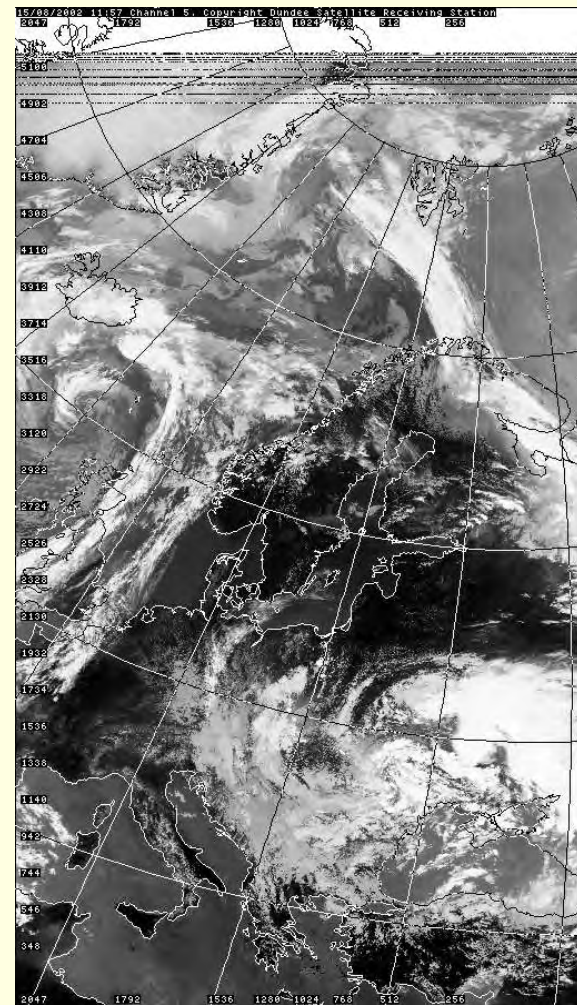
14 August 2002 12:08 UTC



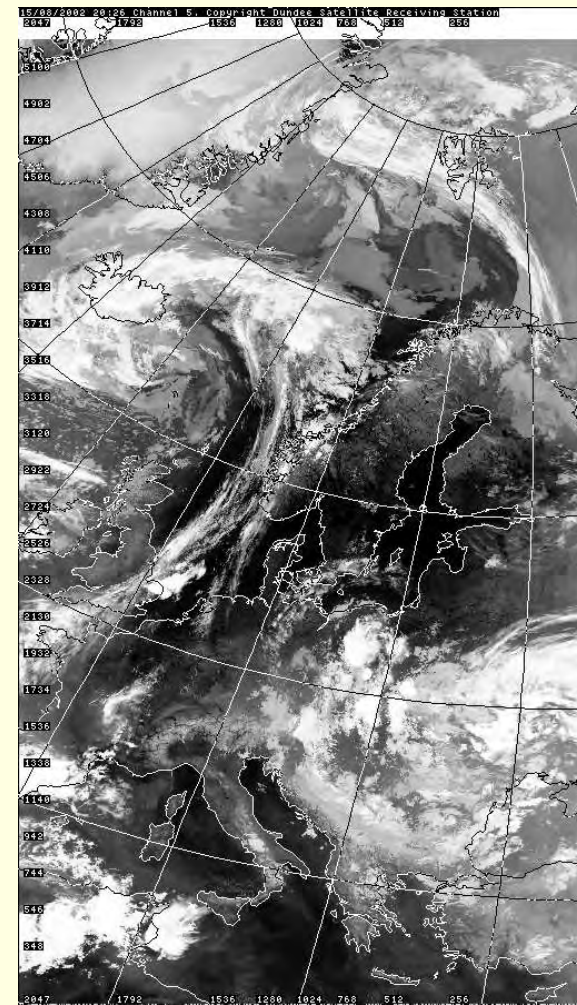
14 August 2002 20:48 UTC



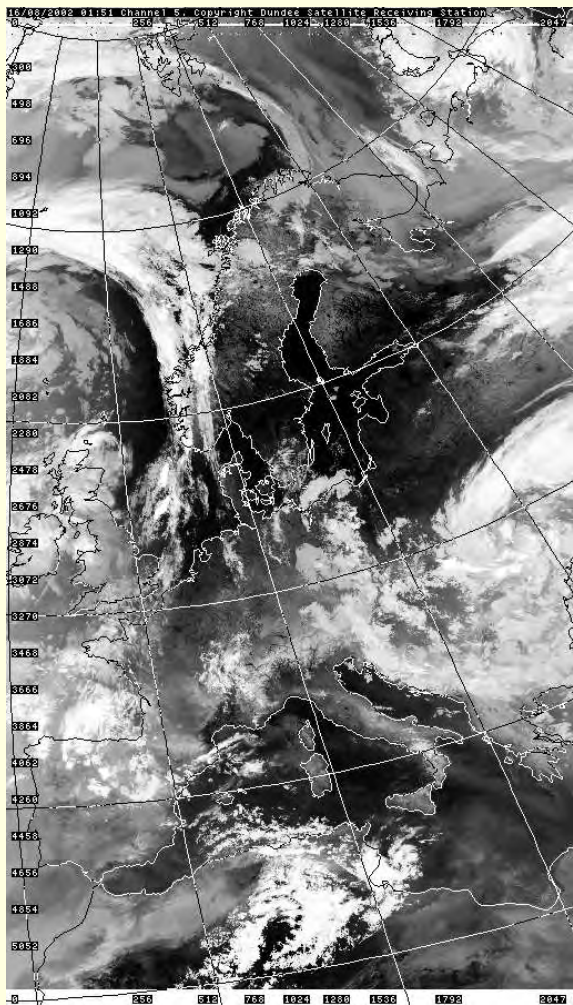
15 August 2002 02:02 UTC



15 August 2002 11:57 UTC



15 August 2002 20:26 UTC

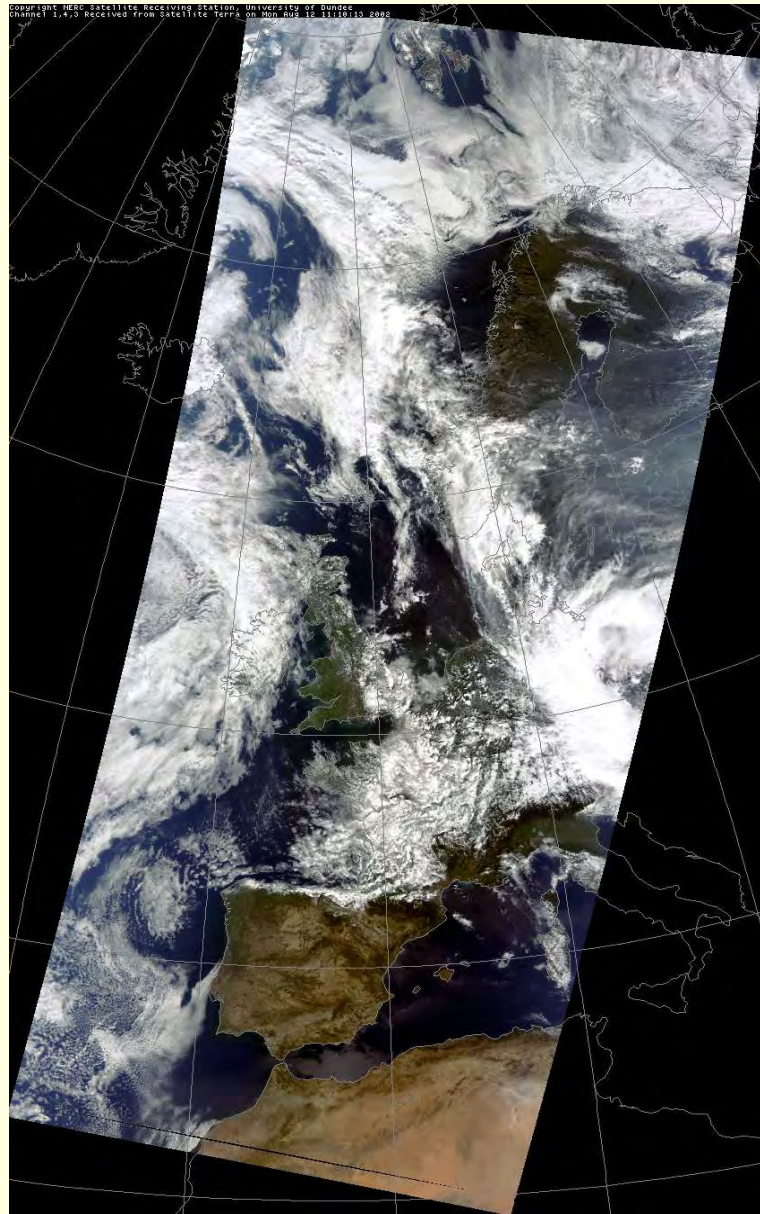


16 August 2002 01:51 UTC

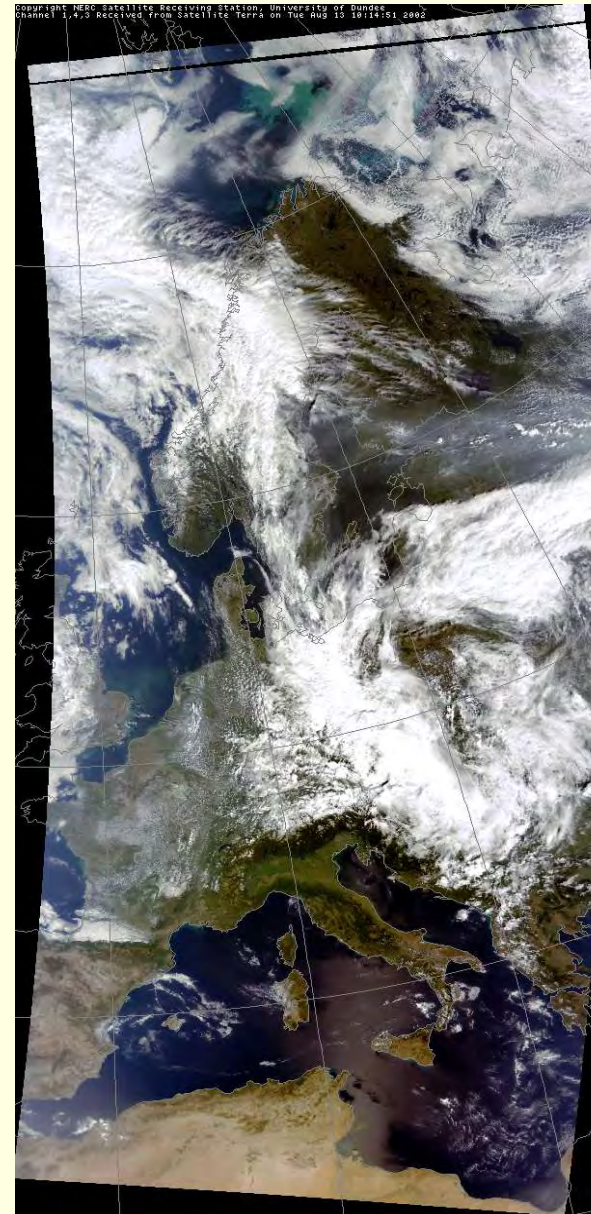
Satellite Images from Dundee Satellite Receiving Station
(<http://www.sat.dundee.ac.uk/auth.html>)

Satellite NOAA
Sensor AVHRR

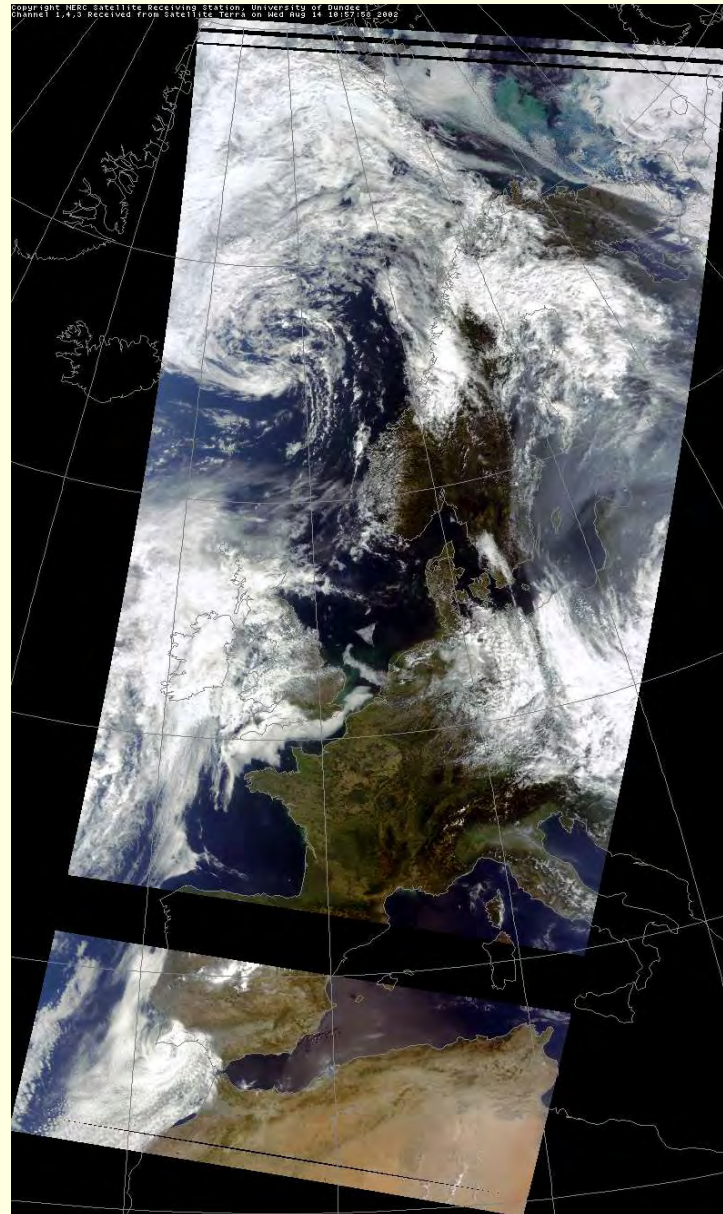
Channel 5 (thermal infra-red, 11.5 - 12.5μm)
500 m resolution



12 August 2002 11:10 UTC



13 August 2002 10:14 UTC



14 August 2002 10:58 UTC



15 August 2002 10:02 UTC



16 August 2002

10:46 UTC

Satellite Images from Dundee Satellite Receiving Station
(<http://www.sat.dundee.ac.uk/auth.html>)

Satellite Terra

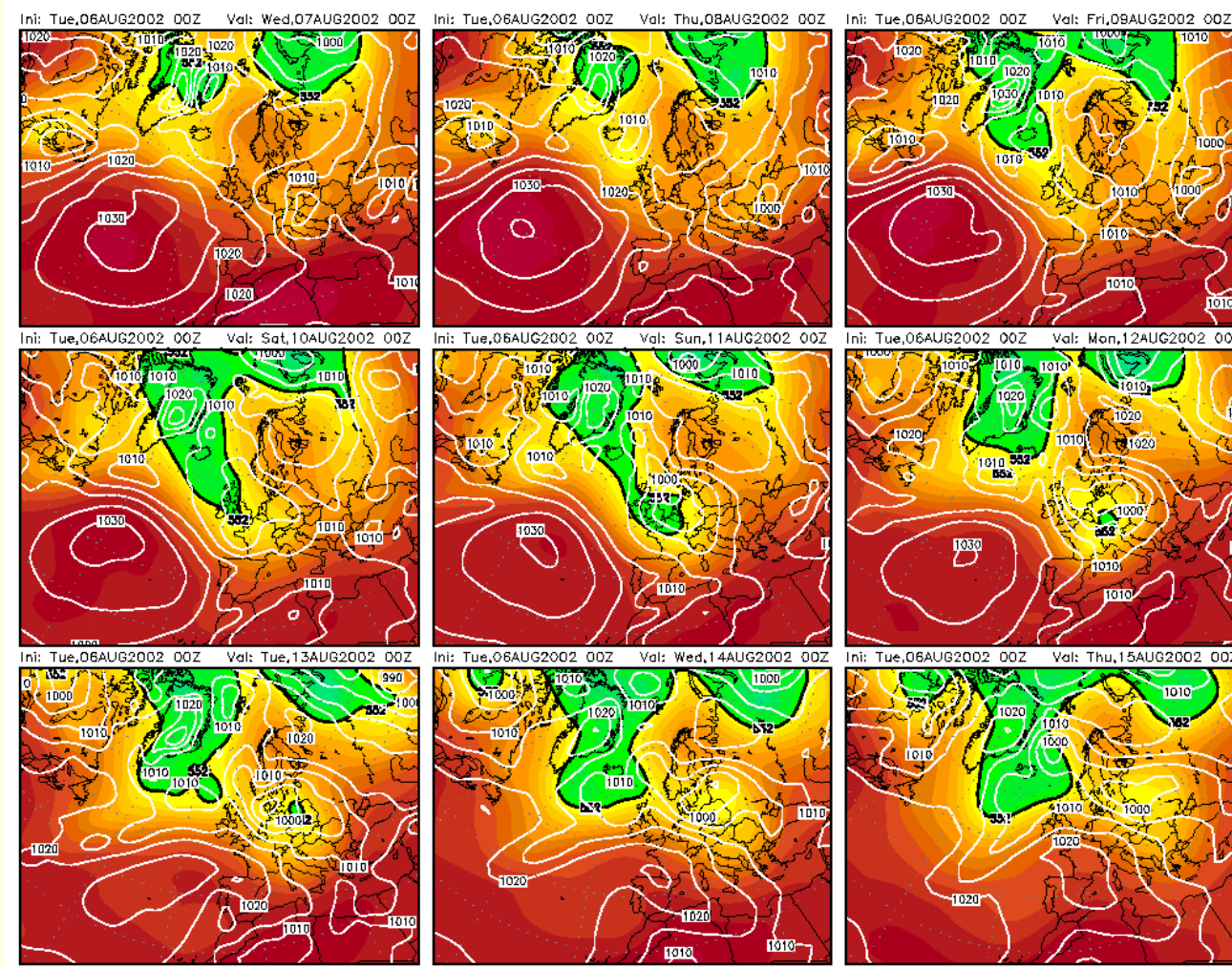
Sensor MODIS

RGB composite image reprojected (RGB 1,4,3 composite)

Band 1 (620 – 670nm) = 250 m resolution

Band 3 (459 – 479nm) and

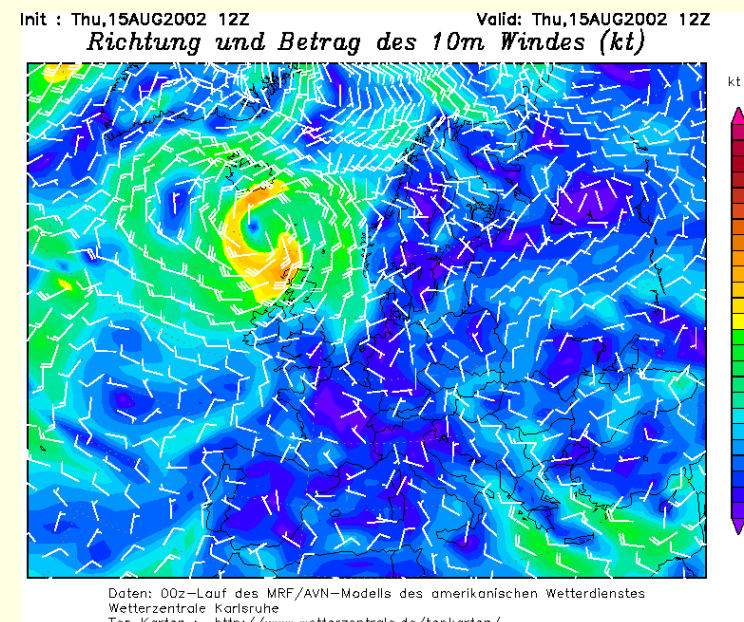
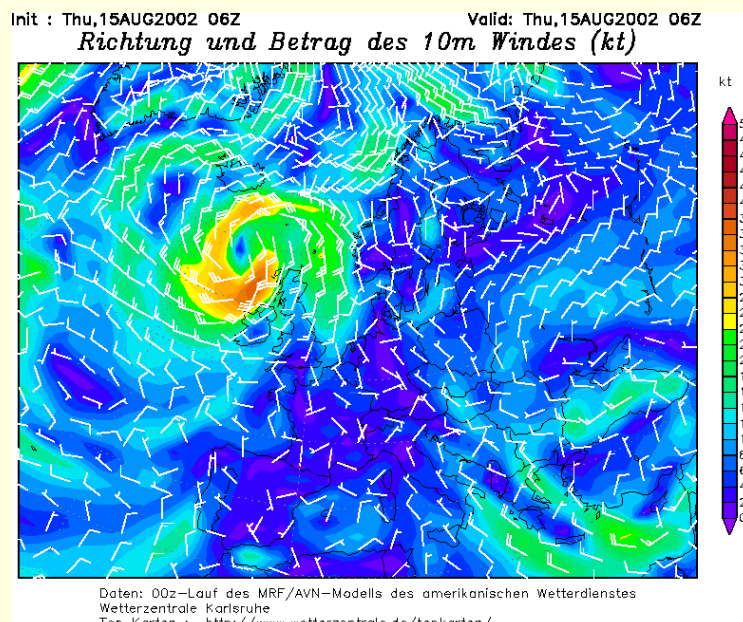
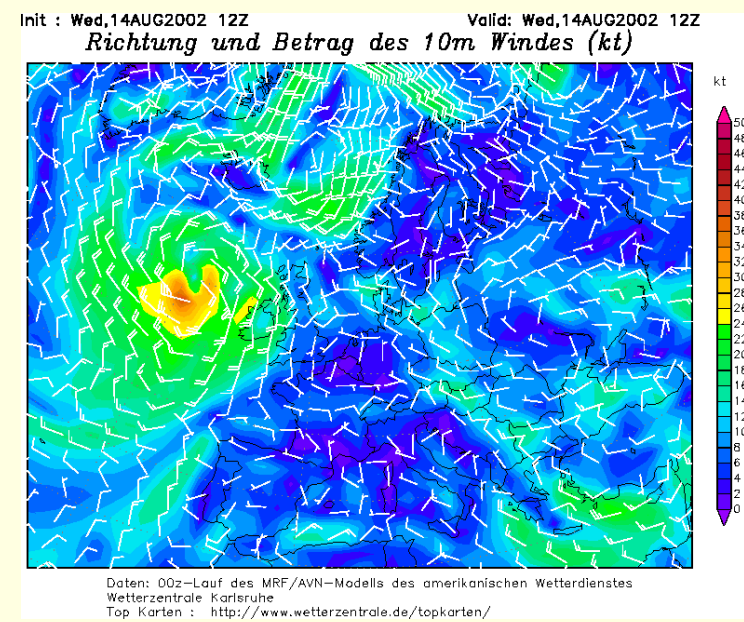
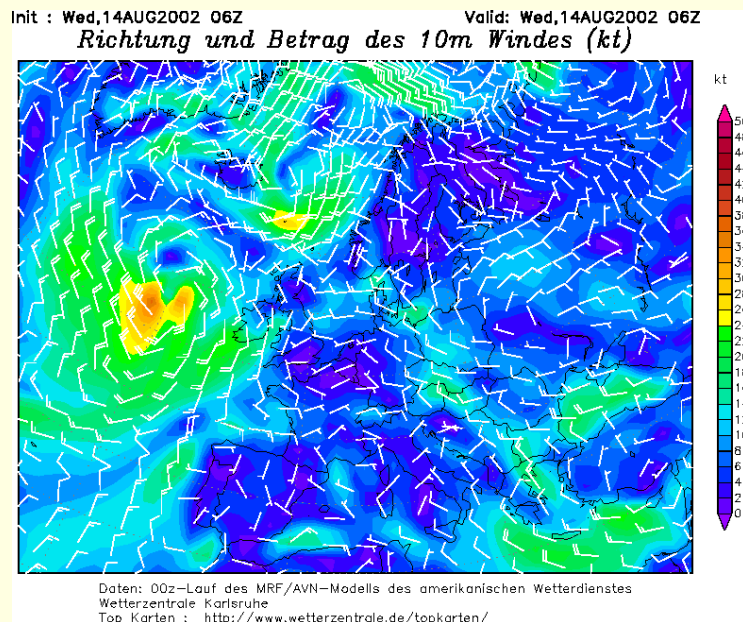
Band 4 (545 – 565nm) = 500 m resolution

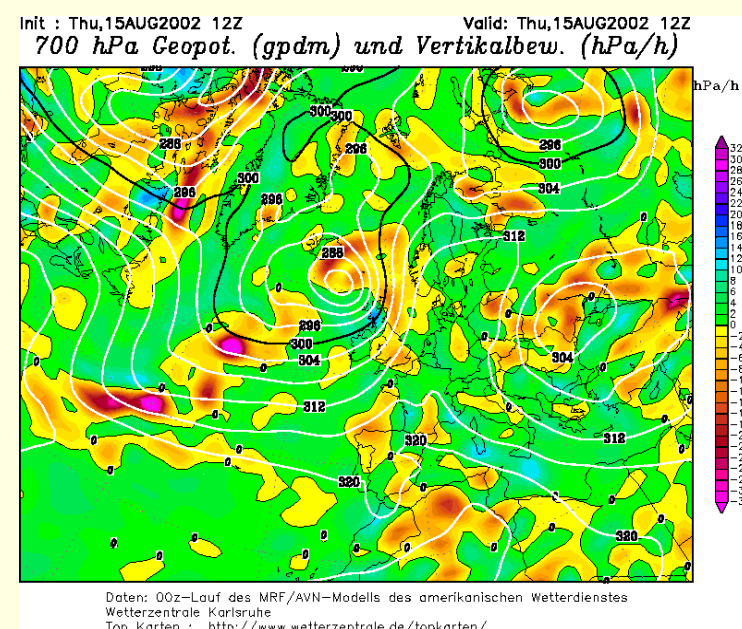
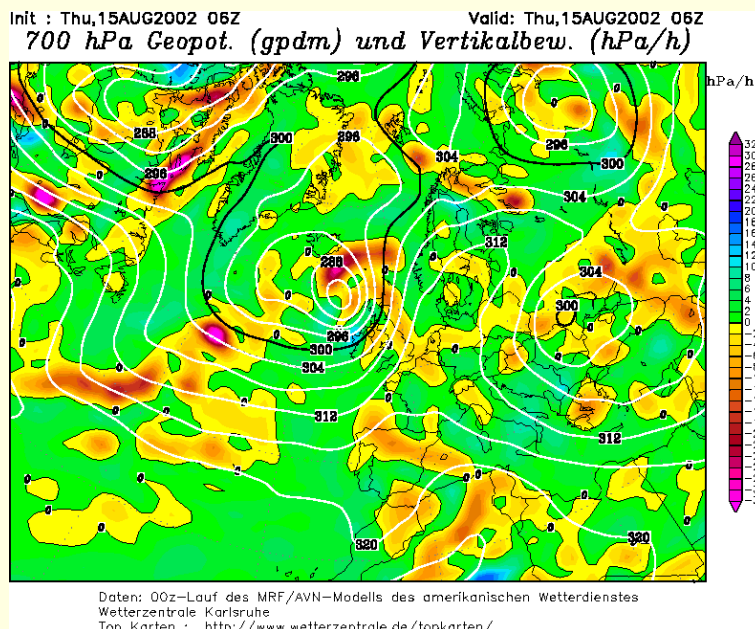
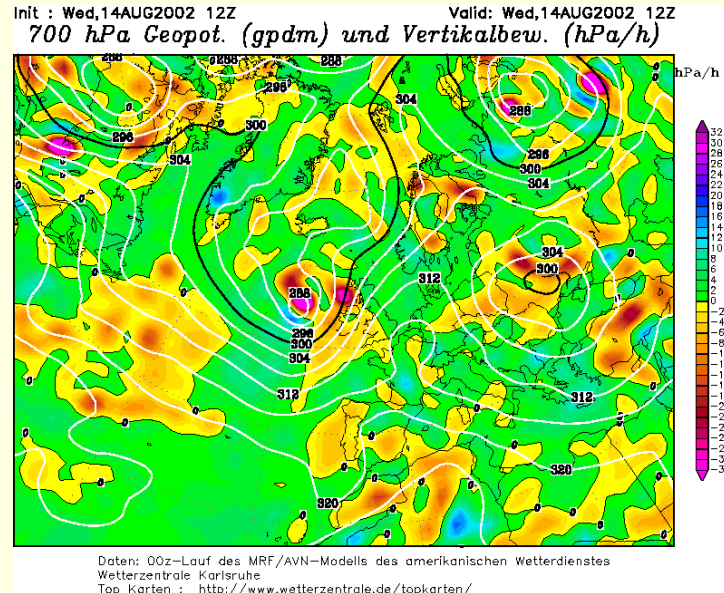
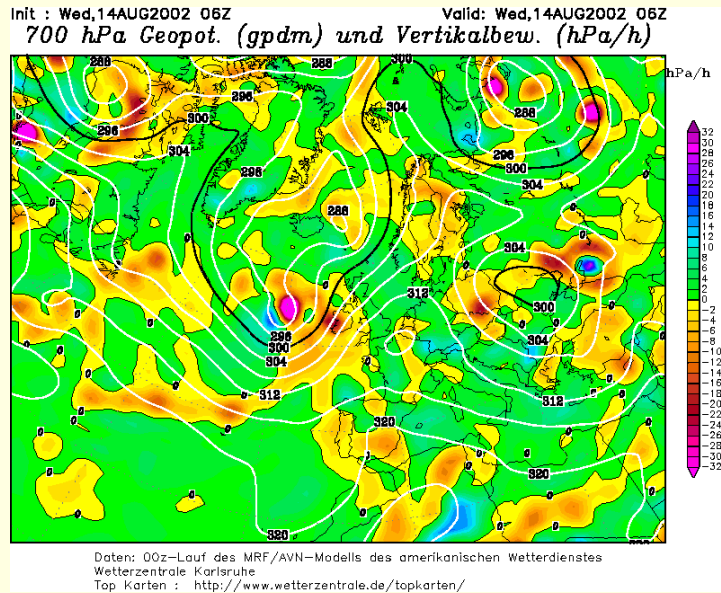


Synoptical analysis data

from Wetterzentrale (<http://www.wetterzentrale.de/topkarten>)

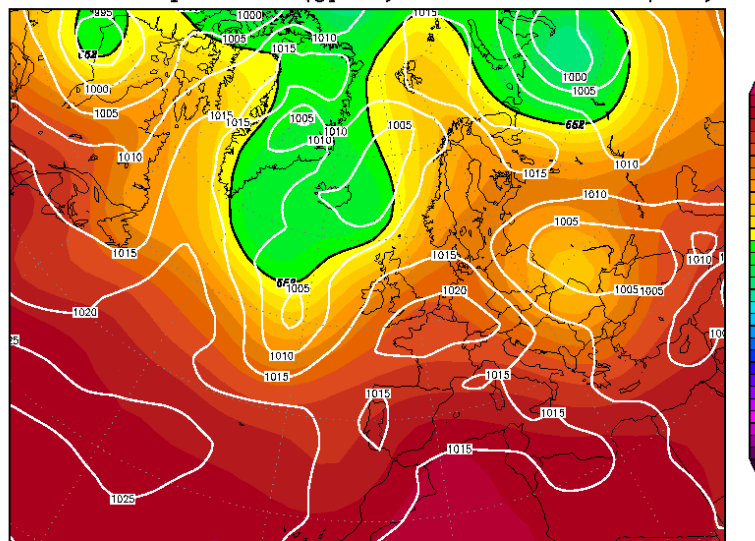
NCEP prediction of ground pressure (above). Next slides display: reanalyses of 10 m wind (direction and velocity), geopotential height of the 700 hPa surface and vertical velocity, and ground pressure and 850 hPa temperature. Upper panels showing data from 14 August, data from 15 August below.





Wed,14AUG2002 00Z

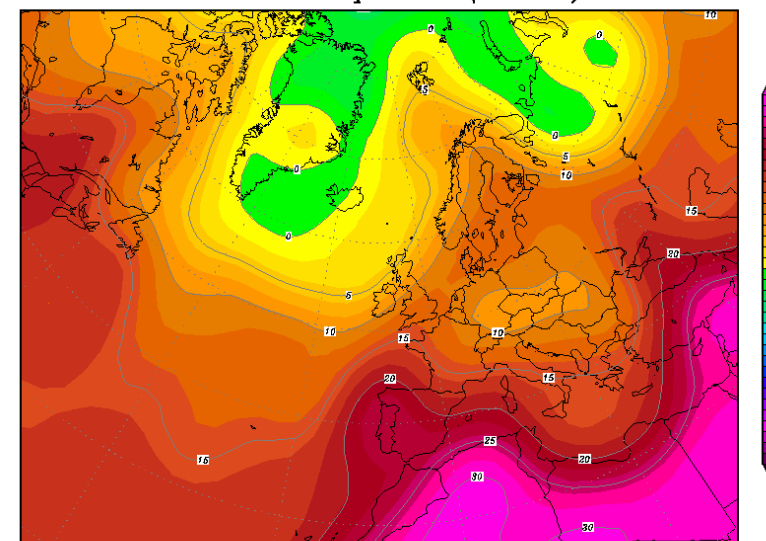
500 hPa Geopotential (gpdm) und Bodendruck (hPa)



Daten: Reanalysis des NCEP
Wetterzentrale Karlsruhe
Top Karten : <http://www.wetterzentrale.de/topkarten/>

Wed,14AUG2002 00Z

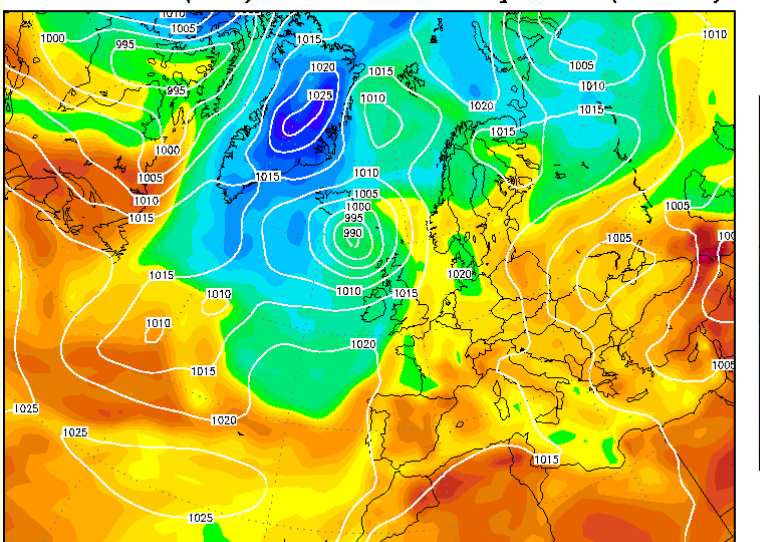
850 hPa Temperatur (Grad C)



Daten: Reanalysis des NCEP
Wetterzentrale Karlsruhe
Top Karten : <http://www.wetterzentrale.de/topkarten/>

Init : Thu,15AUG2002 12Z

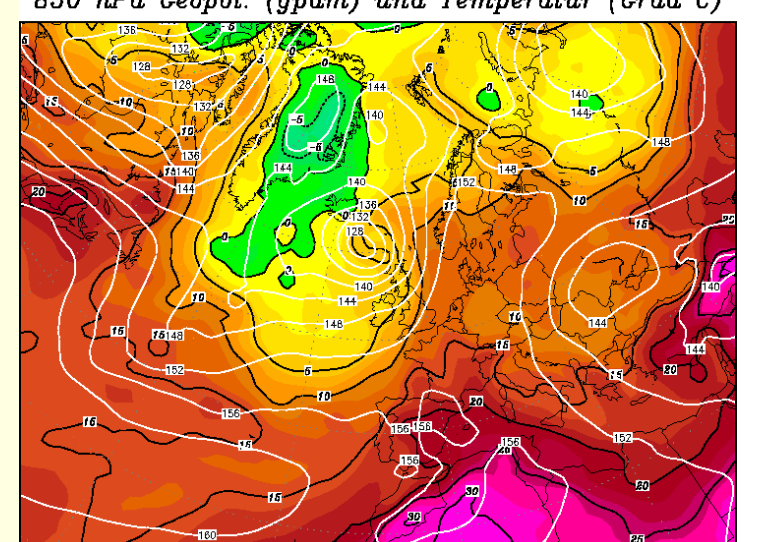
Bodendruck (hPa) und 850 hPa Aeq.Pot.T. (Grad C)



Daten: 00z-Lauf des MRF/AVN-Modells des amerikanischen Wetterdienstes
Wetterzentrale Karlsruhe
Top Karten : <http://www.wetterzentrale.de/topkarten/>

Init : Thu,15AUG2002 12Z

850 hPa Geopot. (gpdm) und Temperatur (Grad C)



Daten: 00z-Lauf des MRF/AVN-Modells des amerikanischen Wetterdienstes
Wetterzentrale Karlsruhe
Top Karten : <http://www.wetterzentrale.de/topkarten/>

The Netherlands Field Campaigns

**14 January – 10 February and
10 to 28 July 2002**



The Netherlands Field Campaigns

14 January – 10 February 2002 and 10 – 28 July 2002

- Titel MODIS satellite image of The Netherlands with frame of the study area (5 June 2000; NASA)
- Figure 1 Satellite Image of the study region with the locations of the vertical profile flights.
- Figure 2 Study site dominated by agriculture use.
- Figure 3 ‘Cabauw’ location – aerial photograph of the tall Cabauw tower and the ground reference site
- Figure 4 Combined measurement activity with the MFP ‘SkyArrow’ above the forest site.
- Figure 5 Ground reference sites ‘Forest’, ‘Maizefield’ and ‘Marshland’.
- Figure 6 MODIS satellite images from 29 January and 2 February 2002.
- Figure 7 Aerial photograph of the marshland area from 150 m above ground. Viewing south.
- Figure 8 Surrounding of the ‘Maizefield’ ground reference site.
- Figure 9 Picture of MFP ‘SkyArrow’ when passing the vertical profile site above the forest location.
- Figure 10 Ground reference site ‘Maizefield’ – pictures from the winter and the summer campaign.
- Figure 11 Aerial photograph of the marshland near the ground reference site.
- Figure 12 MODIS satellite images from 15 and 27 July 2002.

Winter Field Campaign

14 January – 10 February 2002

Flight profile samplings: 25, 29 and 31 January above the ‘Forest’ and the ‘Maize’ location,
30 January above the ‘Forest’ and the ‘Cabauw’ site.

2 February above all three locations ‘Forest’, ‘Maize’ and ‘Cabauw’

Sampling heights: 60, (100), 150, (300) and 900 m above ground.

Sampling times: Morning flights around 10:00 UTC, midday flights around 14:00 UTC.

Aircraft: Piper PA28, 180 HP. Single engine, propeller clockwise. Four seat low wing airplane. Flight speed during sampling procedure 75 knts (~140 km/h), climbing rate 1 m s^{-1} . Tube inlet mounted at left wing tip, approximately 15 cm beneath the profile bottom, facing downwards to the front.

Ground reference samplings: ‘*Loobos*’ on 4 February ‘night time’ [6:30 UTC], on
5 February ‘day time’ [13:00 UTC] and again ‘night time’ on
6 February [6:30 UTC]

‘*Maisfeld*’ on 4 February ‘morning’ [9:00 UTC] and ‘day time’
[13:00 UTC] and on 5 February ‘night time’ [6:30 UTC]

‘*Cabauw*’ on 6 February ‘day time’ [13:00 UTC] and on
7 February ‘night time’ at [6:30 UTC]

The Netherlands Winter Experiment

14 January – 10 February 2002

Test of the improved sampling strategy

A mosaic, formed by four major land form units, is characterizing the study region located within the central Netherlands: Two glacial ridges, orientated from south to north, are bearing mixed coniferous and deciduous forests or heathers. Most prominent is a mixture of agricultural land, commonly maize and grasslands, which is scattered by rural settlements. The marshlands, which are more frequent at the western edge of the study region and along the rivers, are predominately used for animal farming. At the margins and within the study region some large urban agglomerations are located; Rotterdam, Amsterdam and Utrecht, and the smaller cities Amersfoort, Ede and Apeldoorn.

Climatic conditions are specified by mean annual values for temperature of 9.5°C and precipitation of 750 – 950 mm. Compared with the German sites a more maritime character is obvious. Mean wind speed is around 4 m sec.⁻¹, most frequent are south-westerlies. During the campaign took place the weather conditions were quite unstable and in particular with respect to the air temperature not representative. The last decade of January was the warmest period recorded since 1901, the measured 15.5°C at the 2 February was even the highest temperature ever observed at this day of the year. Heavy south-westerly storms passed the region during the night times of the 26 and the 28 January.

Profile flights were performed at three different sites: above a mixed broadleaf and coniferous forest on all days, combined with sampling above a mixed agricultural, scattered populated area on three days and with sampling above marshland north of the tall Cabauw Tower on two days.

From the results of the last laboratory experiment, which was performed to analyse probable impairments caused by the drying agent (see chapter 3.2.2.), the time and operational scheme for flushing and sampling were adjusted to a new flushing duration of each 2 minutes with 10.5 l min⁻¹ respectively 3.0 l min⁻¹ and to a final 2 minute sampling period with a flow rate of 3.0 l min⁻¹.



Figure 1 Satellite image of the study region. The locations where the vertical profile flights were performed are marked by the red stars.



Figure 2 Study area 'Maize' dominated by agriculture use. Viewing north-west.

Picture: afternoon 2 February 2002



Figure 3 'Cabauw' location, viewing west. Marked are the tall 'Cabauw Tower' and the ground reference site where flask samplings were carried out.

Picture: 2 February 2002



Figure 4 Combined measurements with the 'SkyArrow' above the 'Forest site' at highest sampling level
~ 900 m above ground.

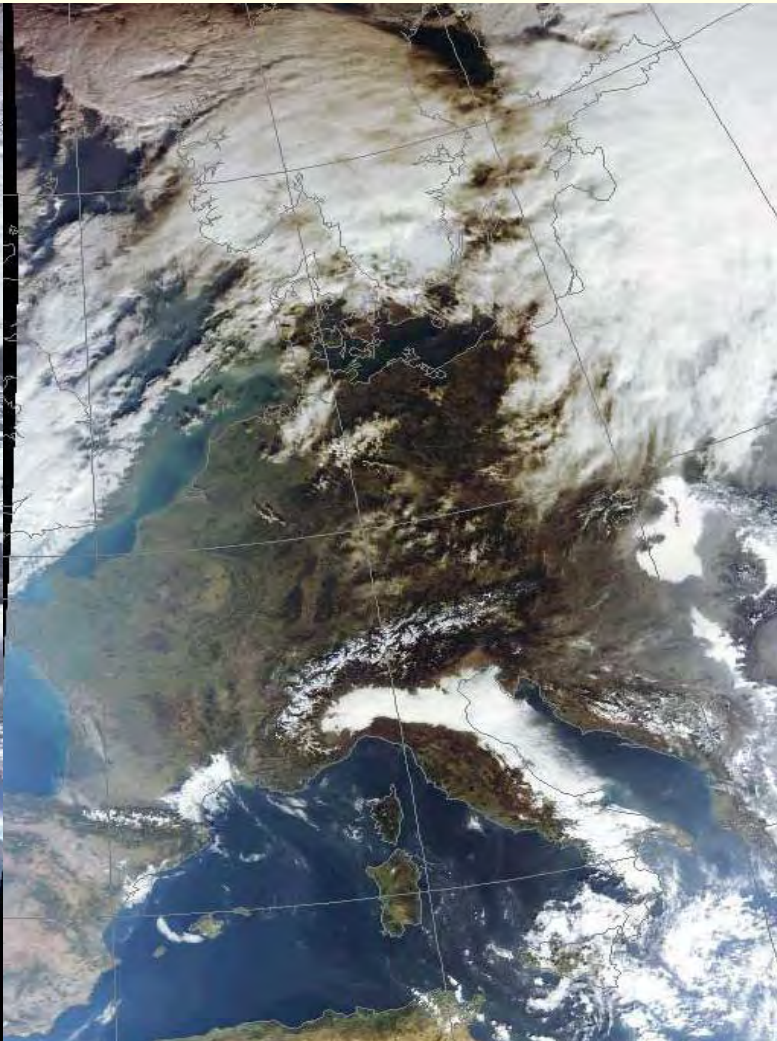
Picture: 29 January 2002



Figure 5 Ground reference sites: ‘Forest’ nearby the Loobos Fluxnet tower (left), the ‘Maizefield’ location (upper right panel) and the ‘Marshland’ site north of the Cabauw Tower.



29 January 2002 10:40 UTC



2 February 2002 10:15 UTC

Figure 6 MODIS Satellite Images (from Dundee Satellite Receiving Station) Satellite: Terra Sensor: MODIS
RGB composite image reprojected (RGB 1,4,3 composite)

Summer Field Campaign

10 – 28 July 2002 Enhancement of the improved sampling strategy

Flight profile samplings: 15, 16 and 27 July above all profile sites ‘Forest’, ‘Maize’ and ‘Cabauw’

Sampling heights: 60, 150, 900 and 1700 m above ground.

Sampling times: Morning flights started around 7:30 UTC, midday flights around 12:30 UTC.

Aircraft: Piper PA28, 180 HP. Single engine, propeller clockwise. Four seat low wing airplane. Flight speed during sampling procedure 75 knts (~140 km/h), climbing rate 1 m s^{-1} . Tube inlet mounted at left wing tip, approximately 15 cm beneath the profile bottom, facing downwards to the front.

Ground reference samplings: within the maizefield on 18 July ‘night time’ [4:00 UTC],
‘midday’ [11:00 UTC] and ‘afternoon’ [15:30 UTC]
above the marshland on 28 July ‘night time’ [4:00 UTC],
‘midday’ [12:30 UTC] and ‘afternoon’ [16:30 UTC]

As during the winter experiment the weather was unstable. Relatively colder and wetter conditions than expected from the long year averages were dominant.

Profiles were carried out at the identical locations as before, but combining this time all sites.

Additional ground reference studies were executed at the identical plots within the maize field and close to the Cabauw tower.



Figure 7 Marshland north of the Cabauw Tower. In the centre the tall 'Cabauw Tower'. Flight altitude approximately 150 m above ground.



Figure 8 Surrounding of the ground reference site 'Maizefield' (marked by the yellow arrow). Picture taken on 27 July from approximately 300 m above ground.



Figure 9 Above the forest study area. The MFP 'SkyArrow' passes the site on its transect while vertical profile is performed for flask sampling.

Picture: 16 July 2002

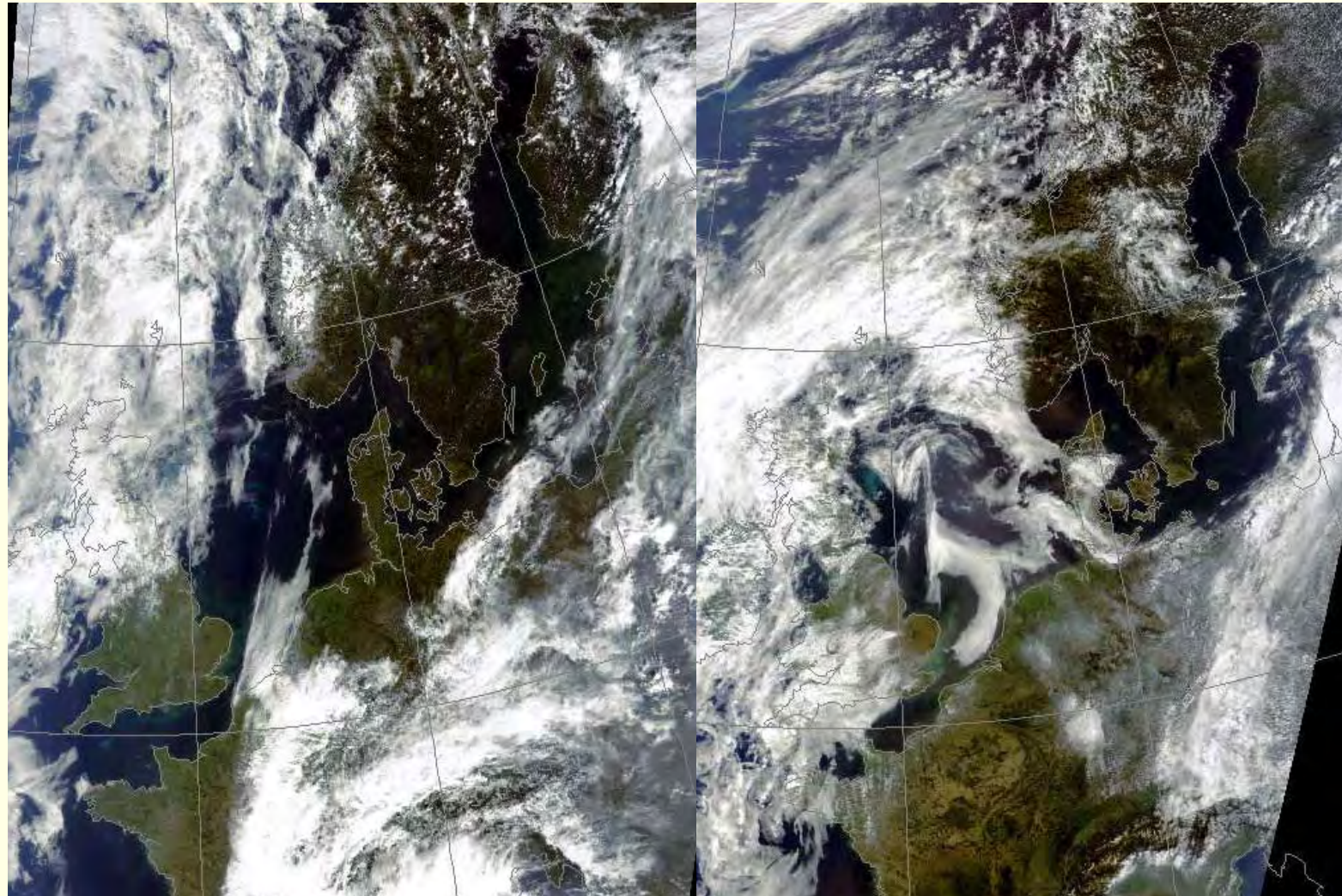


Figure 10 Ground reference site 'Maizefield' – upper panel on 4 February 2002, below on 18 July 2002



Figure 11 Aerial photograph of the marshland area. The ground reference unit was located close to the top left corner (yellow arrow). Flight altitude approximately 150 m above ground, viewing east.

Picture: 27 July 2002



15 July 2002 10:45 UTC

27 July 2002 11:10 UTC

Figure 12 MODIS Satellite Images (from Dundee Satellite Receiving Station) Satellite: Terra Sensor: MODIS
RGB composite image reprojected (RGB 1,4,3 composite)

Description of table parameters

date&time - date and time the sampling procedure was completed in Greenwich Mean Time

Flask code - marking of nameplates for each flask

site - location of the flight pattern, leg length ~2km

Mais - flight track, agricultural area, small villages, isolated farms, fertilizer factory
starting point south-east corner: 52°07'N / 5°40'E

Forst - flight track northwest of Vaassen (Apeldoorn), mixed forest, open heather
starting point south-east corner: 52°16'N / 5°54'E

Cabauw - flight track northeast of the Cabauw tower; marsh lands, small villages
turning point north-west corner: 52°00'N / 4°55'E

Loobos - ground reference sampling within a coniferous forest near the fluxnet tower
site 'Loobos': 52°10'N / 5°44'E

Maisfeld - ground reference sampling at a bare agricultural plot (former maize
cultivation): 52°09'N / 5°43'E

Cabauw - ground reference sampling north of the tall Cabauw Tower at grassland on
wet marsh soil: 51°59'N / 4°56'E

alt - sampling height in meter above ground, referring to the place of departure

init p. - internal flask pressure at the beginning of the analyses

Mixing Ratios

	Precision of the analyses
CH₄ [ppb] - methane mixing ratio in ppb	1.3 ppb
CO₂ [ppm] - carbon dioxide mixing ratio in ppm	0.08 ppm
N₂O [ppb] - nitrous oxide mixing ratio in ppb	0.15 ppb
CO [ppb] - carbon monoxide mixing ratio in ppb	1.0 ppb
H₂ [ppb] - hydrogen mixing ratio in ppb	5.0 ppb
SF₆ [ppt] - sulphur hexafluoride mixing ratio in ppt	0.08 ppt

Isotope Ratios

$$\delta[\$] = (R_{\text{sa}}/R_{\text{ref}} - 1) \cdot 1000 \quad R_{\text{sa}} \text{ and } R_{\text{ref}} \text{ are the sample and reference isotope ratios}$$

del ¹³C [\$] - ratio of the carbon 13 isotope and carbon 12 isotope due to the VPDB isotope ratio scale

del ¹⁸O [\$] - ratio of the oxygen 18 isotope and oxygen 16 isotope due to the VPDB (gas) isotope ratio scale

$$\text{Precision of the analyses} \quad {}^{13}\text{C} = 0.012 \$ \quad {}^{18}\text{O} = 0.02 \$$$

date&time [GMT]	Flask No.	site	alt [m]	init p.	mixing ratio						isotope	
					CH ₄ [ppb]	CO ₂ [ppm]	CO [ppb]	H ₂ [ppb]	SF ₆ [ppt]	N ₂ O [ppb]	del ¹³ C [%]	del ¹⁸ O [%]
25.01.2002 09:23	J185-01	Mais	60	2.3	2126.2	394.8	291.4	575.8	5.27	320.5	-9.465	-0.914
25.01.2002 09:23	J187-01	Mais	60	2.3	2114.8	394.6	290.9	575.1	5.07	320.3	-9.451	-0.964
25.01.2002 09:42	J197-01	Forst	60	2.2	2042.9	394.7	297.8	577.8	7.15	320.1	-9.338	-0.911
25.01.2002 09:42	J186-01	Forst	60	2.2	2060.5	395.7	304.2	577.7	7.03	320.2	-9.357	-0.957
25.01.2002 09:50	J198-01	Forst	107	2.2	1870.7	383.0	202.3	560.8	5.09	318.7	-8.786	-0.641
25.01.2002 09:50	J192-01	Forst	107	2.2	1878.0	383.9	203.8	550.9	5.05	318.6	-8.820	-0.661
25.01.2002 09:59	J193-01	Forst	152	2.2	1857.0	382.8	205.7	615.1	5.05	318.4	-8.762	-0.636
25.01.2002 09:59	J206-01	Forst	152	2.2	1857.4	382.7	202.1	596.5	4.97	318.4	-8.745	-0.615
25.01.2002 10:08	J188-01	Forst	305	2.2	1851.0	381.8	181.2	590.0	5.09	318.2	-8.692	-0.590
25.01.2002 10:08	J204-01	Forst	305	2.2	1847.6	381.3	180.2	584.0	4.95	318.3	-8.664	-0.564
29.01.2002 10:09	J189-01	Mais	60	2.3	1930.4	382.8	342.8	630.6	5.10	320.2	-8.758	-0.221
29.01.2002 10:09	J203-01	Mais	60	2.3	1929.1	382.7	346.3	627.7	5.09	320.1	-8.757	-0.245
29.01.2002 10:25	J090-01	Forst	60	2.3	1915.8	383.3	326.7	619.2	5.15	319.7	-8.804	-0.246
29.01.2002 10:25	J102-01	Forst	60	2.3	1915.0	383.3	323.5	616.7	5.11	319.8	-8.791	-0.271
29.01.2002 10:35	J091-01	Forst	107	2.3	1922.1	383.0	303.9	598.7	5.02	319.8	-8.769	-0.318
29.01.2002 10:35	J089-01	Forst	107	2.3	1915.2	383.1	290.1	592.5	5.18	319.8	-8.771	-0.280
29.01.2002 10:49	J100-01	Forst	152	2.2	1905.3	382.7	288.2	603.8	5.08	319.7	-8.737	-0.333
29.01.2002 10:49	J194-01	Forst	152	2.2	1912.9	382.7	278.3	597.0	5.17	319.7	-8.734	-0.314
29.01.2002 11:00	J199-01	Forst	305	2.2	1896.8	381.5	244.2	585.2	5.04	319.4	-8.687	-0.501
29.01.2002 11:00	J099-01	Forst	305	2.2	1900.2	381.7	242.1	585.3	5.08	319.3	-8.682	-0.261
29.01.2002 11:14	J087-01	Forst	915	2.2	1817.9	375.2	202.6	553.7	5.09	318.0	-8.339	-0.156
29.01.2002 14:26	J115-01	Mais	60	2.3	1917.9	383.2	217.8	562.9	5.37	320.1	-8.716	-0.256
29.01.2002 14:26	J110-01	Mais	60	2.3	1914.3	383.7	221.6	562.0	5.38	320.2	-8.744	-0.255
29.01.2002 14:41	J116-01	Forst	60	2.3	1900.9	381.8	210.0	564.4	5.28	319.9	-8.682	-0.212
29.01.2002 14:41	J118-01	Forst	60	2.2	1899.6	382.0	210.5	563.1	5.35	319.8	-8.667	-0.204
29.01.2002 14:49	J117-01	Forst	107	2.2	1903.3	382.2	208.9	562.9	5.42	320.0	-8.682	-0.270
29.01.2002 14:49	J562-01	Forst	107	2.2	1903.6	382.4	208.6	563.0	5.31	320.0	-8.687	-0.292
29.01.2002 14:57	J561-01	Forst	152	2.2	1903.9	382.4	205.7	574.5	5.45	320.3	-8.677	-0.266
29.01.2002 14:57	J112-01	Forst	152	2.2	1904.2	382.4	205.0	569.7	5.33	320.2	-8.680	-0.289
29.01.2002 15:05	J103-01	Forst	305	2.2	1912.0	382.3	201.4	574.7	5.32	320.2	-8.479	-0.243
29.01.2002 15:05	J565-01	Forst	305	2.2	1904.9	382.3	199.6	570.6	5.19	320.1	-8.668	-0.284
29.01.2002 15:16	J566-01	Forst	915	2.1	1810.7	375.4	142.5	548.0	5.00	318.3	-8.281	-0.021
29.01.2002 15:16	J564-01	Forst	915	2.1	1810.4	375.4	142.5	545.2	4.99	318.3	-8.306	-0.055
30.01.2002 10:03	J607-01	Cabauw	60	2.1	1983.4	391.6	285.1	579.2	5.39	320.4	-9.099	-0.453
30.01.2002 10:03	J606-01	Cabauw	60	2.1	1988.3	390.6	281.1	579.6	5.31	320.3	-9.071	-0.396
30.01.2002 10:11	J578-01	Cabauw	152	2.2	1974.5	390.8	284.4	578.3	5.44	320.5	-9.082	-0.365
30.01.2002 10:11	J568-01	Cabauw	152	2.2	1973.1	390.8	280.0	574.1	5.27	320.4	-9.101	-0.357
30.01.2002 10:19	J569-01	Cabauw	305	2.2	1925.8	387.4	256.3	582.8	5.14	320.5	-8.932	-0.275
30.01.2002 10:19	J580-01	Cabauw	305	2.2	1924.4	387.2	252.8	577.2	5.34	320.2	-8.907	-0.210
30.01.2002 10:30	J605-01	Cabauw	915	2.2	1834.9	375.6	165.2	559.2	5.17	318.9	-8.313	0.120
30.01.2002 11:09	J571-01	Forst	60	2.2	1970.3	384.3	239.0	565.7	5.46	320.0	-8.523	-0.106
30.01.2002 11:09	J567-01	Forst	60	2.2	1966.7	384.2	237.5	562.3	5.45	319.9	-8.732	-0.080
30.01.2002 11:17	J016-01	Forst	152	2.2	1962.3	384.4	226.7	579.6	5.25	319.8	-8.762	-0.140
30.01.2002 11:17	J577-01	Forst	152	2.2	1961.7	384.6	226.2	570.4	5.29	319.9	-8.739	-0.103
30.01.2002 14:14	J581-01	Cabauw	60	2.2	1987.4	385.4	270.0	570.8	5.25	320.9	-8.819	-0.079
30.01.2002 14:14	J584-01	Cabauw	60	2.2	1979.3	386.2	273.0	569.8	5.53	320.7	-8.833	-0.111
30.01.2002 14:24	J119-01	Cabauw	152	2.2	1964.7	386.2	255.9	563.0	5.50	320.9	-8.851	-0.105
30.01.2002 14:24	J586-01	Cabauw	152	2.2	1964.3	385.8	258.2	561.7	5.37	320.7	-8.843	-0.066
30.01.2002 14:33	J587-01	Cabauw	305	2.2	1936.9	385.3	241.1	567.5	5.39	320.8	-8.849	-0.126
30.01.2002 14:33	J593-01	Cabauw	305	2.0	1938.7	385.4	241.6	562.1	5.38	320.7	-8.840	-0.124
30.01.2002 14:45	J582-01	Cabauw	915	2.1	1833.9	372.5	159.2					

02.02.2002 09:57	J021-01	Cabauw	60	2.2	1909.0	386.5	202.1	544.3	5.01	319.6	-8.841	-0.273
02.02.2002 10:07	J032-01	Cabauw	152	2.2	1892.5	384.4	198.4	539.0	5.22	319.6	-8.739	-0.190
02.02.2002 10:07	J041-01	Cabauw	152	2.2	1893.8	386.3	199.4	535.8	4.95	319.5	-8.838	-0.283
02.02.2002 10:19	J033-01	Cabauw	915	2.1	1809.5	374.6	149.6	531.9	4.96	318.2	-8.277	0.151
02.02.2002 10:19	J055-01	Cabauw	915	2.1	1813.0	374.4	149.8	531.2	4.83	318.0	-8.262	0.180
02.02.2002 10:49	J049-01	Mais	60	2.2	1917.1	382.5	217.9	538.4	4.92	319.1	-8.670	-0.082
02.02.2002 10:49	J029-01	Mais	60	2.2	1918.1	382.2	219.8	539.4	5.05	319.3	-8.656	-0.044
02.02.2002 10:59	J051-01	Mais	152	2.2	1900.9	382.4	213.8	537.4	4.96	319.2	-8.670	-0.116
02.02.2002 10:59	J031-01	Mais	152	2.2	1906.0	382.2	211.3	532.5	5.15	319.2	-8.664	-0.039
02.02.2002 11:10	J052-01	Mais	915	2.1	1821.3	375.3	155.6	552.7	5.16	318.4	-8.321	0.164
02.02.2002 11:10	J044-01	Mais	915	2.1	1821.3	375.3	155.9	521.1	4.97	318.2	-8.312	0.136
02.02.2002 11:33	J034-01	Forst	60	2.2	1891.8	380.6	203.4	531.2	5.11	319.1	-8.580	0.010
02.02.2002 11:33	J040-01	Forst	60	2.2	1883.0	380.4	200.9	526.6	5.14	319.2	-8.578	-0.013
02.02.2002 11:42	J042-01	Forst	152	2.2	1878.9	380.7	198.7	537.7	5.04	319.1	-8.582	-0.032
02.02.2002 11:42	J053-01	Forst	152	2.2	1879.8	380.7	198.0	538.5	5.11	319.2	-8.589	0.019
02.02.2002 14:19	J028-01	Cabauw	60	2.2	1888.7	380.7	217.3	542.6	4.95	319.2	-8.596	0.030
02.02.2002 14:19	J043-01	Cabauw	60	2.2	1891.7	381.4	214.7	538.6	5.02	319.3	-8.623	0.005
02.02.2002 14:28	J545-01	Cabauw	152	2.2	1882.6	383.5	212.0	544.1	5.01	319.2	-8.710	-0.251
02.02.2002 14:28	J546-01	Cabauw	152	2.2	1882.0	382.3	211.5	545.0	5.05	319.2	-8.633	-0.070
02.02.2002 14:40	J548-01	Cabauw	915	2.1	1807.2	374.5	142.7	539.1	5.10	318.2	-8.260	0.070
02.02.2002 14:40	J557-01	Cabauw	915	2.1	1806.7	374.4	142.7	538.0	4.98	318.2	-8.257	0.107
02.02.2002 15:11	J553-01	Mais	60	2.2	1915.7	380.0	243.4	545.1	5.15	319.3	-8.550	0.129
02.02.2002 15:11	J550-01	Mais	60	2.2	1911.7	379.9	242.7	540.4	5.07	319.3	-8.506	0.141
02.02.2002 15:19	J551-01	Mais	152	2.2	1890.7	380.0	227.7	547.6	5.07	319.1	-8.525	0.071
02.02.2002 15:19	J059-01	Mais	152	2.2	1893.7	379.9	-999	-999	-999	319.2	-8.534	0.129
02.02.2002 15:31	J556-01	Mais	915	2.1	1812.3	374.8	139.5	547.0	5.02	318.5	-8.259	0.124
02.02.2002 15:31	J056-01	Mais	915	2.1	1812.5	374.8	125.6	504.5	4.82	318.3	-8.249	0.188
02.02.2002 16:04	J069-01	Forst	60	2.2	1875.3	379.4	214.8	539.9	5.07	319.1	-8.520	0.162
02.02.2002 16:04	J555-01	Forst	60	2.2	1875.1	379.4	211.6	533.5	4.95	319.1	-8.496	0.120
02.02.2002 16:13	J554-01	Forst	152	2.2	1875.7	379.8	213.0	541.6	5.10	319.1	-8.535	0.119
02.02.2002 16:13	J549-01	Forst	152	2.2	1873.3	379.7	212.0	538.1	5.18	319.0	-8.540	0.124
04.02.2002 06:40	J532-01	Loobos	0,1	2.3	1883.0	383.6	158.8	483.6	5.11	319.8	-8.751	-0.583
04.02.2002 06:40	J530-01	Loobos	0,1	2.3	1884.8	383.7	158.6	485.6	4.97	319.8	-8.764	-0.659
04.02.2002 07:08	J531-01	Loobos	1,0	2.3	1883.7	383.3	167.9	489.1	4.89	319.3	-8.716	-0.552
04.02.2002 07:08	J559-01	Loobos	1,0	2.3	1882.4	383.3	166.4	487.7	5.05	319.1	-8.701	-0.562
04.02.2002 06:54	J533-01	Loobos	2,0	2.3	1895.5	381.6	160.0	494.7	5.01	319.8	-8.630	-0.452
04.02.2002 06:54	J534-01	Loobos	2,0	2.3	1894.5	381.4	165.7	499.5	5.10	319.8	-8.624	-0.469
04.02.2002 07:24	J560-01	Loobos	5,0	2.2	1895.4	382.7	171.7	514.2	4.97	319.7	-8.682	-0.516
04.02.2002 07:24	J071-01	Loobos	5,0	2.2	1895.3	382.6	171.9	510.0	5.10	319.6	-8.693	-0.509
04.02.2002 09:13	J539-01	Maisfeld	0,1	2.3	1928.2	382.9	180.6	509.3	4.97	319.5	-8.672	-0.516
04.02.2002 09:13	J538-01	Maisfeld	0,1	2.3	1926.8	383.0	181.1	510.2	4.99	319.5	-8.686	-0.538
04.02.2002 09:26	J537-01	Maisfeld	1,0	2.3	1934.6	383.3	-999	-999	-999	319.3	-8.704	-0.510
04.02.2002 09:26	J536-01	Maisfeld	1,0	2.3	1933.8	383.2	178.7	514.6	4.93	319.4	-8.694	-0.531
04.02.2002 09:39	J535-01	Maisfeld	2,0	2.3	1927.6	383.1	177.0	511.9	4.91	319.6	-8.720	-0.491
04.02.2002 09:39	J544-01	Maisfeld	2,0	2.3	1930.4	383.0	176.9	511.3	4.99	319.5	-8.707	-0.483
04.02.2002 09:53	J543-01	Maisfeld	5,0	2.3	1928.4	382.7	176.5	511.3	4.96	319.2	-8.689	-0.470
04.02.2002 09:53	J542-01	Maisfeld	5,0	2.3	1925.2	382.6	175.7	512.1	5.03	319.0	-8.664	-0.507
04.02.2002 13:17	J160-01	Maisfeld	0,1	2.3	1919.0	381.0	178.2	508.7	5.04	319.5	-8.592	-0.354
04.02.2002 13:17	J165-01	Maisfeld	0,1	2.0	1919.9	380.9	178.4	507.4	5.06	319.4	-8.596	-0.405
04.02.2002 13:30	J166-01	Maisfeld	1,0	2.0	1916.0	380.8	174.9	506.1	5.07	319.5	-8.566	-0.350
04.02.2002 13:30	J167-01	Maisfeld	1,0	2.3	1914.4	380.7	174.3	506.5	5.10	319.4	-8.580	-0.327
04.02.2002 13:44	J168-01	Maisfeld	2,0	2.3	1914.5	380.7	178.7	509.2	5.06	319.3	-8.580	-0.346
04.02.2002 13:44	J547-01	Maisfeld	2,0	2.3	1912.4	380.6	177.5	508.6	5.17	319.3	-8.589	-0.313
04.02.2002 13:56	J558-01	Maisfeld	5,0	2.3	1908.8	380.5</td						

06.02.2002 13:48	J371-01	Cabauw	5,0	2.2	1951.6	382.8	208.0	531.4	5.31	319.3	-8.698	-0.545
06.02.2002 13:48	J365-01	Cabauw	5,0	2.3	1947.2	383.0	208.5	530.5	5.30	319.2	-8.708	-0.547
07.02.2002 06:40	J392-01	Cabauw	0,1	2.3	2315.6	400.4	175.0	498.6	5.40	325.9	-9.677	-0.845
07.02.2002 06:40	J382-01	Cabauw	0,1	2.3	2314.6	400.3	174.3	497.3	5.44	325.9	-9.673	-0.772
07.02.2002 06:54	J381-01	Cabauw	1,0	2.3	2056.5	398.4	178.3	503.4	5.35	324.2	-9.592	-0.775
07.02.2002 07:09	J391-01	Cabauw	2,0	2.3	2082.6	402.5	195.8	511.0	5.37	327.5	-9.772	-0.917
07.02.2002 07:09	J389-01	Cabauw	2,0	2.3	2079.1	402.3	195.8	514.3	5.39	327.3	-9.754	-0.843
07.02.2002 07:23	J388-01	Cabauw	5,0	2.3	2243.5	403.7	231.2	533.6	5.47	324.8	-9.822	-1.065
07.02.2002 07:23	J380-01	Cabauw	5,0	2.3	2247.3	403.8	230.8	531.4	5.47	324.8	-9.815	-1.036

Description of table parameters

date&time - date and time the sampling procedure was completed in Greenwich Mean Time

Flask code - marking of nameplates for each flask

site - location of the flight pattern, leg length ~2km

Mais - flight track, agricultural area, small villages, isolated farms, fertilizer factory
starting point south-east corner: 52°07'N / 5°40'E

Forst - flight track northwest of Vaassen (Apeldoorn), mixed forest, open heather
starting point south-east corner: 52°16'N / 5°54'E

Cabauw - flight track northeast of the Cabauw tower; marsh lands, small villages
turning point north-west corner: 52°00'N / 4°55'E

Maisfeld - ground reference sampling at a bare agricultural plot (former maize
cultivation): 52°09'N / 5°43'E

Marsch - ground reference sampling north of the tall Cabauw Tower at grassland on
wet marsh soil: 51°59'N / 4°56'E

alt - sampling height in meter above ground, referring to the place of departure

init p. - internal flask pressure at the beginning of the analyses

Mixing Ratios

	Precision of the analyses
CH₄ [ppb] - methane mixing ratio in ppb	1.3 ppb
CO₂ [ppm] - carbon dioxide mixing ratio in ppm	0.08 ppm
N₂O [ppb] - nitrous oxide mixing ratio in ppb	0.15 ppb
CO [ppb] - carbon monoxide mixing ratio in ppb	1.0 ppb
H₂ [ppb] - hydrogen mixing ratio in ppb	5.0 ppb
SF₆ [ppt] - sulphur hexafluoride mixing ratio in ppt	0.08 ppt

Isotope Ratios

$$\delta[\$] = (R_{\text{sa}}/R_{\text{ref}} - 1) \cdot 1000 \quad R_{\text{sa}} \text{ and } R_{\text{ref}} \text{ are the sample and reference isotope ratios}$$

del ¹³C [\$] - ratio of the carbon 13 isotope and carbon 12 isotope due to the VPDB isotope ratio scale

del ¹⁸O [\$] - ratio of the oxygen 18 isotope and oxygen 16 isotope due to the VPDB (gas) isotope ratio scale

$$\text{Precision of the analyses} \quad {}^{13}\text{C} = 0.012 \$ \quad {}^{18}\text{O} = 0.02 \$$$

date&time [GMT]	flask code	site	alt [m]	init p	mixing ratio						isotope	
					CH ₄ [ppb]	CO ₂ [ppm]	CO [ppb]	H ₂ [ppb]	SF ₆ [ppt]	N ₂ O [ppb]	del ¹³ C [%]	del ¹⁸ O [%]
15.07.2002 07:34	J272-01	Forst	60	2.0	2037.3	389.7	161.0	639.5	5.24	325.8	-9.082	-0.482
15.07.2002 07:34	J262-01	Forst	60	2.0	2040.3	389.7	161.4	632.7	5.26	326.1	-9.054	-0.462
15.07.2002 07:42	J497-01	Forst	152	2.0	1992.8	385.6	165.6	659.7	5.29	324.4	-8.910	-0.407
15.07.2002 07:42	J491-01	Forst	152	2.0	1993.3	385.3	163.9	644.7	5.23	324.3	-8.881	-0.417
15.07.2002 08:03	J490-01	Mais	60	2.0	2026.8	382.3	156.2	661.6	5.23	324.5	-8.712	-0.342
15.07.2002 08:03	J498-01	Mais	60	2.0	2029.6	382.9	157.4	643.0	5.26	324.7	-8.727	-0.413
15.07.2002 08:12	J496-01	Mais	152	2.0	2013.1	381.8	159.2	684.8	5.27	324.4	-8.680	-0.379
15.07.2002 08:12	J495-01	Mais	152	2.0	2009.5	381.4	159.3	676.3	5.30	324.1	-8.650	-0.336
15.07.2002 08:25	J489-01	Mais	915	1.9	1819.1	364.1	116.7	621.4	5.22	318.5	-7.781	0.503
15.07.2002 08:25	J261-01	Mais	915	1.9	1819.4	364.0	116.9	615.6	5.18	318.6	-7.760	0.546
15.07.2002 08:41	J488-01	Mais	1710	1.8	1815.2	364.3	139.1	625.2	5.20	318.7	-7.787	0.682
15.07.2002 08:41	J260-01	Mais	1710	1.8	1816.5	364.3	150.9	617.2	5.20	318.6	-7.794	0.778
15.07.2002 09:05	J494-01	Cabauw	60	2.0	1904.3	362.7	152.5	623.9	5.24	320.1	-7.735	0.301
15.07.2002 09:05	J499-01	Cabauw	60	2.0	1911.0	363.0	157.7	614.2	5.23	320.2	-7.703	0.321
15.07.2002 09:13	J493-01	Cabauw	152	1.5	1903.5	364.0	156.2	658.5	5.24	320.3	-7.720	0.185
15.07.2002 09:13	J492-01	Cabauw	152	1.9	1911.3	364.0	163.3	648.0	5.23	320.2	-7.750	0.192
15.07.2002 09:26	J271-01	Cabauw	915	1.8	1827.6	361.1	170.4	583.2	5.21	318.9	-7.586	0.465
15.07.2002 09:26	J483-01	Cabauw	915	1.8	1828.7	361.4	184.3	565.7	5.20	319.0	-7.596	0.654
15.07.2002 09:39	J484-01	Cabauw	1710	1.8	1819.2	364.1	138.3	595.9	5.23	318.5	-7.754	0.570
15.07.2002 09:39	J486-01	Cabauw	1710	1.8	1819.1	364.1	143.4	592.3	5.21	318.4	-7.771	0.592
15.07.2002 12:18	J362-01	Forst	60	1.9	1888.1	362.6	171.2	581.7	5.22	320.7	-7.769	0.345
15.07.2002 12:18	J363-01	Forst	60	2.0	1892.2	362.7	174.2	572.2	5.26	320.6	-7.771	0.388
15.07.2002 12:28	J376-01	Forst	152	1.9	1893.4	363.2	131.7	581.4	5.25	320.5	-7.785	0.354
15.07.2002 12:28	J267-01	Forst	152	2.0	1892.2	363.6	133.8	559.2	5.28	320.6	-7.776	0.392
15.07.2002 12:43	J270-01	Mais	60	2.0	1891.3	363.2	133.2	613.9	5.29	320.8	-7.824	0.284
15.07.2002 12:43	J362-01	Mais	60	2.0	1889.6	363.2	132.3	599.4	5.24	321.0	-7.799	0.270
15.07.2002 12:53	J264-01	Mais	152	2.0	1880.6	363.5	129.2	648.1	5.24	320.8	-7.790	0.326
15.07.2002 12:53	J257-01	Mais	152	2.0	1881.4	363.6	129.6	618.2	5.26	320.5	-7.801	0.392
15.07.2002 13:08	J266-01	Mais	915	1.9	1875.9	363.4	123.5	602.2	5.25	320.3	-7.741	0.427
15.07.2002 13:25	J361-01	Mais	1710	1.8	1811.0	366.0	113.8	607.5	5.28	318.2	-7.853	0.330
15.07.2002 13:25	J268-01	Mais	1710	1.5	1808.3	366.4	112.5	575.7	5.31	318.1	-7.810	0.391
15.07.2002 13:52	J355-01	Cabauw	60	2.0	1907.8	361.5	135.8	605.2	5.25	320.6	-7.674	0.403
15.07.2002 13:52	J375-01	Cabauw	60	2.0	1909.5	361.5	135.0	583.3	5.22	320.8	-7.647	0.380
15.07.2002 14:01	J377-01	Cabauw	152	1.8	1894.2	362.8	136.3	618.2	5.29	321.1	-7.601	0.017
15.07.2002 14:01	J374-01	Cabauw	152	2.0	1898.6	362.5	135.8	604.9	5.25	320.6	-7.691	0.319
15.07.2002 14:14	J269-01	Cabauw	915	1.9	1878.3	363.4	154.8	634.2	5.26	320.0	-7.760	0.373
15.07.2002 14:14	J373-01	Cabauw	915	1.9	1874.2	363.6	149.2	620.6	5.24	319.8	-7.752	0.328
15.07.2002 14:33	J259-01	Cabauw	1710	1.7	1809.3	364.6	138.8	582.9	5.22	318.8	-7.716	0.774
15.07.2002 14:33	J256-01	Cabauw	1710	1.9	1813.6	364.4	138.3	581.0	5.21	318.5	-7.798	0.641
16.07.2002 06:15	J567-01	Forst	60	2.0	1980.4	383.8	187.2	575.7	5.26	323.0	-8.720	0.350
16.07.2002 06:15	J525-01	Forst	60	1.4	1985.3	384.5	190.8	560.7	5.24	323.2	-8.692	0.393
16.07.2002 06:23	J560-01	Forst	152	2.0	1938.2	378.8	154.1	611.3	5.22	321.7	-8.532	0.251
16.07.2002 06:23	J559-01	Forst	152	2.0	1939.7	378.8	163.5	606.8	5.22	321.7	-8.535	0.289
16.07.2002 06:36	J561-01	Mais	60	2.0	2007.0	381.7	150.7	662.4	5.23	323.2	-8.713	0.209
16.07.2002 06:36	J562-01	Mais	60	2.0	-999	-999	160.0	651.1	5.24	-999	-999	-999
16.07.2002 06:44	J576-01	Mais	152	2.0	1964.6	378.9	151.0	703.3	5.24	322.1	-8.547	0.242
16.07.2002 06:44	J569-01	Mais	152	2.0	1960.8	379.2	164.4	695.8	5.26	322.1	-8.550	0.248
16.07.2002 06:57	J563-01	Mais	915	1.9	1819.6	365.0	157.4	686.2	5.19	318.3	-7.776	0.501
16.07.2002 06:57	J570-01	Mais	915	1.9	1818.5	364.8	167.7	674.1	5.14	318.3	-7.777	0.597
16.07.2002 07:14	J571-01	Mais	1710	1.8	1799.8	367.5	139.5	648.9	5.18	317.9	-7.896	0.406
16.07.2002 07:14	J565-01	Mais	1710	1.8	1800.8	367.5	139.9	638.9	5.			

27.07.2002 06:24	J146-01	Forst	152	2.0	1887.8	373.9	264.3	640.4	5.50	320.2	-8.252	0.388
27.07.2002 06:36	J472-01	Forst	915	1.5	1844.4	367.1	152.5	573.6	5.18	318.7	-7.882	0.399
27.07.2002 06:36	J474-01	Forst	915	1.8	1844.8	367.0	151.9	569.2	5.17	318.6	-7.900	0.370
27.07.2002 07:16	J149-01	Cabauw	60	2.0	2166.4	402.6	197.0	684.3	5.34	326.7	-9.566	-0.587
27.07.2002 07:16	J145-01	Cabauw	60	1.7	2160.2	402.1	202.8	681.0	5.28	326.5	-9.522	-0.576
27.07.2002 07:24	J142-01	Cabauw	152	2.0	2128.0	401.1	201.0	691.9	5.29	325.8	-9.483	-0.572
27.07.2002 07:36	J467-01	Cabauw	915	1.6	1811.2	363.2	154.0	574.3	5.30	318.3	-7.696	0.378
27.07.2002 07:36	J138-01	Cabauw	915	1.9	1811.8	363.2	-999	-999	-999	318.1	-7.701	0.456
27.07.2002 07:51	J466-01	Cabauw	1829	1.8	1782.0	369.2	-999	-999	-999	318.6	-7.988	0.599
27.07.2002 07:51	J160-01	Cabauw	1829	1.8	1782.8	369.1	125.5	563.1	5.15	318.7	-7.986	0.659
27.07.2002 08:15	J143-01	Mais	60	2.0	2107.8	385.4	263.5	594.2	5.45	323.5	-8.733	0.141
27.07.2002 08:15	J468-01	Mais	60	2.0	2139.9	387.8	257.3	595.4	5.50	323.7	-8.829	0.066
27.07.2002 08:23	J463-01	Mais	152	2.0	2120.6	386.8	317.5	633.5	5.48	323.5	-8.797	-0.064
27.07.2002 08:23	J465-01	Mais	152	2.0	2102.5	385.8	331.4	628.8	5.46	323.1	-8.755	-0.036
27.07.2002 08:34	J150-01	Mais	915	1.9	1802.5	364.1	131.4	529.5	5.16	317.6	-7.749	0.040
27.07.2002 08:34	J464-01	Mais	915	1.9	1802.9	364.1	132.4	529.8	5.17	317.6	-7.766	0.800
27.07.2002 08:49	J153-01	Mais	1829	1.7	1782.0	369.1	138.2	564.0	5.17	318.5	-7.764	0.599
27.07.2002 08:49	J151-01	Mais	1829	1.7	1781.8	369.1	133.4	557.7	5.15	318.6	-7.756	0.569
27.07.2002 12:16	J441-01	Forst	60	1.9	1928.2	364.0	161.2	565.3	5.33	320.8	-7.800	0.671
27.07.2002 12:16	J440-01	Forst	60	1.9	1933.7	364.1	162.8	560.9	5.36	320.9	-7.803	0.659
27.07.2002 12:24	J002-01	Forst	152	-999	1924.1	365.0	176.9	566.1	5.35	320.8	-7.767	0.807
27.07.2002 12:24	J014-01	Forst	152	1.9	1922.3	365.1	181.4	558.9	5.38	320.7	-7.766	0.800
27.07.2002 12:35	J009-01	Forst	915	1.9	1904.4	364.3	160.4	565.0	5.32	320.3	-7.764	0.599
27.07.2002 12:35	J444-01	Forst	915	1.9	1907.4	364.2	160.9	562.2	5.35	320.1	-7.756	0.569
27.07.2002 13:08	J012-01	Cabauw	60	2.0	1872.7	365.3	207.6	592.4	5.30	319.7	-7.953	0.435
27.07.2002 13:08	J015-01	Cabauw	60	2.0	1878.1	366.7	218.9	614.2	5.33	320.0	-7.994	0.416
27.07.2002 13:16	J013-01	Cabauw	152	2.0	1884.7	367.2	237.9	614.3	5.32	320.0	-7.998	0.330
27.07.2002 13:16	J001-01	Cabauw	152	1.9	1857.2	366.1	204.6	636.1	5.34	319.7	-8.007	0.325
27.07.2002 13:29	J003-01	Cabauw	915	1.9	1855.9	365.2	193.2	625.2	5.26	319.5	-7.948	0.258
27.07.2002 13:29	J006-01	Cabauw	915	1.9	1772.6	370.0	107.4	564.1	5.07	318.5	-7.910	0.499
27.07.2002 13:44	J008-01	Cabauw	1829	1.8	1772.3	369.7	109.2	561.9	5.09	318.6	-8.028	0.531
27.07.2002 13:44	J442-01	Cabauw	1829	2.0	1911.1	361.1	185.3	610.7	5.35	320.3	-8.041	0.522
27.07.2002 14:09	J007-01	Mais	60	2.0	1909.4	361.0	187.3	607.3	5.34	320.4	-7.728	0.682
27.07.2002 14:09	J005-01	Mais	60	2.0	1906.0	361.8	171.4	649.3	5.34	320.6	-7.719	0.661
27.07.2002 14:18	J004-01	Mais	152	2.0	-999	-999	175.5	641.8	5.36	-999	-7.740	0.550
27.07.2002 14:18	J011-01	Mais	152	2.0	1881.0	365.7	221.4	590.9	5.34	319.9	-999	-999
27.07.2002 14:29	J141-01	Mais	915	1.9	1900.3	361.0	181.2	627.5	5.36	320.3	-7.698	0.754
27.07.2002 14:29	J010-01	Mais	915	1.9	1899.9	361.1	178.5	620.3	5.32	320.3	-7.711	0.710
27.07.2002 14:44	J445-01	Mais	1829	1.9	1776.1	369.2	115.6	563.6	5.16	318.6	-8.022	0.546
27.07.2002 14:44	J139-01	Mais	1829	1.9	1777.5	369.1	117.2	563.5	5.16	318.6	-8.009	0.634
18.07.2002 04:10	J253-01	Maisfeld	0,1	2.1	1841.7	392.6	112.3	473.4	5.16	323.7	-8.597	-0.591
18.07.2002 04:10	J252-01	Maisfeld	0,1	2.1	1841.3	394.1	112.2	472.4	5.12	324.5	-8.639	-0.593
18.07.2002 04:23	J251-01	Maisfeld	0,5	2.1	1926.5	397.9	112.9	485.8	5.15	332.0	-8.762	-0.693
18.07.2002 04:23	J250-01	Maisfeld	0,5	2.1	1928.5	394.0	113.2	486.3	5.17	330.8	-8.663	-0.679
18.07.2002 04:38	J248-01	Maisfeld	1,0	2.1	1889.4	399.6	113.5	472.9	5.14	325.7	-8.771	-0.779
18.07.2002 04:38	J237-01	Maisfeld	1,0	2.1	1888.5	399.4	113.2	470.1	5.15	325.5	-8.780	-0.778
18.07.2002 04:52	J238-01	Maisfeld	2,0	2.1	1879.7	384.6	114.4	484.2	5.13	324.7	-8.444	-0.416
18.07.2002 04:52	J236-01	Maisfeld	2,0	2.1	1883.1	385.9	114.1	482.2	5.15	325.0	-8.480	-0.548
18.07.2002 05:06	J234-01	Maisfeld	5,0	2.0	1926.4	381.8	116.0	494.3	5.13	319.8	-8.460	-0.395
18.07.2002 05:06	J230-01	Maisfeld	5,0	2.1	1925.3	382.2	115.8	492.9	5.13	319.9	-8.473	-0.402
18.07.2002 11:10	J244-01	Maisfeld	0,1	2.1	1820.4	362.9	119.2	496.8	5.17	319.0	-7.879	0.435
18.07.2002 11:10	J243-01	Maisfeld	0,1	2.1	1817.3	361.9	118.6	497.8	5.13	319.0	-7.835	0.445
18.07.2002 11:24	J242-01	Maisfeld	0,5	2.1	1826.9	361.1	121.3	490.4	5.16	320.1	-7.810	0.381
18.07.2002 11:24	J239-01	Maisfeld</										

28.07.2002 13:20	J226-01	Marsch	5,0	2.1	1975.1	370.1	213.0	536.0	5.57	321.7	-7.982	1.032
28.07.2002 13:20	J447-01	Marsch	5,0	2.1	1976.7	370.2	211.1	536.5	5.56	321.8	-7.982	1.038
28.07.2002 16:40	J398-01	Marsch	0,1	2.1	2020.8	358.7	208.6	520.5	5.81	321.9	-7.579	1.610
28.07.2002 16:40	J399-01	Marsch	0,1	2.1	2045.4	362.8	208.9	510.7	5.78	322.5	-7.806	1.497
28.07.2002 16:52	J431-01	Marsch	1,0	2.1	2141.3	367.8	212.5	543.5	5.72	321.4	-7.999	0.868
28.07.2002 16:52	J446-01	Marsch	1,0	2.1	2110.2	366.4	210.9	539.9	5.76	321.4	-7.945	0.920
28.07.2002 17:04	J437-01	Marsch	2,0	2.1	1979.2	362.3	201.7	534.7	5.69	320.5	-7.704	0.984
28.07.2002 17:04	J436-01	Marsch	2,0	2.1	1961.0	362.8	199.4	535.3	5.70	320.5	-7.728	0.926
28.07.2002 17:17	J435-01	Marsch	5,0	2.1	1964.8	360.4	193.3	531.6	5.66	320.4	-7.639	1.043
28.07.2002 17:17	J433-01	Marsch	5,0	2.1	1970.0	360.4	193.4	531.6	5.66	320.4	-7.650	1.077

Summer Field Campaign

Thuringia

15 July – 2 August 2001



Summer Field Campaign

15 July – 2 August 2001

Flight profile samplings on 17, 21, and 23 July above the Gebesee agricultural site and on 24 and 25 July above the Hainich

Sampling heights: Because of clouds the sampling heights had to be adapted sometimes between the flights. Lowest sampling level at Gebesee site was 100 m, above the Hainich 90 m above ground. Since the development of the CBL varied between the days and due to the power capability of the aircraft (related with air temperature) the top height differs from 1800 to 2500 m above ground.

Sampling times: Morning flights around 8:45 UTC, midday flights around 12:30 UTC, afternoon flights around 16:30 UTC.
On 17 and 25 July only two flights per day, caused by fog in the morning and technical problems with the sampling unit, respectively.

Aircraft: Wilga-35, 260 HP. Single 9-cylinder radial engine, propeller clockwise. Four seat shoulder wing airplane. Flight speed during sampling procedure 75 knts (~140 km/h), climbing rate 1 m s^{-1} . Tube inlet mounted at right wing tip, approximately 10 cm beneath the profile bottom, facing downwards to the front

Summer Field Campaign

15 July – 2 August 2001

During the campaign only small air pressure contrasts occurred over Central Europe. A stable high pressure zone over Russia was dominant, faint low pressure cells crossed the region between 19 and 21 July. From 22 July on high pressure conditions were dominating. A low pressure area, generated on 23 July west of Greenland, did not affect the region until the end of the campaign. In July 2001 the temperature anomaly recorded at Erfurt Airport was +1.5°C, the amount of the precipitation was 161% of the 30-year-average (1961 – 1990). Until 15 July the cumulative sum of rain was 67.7 mm, which was 81 % of the monthly total amount. After 21 July no more precipitation was recorded.

Summer Field Campaign

15 July – 2 August 2001

Figure 1 Satellite Image of the study region with the locations of the vertical profile flights.

Figure 2 Aerial photograph of the agricultural study site 'Gebesee'. Viewing south-east.

Figure 3 Hainich Tower from 300 m above ground.

Figure 4 MODIS Satellite Images of Central Europe; 23 and 24 July 2001

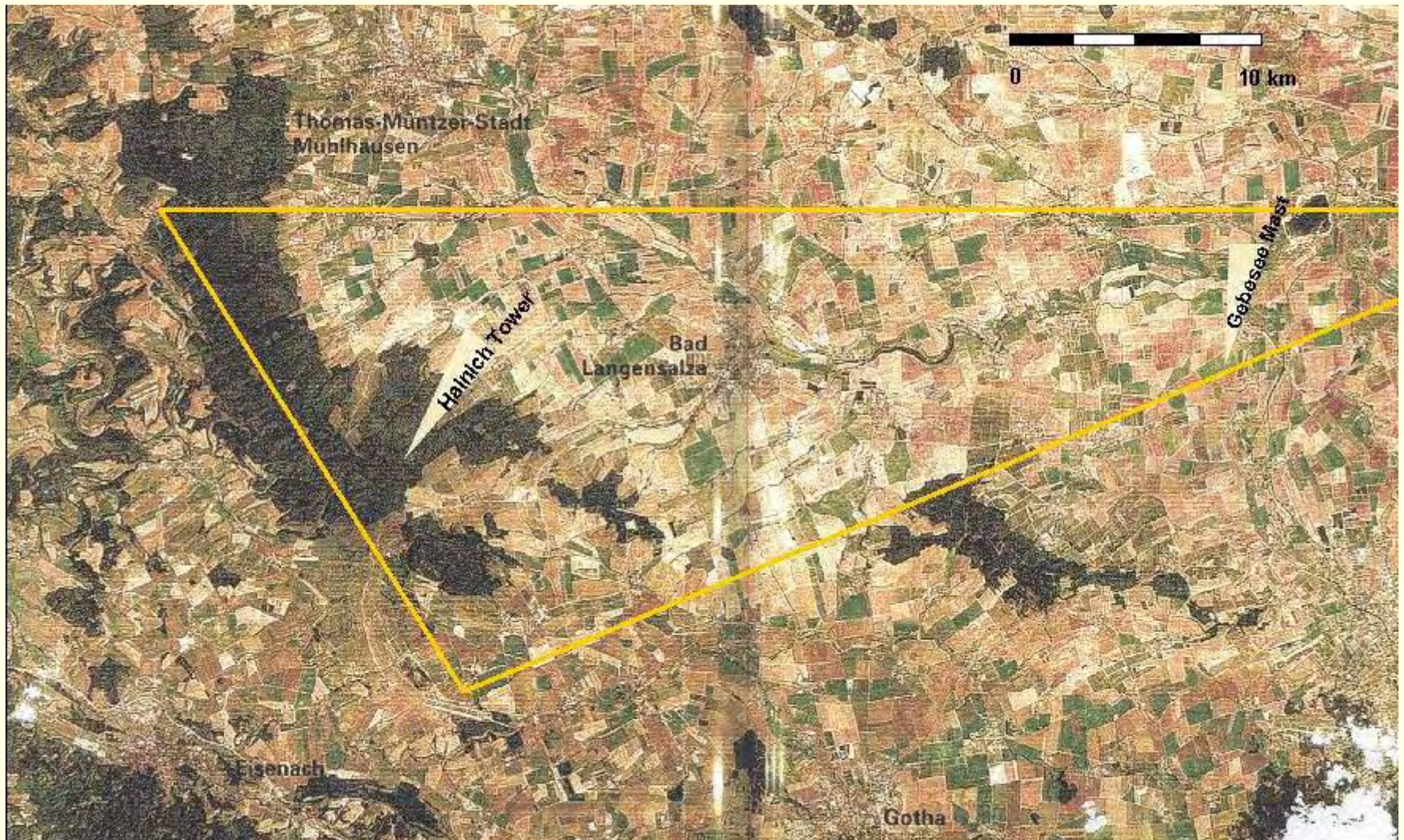


Figure 1 Satellite image of the study region with the locations of the towers, where vertical profile flights were performed, and flight track of the MobileFluxPlatform ‘SkyArrow’.

Image taken from Winter et al. 1998 (modified)



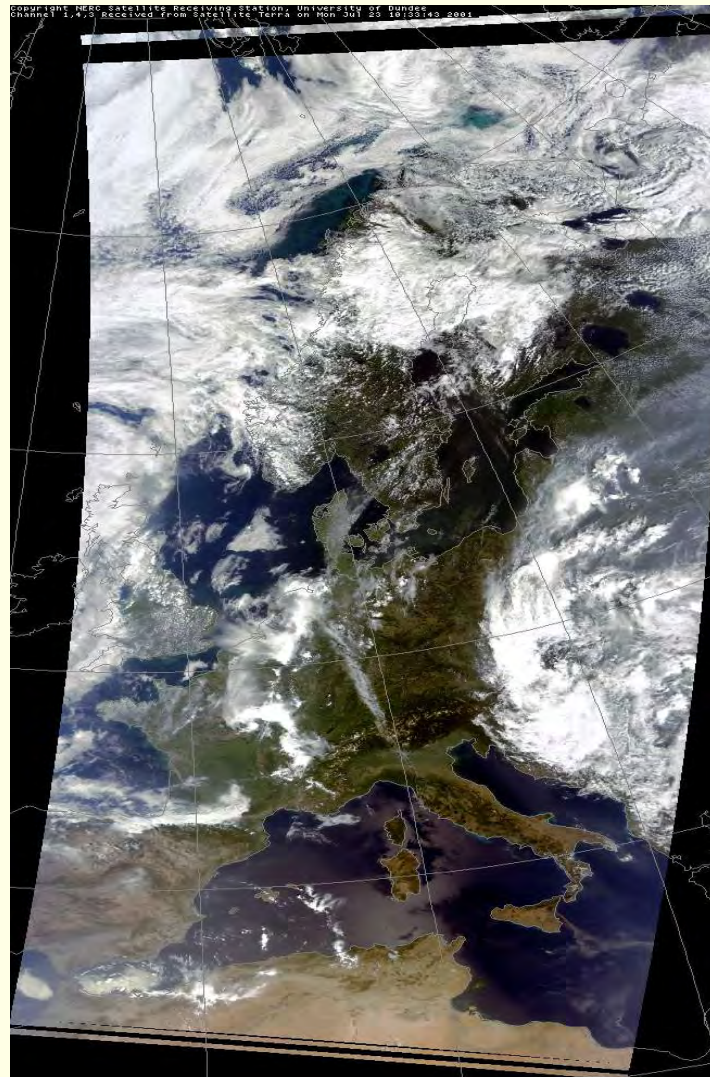
Figure 2 Gebesee agricultural study site. The flux tower is marked by the yellow circle. Most of the grain fields are still harvested. Flight altitude approximately 1000 m above ground, viewing south-east.

Picture: late afternoon 25 July 2001



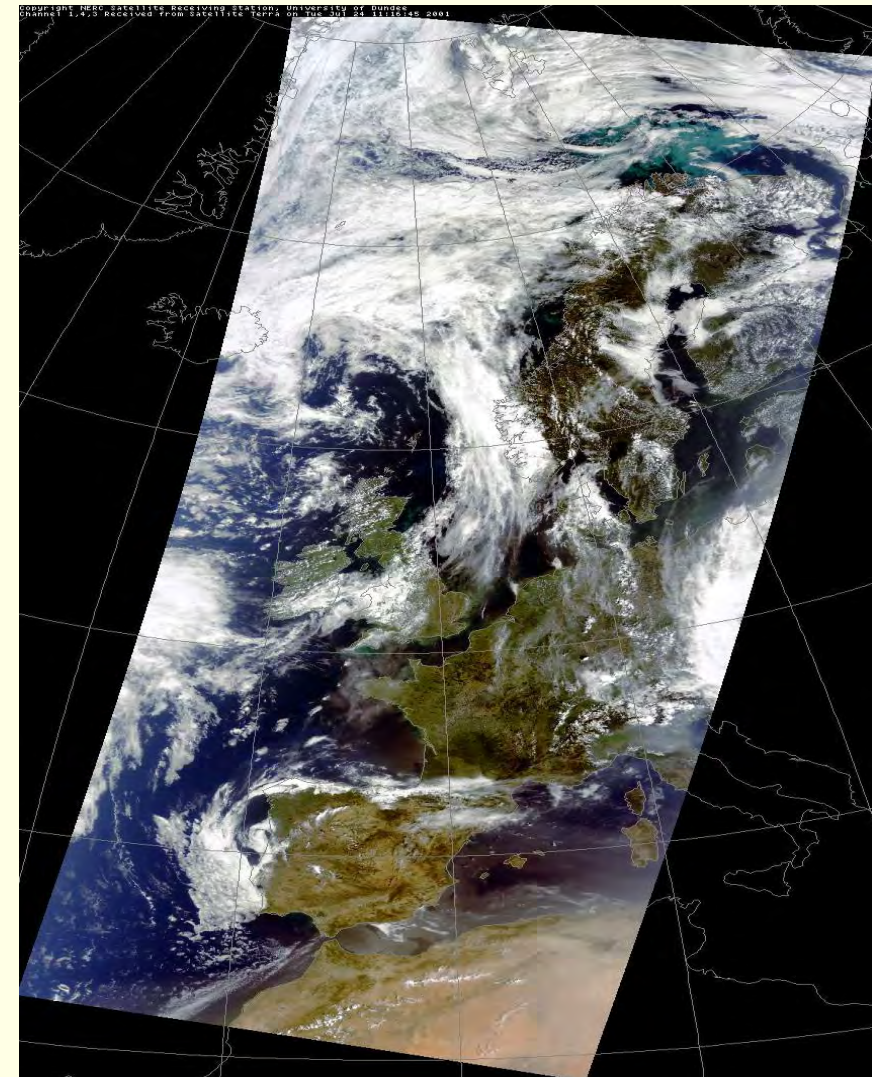
Figure 3 Aerial photograph of the Hainich Tower (located in the center). Flight altitude approximately 300 m above ground.

Picture: 25 July 2001



23 July 2001

10:33 UTC



24 July 2001 11:16 UTC

Figure 4 MODIS Satellite Images (from Dundee Satellite Receiving Station) Satellite: Terra Sensor: MODIS
RGB composite image reprojected (RGB 1,4,3 composite)

Description of table parameters

date&time - date and time the sampling procedure was completed in Greenwich Mean Time

Flask code - marking of nameplates for each flask

Site - location of the flight pattern, tower sites

Gebesee, agricultural site north of Erfurt, 6 m tower; 51°06,1'N / 10°55,0'E, 162 m a.MSL

Hainich, beech forest north of Eisenach, 42 m tower; 51°04,7'N / 10°27,1'E, 439 m a.MSL

alt - sampling height in meter above ground, referring to the place of departure

Mixing ratios

Precision of the analyses

CH4 [ppb] - methan mixing ratio in ppb 1.3 ppb

CO2 [ppm] - carbon dioxide mixing ratio in ppm 0.08 ppm

N2O [ppb] - nitrous oxide mixing ratio in ppb 0.15 ppb

Isotope Ratio

$$\delta[\$] = (R_{\text{sa}}/R_{\text{ref}} - 1) \cdot 1000 \quad R_{\text{sa}} \text{ and } R_{\text{ref}} \text{ are the sample and reference isotope ratios}$$

del 13C - ratio of the carbon 13 isotope and carbon 12 isotope due to the VPDB isotope ratio scale

del 18O - ratio of the oxygen 18 isotope and oxygen 16 isotope due to the VPDB (gas) isotope ratio scale

Precision of the analyses $^{13}\text{C} = 0.012 \$$ $^{18}\text{O} = 0.02 \$$

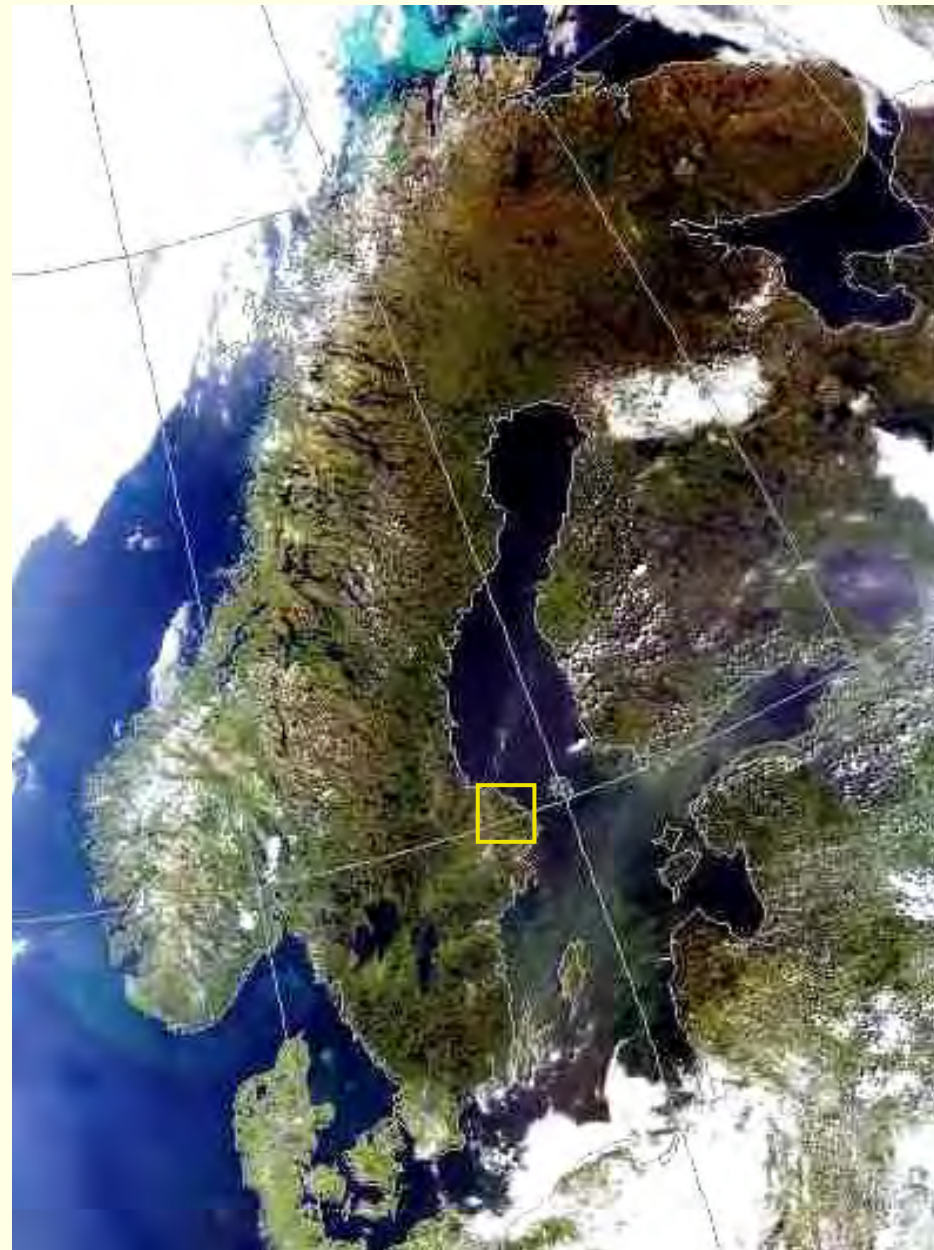
Because of problems with the sampling system a number of flasks (24th and 25th July) were not filled with overpressure. These flasks (laid underneath in yellow colour) were analyzed separately in April 2002 and are not directly comparable – be aware of this!!!

date & time (GMT)	flask code	site	alt [m]	mixing ratio			isotope ratios	
				CH ₄ [ppb]	CO ₂ [ppm]	N ₂ O [ppb]	del δ ¹³ C [%]	del δ ¹⁸ O [%]
17.07.2001 12:55	J399-01	Gebesee	100	1844.7	358.8	316.0	-7.750	-0.290
17.07.2001 12:55	J431-01	Gebesee	100	1846.6	362.4	323.1	-7.750	-0.280
17.07.2001 13:02	J433-01	Gebesee	300	1842.8	355.1	311.6	-7.750	-0.310
17.07.2001 13:02	J432-01	Gebesee	300	1842.0	358.8	314.7	-7.780	-0.280
17.07.2001 13:10	J398-01	Gebesee	500	1842.0	359.1	315.5	-7.790	-0.390
17.07.2001 13:10	J396-01	Gebesee	500	1843.6	362.1	317.4	-7.810	-0.330
17.07.2001 13:19	J393-01	Gebesee	700	1843.8	362.0	317.3	-7.790	-0.460
17.07.2001 13:19	J392-01	Gebesee	700	1841.9	359.6	315.7	-7.800	-0.440
17.07.2001 13:32	J394-01	Gebesee	1400	1838.8	360.6	315.7	-7.800	-0.190
17.07.2001 13:32	J395-01	Gebesee	1400	1838.6	362.1	316.9	-7.810	-0.270
17.07.2001 13:46	J335-01	Gebesee	2000	1820.5	360.0	313.5	-7.850	0.070
17.07.2001 13:46	J397-01	Gebesee	2000	1822.3	362.7	315.3	-7.850	0.000
17.07.2001 16:35	J608-01	Gebesee	340	1858.0	358.2	318.2	-7.570	-0.310
17.07.2001 16:35	J609-01	Gebesee	340	1859.3	358.8	318.0	-7.570	-0.180
17.07.2001 16:47	J516-01	Gebesee	840	1856.0	358.7	317.9	-7.630	-0.270
17.07.2001 16:47	J515-01	Gebesee	840	1854.9	359.7	318.0	-7.650	-0.270
17.07.2001 16:57	J607-01	Gebesee	1140	1854.9	359.3	318.2	-7.640	-0.360
17.07.2001 16:57	J389-01	Gebesee	1140	1855.1	359.9	318.0	-7.670	-0.210
17.07.2001 17:11	J391-01	Gebesee	1740	1843.8	361.9	317.9	-7.760	-0.180
17.07.2001 17:11	J610-01	Gebesee	1740	1840.8	362.5	317.8	-7.790	-0.060
17.07.2001 17:25	J390-01	Gebesee	2040	-999	-999	-999	-999	-999
17.07.2001 17:25	J387-01	Gebesee	2040	-999	-999	-999	-999	-999
21.07.2001 08:49	J488-01	Gebesee	100	1840.8	360.5	317.8	-7.610	-0.260
21.07.2001 08:49	J486-01	Gebesee	100	1842.0	361.4	317.5	-7.670	-0.140
21.07.2001 08:58	J490-01	Gebesee	300	1834.5	361.5	317.6	-7.720	-0.120
21.07.2001 08:58	J484-01	Gebesee	300	1837.6	361.8	317.5	-7.730	-0.070
21.07.2001 09:07	J487-01	Gebesee	500	1835.4	361.5	317.6	-7.700	-0.130
21.07.2001 09:07	J485-01	Gebesee	500	1835.4	361.9	317.5	-7.720	-0.070
21.07.2001 09:17	J489-01	Gebesee	700	1837.0	361.1	317.5	-7.700	-0.130
21.07.2001 09:17	J492-01	Gebesee	700	1837.1	361.7	317.6	-7.700	-0.090
21.07.2001 09:30	J493-01	Gebesee	1400	1806.8	361.1	317.1	-7.660	-0.030
21.07.2001 09:30	J491-01	Gebesee	1400	1805.8	361.2	316.9	-7.690	-0.030
21.07.2001 09:49	J591-01	Gebesee	2500	1807.0	363.6	317.2	-7.800	-0.030
21.07.2001 09:49	J590-01	Gebesee	2500	1806.7	363.7	317.1	-7.810	-0.070
21.07.2001 12:13	J480-01	Gebesee	100	1829.2	356.5	317.3	-7.450	0.080
21.07.2001 12:13	J479-01	Gebesee	100	1828.5	357.0	317.5	-7.500	0.140
21.07.2001 12:21	J514-01	Gebesee	300	1830.7	357.5	317.7	-7.510	0.160
21.07.2001 12:21	J513-01	Gebesee	300	1831.0	357.8	317.5	-7.510	0.160
21.07.2001 12:30	J512-01	Gebesee	500	1828.9	357.7	317.6	-7.520	0.160
21.07.2001 12:30	J511-01	Gebesee	500	1827.9	358.2	317.5	-7.530	0.150
21.07.2001 12:38	J510-01	Gebesee	700	1829.3	357.8	317.4	-7.530	0.160
21.07.2001 12:38	J509-01	Gebesee	700	1829.2	358.1	317.4	-7.540	0.150
21.07.2001 12:51	J508-01	Gebesee	1400	1822.4	358.0	317.6	-7.520	0.070
21.07.2001 12:51	J507-01	Gebesee	1400	1824.1	358.6	317.5	-7.540	0.130
21.07.2001 13:10	J505-01	Gebesee	2300	1815.3	363.1	317.4	-7.760	-0.030
21.07.2001 13:10	J502-01	Gebesee	2300	1814.9	363.4	317.3	-7.750	-0.050
21.07.2001 16:21	J606-01	Gebesee	100	1825.2	355.1	317.5	-7.360	0.220
21.07.2001 16:21	J605-01	Gebesee	100	1826.7	355.6	317.3	-7.430	0.430
21.07.2001 16:30	J497-01	Gebesee	300	1827.1	356.7	317.5	-7.510	0.220
21.07.2001 16:30	J588-01	Gebesee	300	1824.7	356.9	317.5	-999	-999
21.07.2001 16:38	J494-01	Gebesee	500	1824.8	357.2	317.4	-7.540	0.260
21.07.2001 16:38	J496-01	Gebesee	500	1824.6	357.7	317.4	-7.540	0.340
21.07.2001 16:46	J589-01	Gebesee	700	1825.2	357.7	317.6	-7.550	0.250
21.07.2001 16:46	J495-01	Gebesee	700	1825.1	357.7	317.5	-7.540	0.300
21.07.2001 16:59	J604-01	Gebesee	1400	1824.8	357.3	317.5	-7.520	0.280
21.07.2001 16:59	J602-01	Gebesee	1400	1825.3	357.5	317.5	-7.530	0.300
21.07.2001 17:17	J597-01	Gebesee	2200	1793.9	363.9	316.8	-7.780	0.100
21.07.2001 17:17	J603-01	Gebesee	2200	1797.0	364.0	316.7	-7.790	0.180
23.07.2001 08:48	J586-01	Gebesee	100	1971.3	400.3	321.1	-9.620	-0.110
23.07.2001 08:48	J585-01	Gebesee	100	1981.4	403.4	321.6	-9.720	-0.080
23.07.2001 08:59	J583-01	Gebesee	500	1855.2	369.3	318.8	-8.220	0.210
23.07.2001 08:59	J584-01	Gebesee	500	1869.8	373.7	318.8	-8.420	0.240
23.07.2001 09:10	J582-01	Gebesee	900	1859.3	369.8	318.6	-8.200	0.230
23.07.2001 09:10	J580-01	Gebesee	900	1841.9	365.7	318.2	-8.020	0.320
23.07.2001 09:28	J581-01	Gebesee	1600	1780.2	366.0	318.3	-7.880	0.110
23.07.2001 09:28	J579-01	Gebesee	1600	1779.5	364.9	317.4	-7.870	0.370
23.07.2001 09:43	J578-01	Gebesee	1800	1783.8	364.2	317.5	-7.840	0.400
23.07.2001 09:43	J577-01	Gebesee	1800	1781.2	364.4	317.3	-7.860	0.470
23.07.2001 12:34	J483-01	Gebesee	100	1814.9	361.2	317.9	-7.790	0.140
23.07.2001 12:34	J481-01	Gebesee	100	1820.8				

23.07.2001 16:28	J572-01	Gebesee	900	1828.4	363.7	318.2	-7.880	0.420
23.07.2001 16:28	J571-01	Gebesee	900	1825.6	364.0	318.0	-7.910	0.330
23.07.2001 16:44	J570-01	Gebesee	1600	1812.9	363.1	317.9	-7.830	0.300
23.07.2001 16:44	J569-01	Gebesee	1600	1815.3	363.2	318.0	-7.860	0.250
23.07.2001 16:57	J596-01	Gebesee	1950	1797.7	362.0	317.5	-7.770	0.250
23.07.2001 16:57	J482-01	Gebesee	1950	1797.0	362.0	317.3	-7.770	0.210
24.7.01 7:23	J386-01	Hainich	90	1836.7	360.9	318.5	-7.741	0.600
24.7.01 7:23	J385-01	Hainich	90	1837.9	361.4	319.5	-7.555	0.803
24.7.01 7:31	J384-01	Hainich	190	1816.4	362.0	318.6	-7.739	0.538
24.7.01 7:31	J383-01	Hainich	190	1817.1	361.3	318.5	-7.719	0.627
24.7.01 7:42	J382-01	Hainich	590	1812.5	363.0	318.2	-7.810	0.569
24.7.01 7:42	J381-01	Hainich	590	1813.2	362.9	318.3	-7.793	0.589
24.7.01 7:51	J380-01	Hainich	990	1804.9	365.4	318.5	-7.855	0.364
24.7.01 7:51	J364-01	Hainich	990	1805.4	365.4	318.4	-7.884	0.354
24.7.01 8:04	J363-01	Hainich	1390	1800.7	364.6	317.9	-7.841	0.281
24.7.01 8:04	J362-01	Hainich	1390	1801.1	364.6	317.8	-7.821	0.252
24.7.01 8:21	J361-01	Hainich	1890	1839.9	363.6	319.1	-7.798	0.745
24.7.01 8:21	J498-01	Hainich	1890	1838.4	362.6	319.0	-7.732	0.778
24.7.01 12:16	J472-01	Hainich	90	1842.4	374.2	327.7	-7.951	0.229
24.7.01 12:16	J360-01	Hainich	90	1838.6	365.8	321.8	-7.773	-0.523
24.7.01 12:25	J468-01	Hainich	190	1840.4	360.7	317.7	-7.779	-0.004
24.7.01 12:25	J466-01	Hainich	190	1841.0	361.0	317.3	-7.798	-0.599
24.7.01 12:34	J467-01	Hainich	590	1844.9	360.9	317.5	-7.794	0.177
24.7.01 12:34	J465-01	Hainich	590	1841.9	361.0	316.9	-7.796	-0.656
24.7.01 12:45	J464-01	Hainich	990	1833.0	359.9	316.9	-7.751	-0.242
24.7.01 12:45	J478-01	Hainich	990	1841.3	359.0	316.6	-999	-999
24.7.01 12:57	J477-01	Hainich	1390	1843.8	363.5	317.0	-7.752	-0.595
24.7.01 12:57	J476-01	Hainich	1390	1847.2	359.0	316.3	-999	-999
24.7.01 13:16	J475-01	Hainich	1890	1882.0	355.8	318.0	-999	-999
24.7.01 13:16	J474-01	Hainich	1890	1851.9	356.3	316.4	-999	-999
24.7.01 15:44	J456-01	Hainich	90	1873.5	359.1	316.7	-999	-999
24.7.01 15:44	J455-01	Hainich	90	1847.6	359.0	316.8	-7.622	-0.032
24.7.01 15:53	J357-01	Hainich	190	1855.1	360.0	317.5	-999	-999
24.7.01 15:53	J358-01	Hainich	190	1838.4	359.5	317.2	-999	-999
24.7.01 16:03	J359-01	Hainich	590	1827.6	358.3	317.8	-999	-999
24.7.01 16:03	J462-01	Hainich	590	-999	-999	-999	-999	-999
24.7.01 16:14	J463-01	Hainich	990	1827.6	358.3	317.8	-7.659	0.143
24.7.01 16:14	J461-01	Hainich	990	1824.3	357.2	316.6	-7.682	0.543
24.7.01 16:34	J460-01	Hainich	1390	1806.0	358.6	316.6	-999	-999
24.7.01 16:34	J459-01	Hainich	1390	1808.4	358.2	315.7	-7.726	-1.252
24.7.01 16:53	J457-01	Hainich	1790	1805.7	359.2	316.5	-999	-999
24.7.01 16:53	J458-01	Hainich	1790	1812.4	359.0	316.0	-999	-999
25.7.01 8:28	J453-01	Hainich	230	1868.3	367.3	320.2	-8.029	0.524
25.7.01 8:28	J452-01	Hainich	230	1868.1	367.5	320.4	-8.034	0.319
25.7.01 8:38	J454-01	Hainich	480	1866.3	367.1	320.2	-7.980	0.395
25.7.01 8:38	J469-01	Hainich	480	-999	-999	-999	-7.881	-0.204
25.7.01 8:51	J470-01	Hainich	1130	1849.6	365.7	319.0	-7.948	0.276
25.7.01 8:51	J471-01	Hainich	1130	-999	-999	-999	-999	-999
25.7.01 9:05	J450-01	Hainich	1730	1789.8	364.0	316.6	-7.816	-0.373
25.7.01 9:05	J451-01	Hainich	1730	1789.6	364.4	316.9	-7.827	-0.119
25.7.01 9:26	J448-01	Hainich	2430	1794.8	363.1	316.6	-7.759	-0.148
25.7.01 9:26	J568-01	Hainich	2430	1793.9	363.5	316.8	-7.763	-0.260
25.7.01 12:11	J565-01	Hainich	180	1841.4	357.4	317.6	-7.743	0.238
25.7.01 12:11	J566-01	Hainich	180	1842.1	356.7	317.2	-7.747	0.272
25.7.01 12:20	J563-01	Hainich	480	-999	-999	-999	-999	-999
25.7.01 12:20	J564-01	Hainich	480	1839.5	357.2	317.1	-7.710	0.394
25.7.01 12:36	J567-01	Hainich	1130	1842.3	358.0	317.6	-7.741	0.358
25.7.01 12:36	J562-01	Hainich	1130	1842.6	357.9	317.2	-7.735	0.367
25.7.01 12:49	J443-01	Hainich	1730	1668.5	370.5	39.9	-999	-999
25.7.01 12:49	J442-01	Hainich	1730	1811.1	358.6	315.6	-7.753	-0.030
25.7.01 13:01	J441-01	Hainich	2430	1792.5	359.6	315.3	-7.741	-0.335
25.7.01 13:01	J440-01	Hainich	2430	1790.0	359.0	314.8	-7.744	-0.296

Summer Field Campaign

10 August – 9 September 2001



Summer Field Campaign

10 August – 9 September 2001

Flight profile samplings on 16, 17, 18 and 19 August around the Norunda Tower and on 29, 30 August and 1 September above the ‘Florarna’ wetland site

Sampling heights: 60/90, 150, 290, 760/975 and 1980 m above ground.

Sampling times: Morning flights taken place around 5:40 UTC, midday and afternoon flights were executed around 12:00 UTC, respectively 17:00 UTC.

Aircraft: Piper PA28-180, 180 HP. Single engine, propeller clockwise. Four seat low wing airplane. Flight speed during sampling procedure 75 knts (~140 km/h), climbing rate 1 m s^{-1} . Tube inlet mounted at right wing tip, approximately 20 cm beneath the profile bottom, facing downwards to the front

Ground reference samplings: 29 August ‘day time’ [13:00 UTC] and 30 August ‘night time’ [2:30 UTC] above the open swamp

1 September ‘day time’ [13:00 UTC] and 2 September ‘night time’ [2:30 UTC] inside the wooded area (slight rain)

5 September ‘day time’ [13:00 UTC] and 6 September ‘night time’ [2:30 UTC] inside the wooded area

Uppland Summer Experiment

11 August – 9 September 2001

Implementation of additional trace gas analyses

Located about 150 km north of Stockholm the ‘Uppland’ study region was the most northern one within the RECAB project. With its mixture of forests (44 % & 18.5 % clear cuts), agricultural areas (27 %), lakes and wetlands (8 %) the region is representative for the Southern Scandinavian boreal forest zone. The area is topographically and morphologically very uniform; almost flat with an elevation of 30 – 70 m above MSL. In the southern part the soils are dominated by sand and silt, whereas to the north the fraction of till material and bogs increase [Lindroth 2003].

During summer south-westerly winds are prevalent. Because of the location at the margin of the Gulf of Bothnia the area is characterized by relative maritime climatic conditions, compared to the boreal forest further inland. Mean annual temperature is 5.5°C, mean annual precipitation is around 730 mm. On the 16th August a heavy rain shower occurred. Slight rainfall was observed on 20 August, and two more rainy days followed on 27 and 28 August. The maximum of the daily temperature exceeded 20°C on most days. First night with temperature below 0°C was on 30 August.

Data collection was carried out by performing an adapted flight and sampling strategy around the Norunda Tower (coniferous forest with some agricultural used areas in between) and above the Florarna nature reserve (natural wetland). Additional ground level measurements and air sampling was carried out for reference data recordings concurrently with the flight investigations at the Florarna site. Therefore the new mobile mast was installed for a few days within the open swamp and for some more days inside a wooded area of the wetland.

Summer Field Campaign

10 August – 9 September 2001

- Title MODIS image of Scandinavia from 15 July 2003 (10:12 UTC) Dundee Satellite Receiving Station.
- Figure 1 Aerial photograph of the Norunda Tower viewing north.
- Figure 2 Combined measurement flight with the MFP 'SkyArrow' around the Norunda Tower.
- Figure 3 View from the top of the Norunda Tower to the west..
- Figure 4 Map graphics of the profile sites surroundings and landuse classification of the study area.
- Figure 5 Florarna wetland site. View from the ground reference site to the west.
- Figure 6 Ground reference site within the open swamp.
- Figure 7 Ground reference site inside the wooded area.
- Figure 8 MODIS Satellite Images of Scandinavia; 16, 19 and 31 August 2001 (Dundee Satellite Receiving Station)



Figure 1 The Norunda Tower and surroundings, viewing north.

Morning flight 17 August 2001



Figure 2 Combined measurement flight with the 'SkyArrow' around the Norunda Tower.

19 August 2001



Figure 3 View from the top of the Norunda Tower to the west.

Picture: 23 October 2002

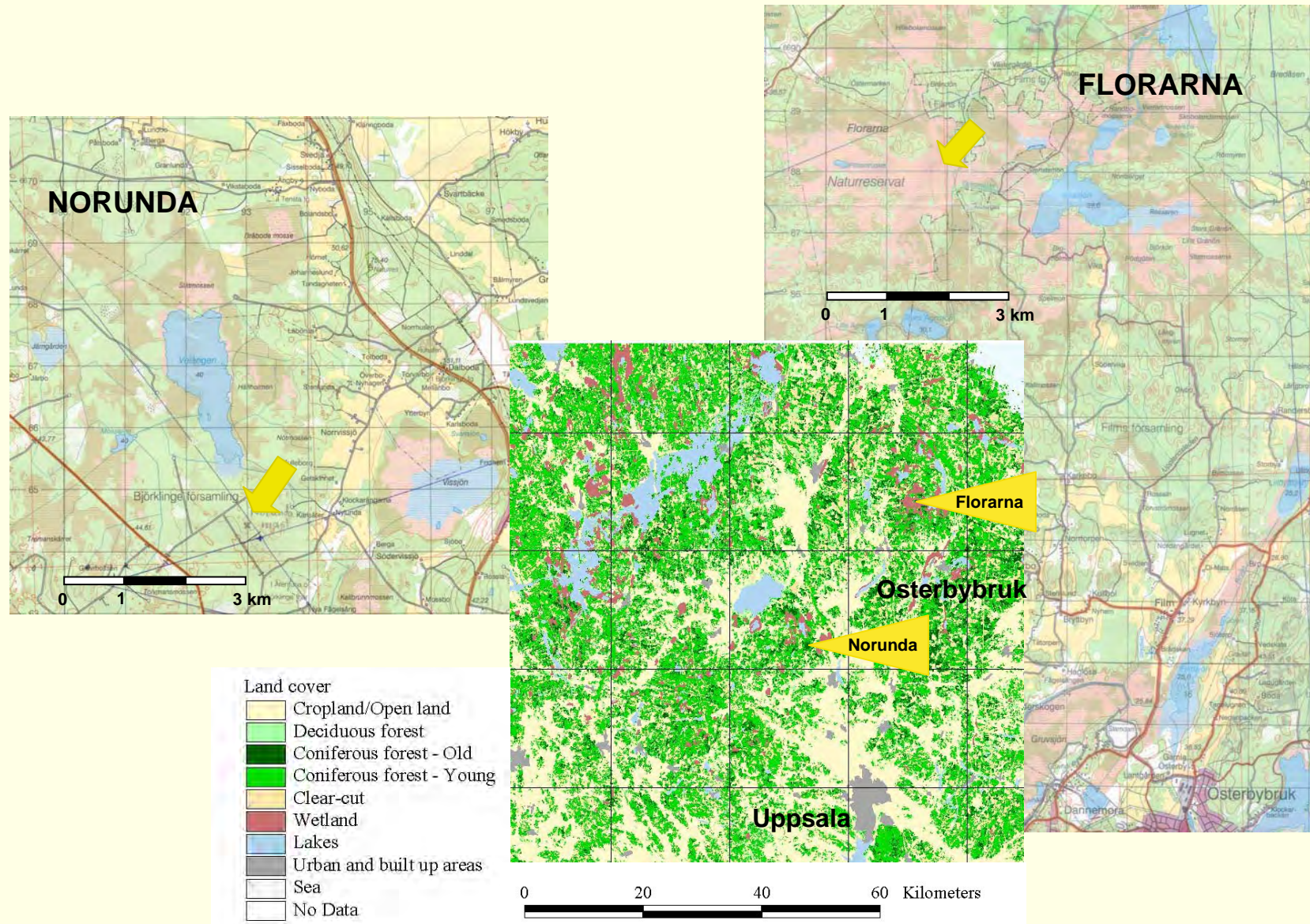


Figure 3 Locations of the profile sites (Topographical Map 1:50.000) and landuse classification for the study area.
(landuse classification taken from Lindroth, A. 2002, Map by Magnus Svensson)



Figure 4 Florarna wetland area. Viewing west from the ground reference site within the open swamp.

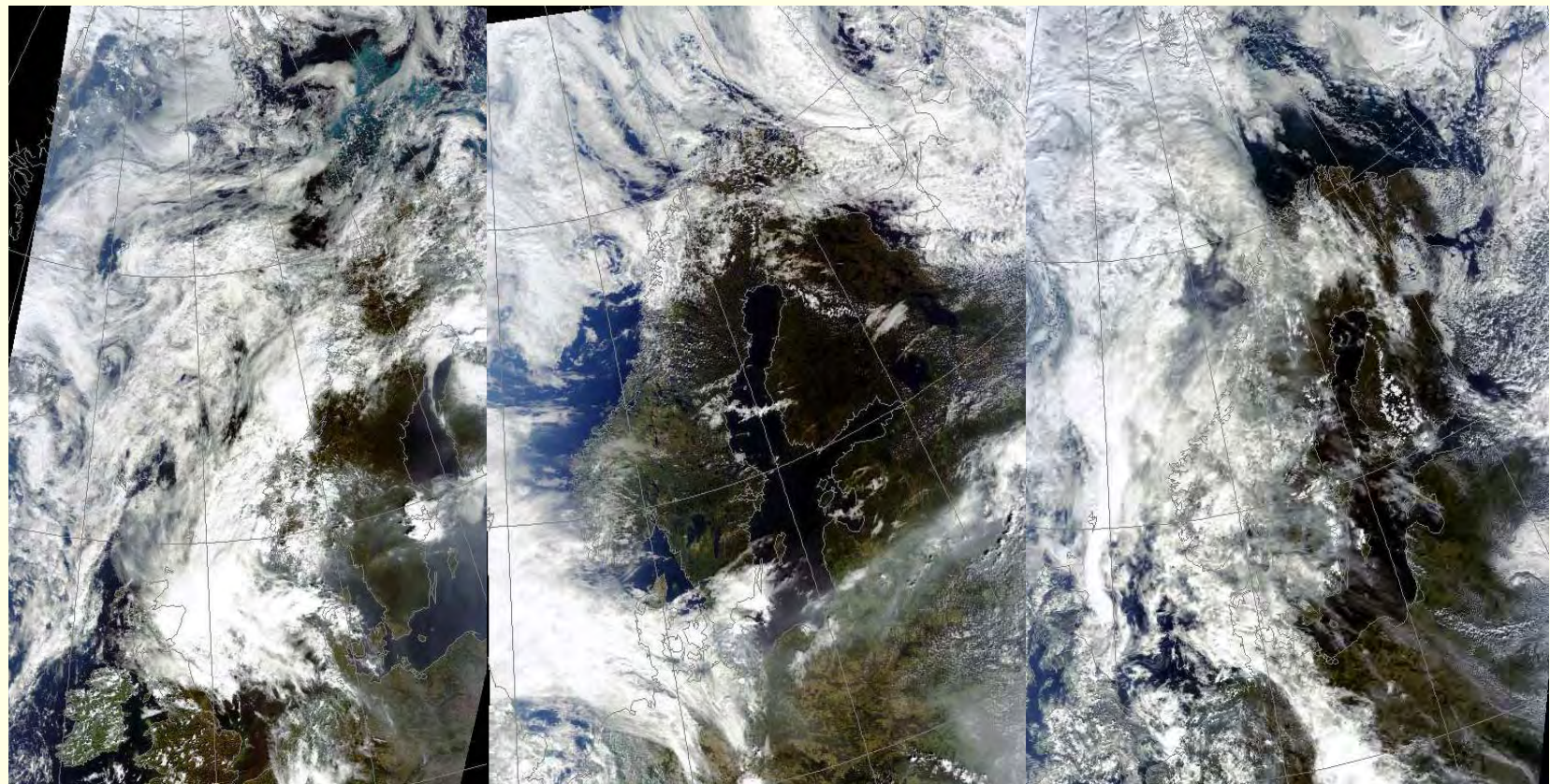
29 August 2001



Figure 5 Open swamp reference site. Top left; download of the data. Top right; view to the south-east. Picture at the bottom was taken from the lowest flight level on 30 August 2001. Yellow arrow indicates ground sampling location.



Figure 6 Forest reference site. Installation of the sensors (left) and the operational measurement equipment.
Pictures: 31 August 2001



16 August 2001 11:22 UTC

19 August 2001 10:14 UTC

31 August 2001 10:38 UTC

Figure 8 MODIS Satellite Images (from Dundee Satellite Receiving Station)

Satellite: Terra Sensor: MODIS
RGB composite image reprojected (RGB 1,4,3 composite)

Description of table parameters

date&time - date and time the sampling procedure was completed in Greenwich Mean Time

Flask code - marking of nameplates for each flask

Flask - position of flask within the sample row

site - location of the flight pattern

Norunda - flight pattern around the Norunda tower north west of Uppsala.
Coniferous forest: 60°05'N / 17°29'E

Florarna - natural sanctuary of swamps and forests north west of Osterbybruk:
60°18'N / 17°48'E

Sumpf - ground reference site within the open swamp: 60°18'N / 17°50'E

Forest - ground reference site inside the wooded area: 60°17'N / 17°48'E

alt - sampling height in meter above ground, referring to the place of departure

init p. - internal flask pressure at the beginning of the analyses

Mixing ratios

Precision of the analyses

CH₄ [ppb]	- methan mixing ratio in ppb	1.3 ppb
CO₂ [ppm]	- carbon dioxide mixing ratio in ppm	0.08 ppm
N₂O [ppb]	- nitrous oxide mixing ratio in ppb	0.15 ppb
CO [ppb]	- carbon monoxide mixing ratio in ppb	1.0 ppb
H₂ [ppb]	- hydrogen mixing ratio in ppb	5.0 ppb
SF₆ [ppt]	- sulfur hexafluoride mixing ratio in ppt	0.08 ppt

Isotope Ratio

$$\delta[\$] = (R_{\text{sa}}/R_{\text{ref}} - 1) \cdot 1000 \quad R_{\text{sa}} \text{ and } R_{\text{ref}} \text{ are the sample and reference isotope ratios}$$

del ¹³C [\$] - ratio of the carbon 13 isotope and carbon 12 isotope due to the VPDB isotope ratio scale

del ¹⁸O [\$] - ratio of the oxygen 18 isotope and oxygen 16 isotope due to the VPDB (gas) isotope ratio scale

$$\text{Precision of the analyses} \quad {}^{13}\text{C} = 0.012 \$ \quad {}^{18}\text{O} = 0.02 \$$$

date&time [GMT]	flask code	site	alt [m]	init p.	mixing ratios						isotope	
					CH ₄ [ppb]	CO ₂ [ppm]	CO [ppb]	H ₂ [ppb]	SF ₆ [ppt]	N ₂ O [ppb]	del ¹³ C [%]	del ¹⁸ O [%]
16.8.01 5:48	J261-01	Norunda	90	-999	1833.0	376.3	-999	-999	-999	318.7	-8.442	-0.291
16.8.01 5:48	J262-01	Norunda	90	-999	1831.9	377.0	-999	-999	-999	318.5	-8.447	-0.154
16.8.01 5:56	J260-01	Norunda	150	-999	1827.0	368.4	-999	-999	-999	318.3	-8.083	-0.089
16.8.01 5:56	J259-01	Norunda	150	-999	1823.3	367.3	-999	-999	-999	318.4	-7.882	0.285
16.8.01 6:05	J254-01	Norunda	290	-999	1844.2	362.0	-999	-999	-999	318.7	-7.782	-0.060
16.8.01 6:05	J256-01	Norunda	290	-999	1842.3	362.5	-999	-999	-999	318.5	-999	-999
16.8.01 6:17	J252-01	Norunda	520	-999	1856.9	362.0	-999	-999	-999	318.8	-7.801	0.153
16.8.01 6:17	J253-01	Norunda	520	-999	1859.6	362.3	-999	-999	-999	319.0	-7.799	0.076
16.8.01 6:27	J251-01	Norunda	975	-999	1758.4	365.2	-999	-999	-999	316.6	-7.882	0.310
16.8.01 6:27	J257-01	Norunda	975	-999	1757.4	364.6	-999	-999	-999	316.7	-7.854	0.180
16.8.01 6:38	J248-01	Norunda	1980	-999	1783.3	363.0	-999	-999	-999	316.3	-7.798	-0.070
16.8.01 6:38	J250-01	Norunda	1980	-999	1785.8	363.4	-999	-999	-999	316.1	-7.807	-0.171
16.8.01 16:45	J265-01	Norunda	90	-999	1852.4	359.9	-999	-999	-999	318.6	-7.692	-0.080
16.8.01 16:45	J391-01	Norunda	90	-999	1851.9	360.6	-999	-999	-999	318.7	-7.716	-0.079
16.8.01 16:53	J385-01	Norunda	150	-999	1854.2	361.2	-999	-999	-999	318.9	-7.743	-0.016
16.8.01 16:53	J392-01	Norunda	150	-999	1851.9	361.6	-999	-999	-999	318.8	-7.757	-0.147
16.8.01 17:01	J378-01	Norunda	290	-999	1860.8	362.5	-999	-999	-999	319.0	-7.835	-0.056
16.8.01 17:01	J386-01	Norunda	290	-999	1861.4	362.9	-999	-999	-999	318.9	-7.830	-0.286
16.8.01 17:12	J595-01	Norunda	520	-999	1872.3	366.5	-999	-999	-999	319.0	-8.077	0.190
16.8.01 17:12	J596-01	Norunda	520	-999	-999	-999	-999	-999	-999	-999	-8.088	-0.110
16.8.01 17:23	J593-01	Norunda	975	1.2	1819.0	363.7	-999	-999	-999	318.0	-7.894	0.066
16.8.01 17:23	J379-01	Norunda	975	1.8	1817.8	363.9	-999	-999	-999	317.8	-7.916	0.088
16.8.01 17:42	J387-01	Norunda	1980	1.7	1824.5	363.6	-999	-999	-999	318.1	-7.944	-0.152
16.8.01 17:42	J605-01	Norunda	1980	2.1	1823.9	364.0	-999	-999	-999	317.7	-7.955	0.632
17.8.01 5:55	J116-01	Norunda	90	2.1	1849.1	375.2	-999	-999	-999	318.7	-8.476	-0.198
17.8.01 5:55	J115-01	Norunda	90	2.1	1848.6	375.5	-999	-999	-999	318.6	-8.505	-0.106
17.8.01 6:03	J122-01	Norunda	150	2.2	1848.7	374.6	-999	-999	-999	318.5	-8.470	-0.304
17.8.01 6:03	J120-01	Norunda	150	2.2	1847.5	375.2	-999	-999	-999	318.7	-8.458	-0.160
17.8.01 6:11	J390-01	Norunda	290	2.1	1844.1	373.4	-999	-999	-999	318.3	-8.376	-0.400
17.8.01 6:11	J119-01	Norunda	290	2.1	1840.7	373.9	-999	-999	-999	318.5	-8.400	-0.153
17.8.01 6:25	J118-01	Norunda	975	2.1	1816.7	366.3	-999	-999	-999	317.0	-8.004	-0.116
17.8.01 6:25	J117-01	Norunda	975	2.1	1815.2	366.8	-999	-999	-999	316.8	-8.003	-0.061
17.8.01 6:43	J594-01	Norunda	1980	2.1	1802.6	360.2	-999	-999	-999	315.7	-7.665	-0.586
17.8.01 6:43	J121-01	Norunda	1980	2.1	1800.7	360.8	-999	-999	-999	315.7	-7.690	-0.360
17.8.01 12:00	J126-01	Norunda	90	2.0	1807.4	356.7	-999	-999	-999	316.3	-7.521	-0.371
17.8.01 12:00	J127-01	Norunda	90	2.0	1808.5	357.2	-999	-999	-999	316.4	-7.546	-0.378
17.8.01 12:10	J124-01	Norunda	150	2.0	1808.1	357.8	-999	-999	-999	316.5	-7.549	-0.392
17.8.01 12:10	J046-01	Norunda	150	2.0	1808.1	358.0	-999	-999	-999	316.6	-7.539	-0.323
17.8.01 12:20	J128-01	Norunda	290	2.0	1807.9	357.6	-999	-999	-999	316.3	-7.543	-0.459
17.8.01 12:20	J045-01	Norunda	290	no	-999	-999	-999	-999	-999	-999	-999	-999
17.8.01 12:40	J130-01	Norunda	975	2.0	1807.5	357.5	-999	-999	-999	316.1	-7.571	-0.409
17.8.01 12:40	J125-01	Norunda	975	2.0	1807.5	358.5	-999	-999	-999	316.2	-7.581	-0.272
17.8.01 12:58	J129-01	Norunda	1980	2.0	1800.9	359.4	-999	-999	-999	315.9	-7.663	-0.530
17.8.01 12:58	J264-01	Norunda	1980	2.0	1804.0	359.9	-999	-999	-999	316.0	-7.662	-0.548
17.8.01 16:42	J038-01	Norunda	90	2.0	1809.4	355.3	-999	-999	-999	316.3	-7.464	-0.370
17.8.01 16:42	J039-01	Norunda	90	2.0	1811.7	356.1	-999	-999	-999	316.3	-7.466	-0.364
17.8.01 16:52	J041-01	Norunda	150	2.0	1808.8	356.2	-999	-999	-999	316.1	-7.509	-0.433
17.8.01 16:52	J049-01	Norunda	150	-999	1811.2	356.7	-999	-999	-999	316.4	-7.497	-0.358
17.8.01 17:02	J042-01	Norunda	290	-999	1812.3	356.3	-999	-999	-999	316.4	-7.497	-0.498
17.8.01 17:02	J044-01	Norunda	290	-999	1811.2	356.8	-999	-999	-999	316.3	-7.503	-0.365
17.8.01 17:23	J389-01	Norunda	975	-999	1812.2	356.1	-999	-999	-999	316.1	-7.482	-0.514
17.8.01 17:23	J043-01	Norunda	975	-999	1811.5	356.7	-999	-999	-999	316.2	-7.497	-0.457
17.8.01 17:40	J388-01	Norunda	1980	-999	1810.3	359.7	-999	-999	-999	316.3	-7.656	-0.787
17.8.01 17:40	J047-01	Norunda	1980	-999	1813.0	360.3	-999	-999	-999	316.4	-7.696	-0.567

18.8.01 17:11	J524-01	Norunda	520	-999	1815.6	356.4	-999	-999	-999	316.3	-7.503	-0.284
18.8.01 17:11	J525-01	Norunda	520	-999	1814.3	357.4	-999	-999	-999	316.7	-7.465	-0.402
18.8.01 17:21	J527-01	Norunda	975	-999	1818.5	356.4	-999	-999	-999	316.3	-7.520	-0.263
18.8.01 17:21	J528-01	Norunda	975	-999	1816.3	356.9	-999	-999	-999	316.3	-7.518	-0.334
18.8.01 17:37	J522-01	Norunda	1980	-999	1804.4	360.1	-999	-999	-999	315.7	-7.692	-0.646
18.8.01 17:37	J521-01	Norunda	1980	-999	1807.5	360.9	-999	-999	-999	315.7	-7.713	-0.518
19.8.01 5:16	J180-01	Norunda	90	-999	1826.7	373.4	-999	-999	-999	316.5	-8.395	-0.104
19.8.01 5:16	J179-01	Norunda	90	-999	1827.1	374.0	102.2	445.0	4.90	317.1	-8.380	-0.040
19.8.01 5:23	J131-01	Norunda	150	-999	1817.8	358.4	99.8	470.5	4.85	316.7	-7.583	-0.069
19.8.01 5:23	J136-01	Norunda	150	-999	1818.9	359.2	101.6	466.1	4.92	316.7	-7.606	-0.190
19.8.01 5:31	J133-01	Norunda	290	-999	1817.3	357.7	98.4	480.5	4.92	316.8	-7.533	-0.215
19.8.01 5:31	J134-01	Norunda	290	-999	1816.7	358.2	97.8	472.6	4.88	316.7	-7.557	-0.272
19.8.01 5:41	J138-01	Norunda	520	-999	1816.1	356.5	97.8	475.1	4.93	316.7	-7.466	-0.160
19.8.01 5:41	J139-01	Norunda	520	-999	1815.9	357.0	97.4	469.1	5.01	316.8	-7.473	-0.138
19.8.01 5:52	J132-01	Norunda	975	-999	1815.0	357.0	99.3	467.3	5.00	316.6	-7.503	-0.341
19.8.01 5:52	J137-01	Norunda	975	-999	1818.1	357.4	98.4	462.2	4.93	316.6	-7.510	-0.133
19.8.01 6:08	J140-01	Norunda	1980	-999	1813.7	359.8	98.0	476.0	4.94	321.0	-7.640	-0.240
19.8.01 6:08	J141-01	Norunda	1980	-999	1810.8	360.3	95.8	473.7	4.87	316.2	-7.671	-0.253
19.8.01 11:17	J181-01	Norunda	90	-999	1808.5	356.7	101.4	453.7	5.07	317.8	-7.292	-0.343
19.8.01 11:17	J182-01	Norunda	90	-999	1818.3	356.2	100.1	458.6	5.00	316.6	-7.477	-0.250
19.8.01 11:24	J183-01	Norunda	150	-999	1815.6	356.4	101.0	469.4	5.00	316.9	-7.499	-0.151
19.8.01 11:24	J189-01	Norunda	150	-999	1815.5	356.8	100.1	463.7	5.10	316.9	-7.485	-0.145
19.8.01 11:32	J188-01	Norunda	290	-999	1817.2	356.7	102.0	472.6	4.95	316.9	-7.500	-0.274
19.8.01 11:32	J193-01	Norunda	290	-999	1817.4	357.0	101.3	465.6	4.93	316.7	-7.494	-0.230
19.8.01 11:44	J187-01	Norunda	520	-999	1815.4	356.3	101.0	469.9	4.87	316.7	-7.506	-0.164
19.8.01 11:44	J186-01	Norunda	520	-999	1815.6	356.7	100.5	462.6	4.87	316.7	-7.502	-0.083
19.8.01 11:54	J194-01	Norunda	975	-999	1815.1	356.5	101.4	468.4	5.11	316.7	-7.512	-0.178
19.8.01 11:54	J190-01	Norunda	975	-999	1816.6	356.7	101.2	463.1	4.98	316.5	-7.496	-0.125
19.8.01 12:15	J191-01	Norunda	2440	-999	1802.8	359.5	97.6	479.8	4.83	315.7	-7.676	-0.894
19.8.01 12:15	J185-01	Norunda	2440	-999	1803.1	359.8	95.9	476.0	4.85	315.6	-7.668	-0.515
19.8.01 16:45	J148-01	Norunda	90	-999	1825.5	354.8	108.6	468.1	4.88	317.0	-7.444	0.044
19.8.01 16:45	J151-01	Norunda	90	-999	1824.9	355.6	106.0	463.5	4.92	317.0	-7.477	0.013
19.8.01 16:54	J152-01	Norunda	150	-999	1823.0	355.5	108.0	468.7	4.97	317.1	-7.463	-0.018
19.8.01 16:54	J149-01	Norunda	150	-999	1824.8	355.9	109.9	464.8	4.86	316.7	-7.481	0.093
19.8.01 17:03	J435-01	Norunda	290	-999	1825.6	355.9	111.4	469.2	4.97	316.7	-7.479	-0.598
19.8.01 17:03	J147-01	Norunda	290	-999	1829.5	356.0	110.1	464.4	4.99	316.7	-7.480	-0.062
19.8.01 17:14	J150-01	Norunda	520	-999	1825.6	356.2	113.6	471.1	4.87	316.6	-7.502	-0.118
19.8.01 17:14	J155-01	Norunda	520	-999	1825.0	356.7	113.6	467.3	4.94	317.1	-7.518	-0.168
19.8.01 17:25	J523-01	Norunda	975	-999	1825.6	356.4	116.3	471.4	4.94	316.9	-7.518	-0.461
19.8.01 17:25	J153-01	Norunda	975	-999	1825.9	356.7	115.6	466.2	4.95	316.9	-7.519	-0.116
19.8.01 17:49	J156-01	Norunda	2440	-999	1805.4	359.9	112.1	481.3	4.94	315.9	-7.697	-0.774
19.8.01 17:49	J158-01	Norunda	2440	-999	1804.1	360.2	111.7	478.1	4.96	315.8	-7.681	-0.649
29.8.01 5:19	J157-01	Florarna	60	-999	1871.7	361.2	119.7	460.9	-999	318.6	-7.439	-2.344
29.8.01 5:19	J159-01	Florarna	60	-999	1889.3	359.9	117.1	461.3	4.92	316.6	-7.678	-2.274
29.8.01 5:27	J240-01	Florarna	125	-999	1885.2	358.8	113.2	455.9	5.02	316.9	-7.711	-2.646
29.8.01 5:27	J239-01	Florarna	125	-999	1884.1	359.3	112.0	448.9	4.96	316.6	-7.665	-2.202
29.8.01 5:35	J238-01	Florarna	275	-999	1880.9	357.1	111.1	451.3	4.90	316.5	-7.559	-2.096
29.8.01 5:35	J236-01	Florarna	275	-999	1880.5	357.7	110.3	452.5	4.99	316.3	-7.556	-2.251
29.8.01 5:45	J237-01	Florarna	760	-999	1878.9	358.2	112.2	453.2	4.94	316.1	-7.601	-1.809
29.8.01 5:45	J233-01	Florarna	760	-999	1878.3	358.9	113.4	450.5	4.91	316.1	-7.613	-1.666
29.8.01 6:08	J234-01	Florarna	1980	-999	1805.2	359.5	110.0	491.8	4.96	316.0	-7.682	-0.275
29.8.01 6:08	J235-01	Florarna	1980	-999	1804.2	360.0	105.6	486.4	4.94	315.9	-7.686	-0.202
29.8.01 12:41	J163-01	Florarna	60	2.1	1853.8	351.0	112.5	459.8	4.87	316.0	-7.229	-1.428
29.8.01 12:41	J215-01	Florarna	60	2.0	1853.8	352.2	111.3	452.5	4.92	316.1	-7.249	-1.207
29.8.01 12:50	J241-01	Florarna	125	2.1	1853.4	352.4	111.5	457.6	4.86	316.0	-7.293	-1.477
29.8.01 12												

30.8.01 13:14	J112-01	Florarna	760	-999	1855.3	352.7	119.1	450.9	4.91	316.3	-7.286	-1.383
30.8.01 13:14	J263-01	Florarna	760	-999	1853.7	353.7	118.0	447.5	-999	316.3	-7.313	-1.432
30.8.01 13:31	J111-01	Florarna	1980	-999	1838.8	357.3	108.6	461.7	4.84	316.3	-7.553	-0.961
30.8.01 13:31	J514-01	Florarna	1980	-999	1837.4	358.2	108.6	456.4	4.78	316.3	-7.579	-0.939
30.8.01 16:48	J114-01	Florarna	60	-999	1867.6	349.5	118.4	450.1	4.95	316.6	-7.077	-1.495
30.8.01 16:48	J102-01	Florarna	60	-999	1864.7	350.8	117.9	444.9	4.90	316.8	-7.108	-1.119
30.8.01 16:56	J097-01	Florarna	125	-999	1862.6	351.0	116.1	450.4	4.98	316.7	-7.170	-1.432
30.8.01 16:56	J091-01	Florarna	125	-999	1861.8	351.9	115.5	442.5	4.93	316.9	-7.188	-1.284
30.8.01 17:04	J099-01	Florarna	275	-999	1860.5	351.5	118.2	457.1	4.99	316.6	-7.188	-1.471
30.8.01 17:04	J090-01	Florarna	275	-999	1860.6	352.4	117.2	449.1	4.99	316.8	-7.196	-1.316
30.8.01 17:13	J103-01	Florarna	760	-999	1861.3	351.2	122.0	456.6	5.04	316.5	-7.148	-1.151
30.8.01 17:13	J089-01	Florarna	760	-999	1861.7	352.2	120.8	447.5	4.96	316.8	-7.163	-1.181
30.8.01 17:32	J092-01	Florarna	1980	-999	1847.7	359.6	114.1	455.4	4.96	316.2	-7.648	-1.151
30.8.01 17:32	J040-01	Florarna	1980	2.2	1849.9	360.6	114.9	452.4	4.88	316.4	-7.662	-1.160
1.9.01 7:18	J606-01	Florarna	60	2.2	1882.0	359.4	121.1	473.5	4.89	316.2	-7.666	-1.858
1.9.01 7:18	J178-01	Florarna	60	2.2	1880.5	361.1	120.7	458.2	4.91	316.6	-7.679	-1.572
1.9.01 7:26	J607-01	Florarna	125	2.2	1874.2	359.4	118.9	463.2	4.87	316.2	-7.655	-1.759
1.9.01 7:26	J177-01	Florarna	125	2.2	1874.8	360.5	116.7	453.3	4.94	316.5	-7.666	-1.316
1.9.01 7:34	J608-01	Florarna	275	2.2	1877.4	354.4	118.4	464.3	4.96	316.2	-7.349	-1.297
1.9.01 7:34	J154-01	Florarna	275	-999	-999	-999	121.5	470.6	-999	-999	-999	-999
1.9.01 7:44	J365-01	Florarna	760	2.2	1885.9	355.7	121.2	460.3	4.88	316.2	-7.416	-1.276
1.9.01 7:44	J245-01	Florarna	760	2.2	1884.8	356.6	117.3	462.6	4.84	316.4	-7.435	-1.146
1.9.01 8:06	J366-01	Florarna	2290	2.2	1861.3	356.5	117.3	462.6	4.84	316.0	-7.482	-0.991
1.9.01 8:06	J231-01	Florarna	2290	-999	-999	-999	-999	-999	-999	-999	-999	-999
1.9.01 12:40	J164-01	Florarna	60	2.1	1881.4	349.8	133.1	463.1	4.94	316.3	-7.103	-0.799
1.9.01 12:40	J176-01	Florarna	60	2.1	1883.4	350.9	133.6	453.3	4.89	316.4	-7.125	-0.613
1.9.01 12:49	J165-01	Florarna	125	1.4	1880.0	351.1	135.5	456.0	4.97	316.4	-7.169	-0.871
1.9.01 12:49	J175-01	Florarna	125	2.1	1879.8	352.2	134.5	451.9	4.93	316.6	-7.197	-0.729
1.9.01 12:58	J166-01	Florarna	275	1.1	1886.3	352.5	135.1	452.2	-999	-999	-999	-999
1.9.01 12:58	J219-01	Florarna	275	1.7	1884.9	352.7	133.8	450.0	-999	316.5	-999	-999
1.9.01 13:08	J167-01	Florarna	760	1.7	1883.6	352.0	127.5	459.4	-999	316.2	-999	-999
1.9.01 13:08	J242-01	Florarna	760	-999	1878.0	353.4	127.4	451.4	-999	316.9	-999	-999
1.9.01 13:32	J168-01	Florarna	2290	-999	1868.8	355.2	121.3	461.1	-999	315.8	-7.425	-0.972
1.9.01 13:32	Test 1	Florarna	2290	-999	1867.6	356.4	121.6	457.3	5.01	316.3	-7.464	-1.176
29.8.01 12:40	J050-01	Sumpf	0.1	-999	1924.1	354.5	114.1	439.0	-999	317.0	-7.156	-0.749
29.8.01 12:40	J051-01	Sumpf	0.1	-999	1937.4	354.2	114.5	437.8	-999	317.3	-7.143	-0.685
29.8.01 12:56	J052-01	Sumpf	0.5	-999	1896.4	353.8	113.0	436.3	-999	317.3	-7.150	-0.823
29.8.01 12:56	J053-01	Sumpf	0.5	-999	1896.6	353.9	113.3	437.3	-999	317.2	-7.139	-0.787
29.8.01 13:14	J055-01	Sumpf	1	-999	1882.9	354.4	111.9	436.0	-999	317.3	-7.182	-0.831
29.8.01 13:14	J056-01	Sumpf	1	-999	1888.5	354.2	112.1	436.1	-999	317.3	-7.167	-0.833
29.8.01 13:29	J058-01	Sumpf	2	-999	1880.7	353.9	111.4	435.6	-999	317.2	-7.175	-0.895
29.8.01 13:29	J059-01	Sumpf	2	-999	1876.1	354.1	111.1	433.6	-999	317.2	-7.163	-0.855
29.8.01 13:46	J069-01	Sumpf	5	-999	1871.7	355.1	110.3	433.5	-999	317.2	-7.253	-0.916
29.8.01 13:46	J066-01	Sumpf	5	-999	1869.9	355.3	110.5	434.1	-999	317.2	-7.252	-0.908
30.8.01 2:13	J379-01	Sumpf	0.1	-999	6692.0	606.8	64.1	257.2	-999	311.2	-15.273	-6.055
30.8.01 2:13	J374-01	Sumpf	0.1	-999	6561.2	606.5	63.7	256.6	-999	320.5	-15.286	-6.074
30.8.01 2:28	J377-01	Sumpf	0.5	-999	5690.4	600.2	69.0	313.9	-999	321.9	-14.861	-6.186
30.8.01 2:28	J375-01	Sumpf	0.5	-999	5718.7	596.0	68.5	258.1	-999	320.8	-15.113	-5.876
30.8.01 2:43	J373-01	Sumpf	1	-999	5896.7	591.4	71.1	252.3	-999	320.3	-15.053	-5.754
30.8.01 2:43	J088-01	Sumpf	1	-999	5870.9	591.6	69.8	250.8	4.94	320.0	-15.033	-5.712
30.8.01 2:59	J087-01	Sumpf	2	-999	3953.4	550.8	85.1	264.4	4.86	320.1	-14.272	-4.815
30.8.01 2:59	J086-01	Sumpf	2	-999	3987.4	551.7	84.6	264.1	4.97	319.9	-14.292	-4.829
30.8.01 3:15	J083-01	Sumpf	5	-999	3168.1	529.9	93.2	271.2	4.97	319.8	-13.819	-4.329
30.8.01 3:15	J071-01	Sumpf	5	-999	3161.8	529.6	92.8	270.5	4.90	320.0	-13.794	-4.347
1.9.01 12:40	J487-01	Forest	0.1	-999	1877.3	361.6	130.9	415.4	4.92	317.8	-7.491	-0.866
1.9.01 12:40	J489-01	Forest	0.1	-999								

6.9.01 2:28	J206-01	Forest	1	-999	1900.9	481.3	131.0	302.8	4.95	318.6	-12.420	-4.591
6.9.01 2:43	J169-01	Forest	2	-999	1912.8	474.4	127.1	310.2	4.90	318.6	-12.233	-4.827
6.9.01 2:43	J207-01	Forest	2	-999	1912.6	475.7	126.8	309.0	4.87	318.7	-12.277	-4.866
6.9.01 2:58	J210-01	Forest	5	-999	1900.1	448.2	128.4	342.8	4.85	318.6	-11.353	-4.131
6.9.01 2:58	Test 2	Forest	5	-999	1900.5	448.2	127.4	339.5	4.88	318.7	-11.347	-3.890

Spain Field Campaigns

17 June – 7 July 2001 and
17 November – 16 December 2001



Spain Field Campaigns

17 June – 7 July 2001 and 17 November – 16 December 2001

- Titel Satellite image of the Iberian Peninsula (SeaWiFS scene from 8 July 2000; NASA)
- Figure 1 Satellite image of the study region with the locations of the vertical profile flights.
- Figure 2 Aerial photograph of the orchard study area. Viewing to the Mediterranean Sea.
- Figure 3 'Orchard' ground reference site; pictures from summer and winter time.
- Figure 4 Smoke plume from biomass combustion as observed most frequently during the morning flights.
- Figure 5 Satellite Images of Central Europe from 2, 3 and 4 July 2001.
- Figure 6 Aerial photograph of the study region viewing west: Location of the rice field ground reference site and scheme of the flight track.
- Figure 7 Aircraft during lowest level flight and aerial photographs of the rice field ground reference location.
- Figure 8 Aerial photograph of the ground reference location at the remote mountain site 'Cortes des Pallás'.
- Figure 9 Scheme of the land-sea-wind circulation during day and night time. Locations of the ground reference sampling.
- Figure 10 Results from the ground reference sampling above the rice fields, the orchard, the remote mountain site and close to the highway.
- Figure 11 Ground reference sites: installation of the equipment at the rice field, reference mast inside a orange plantation and at the mountain site.
- Figure 12 MODIS Satellite Images of Central Europe; 5, 6 and 12 December 2001.

Valencia Summer Experiment

17 June – 7 July 2001

First experiment with the modified flight sampling system

The spatial frame of the study region enclosed a coastal plain from the Mediterranean Sea in the East to the slopes of the Iberian Plateau in the West, with an extension of 20 – 30 km. The northern edge was defined by the Lagoon ‘Albufera’, the southern border was marked by the Júcar River. Very intensive agriculture use characterizes the coastal plain, from east to west: a zone of paddy fields along the shore line passes over to citrus and apricot orchards on the higher parts of the plain, where also the urban settlements are located. Two main roads transect the study area in north-south direction.

Synoptic conditions typical for the region during the campaign: forced by thermal lows over the Iberian Peninsula surface inland winds established during day time with a compensatory large-scale subsidence over the coastal zones, whereas during night time a land-sea circulation developed.



Figure 1

Satellite image of the study region. The locations where the vertical profile flights were performed are marked by the yellow arrows.

Image taken from
Beckel [ed.] 1997
(modified)

Summer Field Campaign

17 June – 7 July 2001

Flight profile samplings: on 25, 26, 28 June / 2, 3 July above the orchards and
on 4 July above the ricefields

On 27 June in the late afternoon an additional comparison flight was performed with the
MFP ‘SkyArrow’ parallel to the coast line (VFlug).

Sampling heights: Lowest sampling level was 100 m above ground, the top height differs from 1500 to
2000 m above ground.

Sampling times: Morning flights around 7:00 UTC, midday flights around 10:30 UTC and afternoon
flights around 14:30 UTC.

Aircraft: Morane Socata, 160 HP. Single engine, propeller clockwise. Four seat low wing
airplane. Flight speed during sampling procedure 75 knts (~140 km/h), climbing rate
 1 m s^{-1} . Tube inlet mounted at right wing tip, approximately 15 cm beneath the
profile bottom, facing downwards to the front.

Ground reference samplings: 3 July ‘night time’ [3:30 UTC] and 5 July ‘day time’ [12:00 UTC]
in the apricot orchard.

4 July ‘day time’ [13:00 UTC] above the rice fields.



Figure 2 Study area dominated by citrus and apricot orchards. The yellow arrow marks the ground reference sampling site. View direction is eastwards to the Mediterranean Sea.

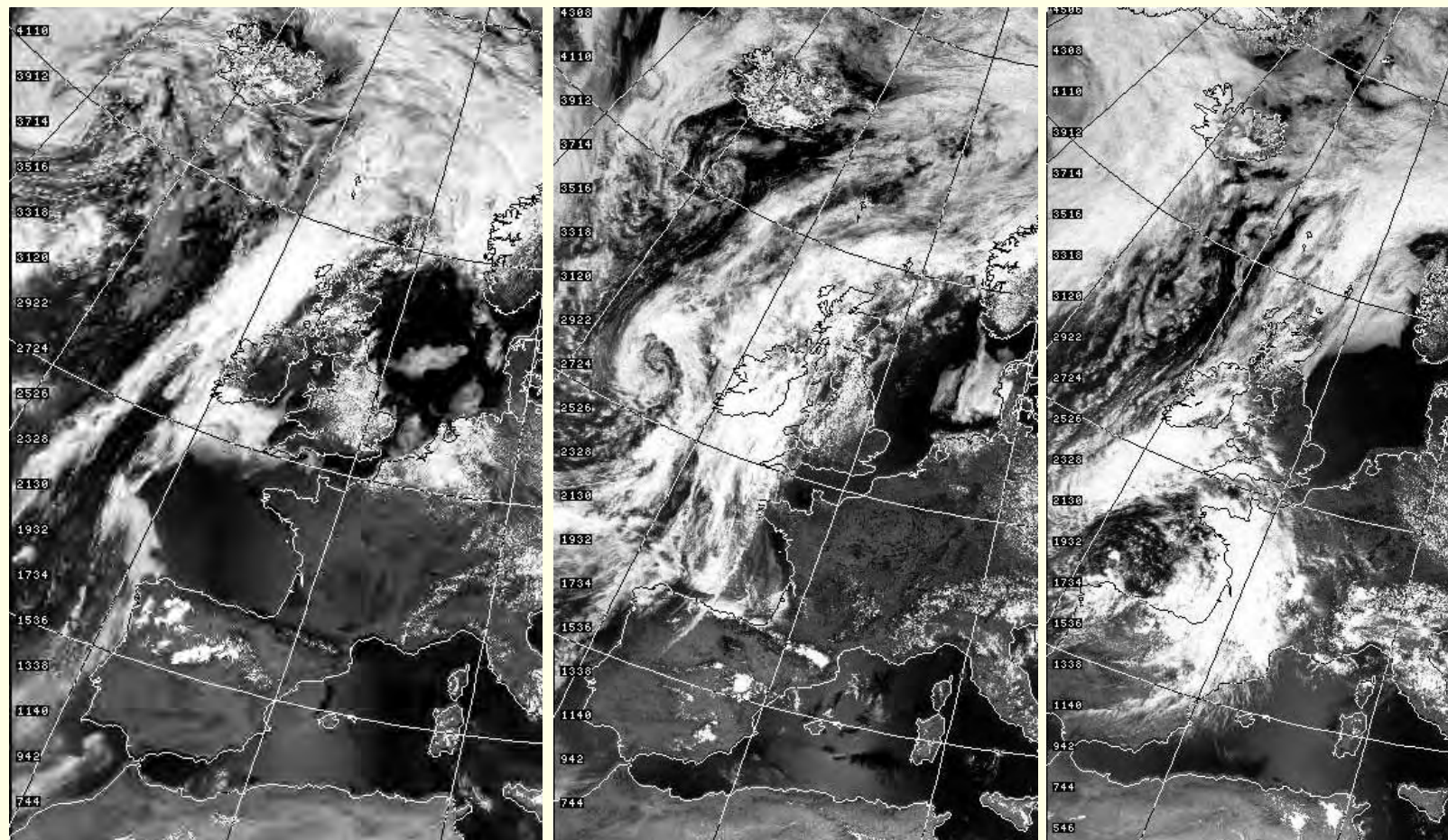
Picture: late afternoon 4 July 2001



Figure 3 'Orchard' ground reference site. Upper picture was taken on 5 July 2001, the picture below showing the same spot on 11 December 2001.



Figure 4 Combustion of green material within the orchards as observed most frequently during the campaign.
Flight altitude approximately 300 m above ground.



2 July 2001 13:10 UTC

3 July 2001 12:59 UTC

4 July 2001 12:49 UTC

Figure 5 Satellite Images (from Dundee Satellite Receiving Station)

NOAA 16 Channel 1 (visible 0.58 – 0.68 μm)

Winter Field Campaign

17 November – 16 December 2001

Flight profile samplings: on 1, 2, 4, 5 and 6 December above the ricefields, and
on 12 December above the mountain site.

Sampling heights: Lowest sampling level was 10 m above ground, common used heights were 20, 80, 150, 230 up to 1000 m above ground.

Sampling times: Morning flights around 7:00 UTC, midday around 11:30 UTC and afternoon flights around 14:30 UTC.

Aircraft: Morane Socata, 160 HP. Single engine, propeller clockwise. Four seat low wing airplane. Flight speed during sampling procedure 75 knts (~140 km/h), climbing rate 1 m s^{-1} . Tube inlet mounted at right wing tip, approximately 15 cm beneath the profile bottom, facing downwards to the front.

Ground reference samplings: 30 November ‘day time’ in the orange plantation [12:30 UTC] and above the rice field [15:30 UTC].
3 December ‘night time’ above the rice field [4:30 UTC] and in the orange plantation [7:50 UTC].
13 December ‘night time’ [7:10 UTC] and ‘day time’ [13:20 UTC] above the mountain site.
13 December close to the highway [20:30 UTC].

Valencia Winter Experiment

16 November – 15 December 2001

Final configuration of the modified flight sampling system

During the campaign a high pressure cell centred above the Iberian Peninsula dominated the weather conditions. Because of clear sky and daily temperatures above 15°C like in summer a land-sea-wind circulation developed, however less intensive and extended than in June and July.

Because of frequent biomass burning activity the orchard site area was this time excluded from flight sampling. Vertical profiles were executed above the rice fields (including one sample taken off shore during the noon flight) and above a mountain site about 50 km inland. The rice fields had been harvested, but uncontrolled growth occurred because heavy rainfalls flooded the fields the weeks before. Additional ground level measurements and samplings were carried out above the rice fields, in a citrus orchard, above the mountain site and close to a highway.

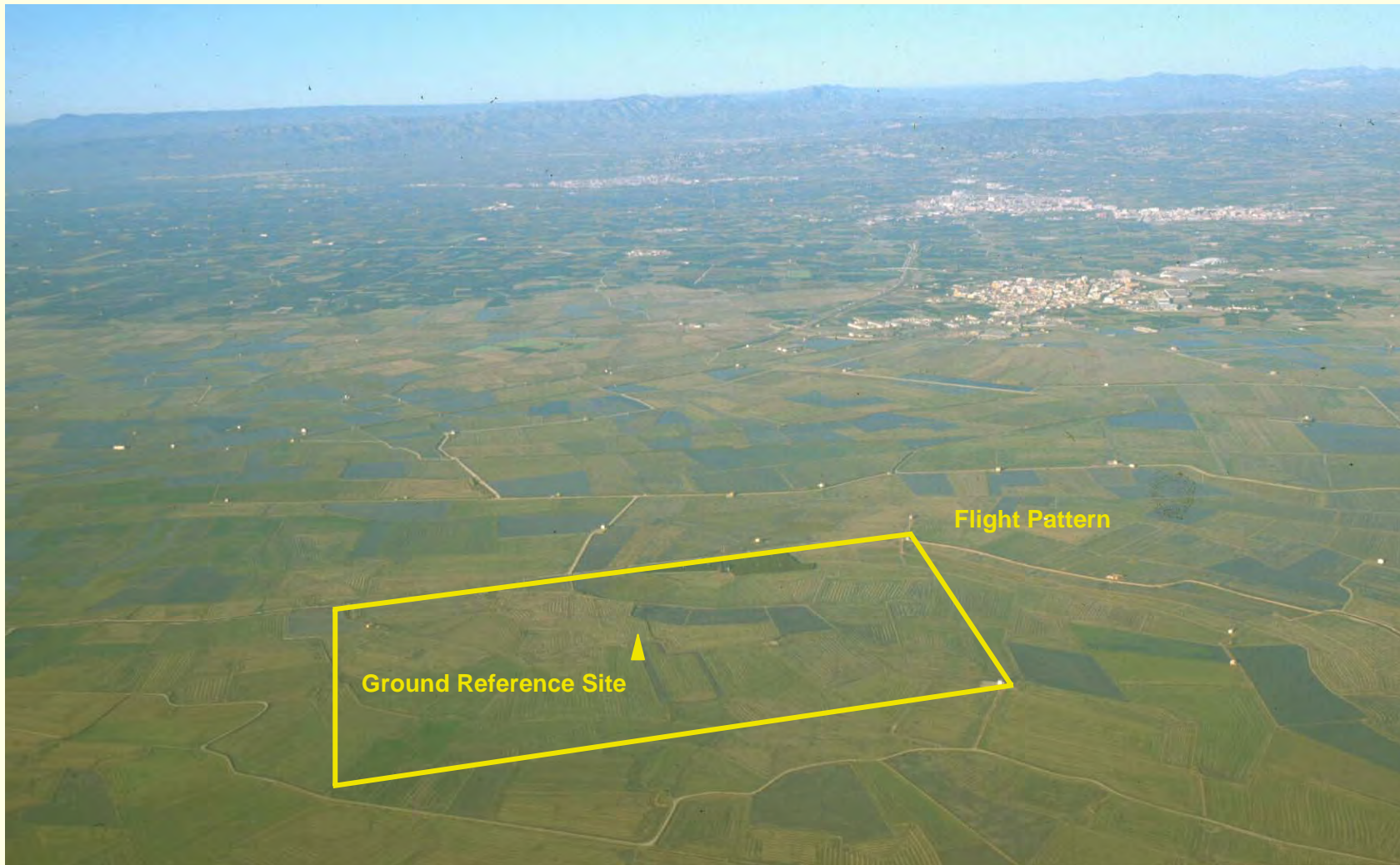


Figure 6 Flight pattern and location of the ground reference site. View above the Ricefields, the Orchards and the Coast Mountains to the West.

Picture: 6 December 2001



Reference Unit

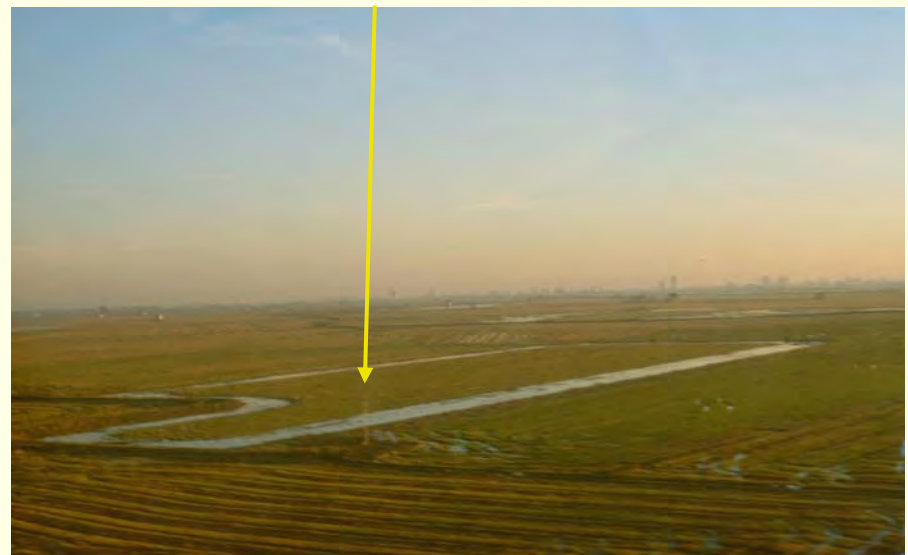


Figure 7

Comparison experiment between the
Flight- and Ground Reference
sampling Unit.

Pictures: 6 December 2001
(‘Aircraft and Mast’ by Waldemar Ziegler)



Figure 8 Aerial photograph of the remote mountain location ‘Cortes des Pallás’. The ground reference unit is visible in the front. Flight altitude approximately 150 m above ground, viewing north-west.

Picture: 12 December 2001

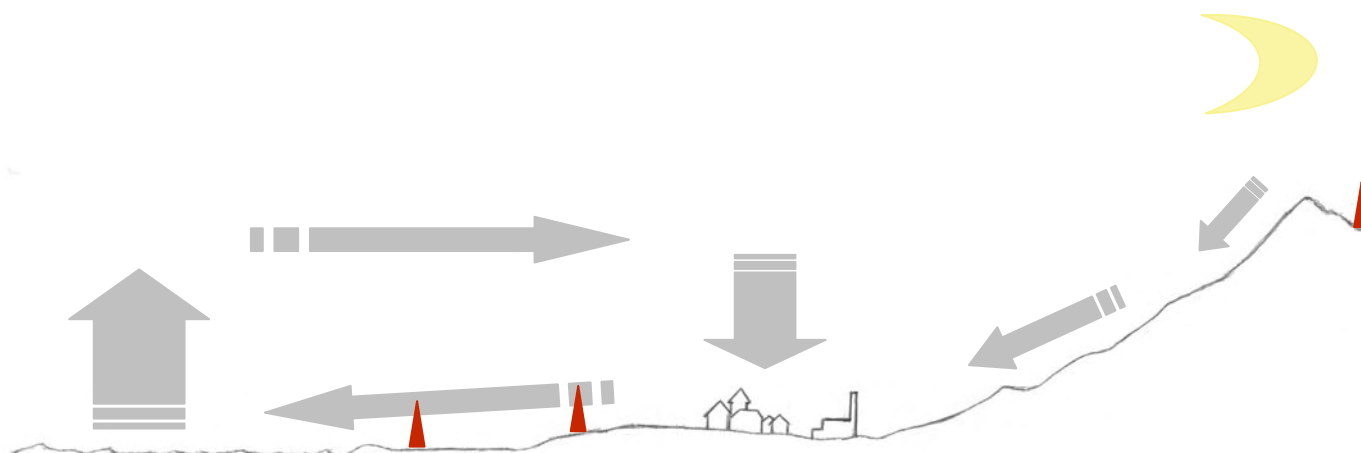
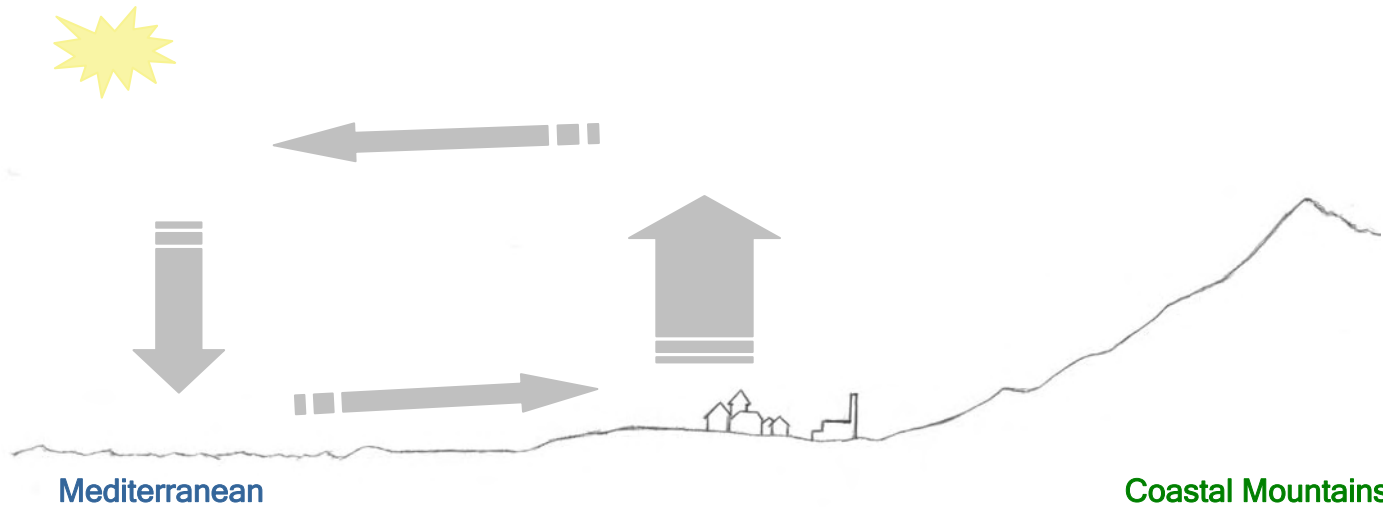


Figure 9 Scheme of the land-sea-wind circulation during day and night time. The locations of the ground reference sampling sites are marked by red triangles.

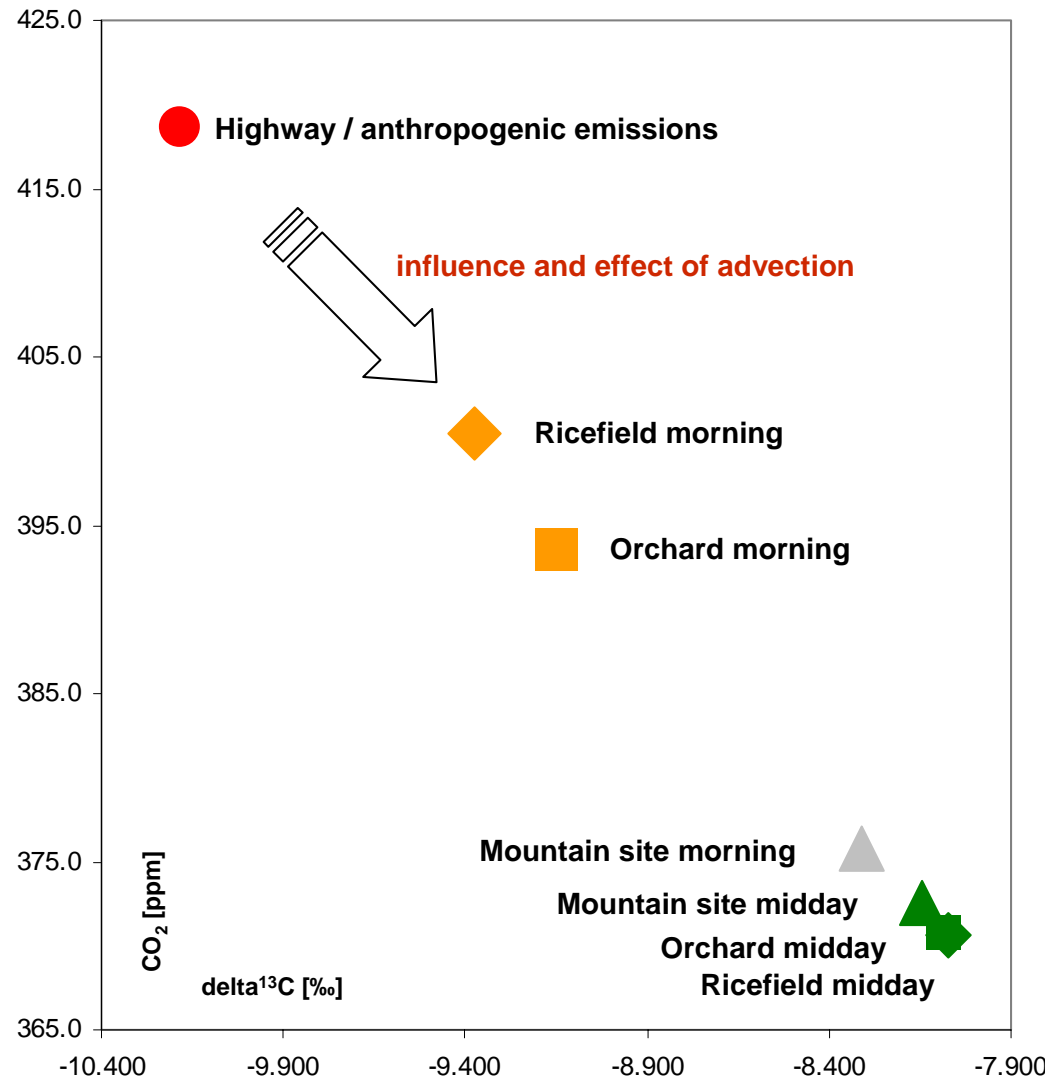


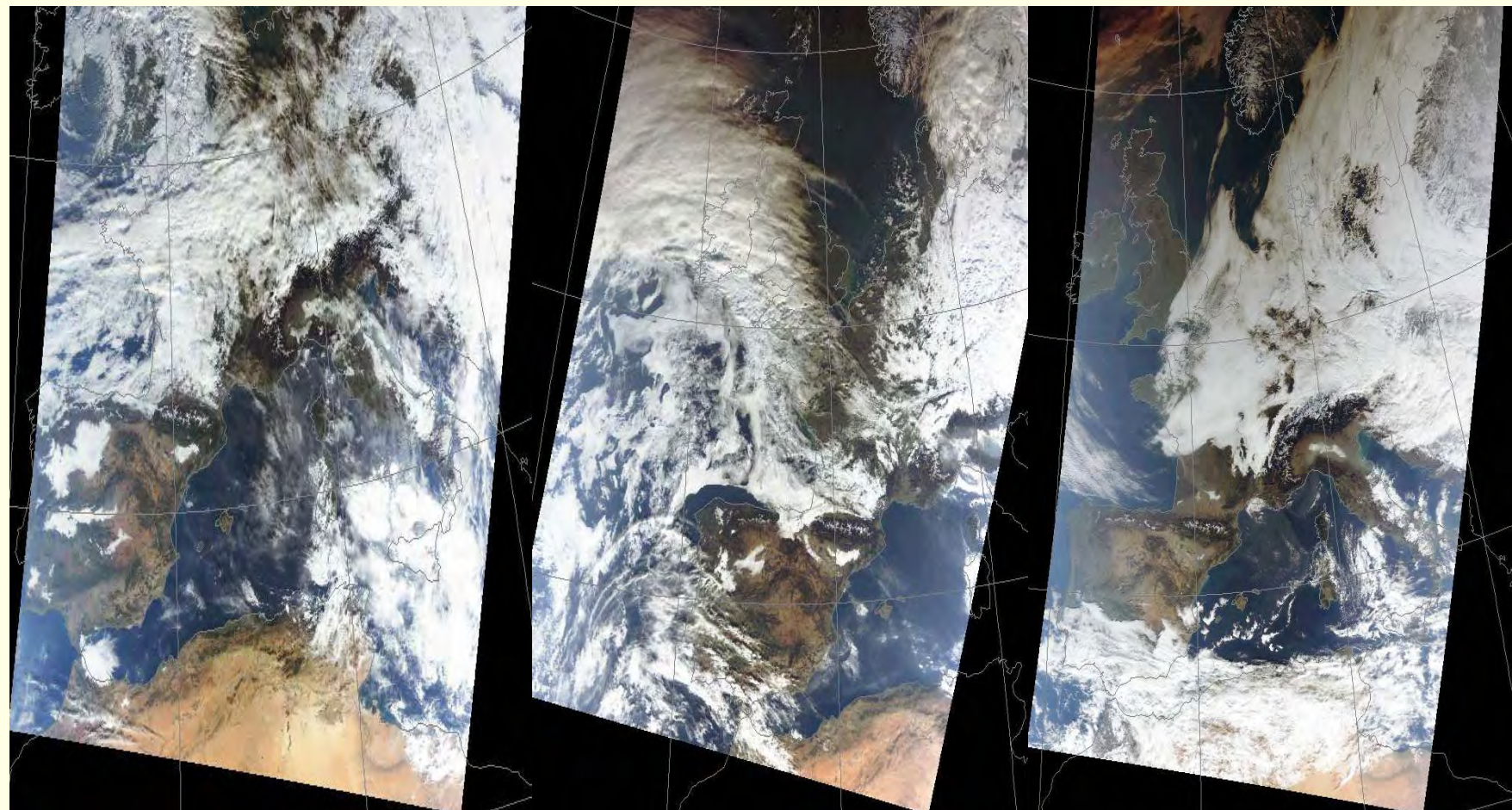
Figure 10 Results from the ground level flask sampling above the rice fields, the orchard, the remote mountain site and nearby the highway reflecting the effect of horizontal advection.



Figure 11

Installation of the Ground Reference Unit at the rice field site (top left). The Ground Reference Unit within the orange plantation (top right).

Ground Reference Unit at the remote mountain location site 'Cortes des Pallás'.



5 December 2001 10:35 UTC

6 December 2001 11:18 UTC

12 December 2001 10:41 UTC

Figure 12 MODIS Satellite Images (from Dundee Satellite Receiving Station)

Satellite: Terra Sensor: MODIS
RGB composite image reprojected (RGB 1,4,3 composite)

PARAMETER/VARIABLE DESCRIPTION

date&time (GMT) - date and time the sampling procedure was completed in Greenwich Mean Time

flask code - marking of nameplates for each flask

site - location of the flight pattern / ground reference site

Valzi	- south of Valencia above the citrus and apricot plantations [39°15.0'N / 000°26.7'W]
Reis	- above the paddy fields south of Lake Albufera [39°15.8'N / 000°20.6'W]
Mare	- around 1 km off shore, east of Tamarit al
P-Plant	- inside the apricot plantation
Reis-Bo	- at the temporary field site in the paddy field

alt - sampling height in meter above ground

init p. - internal flask pressure at the beginning of the analyses

Mixing ratios

Precision of the analyses

CH₄ [ppb] -	methan concentration in ppb	1.3 ppb
CO₂ [ppm] -	carbon dioxide concentration in ppm	0.08 ppm
N₂O [ppb] -	nitrous oxide concentration in ppb	0.15 ppb

Isotope Ratio

$$\delta[\$] = (R_{\text{sa}}/R_{\text{ref}} - 1) \cdot 1000 \quad R_{\text{sa}} \text{ and } R_{\text{ref}} \text{ are the sample and reference isotope ratios}$$

del ¹³C [\$] - ratio of the carbon 13 isotope and carbon 12 isotope due to the VPDB isotope ratio scale

del ¹⁸O [\$] - ratio of the oxygen 18 isotope and oxygen 16 isotope due to the VPDB (gas) isotope ratio scale

$$\text{Precision of the analyses} \quad {}^{13}\text{C} = 0.012 \$ \quad {}^{18}\text{O} = 0.02 \$$$

date&time [GMT]	flask code	site	alt [m]	init p.	mixing ratio			isotope	
					CH ₄ [ppb]	CO ₂ [ppm]	N ₂ O [ppb]	del ¹³ C [%]	del ¹⁸ O [%]
25.6.01 8:28	J151-01	Valzi	100	1.8	1819.7	371.3	318.4	-8.392	1.421
25.6.01 8:28	J144-01	Valzi	100	1.8	1828.4	373.5	319.0	-8.382	1.544
25.6.01 8:43	J155-01	Valzi	500	1.8	1770.8	368.0	317.3	-8.110	0.879
25.6.01 8:43	J156-01	Valzi	500	1.8	1770.8	368.9	317.3	-8.118	0.905
25.6.01 8:57	J153-01	Valzi	1000	1.7	1772.8	368.6	317.1	-8.126	0.869
25.6.01 8:57	J154-01	Valzi	1000	1.0	-999	-999	-999	-8.840	0.774
25.6.01 9:11	J152-01	Valzi	1500	1.7	1779.4	368.6	317.0	-8.122	0.946
25.6.01 9:11	J150-01	Valzi	1500	1.7	1804.4	371.4	318.0	-8.124	0.967
25.6.01 9:27	J141-01	Valzi	2000	1.7	1777.8	368.5	317.2	-8.126	0.634
25.6.01 9:27	J142-01	Valzi	2000	1.6	1774.8	369.3	317.1	-8.132	0.654
25.6.01 12:30	J143-01	Valzi	150	1.8	1802.6	371.3	319.1	-8.267	0.871
25.6.01 12:30	J145-01	Valzi	150	1.8	1802.1	372.3	318.8	-8.271	0.881
25.6.01 12:42	J170-01	Valzi	500	1.8	1765.4	368.9	317.1	-8.114	0.836
25.6.01 12:42	J171-01	Valzi	500	1.8	1765.1	369.7	317.2	-8.112	0.845
26.6.01 5:24	J160-01	Valzi	100	1.9	1816.2	377.4	318.3	-8.549	1.009
26.6.01 5:24	J159-01	Valzi	100	1.8	1815.5	377.8	318.0	-8.545	0.992
26.6.01 5:34	J164-01	Valzi	500	1.9	1802.8	372.0	317.9	-8.288	0.917
26.6.01 5:34	J162-01	Valzi	500	1.9	1804.0	371.8	317.6	-8.274	0.971
26.6.01 5:49	J166-01	Valzi	1000	1.8	1779.3	370.3	317.3	-8.187	0.821
26.6.01 5:49	J167-01	Valzi	1000	1.8	1779.2	370.6	317.1	-8.186	0.841
26.6.01 6:11	J165-01	Valzi	1500	1.6	1779.3	368.8	317.2	-8.106	0.830
26.6.01 6:11	J163-01	Valzi	1500	1.6	1781.5	369.3	317.0	-8.122	0.827
26.6.01 8:47	J157-01	Valzi	100	1.4	1871.2	379.8	321.0	-8.602	1.213
26.6.01 8:47	J158-01	Valzi	100	1.5	1866.9	380.1	320.4	-8.638	1.159
26.6.01 9:00	J140-01	Valzi	500	1.4	1808.2	371.8	323.8	-8.224	1.106
26.6.01 9:00	J139-01	Valzi	500	1.4	1809.6	372.2	317.8	-8.237	1.097
26.6.01 9:13	J138-01	Valzi	1000	1.4	1784.6	370.0	317.4	-8.139	0.857
26.6.01 9:13	J168-01	Valzi	1000	1.4	1783.8	370.4	317.2	-8.156	0.864
26.6.01 9:30	J194-01	Valzi	1500	1.4	1779.0	369.5	317.3	-8.129	0.746
26.6.01 9:30	J193-01	Valzi	1500	1.4	1779.8	369.8	317.0	-8.150	0.767
26.6.01 9:44	J191-01	Valzi	1750	1.1	1782.0	379.2	319.8	-8.229	0.677
26.6.01 9:44	J192-01	Valzi	1750	1.0	-999	-999	-999	-8.335	0.624
26.6.01 11:59	J190-01	Valzi	100	1.5	1811.0	367.7	318.3	-8.162	0.813
26.6.01 11:59	J189-01	Valzi	100	1.5	1813.4	369.9	318.5	-8.183	0.871
26.6.01 12:11	J188-01	Valzi	500	1.3	1836.6	369.4	318.6	-8.289	1.026
26.6.01 12:11	J187-01	Valzi	500	1.3	1840.6	373.2	318.5	-8.311	1.066
26.6.01 12:26	J186-01	Valzi	1000	1.3	1787.3	369.1	317.5	-8.138	0.801
26.6.01 12:26	J177-01	Valzi	1000	1.3	1787.1	369.4	317.1	-8.161	0.804
26.6.01 12:41	J181-01	Valzi	1500	1.3	1772.6	369.0	317.5	-8.118	0.543
26.6.01 12:41	J182-01	Valzi	1500	1.3	1777.3	368.9	317.1	-8.141	0.733
26.6.01 12:55	J046-01	Valzi	1750	1.3	1764.4	368.9	317.2	-8.134	0.626
26.6.01 12:55	J175-01	Valzi	1750	1.3	1763.7	369.0	316.9	-8.141	0.620
27.6.01 18:14	J173-01	VFlug	180	1.7	1819.0	368.6	317.8	-8.163	0.752
27.6.01 18:14	J174-01	VFlug	180	1.6	1817.2	368.9	317.6	-8.147	0.830
28.6.01 5:28	J035-01	Valzi	100	3.5	1833.2	377.6	318.5	-8.431	0.898
28.6.01 5:28	J037-01	Valzi	100	3.0	1831.9	378.0	318.8	-8.456	0.894
28.6.01 5:37	J049-01	Valzi	335	3.1	1821.3	375.4	318.6	-8.333	0.859
28.6.01 5:37	J047-01	Valzi	335	3.0	1817.3	375.3	318.5	-8.304	0.798
28.6.01 5:46	J038-01	Valzi	500	3.0	1819.6	373.9	318.6	-8.258	0.835
28.6.01 5:46	J039-01	Valzi	500	2.7	1818.0	374.4	318.8	-8.260	0.788
28.6.01 5:56	J044-01	Valzi	1000	2.9	1803.6	368.7	317.7	-8.054	0.750
28.6.01 5:56	J040-01	Valzi	1000	2.9	1804.6	369.8	317.7	-8.078	0.684
28.6.01 6:08	J041-01	Valzi	1500	2.9	1801.0	369.1	317.4	-8.015	0.610
28.6.01 6:08	J048-01	Valzi	1500	2.8	1801.1	369.3	317.6	-8.047	0.592
28.6.01 6:23	J043-01	Valzi	2000	2.4	1803.6	368.8	318.1	-8.016	0.806
28.6.01 6:23	J042-01	Valzi	2000	2.4	1805.1	368.7	317.8	-8.007	0.797
28.6.01 8:44	J132-01	Valzi	100	1.6	1852.9	371.0	318.7	-7.990	1.399
28.6.01 8:44	J133-01	Valzi	100	1.6	1846.8	371.6	318.5	-7.937	1.640
28.6.01 8:53	J130-01	Valzi	335	1.5	1832.0	370.8	318.3	-8.216	0.923
28.6.01 8:53	J131-01	Valzi	335	1.5	1830.1	370.9	318.1	-8.203	0.966
28.6.01 9:02	J128-01	Valzi	500	1.5	1834.7	370.3	318.2	-8.173	0.866
28.6.01 9:02	J129-01	Valzi	500	1.5	1830.4	370.6	317.9	-8.182	0.927
28.6.01 9:12	J127-01	Valzi	1000	1.5	1799.6	365.4	316.7	-7.948	0.524
28.6.01 9:12	J134-01	Valzi	1000	1.5	1799.7	365.8	316.6	-7.984	0.621
28.6.01 9:23	J137-01	Valzi	1500	1.4	1798.1	364.3	316.6	-7.928	0.536
28.6.01 9:23	J136-01	Valzi	1500	1.4	1797.5	365.1	316.5	-7.970	0.530
28.6.01 9:37	J125-01	Valzi	2000	1.4	1802.2	363.6	316.6	-7.940	0.7

2.7.01 7:53	J103-01	Valzi	250	2.1	1837.4	373.8	319.0	-8.286	0.983
2.7.01 8:04	J120-01	Valzi	500	2.6	1814.3	368.7	318.4	-8.013	0.963
2.7.01 8:04	J114-01	Valzi	500	2.6	1814.9	368.7	318.5	-7.990	0.942
2.7.01 8:18	J118-01	Valzi	1000	2.3	1796.1	369.1	318.0	-8.032	0.900
2.7.01 8:18	J121-01	Valzi	1000	2.3	1794.0	369.0	318.0	-8.032	0.935
2.7.01 8:31	J117-01	Valzi	1500	2.3	1787.7	368.7	317.8	-8.013	0.916
2.7.01 8:31	J115-01	Valzi	1500	2.3	1786.7	368.4	317.9	-7.996	0.902
2.7.01 8:52	J119-01	Mare	100	2.5	1912.1	375.7	322.0	-8.384	0.900
2.7.01 8:52	J112-01	Mare	100	2.5	1911.5	375.6	321.8	-8.393	0.837
2.7.01 11:21	J242-01	Valzi	100	1.8	1857.1	365.9	319.6	-7.967	1.088
2.7.01 11:21	J214-01	Valzi	100	2.0	1861.2	366.5	319.3	-8.017	1.083
2.7.01 11:29	J110-01	Valzi	250	2.0	1845.9	366.6	319.1	-8.019	1.048
2.7.01 11:29	J245-01	Valzi	250	2.0	1844.0	367.2	318.9	-8.033	1.051
2.7.01 11:38	J107-01	Valzi	500	1.9	1806.2	367.8	317.8	-8.062	0.843
2.7.01 11:38	J215-01	Valzi	500	1.9	1805.9	368.5	317.8	-8.075	0.872
2.7.01 11:48	J104-01	Valzi	1000	1.9	1788.1	366.0	317.2	-8.017	0.745
2.7.01 11:48	J216-01	Valzi	1000	1.9	1790.7	367.2	317.2	-7.998	0.749
2.7.01 11:59	J213-01	Valzi	1500	1.9	1790.8	366.4	317.1	-7.984	0.815
2.7.01 11:59	J218-01	Valzi	1500	1.9	1792.0	366.8	317.0	-7.995	0.803
2.7.01 12:19	J243-01	Mare	100	2.0	1830.5	363.6	317.9	-7.889	1.113
2.7.01 12:19	J244-01	Mare	100	2.0	1827.5	364.2	318.1	-7.918	1.083
2.7.01 14:51	J241-01	Valzi	100	2.0	1816.7	363.4	318.0	-7.866	0.860
2.7.01 14:51	J239-01	Valzi	100	2.0	1817.9	363.9	317.9	-7.871	0.956
2.7.01 15:01	J237-01	Valzi	250	2.0	1811.6	364.6	317.9	-7.898	0.860
2.7.01 15:01	J240-01	Valzi	250	2.0	1812.9	365.1	317.9	-7.915	0.820
2.7.01 15:10	J238-01	Valzi	500	1.9	1811.8	366.5	317.9	-8.009	0.892
2.7.01 15:10	J231-01	Valzi	500	1.7	1811.8	366.9	317.9	-9.009	0.328
2.7.01 15:20	J235-01	Valzi	1000	1.9	1809.3	367.1	317.9	-8.030	0.857
2.7.01 15:20	J236-01	Valzi	1000	1.9	1808.7	367.7	318.1	-8.041	0.906
2.7.01 15:34	J233-01	Valzi	1500	1.9	1793.2	366.8	317.3	-8.019	0.776
2.7.01 15:34	J232-01	Valzi	1500	1.9	1794.7	367.5	317.2	-8.018	0.804
2.7.01 16:07	J234-01	Mare	100	2.0	1816.0	364.1	317.8	-7.940	0.902
2.7.01 16:07	J034-01	Mare	100	2.0	1812.9	365.5	317.6	-7.960	0.957
3.7.01 7:43	J023-01	Valzi	100	2.1	1883.2	370.7	322.0	-8.263	0.931
3.7.01 7:43	J033-01	Valzi	100	2.1	1875.7	370.7	322.5	-8.212	0.991
3.7.01 7:51	J026-01	Valzi	250	2.1	1867.7	370.4	321.6	-8.221	0.928
3.7.01 7:51	J030-01	Valzi	250	2.1	1867.0	371.7	321.6	-8.252	0.931
3.7.01 8:00	J028-01	Valzi	500	2.1	1821.1	367.1	318.1	-8.068	0.931
3.7.01 8:00	J031-01	Valzi	500	2.1	1821.8	368.3	318.5	-8.076	0.921
3.7.01 8:10	J027-01	Valzi	1000	2.1	1804.0	366.5	317.5	-8.009	0.629
3.7.01 8:10	J032-01	Valzi	1000	2.1	1802.7	367.1	317.2	-8.024	0.707
3.7.01 8:21	J024-01	Valzi	1500	2.0	1801.6	366.5	317.2	-7.995	0.747
3.7.01 8:21	J021-01	Valzi	1500	2.0	1799.4	367.1	317.1	-8.004	0.831
3.7.01 8:50	J022-01	Mare	100	2.1	1862.9	371.3	320.1	-8.207	0.758
3.7.01 8:50	J020-01	Mare	100	2.1	1863.8	370.5	320.0	-8.195	0.770
3.7.01 11:05	J029-01	Valzi	100	2.0	1851.4	366.7	319.5	-8.097	0.726
3.7.01 11:05	J025-01	Valzi	100	2.0	1851.6	367.6	319.6	-8.123	0.725
3.7.01 11:13	J203-01	Valzi	250	2.0	1853.5	367.5	319.5	-8.136	0.668
3.7.01 11:13	J205-01	Valzi	250	2.0	1852.9	368.8	319.4	-8.139	0.741
3.7.01 11:22	J204-01	Valzi	500	1.9	1818.2	366.7	317.9	-8.021	0.869
3.7.01 11:22	J211-01	Valzi	500	1.9	1821.5	367.1	318.2	-8.047	0.870
3.7.01 11:32	J212-01	Valzi	1000	1.9	1806.5	366.7	317.5	-8.058	0.815
3.7.01 11:32	J210-01	Valzi	1000	1.9	1805.6	367.6	317.5	-8.065	0.837
3.7.01 11:47	J209-01	Valzi	1500	1.8	1793.0	368.5	317.3	-8.086	0.649
3.7.01 11:47	J208-01	Valzi	1500	1.8	1793.3	369.0	317.2	-8.092	0.791
3.7.01 12:15	J206-01	Mare	100	2.0	1830.0	367.2	318.0	-8.085	0.867
3.7.01 12:15	J207-01	Mare	100	2.0	1829.4	367.9	318.1	-8.087	0.784
3.7.01 14:49	J197-01	Valzi	100	2.0	1816.0	360.3	317.7	-7.746	0.893
3.7.01 14:49	J198-01	Valzi	100	2.0	1816.6	361.4	317.8	-7.773	0.974
3.7.01 14:58	J099-01	Valzi	250	2.0	1811.8	363.4	317.5	-7.871	0.884
3.7.01 14:58	J100-01	Valzi	250	2.0	1813.4	364.0	317.7	-7.871	0.861
3.7.01 15:07	J093-01	Valzi	500	1.9	1811.4	365.9	317.5	-7.996	0.840
3.7.01 15:07	J097-01	Valzi	500	1.9	1810.4	366.5	317.5	-7.976	0.821
3.7.01 15:18	J098-01	Valzi	1000	1.9	1815.7	366.3	317.7	-8.030	0.813
3.7.01 15:18	J200-01	Valzi	1000	1.9	1814.7	367.3	317.8	-8.043	0.830
3.7.01 15:34	J199-01	Valzi	1500	1.9	1807.2	366.8	317.8	-8.012	0.197
3.7.01 15:34	J202-01	Valzi	1500	1.9	1808.6	367.0	317.6	-8.018	0.771
3.7.01 16:02	J092-01	Mare	100	2.0	1806.1	365.4	317.5	-7.967	0.815
3.7.01 16:02	J091-01	Mare	100	2.0	1807.9	365.7	317.5	-7.975	0.886
4.7.01 8:47	J075-01	Reis	100	2.0	1919.4	367.3	322.3	-8.065	0.743
4.7.01 8:47	J071-01	Reis	100	2.0					

4.7.01 12:30	J379-01	Reis	500	2.0	1826.6	369.5	318.1	-8.133	0.778
4.7.01 12:39	J090-01	Reis	1000	2.0	1812.2	367.3	317.6	-8.049	0.880
4.7.01 12:39	J373-01	Reis	1000	2.0	1811.1	367.9	317.6	-8.062	0.723
4.7.01 12:54	J375-01	Reis	1500	2.2	1801.8	366.4	317.4	-8.019	0.572
4.7.01 12:54	J376-01	Reis	1500	2.1	1800.7	366.9	317.3	-8.009	0.740
4.7.01 13:15	J377-01	Mare	100	2.0	1812.1	370.2	318.3	-8.063	-0.308
4.7.01 13:15	J378-01	Mare	100	2.0	1813.7	369.9	318.1	-8.152	0.566
4.7.01 15:24	J258-01	Reis	100	2.0	1813.4	368.1	317.8	-8.108	0.682
4.7.01 15:24	J253-01	Reis	100	2.0	1813.4	369.0	317.8	-8.126	0.612
4.7.01 15:32	J322-01	Reis	250	1.9	1808.8	368.5	317.6	-8.076	0.554
4.7.01 15:32	J270-01	Reis	250	1.9	1808.5	369.1	317.8	-8.116	0.650
4.7.01 15:41	J321-01	Reis	500	1.9	1804.5	368.5	317.5	-8.091	0.655
4.7.01 15:41	J266-01	Reis	500	1.9	1802.9	369.1	317.6	-8.090	0.737
4.7.01 15:51	J320-01	Reis	1000	1.9	1804.5	368.1	317.5	-8.060	0.712
4.7.01 15:51	J267-01	Reis	1000	1.9	1804.7	368.7	317.5	-8.071	0.622
4.7.01 16:03	J260-01	Reis	1500	1.9	1809.3	367.7	317.2	-8.071	0.770
4.7.01 16:03	J265-01	Reis	1500	1.9	1808.2	369.1	317.8	-8.085	0.686
4.7.01 16:28	J255-01	Mare	100	1.9	1799.7	367.7	317.3	-8.052	0.552
4.7.01 16:28	J259-01	Mare	100	1.9	1798.4	368.8	317.6	-7.985	0.780
3.7.01 3:34	J530-01	P-Plant	0.5	2.0	1975.9	428.7	336.0	-10.308	0.291
3.7.01 3:34	J531-01	P-Plant	0.5	2.0	1978.6	428.1	335.8	-10.283	0.344
3.7.01 3:49	J529-01	P-Plant	1	2.0	1954.7	421.6	332.2	-10.099	0.414
3.7.01 3:49	J527-01	P-Plant	1	2.0	1955.5	420.3	332.1	-10.055	0.397
3.7.01 4:06	J526-01	P-Plant	2	2.0	1841.5	363.5	314.9	-8.286	-0.926
3.7.01 4:06	J528-01	P-Plant	2	2.0	1842.8	364.1	315.0	-8.298	-0.771
3.7.01 4:25	J525-01	P-Plant	3	1.9	1841.7	363.8	314.9	-8.259	-1.103
3.7.01 4:25	J524-01	P-Plant	3	2.0	1842.6	364.1	314.9	-8.273	-0.797
3.7.01 4:40	J523-01	P-Plant	4.5	1.9	1842.6	363.4	314.7	-8.266	-1.007
3.7.01 4:40	J522-01	P-Plant	4.5	2.0	1845.8	363.9	314.7	-8.261	-0.872
5.7.01 12:10	J248-01	P-Plant	0.5	1.9	1817.1	367.0	317.9	-7.911	1.096
5.7.01 12:10	J252-01	P-Plant	0.5	1.9	1818.8	366.7	317.7	-7.892	1.093
5.7.01 12:25	J052-01	P-Plant	1	1.9	1805.1	365.7	317.6	-7.867	1.052
5.7.01 12:25	J051-01	P-Plant	1	1.9	1804.7	365.6	317.4	-7.874	1.094
5.7.01 12:45	J249-01	P-Plant	2	1.8	1804.5	364.1	317.5	-7.776	1.181
5.7.01 12:45	J521-01	P-Plant	2	1.9	1803.4	364.3	317.6	-7.784	1.214
5.7.01 13:03	J520-01	P-Plant	3	1.8	1802.5	365.5	317.4	-7.830	0.905
5.7.01 13:03	J519-01	P-Plant	3	-999	1801.8	365.5	317.3	-7.822	0.813
5.7.01 13:19	J517-01	P-Plant	4.15	-999	1802.8	366.5	317.8	-7.894	0.812
5.7.01 13:19	J518-01	P-Plant	4.15	-999	1803.1	366.3	317.6	-7.892	0.784
4.7.01 14:33	J054-01	Reis-Bo	0.1	1.9	1920.1	342.2	318.6	-6.460	1.487
4.7.01 14:33	J055-01	Reis-Bo	0.1	1.9	1923.0	342.0	318.7	-6.418	1.454
4.7.01 13:05	J062-01	Reis-Bo	0.5	1.9	1837.6	351.8	318.7	-6.932	1.482
4.7.01 13:05	J069-01	Reis-Bo	0.5	1.8	1837.3	353.0	318.7	-6.997	1.432
4.7.01 13:20	J070-01	Reis-Bo	1	1.9	1830.7	356.5	318.9	-6.777	2.017
4.7.01 13:20	J066-01	Reis-Bo	1	1.9	1829.1	357.0	318.8	-6.780	2.081
4.7.01 13:36	J065-01	Reis-Bo	2	1.9	1824.1	352.9	318.9	-7.101	1.158
4.7.01 13:36	J056-01	Reis-Bo	2	-999	1823.6	352.5	318.9	-7.098	1.169
4.7.01 13:52	J057-01	Reis-Bo	3	-999	1824.8	357.1	319.0	-7.333	1.132
4.7.01 13:52	J058-01	Reis-Bo	3	1.2	1824.7	357.4	319.0	-7.358	1.081
4.7.01 14:11	J060-01	Reis-Bo	3.75	-999	1825.3	357.6	318.5	-7.333	1.203
4.7.01 14:11	J059-01	Reis-Bo	3.75	-999	1824.1	358.3	318.6	-7.382	1.247

PARAMETER/VARIABLE DESCRIPTION

date&time (GMT) - date and time the sampling procedure was completed in Greenwich Mean Time

flask code - marking of nameplates for each flask

site - location of the flight pattern / ground reference site

Rice - flight track around the temporal CEAM flux tower at the ricefield site south-east of Sollana (Waypoints: NE 39,27874°N / 000,33356°W, NW 39,28093°N / 000,34595°W, SE 39,26414°N / 000,33343°W, SW 39,26694°N / 000,34417°W; Tower for ground reference 39,26453°N / 000,34329°W)

Cortes - flight track above vegetation type of macchie, mountain site, Slightly rolling plateau ~ 750m a.s.l. (Tower for ground reference 39,22550°N / 000,82689°W)

alt - sampling height in meter above ground

init p. - internal flask pressure at the beginning of the analyses

Mixing Ratios

	Precision of the analyses
CH₄ [ppb] - methan concentration in ppb	1.3 ppb
CO₂ [ppm] - carbon dioxide concentration in ppm	0.08 ppm
N₂O [ppb] - nitrous oxide concentration in ppb	0.15 ppb
CO [ppb] - carbon monoxide concentration in ppb	1.0 ppb
H₂ [ppb] - hydrogen concentration in ppb	5.0 ppb
SF₆ [ppt] - sulfur hexafluoride in ppt	0.08 ppt

Isotope Ratio

$$\delta[\$] = (R_{\text{sa}}/R_{\text{ref}} - 1) \cdot 1000 \quad R_{\text{sa}} \text{ and } R_{\text{ref}} \text{ are the sample and reference isotope ratios}$$

del ¹³C [\$] - ratio of the carbon 13 isotope and carbon 12 isotope due to the VPDB isotope ratio scale

del ¹⁸O [\$] - ratio of the oxygen 18 isotope and oxygen 16 isotope due to the VPDB (gas) isotope ratio scale

$$\text{Precision of the analyses} \quad {}^{13}\text{C} = 0.012 \$ \quad {}^{18}\text{O} = 0.02 \$$$

date&time [GMT]	Flask No.	site	alt [m]	init p.	mixing ratio						isotope	
					CH ₄ [ppb]	CO ₂ [ppm]	CO [ppb]	H ₂ [ppb]	SF ₆ [ppt]	N ₂ O [ppb]	del ¹³ C [%]	del ¹⁸ O [%]
01.12.2001 07:37	J130-1	Rice	46	2.2	1865.2	375.0	206.0	483.2	5.08	318.7	-8.394	0.016
01.12.2001 07:37	J127-1	Rice	46	2.2	1865.6	376.4	207.2	476.2	5.11	318.9	-8.393	0.030
01.12.2001 07:46	J128-1	Rice	91	2.2	1853.4	372.4	147.9	469.9	5.18	318.4	-8.220	0.025
01.12.2001 07:46	J138-1	Rice	91	2.1	1854.9	373.6	158.5	464.7	5.15	318.6	-8.240	0.057
01.12.2001 07:57	J139-1	Rice	152	2.1	1848.0	371.9	136.4	471.3	5.33	318.3	-8.217	-0.078
01.12.2001 07:57	J129-1	Rice	152	2.1	1846.5	372.7	135.6	460.9	5.22	318.4	-8.197	-0.045
01.12.2001 08:19	J137-1	Rice	823	2.0	1805.9	369.1	115.5	472.4	4.94	318.0	-8.075	-0.121
01.12.2001 08:19	J134-1	Rice	823	2.0	1806.6	369.9	115.3	469.0	4.94	317.9	-8.069	-0.052
01.12.2001 12:35	J132-1	Mare	30	2.0	1831.6	367.5	135.2	465.1	5.13	318.2	-8.051	-0.257
01.12.2001 12:35	J136-1	Mare	30	2.1	1830.7	368.3	134.1	460.6	5.06	318.2	-8.035	-0.116
01.12.2001 14:56	J118-1	Rice	46	2.0	1868.8	375.6	268.2	479.3	5.20	319.3	-8.538	-0.138
01.12.2001 14:56	J117-1	Rice	46	2.2	1867.8	376.7	272.9	479.4	5.25	319.4	-8.514	-0.059
01.12.2001 15:05	J125-1	Rice	91	2.2	1866.9	376.7	249.2	473.0	5.04	319.7	-8.536	-0.070
01.12.2001 15:05	J126-1	Rice	91	2.1	1867.3	377.7	245.0	466.3	5.16	319.7	-8.521	-0.019
01.12.2001 15:13	J453-1	Rice	152	2.1	1852.5	374.5	207.9	464.8	5.21	319.2	-8.373	-0.144
01.12.2001 15:13	J454-1	Rice	152	2.1	1851.2	375.1	200.5	459.9	5.19	319.2	-8.372	-0.172
01.12.2001 15:32	J124-1	Rice	823	2.1	1845.6	367.0	135.0	441.7	5.18	318.2	-8.051	-0.124
01.12.2001 15:32	J451-1	Rice	823	2.1	1844.3	368.1	134.4	439.3	5.12	318.5	-8.041	-0.015
02.12.2001 07:26	J439-1	Rice	30	2.1	1956.8	385.9	267.1	459.6	5.05	319.8	-8.920	-0.333
02.12.2001 07:26	J444-1	Rice	30	2.1	1957.5	387.3	261.2	449.1	5.18	319.8	-8.976	-0.347
02.12.2001 07:35	J440-1	Rice	76	2.2	1929.8	385.0	221.3	460.7	5.00	319.5	-8.882	-0.376
02.12.2001 07:35	J447-1	Rice	76	2.2	1928.9	386.8	222.6	497.7	5.07	319.8	-8.913	-0.295
02.12.2001 07:44	J446-1	Rice	152	2.1	1893.7	381.6	203.7	463.0	5.09	320.7	-8.707	-0.598
02.12.2001 07:44	J445-1	Rice	152	2.0	1893.2	381.3	198.3	452.5	5.16	320.7	-8.621	-0.341
02.12.2001 07:53	J449-1	Rice	229	2.1	1889.8	380.4	202.0	464.8	5.11	322.4	-8.603	-0.481
02.12.2001 07:53	J448-1	Rice	229	2.1	1893.6	381.4	202.1	460.4	5.18	322.8	-8.599	-0.471
02.12.2001 12:52	J450-1	Mare	30	2.2	1932.2	379.6	260.7	472.0	5.11	319.5	-8.554	-0.306
02.12.2001 12:52	J441-1	Mare	30	2.1	1933.0	378.3	258.1	473.2	5.16	319.5	-8.561	-0.587
02.12.2001 14:50	J452-1	Rice	30	2.0	1881.9	375.0	196.8	466.4	8.05	318.8	-8.404	-0.583
02.12.2001 14:50	J442-1	Rice	30	2.0	1884.1	375.5	197.7	462.0	7.89	318.8	-8.405	-0.321
02.12.2001 14:59	J568-1	Rice	76	2.2	1885.3	375.7	204.3	472.5	5.04	318.9	-8.446	-0.530
02.12.2001 14:59	J017-1	Rice	76	2.2	1878.9	376.8	199.5	466.5	5.04	318.8	-8.449	-0.269
02.12.2001 15:08	J571-1	Rice	152	2.1	1863.5	375.4	182.3	485.4	4.90	318.6	-8.409	-0.510
02.12.2001 15:08	J566-1	Rice	152	2.1	1864.9	376.1	180.2	477.8	4.93	318.8	-8.420	-0.367
02.12.2001 15:16	J567-1	Rice	229	2.2	1845.3	374.4	153.7	485.6	5.00	318.5	-8.363	-0.538
02.12.2001 15:16	J564-1	Rice	229	2.2	1848.3	375.3	153.8	477.5	4.99	318.4	-8.400	-0.420
02.12.2001 15:38	J565-1	Rice	1005	2.1	1850.7	371.8	166.9	463.3	4.97	318.5	-8.286	-0.309
02.12.2001 15:38	J569-1	Rice	1005	2.1	1850.5	373.0	-999	-999	-999	318.6	-8.270	-0.296
04.12.2001 07:30	J393-1	Rice	15	2.2	1884.4	381.9	-999	-999	-999	319.2	-8.750	-0.652
04.12.2001 07:30	J394-1	Rice	15	2.2	1882.7	382.2	-999	-999	-999	319.2	-8.724	-0.460
04.12.2001 07:39	J572-1	Rice	76	2.2	1872.3	379.2	-999	-999	-999	318.7	-8.573	-0.424
04.12.2001 07:39	J576-1	Rice	76	2.2	1872.8	380.2	-999	-999	-999	318.9	-8.612	-0.383
04.12.2001 07:49	J573-1	Rice	152	2.2	1860.7	376.4	-999	-999	-999	318.5	-8.410	-0.393
04.12.2001 07:49	J396-1	Rice	152	2.2	1863.4	377.3	-999	-999	-999	318.7	-8.431	-0.374
04.12.2001 07:58	J574-1	Rice	229	2.2	1855.5	374.4	-999	-999	-999	318.5	-8.320	-0.461
04.12.2001 07:58	J397-1	Rice	229	-999	1854.0	375.4	-999	-999	-999	318.6	-8.317	-0.328
04.12.2001 08:16	J575-1	Rice	1006	2.0	1805.1	368.4	116.4	466.7	4.85	318.2	-8.029	0.015
04.12.2001 08:16	J398-1	Rice	1006	2.0	1807.1	369.3	116.5	466.7	4.93	318.2	-8.031	-0.132
04.12.2001 12:36	J570-1	Mare	15	2.2	1868.5	372.6	201.3	428.2	5.03	318.9	-8.330	-0.479
04.12.2001 12:36	J395-1	Mare	15	2.2	1866.6	373.3	200.9	426.8	5.03	318.9	-8.332	-0.529
04.12.2001 14:50	J432-1	Rice	15	2.2	1855.0	371.4	188.9	437.5	4.85	318.7	-8.299	-0.560</td

05.12.2001	16:01	J336-1	Rice	1006	2.1	1794.8	366.9	106.9	473.7	4.96	317.9	-7.997	0.019
06.12.2001	07:32	J340-1	Rice	6	2.2	1898.2	387.5	234.3	393.8	5.05	319.3	-9.064	0.078
06.12.2001	07:32	J339-1	Rice	6	-999	1899.6	388.7	-999	-999	-999	319.2	-9.039	0.084
06.12.2001	07:41	J331-1	Rice	76	2.2	1877.6	380.8				318.9	-8.611	0.034
06.12.2001	07:41	J332-1	Rice	76	2.2	1879.7	382.0	241.9	397.9	4.81	318.8	-8.641	0.091
06.12.2001	07:52	J592-1	Rice	152	2.2	1867.3	378.7	200.0	395.0	5.07	318.9	-8.482	0.035
06.12.2001	07:52	J598-1	Rice	152	2.1	1867.4	379.3	205.5	394.7	5.03	319.1	-8.473	-0.057
06.12.2001	08:01	J328-1	Rice	229	2.2	1857.4	377.8	199.4	407.7	4.95	319.2	-8.444	-0.078
06.12.2001	08:01	J594-1	Rice	229	2.1	1854.9	378.6	199.9	421.9	4.92	319.3	-8.456	-0.054
06.12.2001	08:24	J330-1	Rice	1006	2.0	1803.5	368.7	120.5	459.5	4.85	318.1	-8.050	0.085
06.12.2001	08:24	J597-1	Rice	1006	2.0	1805.6	369.6	119.7	456.4	4.94	318.2	-8.074	0.058
06.12.2001	14:56	J599-1	Rice	6	2.2	1854.6	375.6	217.2	435.5	5.01	319.4	-8.382	-0.183
06.12.2001	14:56	J329-1	Rice	6	2.2	1854.1	376.6	216.2	435.2	4.95	319.5	-8.408	0.017
06.12.2001	15:05	J600-1	Rice	76	2.2	1852.2	376.1	212.0	434.7	5.00	319.3	-8.407	-0.157
06.12.2001	15:05	J601-1	Rice	76	2.1	1851.1	376.9	212.3	434.8	4.87	319.4	-8.401	-0.017
06.12.2001	15:13	J603-1	Rice	152	2.1	1849.3	374.3	211.7	420.4	4.94	319.3	-8.339	-0.119
06.12.2001	15:13	J604-1	Rice	152	2.1	1848.5	375.5	205.6	425.5	5.12	319.4	-8.352	0.109
06.12.2001	15:21	J611-1	Rice	229	2.1	1848.3	374.9	220.2	432.4	4.96	319.2	-8.349	0.002
06.12.2001	15:21	J610-1	Rice	229	2.1	1850.5	375.2	219.9	432.5	5.04	319.4	-8.348	0.024
06.12.2001	15:39	J612-1	Rice	1006	1.8	1800.9	367.9	113.8	462.8	5.12	318.1	-8.041	-0.024
06.12.2001	15:39	J609-1	Rice	1006	2.0	1802.4	368.8	111.9	462.3	5.10	318.1	-8.034	-0.022
12.12.2001	10:10	J602-1	Cortes	15	2.1	1830.5	371.0	147.9	471.3	5.09	318.2	-8.230	-0.238
12.12.2001	10:10	J613-1	Cortes	15	2.1	1830.3	372.1	150.5	472.1	5.08	318.3	-8.233	-0.160
12.12.2001	10:18	J529-1	Cortes	30	2.1	1829.4	371.6	145.3	473.0	4.95	318.2	-8.219	-0.186
12.12.2001	10:18	J515-1	Cortes	30	2.1	1829.8	372.7	145.5	472.4	5.10	318.3	-8.222	-0.207
12.12.2001	10:26	J518-1	Cortes	76	2.1	1828.2	371.6	139.8	470.8	5.07	318.2	-8.231	-0.260
12.12.2001	10:26	J519-1	Cortes	76	2.1	1828.9	372.5	142.0	470.2	5.04	318.2	-8.216	-0.257
12.12.2001	10:35	J517-1	Cortes	152	2.1	1829.5	372.1	137.1	472.2	5.02	318.2	-8.241	-0.318
12.12.2001	10:35	J496-1	Cortes	152	2.1	1829.6	372.8	136.6	469.7	4.96	318.3	-8.229	-0.239
12.12.2001	10:44	J528-1	Cortes	229	2.1	1833.8	372.8	143.4	474.7	5.09	318.3	-8.286	-0.344
12.12.2001	10:44	J522-1	Cortes	229	2.1	1835.6	373.6	144.1	471.4	5.09	318.2	-8.265	-0.277
12.12.2001	10:56	J516-1	Cortes	762	2.0	1825.5	371.7	138.3	475.5	5.04	318.1	-8.220	-0.266
12.12.2001	10:56	J498-1	Cortes	762	2.0	1826.2	372.6	136.9	474.8	5.02	318.3	-8.224	-0.337
12.12.2001	15:17	J521-1	Cortes	15	2.1	1839.2	371.8	150.1	474.8	5.09	318.2	-8.215	-0.236
12.12.2001	15:17	J497-1	Cortes	15	-999	1838.8	372.6	149.7	473.9	5.10	318.4	-8.231	-0.147
12.12.2001	15:25	J353-1	Cortes	30	-999	1836.1	371.9	146.1	473.6	5.05	318.3	-8.219	-0.172
12.12.2001	15:25	J352-1	Cortes	30	2.1	1837.4	372.8	144.9	472.1	5.18	318.4	-8.227	-0.218
12.12.2001	15:33	J349-1	Cortes	76	2.1	1835.3	372.1	142.9	473.9	5.12	318.3	-8.211	-0.367
12.12.2001	15:33	J348-1	Cortes	76	2.1	1837.3	372.7	144.2	470.8	5.32	318.4	-8.227	-0.199
12.12.2001	15:41	J356-1	Cortes	152	2.1	1837.9	372.1	143.2	475.1	5.17	318.3	-8.237	-0.226
12.12.2001	15:41	J354-1	Cortes	152	2.1	1835.1	372.7	141.3	472.9	5.14	318.3	-8.225	-0.152
30.11.2001	13:11	J505-1	OPlant	0,1	2.2	1856.3	371.2	160.9	410.1	5.05	318.6	-8.100	0.311
30.11.2001	13:11	J506-1	OPlant	0,1	2.2	1855.6	371.6	160.2	411.1	5.09	318.6	-8.095	0.263
30.11.2001	12:58	J503-1	OPlant	1,0	2.2	1862.7	370.9	170.0	413.9	5.11	318.7	-8.087	0.340
30.11.2001	12:58	J504-1	OPlant	1,0	2.2	1864.9	370.7	169.8	413.0	5.10	318.6	-8.086	0.357
30.11.2001	12:45	J501-1	OPlant	2,0	2.2	1870.0	371.3	178.2	414.4	5.09	318.8	-8.119	0.302
30.11.2001	12:45	J502-1	OPlant	2,0	2.2	1868.6	371.4	177.3	412.7	5.07	318.7	-8.085	0.351
30.11.2001	12:32	J499-1	OPlant	5,0	2.2	1875.8	373.4	179.6	411.7	5.13	318.7	-8.192	0.234
30.11.2001	12:32	J500-1	OPlant	5,0	2.2	1874.7	373.5	180.0	411.4	5.17	318.6	-8.206	0.208
30.11.2001	16:08	J510-1	RFeld	0,1	2.2	1846.5	368.2	155.8	434.7	5.19	318.6	-7.911	0.498
30.11.2001	16:08	J231-1	RFeld	0,1	2.2	1844.4	367.8	158.1	434.4	5.09	318.6	-7.919	0.479
30.11.2001	15:53	J513-1	RFeld	1,0	2.2	1858.5	370.6	150.6	431.6	5.22	318.6	-8.071	0.202
30.11.2001	15:53	J509-1	RFeld	1,0	2.2	1857.4	370.7	150.5	431.1	5.09	3		

13.12.2001	13:17	J323-1	Macchie	0,1	2.1	1822.1	371.0	130.1	451.1	5.06	318.3	-8.087	0.263
13.12.2001	13:38	J346-1	Macchie	0,5	2.1	1822.8	371.8	130.0	454.2	4.94	318.3	-8.127	0.145
13.12.2001	13:38	J345-1	Macchie	0,5	2.2	1821.7	371.7	129.9	455.6	4.94	318.2	-8.114	0.066
13.12.2001	13:56	J350-1	Macchie	1,0	2.1	1826.0	372.5	133.3	448.8	4.98	318.3	-8.143	0.191
13.12.2001	13:56	J351-1	Macchie	1,0	2.1	1826.4	372.4	133.1	453.4	5.04	318.3	-8.162	0.163
13.12.2001	14:10	J343-1	Macchie	2,0	2.1	1830.2	373.0	138.1	448.6	5.06	318.4	-8.200	0.037
13.12.2001	14:10	J342-1	Macchie	2,0	2.1	1830.3	373.1	137.4	450.1	5.21	318.4	-8.195	0.058
13.12.2001	14:23	J527-1	Macchie	5,0	2.1	1830.9	373.8	141.8	440.3	5.08	318.5	-8.225	0.136
13.12.2001	14:23	J525-1	Macchie	5,0	1.8	1828.5	373.7	142.7	434.7	5.03	318.6	-8.193	0.045
13.12.2001	20:35	J479-1	N221	0,0	2.3	2172.7	426.2	1572.6	875.3	5.07	327.9	-10.497	0.762
13.12.2001	20:35	J480-1	N221	0,0	2.3	2170.4	427.2	1567.9	863.5	5.08	327.5	-10.550	0.680
13.12.2001	20:50	J470-1	N221	1,0	2.1	2306.6	418.7	687.5	532.8	5.11	325.0	-10.183	1.159
13.12.2001	20:50	J473-1	N221	1,0	2.3	2311.6	421.5	739.6	553.6	5.14	324.9	-10.338	1.040
13.12.2001	21:05	J481-1	N221	4,0	2.3	2210.4	404.6	687.4	591.9	5.18	324.8	-9.645	1.299
13.12.2001	21:05	J469-1	N221	4,0	2.3	2216.2	407.6	706.8	596.5	5.03	325.0	-9.789	1.117

Instrumentation – Flight Sampling Systems

- Figure 1 Flask Sampling System used until May 2001
- Figure 2 Sampling System inside the WILGA-35, October 2000.
Description of the Flask Sampling System
- Figure 3 Modified Flight Sampling Unit constructed within the study
Description of the modified Flight Sampling Unit
- Figure 4 Sketch of the Flight Sampling Unit
- Figure 5 Installation of the flight equipment (Montorotondo Airfield, Italy)
- Figure 6 Pump and power supply installed inside the cabin
- Figure 7 Flight Sampling Unit and equipment of the continuos measurement system installed at the aircraft operated in Italy

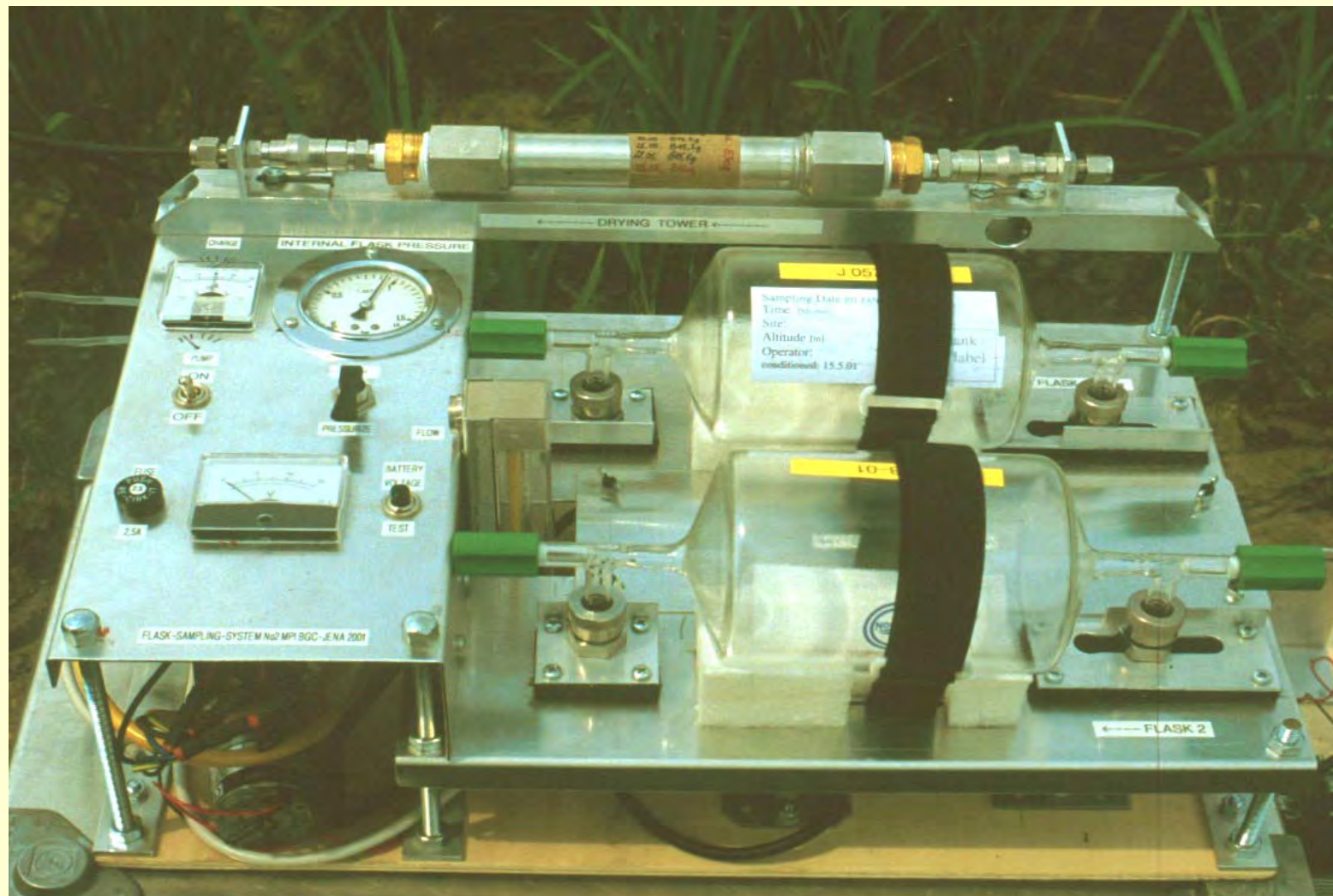


Figure 1 Traditional Flask-Sampling-System of the MPI-BGC with the configuration used within this study until Spring 2001. The original plastic tubes are already replaced by decarbon pipes.

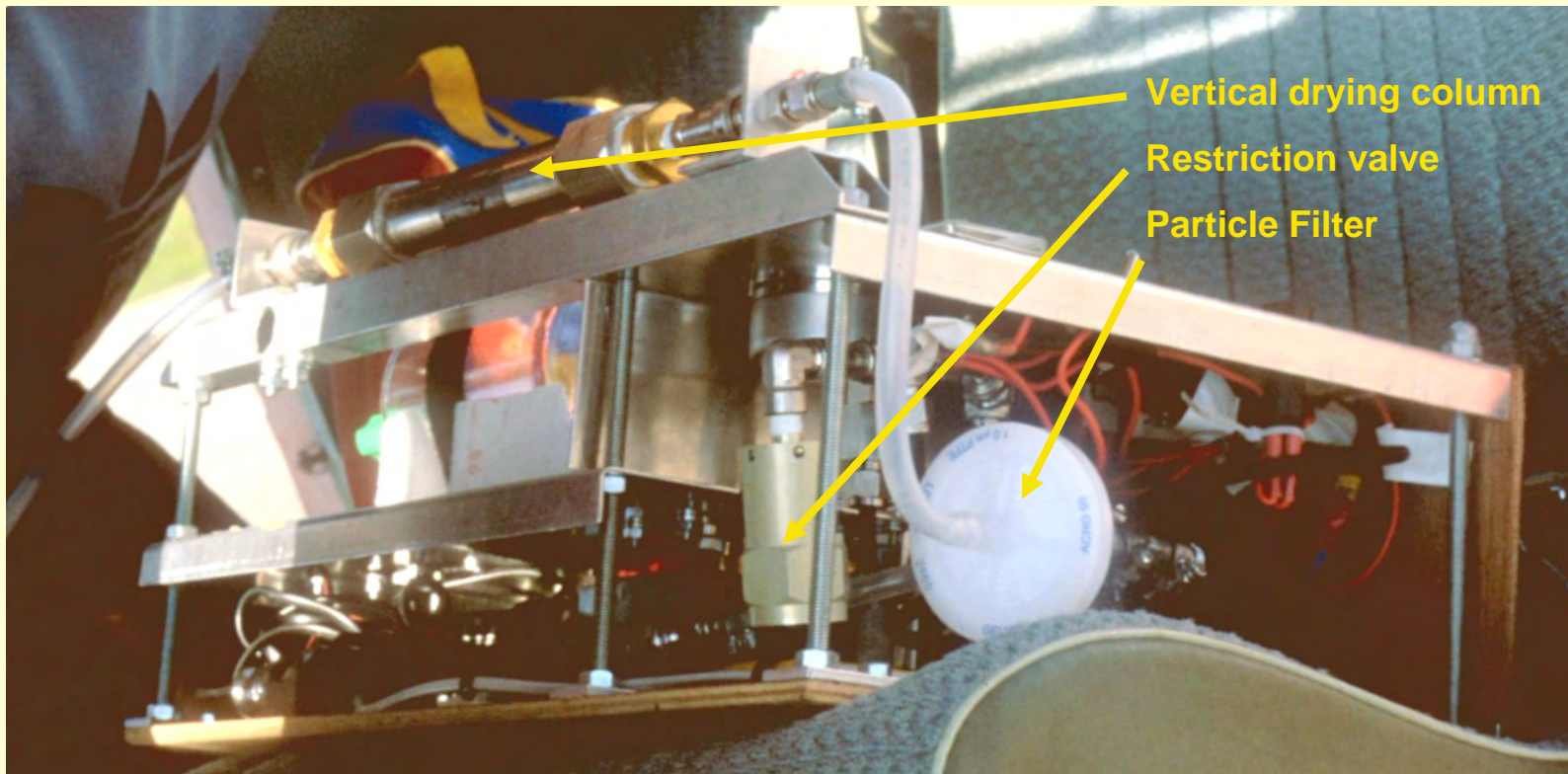


Figure 2 Traditional Flask-Sampling-System inside the cabin of the WILGA-35 used for the German flights. Notice the horizontal drying column, the tubes as well as the particle filter from plastics and the TAVCO restriction valve.

October 2000

Original flight sampling unit:

½“ Teflon® tube (length 650 cm) from wing tip to horizontal drying column (stainless steel) with Mg(ClO₄)₂ [~ 65 g] as binder medium (Fluka Chemika) – ¼“ Teflon® tube (all lines within the sample unit) – particle filter (Gelman, 1.0 micron) – pump (KNF N 814 KNDC) – unidirectional restrictor valve (Swagelok) – sample flasks (1 l bor-silicate 3.3 glass flasks [Schott], with two valves [Glas Expansion, Australia] sealed with Teflon® PFA O-rings, prefilled with calibration gas of known trace gas concentrations [2 bar abs.] - in and out fixed by ½” Cajon Ultratorr shafts (Swagelok) – 3-way-valve (Swagelok; 1 – in, 2 – out →flushing, 3 – out →sampling);

for flushing: – mechanical flow controller (Krohne 0/232939.2) – outlet

for sampling: – analog manometer (Empeo, NR63.14 0-2.5 bar) – restriction
outlet 2 bar abs (TAVCO, 2391244-8-3)

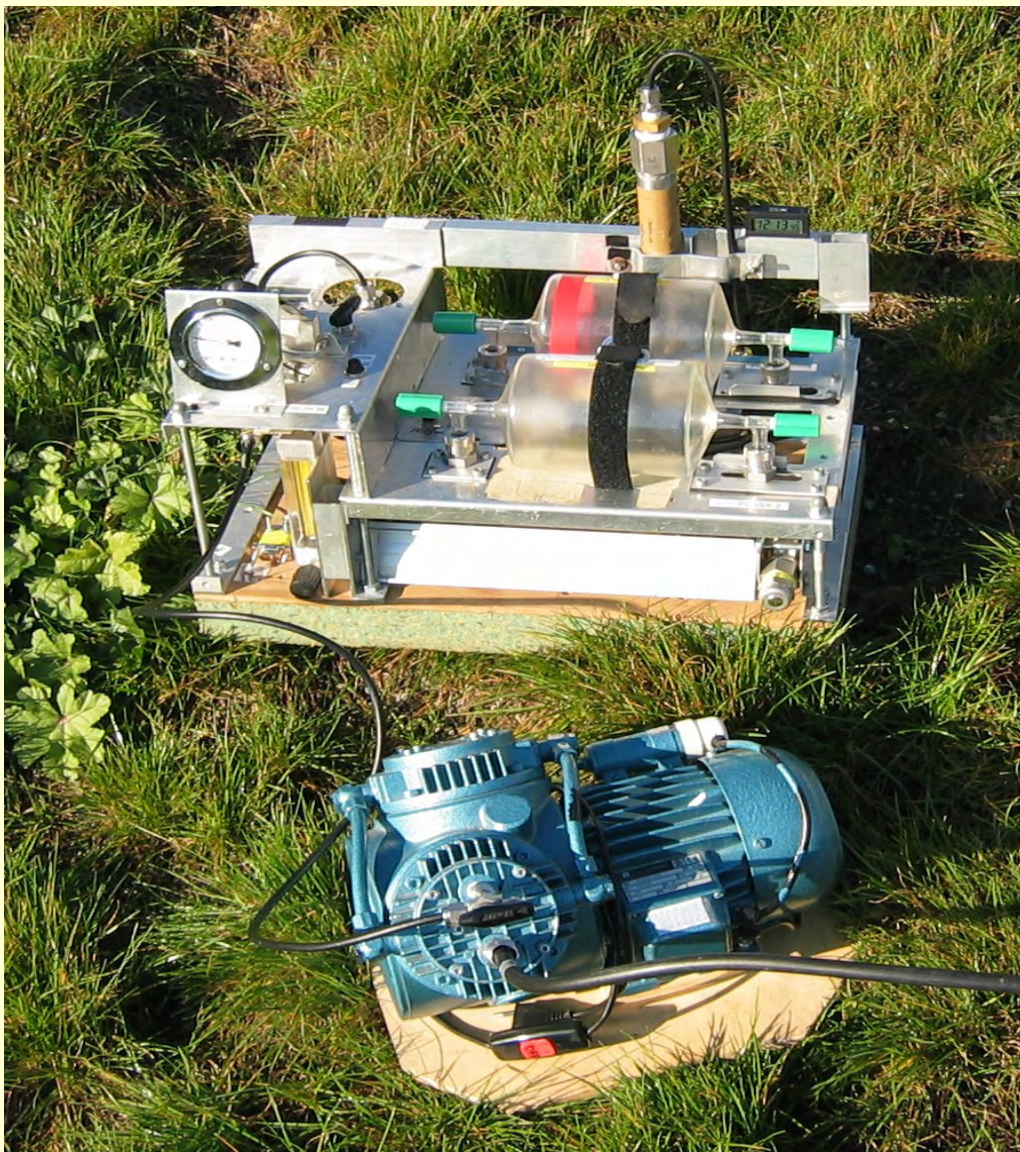


Figure 3

Modified Flight Sampling Unit.

Used in this configuration since the Valencia Winter campaign in November 2001.

Modified Flight Sampling Unit:

½“ Decarbon® tube (length 650 cm) from wing tip to pump (KNF N 145.1.2.AVE) – ¼“ steel tube outlet – 3-way-valve (Swagelok; 1 – pump out, 2 – sample unit, 3 – cockpit) – ¼“ Decarbon® tube (all lines within the sample unit) - coalescing filter (stainless steel NUPRO FC Series [Swagelok] with 0.3 micron filter [GE-15K-FC-03]) – massflow controller (Bronkhorst F201C-FACß22-V [flushing rate ~10.5 l min-1, sampling rate 3.0 l min-1 at 2 bar abs.]) – vertical drying column (stainless steel) with Mg(ClO₄)₂ [~ 70 g] as binder medium (Fluka Chemika) – particle filter (stainless steel NUPRO FC Series [Swagelok] with 0.3 micron filter [GS-15K-FC-03]) – unidirectional restrictor valve (Swagelok) - mechanical flow controller (only for control purpose, Krohne 0/232939.2) – 3-way-valve (Swagelok; 1 – in, 2 – out →sample unit, 3 – out →restriction outlet 1 bar rel. [Swagelok RL4 (0.7-15bar)]) – analog manometer (Empeo, NR63.14 0-2.5 bar) – sample flasks (1 l borosilicate 3.3 glass flasks [Schott], with two valves [Glas Expansion, Australia] sealed with Teflon® PFA O-rings, prefilled with calibration gas of known trace gas concentrations [2 bar abs.] - in and out fixed by ½” Cajon Ultratorr shafts (Swagelok) – pressure controller (Bronkorst P702C-FAC-22-V; restriction 2 bar abs.)

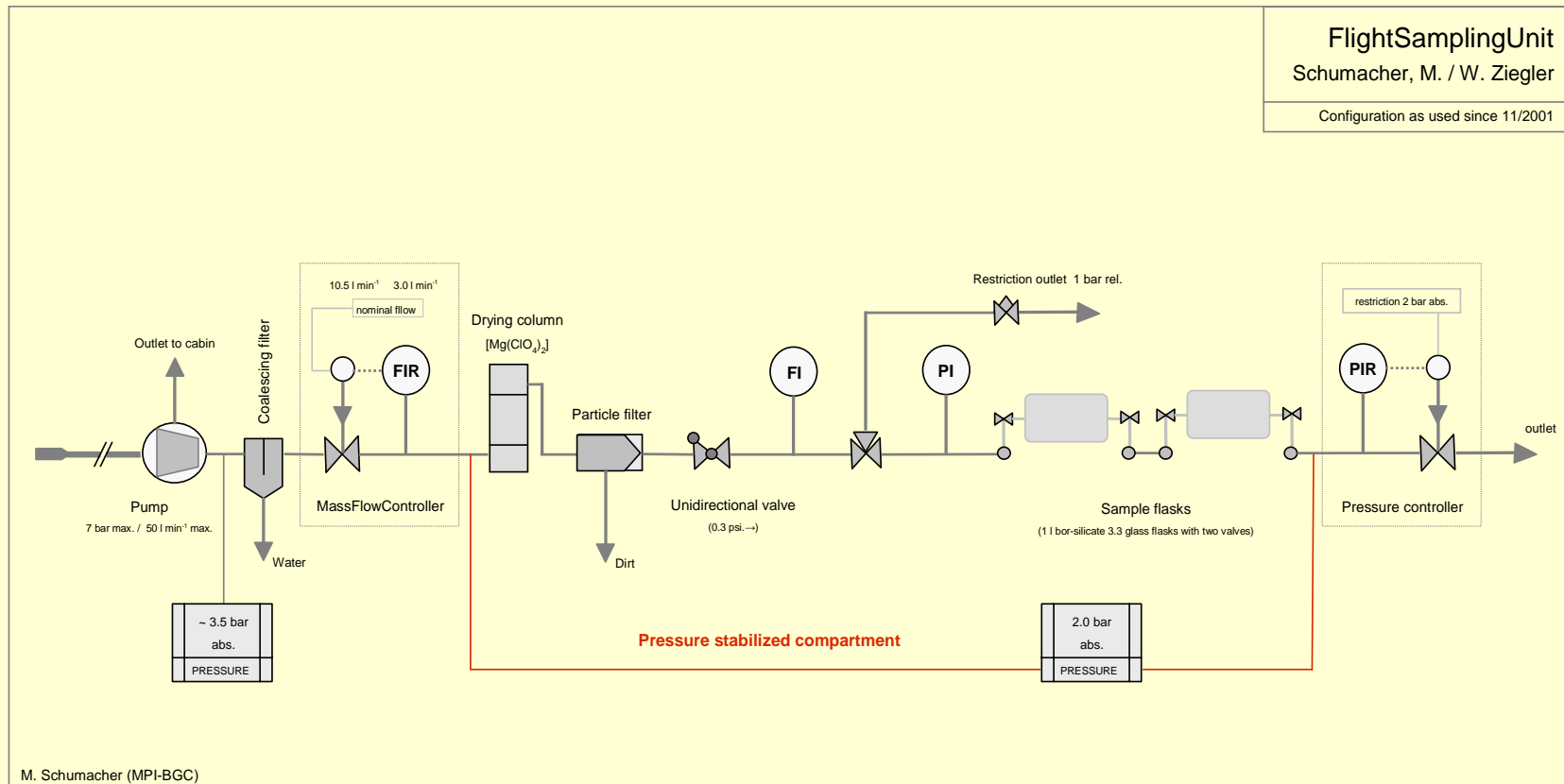


Figure 4 Configuration of the modified FlightSamplingUnit. Operated in this configuration since the Valencia Winter Experiment 2001.



Figure 5 Installation of the flight equipment at the Montorotondo Airfield in Italy. Location of the air inlet was on the right wing tip. The tube is covered by the wing nose, becoming visible at the white taped section. Aircraft is a Morane Socata.



Figure 6 Pump and power supply installed at the copilots place inside the cabin.



Figure 7 FlightSamplingUnit, GPS (on the barrier between front and rear seat), switch box of the continuous measurement system in front of the GPS. Laptop for system controlling and data recording – during the flight fixed on the operators thigh. Sample flasks are stored in the rear of the cabin Recognizable are on the left wing the mounted sensors for air temperature and humidity, dynamic and static pressure and the compass module.

Instrumentation – Ground Sampling and Reference System

Figure 1 Flask Sampling System

Description of the Ground Sampling System

Figure 2 Instrumentation of the Ground Reference System (6 m light weight mast construction)



Figure 1 Flask Sampling System used for the ground reference sampling.

Ground sampling system:

½“ Decarbon® tube from mast to pump unit (two pumps in row: KNF N 828 KNDC & KNF N 814 KNDC) – ¼“ Decarbon® tube (all lines within the sample unit) – horizontal drying column (stainless steel) with Mg(ClO₄)₂ [~ 65 g] as binder medium (Fluka Chemika) – particle filter (Gelman, 0.3 micron) – mechanical flow controller (Krohne 0/232939.2) – unidirectional restrictor valve (Swagelok) – analog manometer (Empeo, NR63.14 0-2.5 bar) – sample flasks (1 l borosilicate 3.3 glass flasks [Schott], with two valves [Glas Expansion, Australia] sealed with Teflon® PFA O-rings, prefilled with calibration gas of known trace gas mixing ratio [2 bar abs.] - in and out fixed by ½" Cajon Ultratorr shafts (Swagelok) – restriction outlet 1 bar rel. (Swagelok RL4 (0.7-15bar))

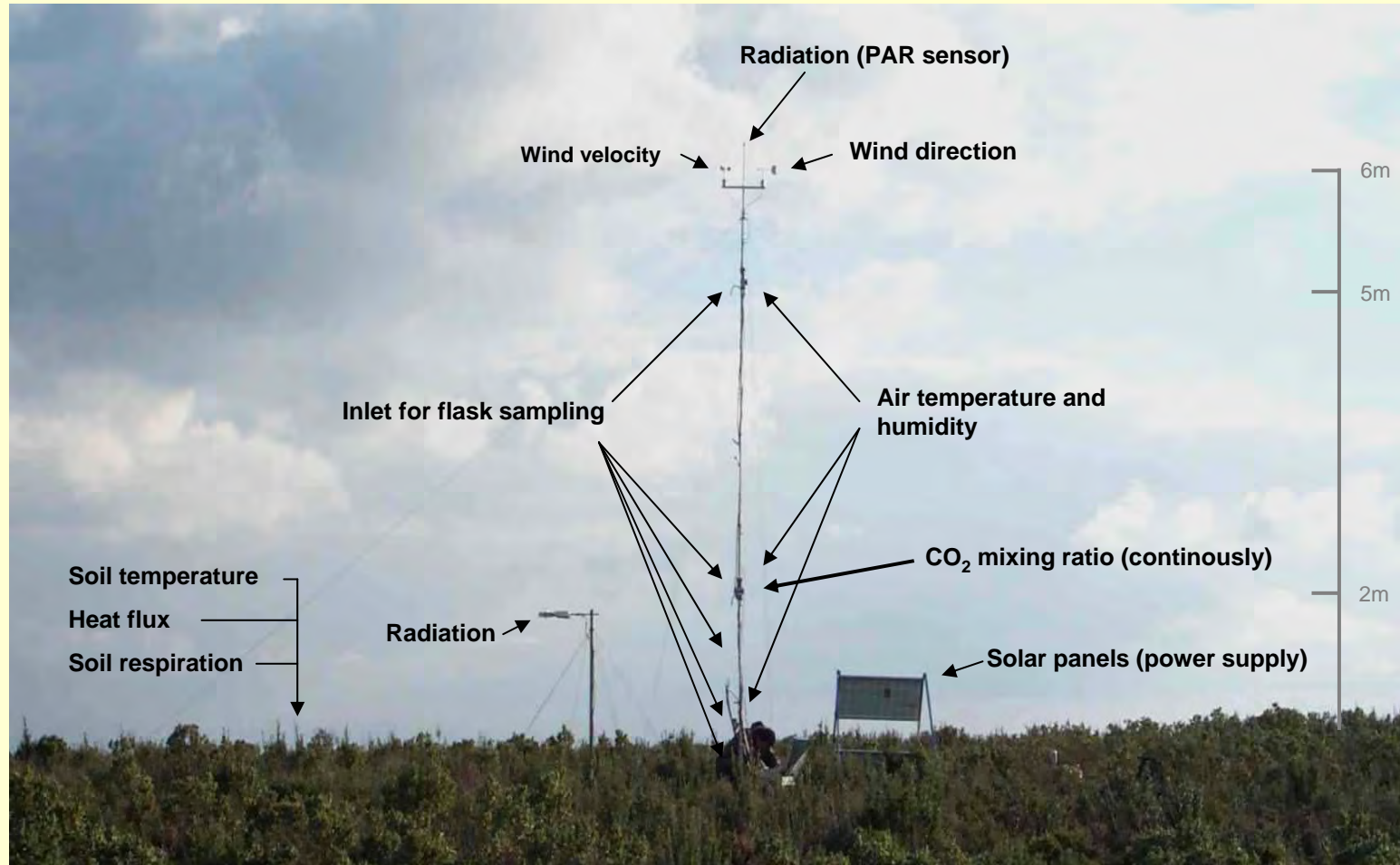


Figure 2 Instrumentation of the ground reference system.

Picture taken at the mountain site 'Cortes des Pallás', December 2001